Vol. 104 No. 2 February 1, 1979
Completing Vol. 104

ISSN 0003-2670

ANALYTICA CHIMICA ACTA

International journal devoted to all branches of analytical chemistry

ELSEVIER SCIENTIFIC PUBLISHING COMPANY

ANALYTICA CHIMICA ACTA

International journal devoted to all branches of analytical chemistry
Revue internationale consacrée à tous les domaines de la chimie analytique
Internationale Zeitschrift für alle Gebiete der analytischen Chemie

PUBLICATION SCHEDULE FOR 1979 (incorporating the section on Computer Techniques and Optimization).

	J	F	M	A	M	J	J	A	S	O	N	D
Analytica Chimica Acta	104/1	104/2	105	106/1	106/2	107	108	109/1	109/2	110/1	110/2	111
Section on Computer Techniques and Optimization			112/1			112/2			112/3			112/4

Scope. *Analytica Chimica Acta* publishes original papers, short communications, and reviews dealing with every aspect of modern chemical analysis, both fundamental and applied. The section on *Computer Techniques and Optimization* is devoted to new developments in chemical analysis by the application of computer techniques and by interdisciplinary approaches, including statistics, systems theory and operation research. The section deals with the following topics: Computerized acquisition, processing and evaluation of data. Computerized methods for the interpretation of analytical data including chemometrics, cluster analysis, and pattern recognition. Storage and retrieval systems. Optimization procedures and their application. Automated analysis for industrial processes and quality control. Organizational problems.

Submission of Papers. Manuscripts (three copies) should be submitted to:
for *Analytica Chimica Acta:* Dr. A. M. G. Macdonald, Department of Chemistry, The University, P.O. Box 363, Birmingham B15 2TT, England;
for the section on *Computer Techniques and Optimization:* Dr. J. T. Clerc, Universität Bern, Pharmazeutisches Institut, Sahlistrasse 10, CH-3012 Bern, Switzerland.

Information for Authors. Papers in English, French and German are published. There are no page charges. Manuscripts should conform in layout and style to the papers published in this Volume. Authors should consult Vol. 102, p. 253 for detailed information. Reprints of this information are available from the Editors or from: Elsevier Editorial Services Ltd., Mayfield House, 256 Banbury Road, Oxford OX2 7DE (Great Britain).

Reprints. Fifty reprints will be supplied free of charge. Additional reprints (minimum 100) can be ordered. An order form containing price quotations will be sent to the authors together with the proofs of their article.

Advertisements. Advertisement rates are available from the publisher.

Subscriptions. Subscriptions should be sent to: Elsevier Scientific Publishing Company, P.O. Box 211, 1000 AE Amsterdam, The Netherlands. The section on *Computer Techniques and Optimization* can be subscribed to separately.

Publication. *Analytica Chimica Acta* (including the section on *Computer Techniques and Optimization*) appears in 9 volumes in 1979. The subscription for 1979 (Vols. 104–112) is Dfl. 1179.00 plus Dfl. 135.00 (postage) (Total approx. U.S. $640.98). The subscription for the *Computer Techniques and Optimization* section only (Vol. 112) is Dfl. 131.00 plus Dfl. 15.00 (postage) (Total approx. U.S. $71.22). Journals are sent automatically by air mail to the U.S.A. and Canada at no extra cost and to Japan, Australia and New Zealand for a small additional postal charge. All earlier volumes (Vols. 1–95) except Vols. 23 and 28 are available at Dfl. 144.00 (U.S. $70.24), plus Dfl. 10.00 (U.S. $4.88) postage and handling, per volume.

Claims for issues not received should be made within three months of publication of the issue, otherwise they cannot be honoured free of charge.

Customers in the U.S.A. and Canada who wish to obtain additional bibliographic information on this and other Elsevier journals should contact Elsevier/North Holland Inc., Journal Information Center, 52, Vanderbilt Avenue, New York, NY 10017. Tel: (212) 867-9040.

Analytica Chimica Acta, 104 (1979) 195—203

ELECTROCHEMICAL BIOSENSORS IN THE ASSAY OF ANTIBIOTICS

MICHAEL THOMPSON*, P. J. WORSFOLD, J. M. HOLUK and E. A. STUBLEY

Department of Chemistry, University of Toronto, 80 St. George Street, Toronto, Ontario, M5S 1A1 (Canada)

(Received 10th August 1978)

SUMMARY

Certain antibiotics such as amphotericin B and nystatin are known to interact selectively with cholesterol in bilayer lipid membranes, resulting in changes in the transmembrane electrical properties. The possibilities for use of this effect in selective trace organic analysis are demonstrated by experiments performed with a simple electrical circuit incorporating a conventional research pH meter. Transmembrane resistance-based responses correlate with aqueous antibiotic concentration and are rapid and reversible. The limit of detection of the technique is approximately 10^{-9} M of stimulant.

In recent years, ion-selective electrodes have become an established weapon in the armament of the inorganic analytical chemist [1—3]. The major reasons for their acceptance are undoubtedly their low cost, mobility, relative ease of construction and incorporation into automated systems and, in particular, their selectivity. Parallel development for the selective sensing of organic molecules would have an equally significant impact in analytical chemistry. For example, one problem area is the detection of species in vivo such as the sensing of glucose in conjunction with the operation of an artificial pancreas unit. To date, attempts to monitor organic molecules with electrodes have been restricted predominantly to the determination of a secondary ionic species by using the product of an enzyme—substrate [4, 5] or antibody—antigen reaction [6]. Promising developments in the discipline of medical science with regard to the use of artificial bilayer lipid membranes (BLM) [7] in the sensing of organic molecules have not attracted attention for analytical purposes, probably because of the delicate nature of the systems involved.

The advances in the area were initiated by del Castillo et al. [8] who were able to detect anti-insulin antibodies via resistance changes across BLM. Further work involved enzyme—substrate reactions on one side of a thin phospholipid film [9]. Subsequently, it was demonstrated that certain antibiotics such as gramicidin A and amphotericin B cause resistance drops across BLM [10—12]. There is evidence from these studies that the decreased transmembrane resistance is due to the creation of aqueous pores across the membrane.

The membrane systems described above are delicate from an experimental standpoint and, therefore, are clearly unsuitable for application to practical

analytical problems. However, the electrogenic processes involved are phenomenologically similar to those postulated for the transducer action associated with chemoreception in natural sensory systems [13]. The latter are much more robust in character. For example, it is well documented that insects can detect very low concentrations of a specific pheromone in the presence of high concentrations of a mixture of other organic molecules [14]. That there is an electrical response resulting from interaction of compounds with membranes has been shown by the insertion of micro-electrodes into single cells of the insect [15]. The technique of electroantennography has become a standard procedure in the study of insect antenna—stimulant interactions in recent years. A less selective ability to distinguish and respond to different organic molecules is exhibited by the olfactory and gustatory systems of *homo sapiens* [16].

In summary, there appears to be considerable potential in analytical chemistry for the development of sensors based on the transducer action of membranes capable of chemoreception. This paper describes some new studies, with an analytical bias, on the electrochemical characteristics of BLM interaction with antibiotics.

EXPERIMENTAL

Reagents

The lipids used for BLM formation were predominantly phosphatidyl ethanolamine (PE) and phosphatidyl serine (PS) obtained from egg yolk (Serdary Research Laboratories Inc., London, Ontario). Oxidized cholesterol, rather than the pure compound, has been found to produce very stable BLM [17]. This material was prepared by refluxing cholesterol in n-octane in the presence of oxygen for several hours. The antibiotics used were nystatin (Sigma Chemical Co., St. Louis) and amphotericin B (P-L Biochemicals Inc., Wisconsin).

Apparatus

The membrane housing consisted of a machined Teflon block enclosed in a thermostatted cell (Fig. 1). Transmembrane resistance properties were studied by using single junction silver—silver chloride reference electrodes (Orion Research Inc., Cambridge, Mass.) in conjunction with a research pH meter (PHM 64, Radiometer, Copenhagen) in the electrical circuit shown in Fig. 2. The high resistances of the BLM necessitated careful shielding where appropriat

Procedures

For BLM formation, lipid solutions (<1% w/v) in a 1:1 chloroform—n-tetradecane mixture were introduced into the aperture (1—2 mm diameter) of the Teflon block with a 10-μl syringe. The volume of solution required to fill the aperture completely was 1.5—3.0 μl. The solvent then diffused into the aqueous electrolyte (0.1 M NaCl) leaving a thin lipid membrane. The temperature of the stirred electrolyte was controlled to ±0.1°C between 20°C and 35°C.

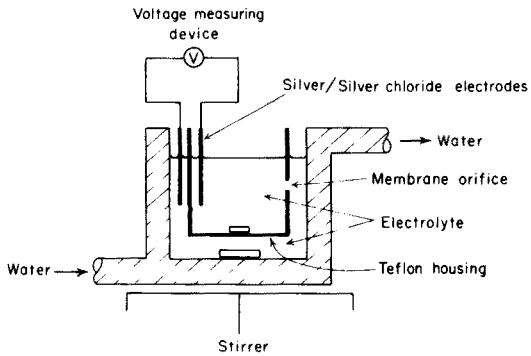

Fig. 1. Schematic diagram of experimental arrangement for BLM studies.

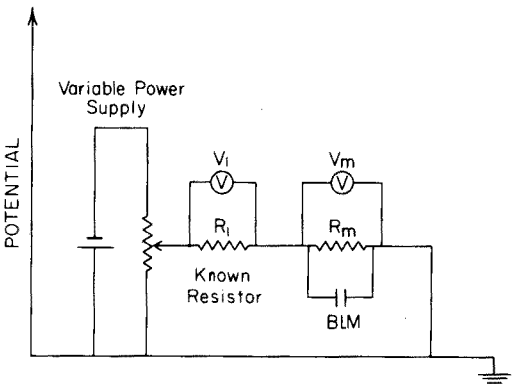

Fig. 2. Electrical circuit for resistance measurements.

The thickness of the membrane, an essential parameter, was estimated by optical reflectance [18] and capacitance measurements. The latter were derived from the assumption that the membrane acts as a parallel plate condenser. From measurements of maximum voltage against time, the leakage current of the millivoltmeter and an estimate of BLM dielectric constant of 2.66 [18], the membrane thickness was calculated to be approximately 6 nm. Despite the inherently approximate nature of the procedure, this result compares reasonably with the value of 7.2 ± 1 nm obtained from optical reflectance data [19].

Various electrical properties of the BLM were studied. These were voltage—time characteristics to monitor the membrane thinning process, current—voltage relationships to investigate the "reversibility" of BLM, and transmembrane resistance to act as a reference for membrane transport experiments. For the latter, solutions of the antibiotics in absolute ethanol were introduced by variable-volume pipette into the stirred electrolyte on both sides of the completely thinned and stable membrane.

RESULTS AND DISCUSSION

Membrane formation

A unique property of lipids is their amphipathic solubility. When introduced at an oil—water interface, lipids will align with the hydrocarbon tail in the oil phase and the polar head group in the aqueous phase, so as to reduce interfacial tension. By extension of this concept, when a lipid is introduced into an aperture in a thin hydrophobic support between two aqueous layers, it will generally thin spontaneously to a bilayer, with the polar head groups facing the aqueous layers.

Previous studies have shown that several factors need to be controlled in order to achieve satisfactory BLM formation. Among these are the hydrophobic nature and cleanliness of the membrane housing, aperture size, lipid solvent, temperature, and method of introduction. In the present work, exhaustive studies showed that a 1:1 mixture of chloroform and n-tetradecane gave the required density and polarity for lipid solubilization and BLM formation. A Teflon housing machined to allow for various apertures was used to optimize the hole size at 1.5—2.0 mm.

Electrical properties

The increasing potential observed as a function of time from the inception of the BLM (Fig. 3) is a combination of two distinct components, these being the thinning of the BLM and the charging of the BLM caused by the current flowing through the circuit. The shape of the curve obtained in all instances was exponential, rising to a maximum potential after a certain time. The maximum potential varied for different membranes of similar composition and for membranes of different composition, but the majority of BLM gave voltage maxima between 300 mV and 400 mV. The time taken to reach these maxima was inversely related to current flowing, as would be expected. In a true potentiometric situation, the steady-state transmembrane voltage is generally between +50 mV and —50 mV.

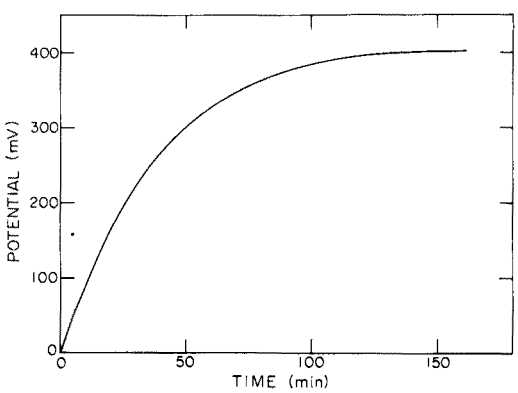

Fig. 3. Voltage—time relationship for an oxidized cholesterol BLM.

The shape of the curve can be rationalized if the membrane is considered as a parallel plate capacitor. As the membrane thins and the molecules therein become more aligned, the capacitance will increase, and in a constant-current situation, the voltage will also increase. This effect will be superimposed on the conventional capacitance charging curve.

Typical current—voltage relationships were obtained (not shown) which were characteristic of a partially polarizable resistor [20]. This result justifies the representation of BLM as capacitive resistors in electrical circuits and is one reason why the voltage across BLM stabilizes at low current only after a considerable period of time (hours). Other reasons include the fluidity of the membrane, electrostatic interference and cable capacitance effects. The response, in terms of voltage change, when direct current is suddenly applied to a BLM at a steady-state resting potential also indicates the slow reaction of unmodified BLM to change (Fig. 4). The response when the current is removed is equally slow. These results indicate that the BLM is a good choice of medium for the "framework" of an electrochemical sensor, provided that some other species can be integrated with the membrane to give selective, as well as rapid, changes in transmembrane electrical properties.

Incorporation of a conventional research pH meter into the simple electrical circuit shown in Fig. 2 proved to be adequate for resistance measurements when tested with a series of known resistors. The results for one particular BLM measured under different circuit conditions showed reasonable consistency

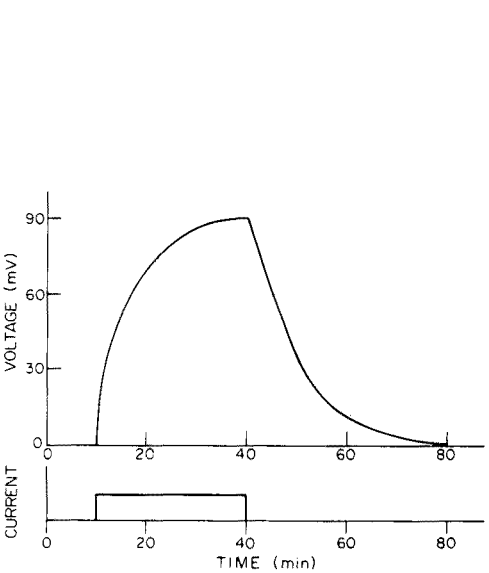

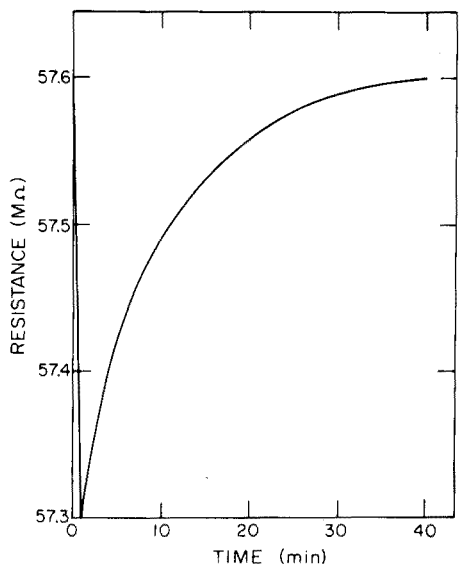

Fig. 4. Voltage response to a current pulse for a phosphatidyl serine BLM.

Fig. 5. Typical resistance—time curve for interaction of 1×10^{-6} M amphotericin B with a phosphatidyl ethanolamine—cholesterol BLM.

TABLE 1

Resistance measurements of oxidized cholesterol BLM
(R_m at 25°C and membrane area of 0.017 cm^2)

R_i ($\times 10^6$ Ω)	V_i (mV)	V_m (mV)	R_m ($\times 10^6$ Ω)	R_m ($\times 10^6$ Ω cm^2)
10	471	29	168	2.9
100	357	143	275	4.7
110	351	149	245	4.2
10[a]	481	18	267	4.5
100[a]	363	137	264	4.5
110[a]	354	146	266	4.5

[a]Direction of current reversed.

(Table 1). However, the resistance of a number of membranes varied widely over the range 10^6—10^9 Ω. This is undoubtedly associated with variations in the structure (packing) of the membrane and the nature of the Plateau—Gibbs border. These effects are related to the method of membrane preparation, i.e. the injection of lipid solution into the aperture.

Membrane transport and analytical responses

The addition of amphotericin B or nystatin on both sides of a BLM containin cholesterol causes a lowering of the membrane resistance [10—12]. In the work discussed here, analytical parameters associated with this "signal" were investigated, i.e. concentration dependence, limit of detection and response—time relationships. Despite the variation in initial resistance, there appears to be a quantitative correlation between the maximum resistance drop expressed as a fraction of the starting resistance and concentration of amphotericin B (Table 2). In these experiments, antibiotic was injected into the electrolyte solution on both sides of the membrane. The resistance drops from 10^9 Ω to 10^3 Ω found previously [10] could not be corroborated. Similar results for the effects of nystatin are also given in Table 2. Higher concentrations of the antibiotics considerably reduce the lifetime of the membrane. The limit of detection of the technique is in the vicinity of 10^{-9} M antibiotic.

A typical resistance—time curve (Fig. 5) at the relatively low amphotericin B concentration of 1×10^{-8} M exhibits a sharp initial decrease followed by a slow climb back to the original transmembrane resistance. Interestingly, at higher antibiotic concentrations the resistance of the membrane does not return to its original value.

In order to rationalize the results described above, it is instructive to conside the "pore" hypothesis of Finkelstein and Holz [21]. Interaction of the antibiotic with cholesterol in the membrane results in the packing of antibiotic molecules to produce a cylindrical structure in each half of the BLM; the halves are held together in the centre of the bilayer by a ring of hydrogen-

TABLE 2

Response of PE—cholesterol BLM to amphotericin B and nystatin

Antibiotic Concn.[a] (M)	Initial membrane resistance ($\times 10^9$ Ω)	Maximum resistance drop ($\times 10^9$ Ω)	Resistance drop (%)
Amphotericin B			
6.6×10^{-9}	5.70	0.27	0.5
	5.70	0.20	0.3
	6.80	0.15	0.2
	6.80	0.10	0.2
5.0×10^{-8}	6.30	0.78	12.4
	5.34	0.69	12.9
	6.43	0.95	14.8
1.5×10^{-7}	8.37	2.86	34.2
	7.28	2.20	30.2
5.0×10^{-7}	21.0	13.19	62.8
Nystatin			
1.0×10^{-6}	2.6	0.012	0.5
	2.2	0.012	0.5
	2.1	0.009	0.4
5.0×10^{-6}	3.1	0.17	5.5
	3.4	0.32	9.4
	3.4	0.24	7.1
	3.6	0.19	5.3

[a] Average of concentrations for each side of BLM.

bonded hydroxyl groups. The significant feature of this structure is that it provides a water-filled region of high dielectric constant for ion transport within a non-polar hydrocarbon exterior.

The concentration correlation is clearly governed by the number of pores that are formed initially and the limit of detection is probably related to a "threshold" mechanism involving membrane association of antibiotic molecules. Furthermore, rupture at high concentration is caused by a destabilizing effect corresponding to a critical number of pores. It is more difficult to explain the nature of the resistance—time experiments. If it can be assumed that pore formation is a dynamic (equilibrium) process, as is thought to be the case, then one can only speculate that at the lower antibiotic concentrations slow pore removal is effected. Such a theory would necessitate gradual removal of antibiotic in some way. In view of the amphipathic character of the process, aggregation in aqueous solution is a possibility. It is interesting to note that introduction of a fresh sample of antibiotic causes the resistance to drop sharply again. At the higher concentrations, enough monomer must be present in solution to drive the BLM—solution equilibrium to continual pore replacement.

CONCLUSIONS

The present paper indicates the possibilities of lipid membranes for trace organic analysis. The systems can be used to give a concentration-dependent signal; unlike ion-selective electrodes, the response is resistance-based. The technique appears to offer very high sensitivity and a low limit of detection. Further work is proceeding in the following areas.

(1) The results cited above were obtained with a simple circuit. The disadvantages of this system may be overcome through use of more sophisticated electrometer-based equipment which is microprocessor-controlled. This enables several membrane—stimulant interaction experiments to be monitored in a very rapid sequential manner through a scanning device. The BLM described above are delicate and have a limited lifetime. Methods of producing more robust systems are being studied.

(2) Electron microscopy offers the possibility of "seeing" membrane receptor sites and pores as well as transmembrane structure. As preliminaries to electron microscopy, the freeze-fracture technique and fixing procedures are being studied.

(3) It should be possible to incorporate selectivity into the membrane in terms of stimulant—membrane interaction. A good example of this is the work of Reader et al. [22] who were able to incorporate hydrophobic protein receptors into BLM for interaction with pharmacological agents such as acetylcholine present in the aqueous phase.

We are indebted to the Natural Sciences and Engineering Research Council of Canada for support for this work. Also, we are particularly appreciative of funds for equipment provision from the Atkinson Foundation of Toronto, Ontario.

REFERENCES

1 R. P. Buck, Anal. Chem., 50 (1978) 17R.
2 J. Koryta, Anal. Chim. Acta, 91 (1977) 1.
3 See, e.g., P. L. Bailey, Analysis with Ion-selective Electrodes, Heyden, London, 1976.
4 See, e.g., G. G. Guilbault, in G. Svehla, Ed., Comprehensive Analytical Chemistry, Vol. VIII, Elsevier, Amsterdam, 1977, p. 1.
5 D. N. Gray, M. H. Keyes and B. Watson, Anal. Chem., 49 (1977) 1067A.
6 P. D'Orazio and G. A. Rechnitz, Anal. Chem., 49 (1977) 2083.
7 P. Mueller, D. O. Rudin, H. Ti Tien and W. C. Wescott, Nature, 194 (1962) 979.
8 J. del Castillo, A. Rodriguez, C. A. Romero and V. Sanchez, Science, 153 (1966) 185.
9 E. Toro-Goyco, A. Rodriguez and J. del Castillo, Biochem. Biophys. Res. Commun., 23 (1966) 341.
10 T. E. Andreoli and M. Monahan, J. Gen. Physiol., 52 (1968) 300.
11 A. Cass, A. Finkelstein and V. Krespi, J. Gen. Physiol., 56 (1970) 100.
12 R. Holz and A. Finkelstein, J. Gen. Physiol., 56 (1970) 125.
13 T. M. Poynder (Ed.), Transduction Mechanisms in Chemoreception, Information Retrieval Limited, London, 1974.

14 L. L. Sower, L. K. Gaston and H. H. Shorey, Ann. Entomol. Soc. Am., 64 (1971) 1148.
15 See, e.g., L. Frisch (Ed.), Cold Spring Harbor Symposia on Quantitative Biology, Vol. 30, Long Island, New York, 1965.
16 G. E. W. Wolstenholme and T. Knight (Eds.), Symposium on Taste and Smell in Vertebrates, Churchill, London, 1969.
17 H. Ti Tien, S. Carbone and E. Dawidowicz, Nature, 212 (1966) 718.
18 H. Ti Tien, J. Gen. Physiol., 52 (1968) 125.
19 H. Ti Tien, J. Mol. Biol., 16 (1966) 576.
20 E. Gileadi, E. Kirowa-Eisener and J. Penciner, Interfacial Electrochemistry — An Experimental Approach, Addison-Wesley, Reading, Mass., 1975.
21 A. Finkelstein and R. Holz in G. Eisenman (Ed.), Membranes 2, Lipid Bilayers and Antibiotics, M. Dekker, New York, 1973, p. 399.
22 T. A. Reader, S. Fiszer de Plazas, P. J. I. Salas and E. De Robertis in P. E. Roy and N. S. Dhalla (Eds.), Recent Advances in Studies on Cardiac Structure and Metabolism, Vol. 9, The Sarcolemma, University Park Press, Baltimore, 1976, p. 149.

Analytica Chimica Acta, 104 (1979) 205—213

THE APPLICATION OF THE pH-STAT METHOD TO METAL ION-CATALYZED REACTIONS

SIEGBERT PANTEL

Lehrstuhl für Analytische Chemie, Chemisches Laboratorium der Universität, Freiburg i.Br. (Federal Republic of Germany)

(Received 16th June 1978)

SUMMARY

The pH-stat method, which is well known in organic chemistry and biochemistry, is used for the kinetic determination of metal ion catalysts. Indicator reactions that involve protons can be followed by controlled addition of standard base or acid. This is illustrated by the following examples: determination of copper(II) (0.03—0.3 $\mu g\ ml^{-1}$) with the indicator reaction ascorbic acid—peroxydisulphate; determination of molybdenum(VI) (0.2—2.5 $\mu g\ ml^{-1}$) with the indicator reaction thiosulphate—hydrogen peroxide; determination of zirconium(IV) (0.2—2 $\mu g\ ml^{-1}$) with the indicator reaction iodide—hydrogen peroxide; and determination of vanadium(V) (0.2—2 $\mu g\ ml^{-1}$) with the indicator reaction iodide—bromate. For one example, the copper—ascorbic acid—peroxydisulphate reaction, it is shown that the pH-stat method has distinct advantages over closed systems, giving considerably better sensitivity for the determination of copper (0.5—5 $ng\ ml^{-1}$).

"Stat" methods are one possibility of using open systems for the catalytic-kinetic determination of catalysts. In these methods, a preset state of the indicator reaction $A + B \overset{Cat.}{\rightarrow} X + Y$, is kept constant by stepwise addition of one of the reactants A or B depending on its consumption, or of a suitable substance which reacts quickly with one of the reaction products X or Y. The speed of addition is controlled by following some physical property of the indicator substance which is changed by the chemical reaction in the system. The physical phenomenon may be pH (pH-stat) [1, 2], redox potential (potentiostat) [3—5], colour intensity (absorptiostat) [6], polarization current (biamperostat) [7] or the chemiluminescence (luminostat) [8].

Examples of the application of the pH-stat method are mainly known in enzymatic reactions, in organic chemistry and in general biochemistry [9—16]. In this paper it will be shown that the pH-stat method can also be used for the determination of catalytically active metal ions such as copper(II), molybdenum(VI), zirconium(IV) or vanadium(V), based on catalyzed oxidations of organic or inorganic substrates with peroxydisulphate, hydrogen peroxide or bromate.

In pH-stat methods, buffers obviously cannot be used but several catalyzable redox systems have a more or less marked buffering action. This can be shown

by titrating an acidified solution of the indicator reaction system (but without catalyst) with a standard solution of sodium hydroxide and monitoring with a recording pH meter. This was done with 5 substrate pairs for the copper- or molybdenum-catalyzed oxidation systems. Figure 1 (a—e) shows the corresponding titration curves achieved with 1 M sodium hydroxide. It can be seen that for the various systems the maximum sensitivity lies in different pH regions. However, the catalyzed reaction is at its optimum only in a more or less narrow pH region; only when the maximum pH change caused by NaOH addition and the optimal pH for the catalyzed reaction are in the same region can the highest sensitivity of the method be achieved.

In cases where the pH optimum for the catalyzed reaction lies in the upper or lower curved part (Fig. 1), more hydrogen ion or hydroxide must be applied to achieve the same measuring effect; but "titrating" solutions of too high concentration would cause an "overshoot" at every addition because of the sluggishness of the glass electrode.

EXPERIMENTAL

Apparatus

The preset working potential (pH value) was kept constant by using a Combi-Titrator 3 D (Metrohm, Herisau); this consists of a mV/pH meter, controller (Impulsomat) and automatic burette (1 ml) with a mechanically coupled recorder (Multidosigraph). The electrode used was a uranium glass electrode (Ingold LOT 401) with inner reference standard.

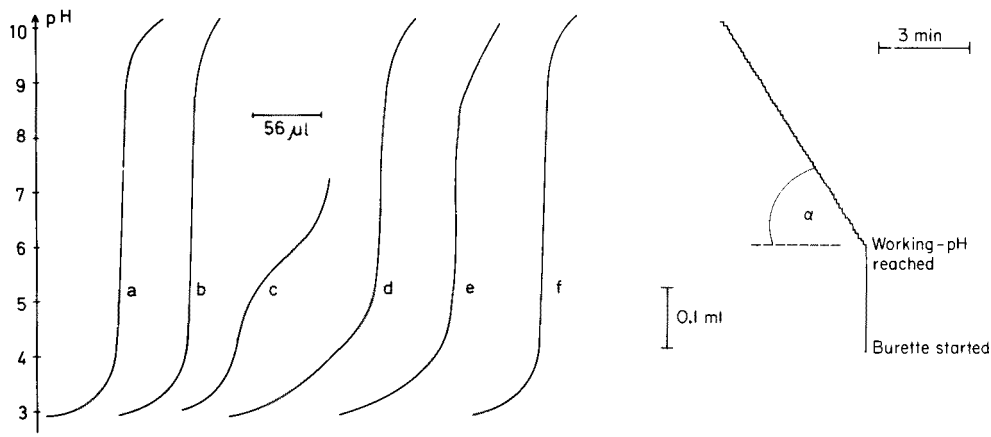

Fig. 1. Titration curves for some redox systems with 1 M NaOH in the absence of catalysts; all solutions are 0.002 M in oxidant and reductant concentration. Glass electrode as indicator system. (a) $S_2O_3^{2-}/H_2O_2$; (b) $N_2H_4/S_2O_8^{2-}$; (c) $NH_2OH/S_2O_8^{2-}$; (d) ascorbic acid/$S_2O_8^{2-}$; (e) gluconic acid/$S_2O_8^{2-}$; (f) 0.001 M H_2SO_4 for comparison.

Fig. 2. Recorder graph for the pH-controlled addition of 0.05 M NaOH in the copper-catalyzed oxidation of ascorbic acid with peroxydisulphate.

In the Combi-Titrator 3 D, a measured actual potential is compared electronically with a preset working potential, e.g. the pH of the solution to be kept constant. The difference between the two supplies an impulse to the burette, so that a suitable reagent (acid or base) is added to the system until the two potentials are again identical. The addition steps are monitored vs. time as shown in Fig. 2.

A 50-ml beaker (tall form) with a PVC cover (with appropriate holes) was used as reaction vessel. This beaker was fixed in a hollow aluminium block connected to a thermostat, thus being kept constant at 22.5 ± 0.1°C in all cases. The recorder speed was 10 mm min^{-1}; pH meter and electrode were standardized with 0.050 molal potassium hydrogenphthalate solution (pH 4.0 at 20°C).

All solutions were prepared with deionized—distilled water from p.a. chemicals.

OXIDATION REACTIONS WITH POTASSIUM PEROXYDISULPHATE

Peroxydisulphate is a typical dehydrogenating oxidant [17, 18] in acidic, neutral and alkaline solution. The sodium salt has a higher solubility, the potassium salt crystallizes with higher purity, and the ammonium salt is unstable.

Oxidations with peroxydisulphate are strongly catalyzed by silver(I) [19, 20] and copper(II) [21—23]; the catalytic activity of osmium(VIII), nickel, vanadium(II) and gold(III) is lower.

Determination of copper(II) in the microgram range

The copper(II)-catalyzed oxidation of ascorbic acid with peroxydisulphate,

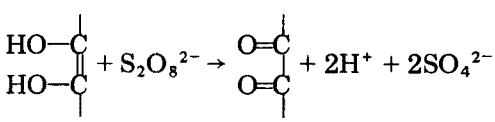

proceeds very slowly below pH 2.5; above pH 5.5, even the uncatalyzed reaction is fast. The titration curve for the system (Fig. 1d) with 1 M NaOH shows that the highest sensitivity lies between pH 5 and 9. As there is no agreement between the pH values for optimal sensitivity and optimal reaction, the determination of copper(II) was done at pH 3.5, where the uncatalyzed reaction is still slow enough; 0.05 M NaOH proved to be a suitable concentration for keeping the preset pH constant.

Procedure for the microgram range. To the measuring vessel are added 1 ml of an aqueous solution of ascorbic acid (10 mg ml^{-1}), 50 μl of 0.1 M sulphuric acid and 0.5 ml of copper standard solution (2—20 μg ml^{-1}) for the calibration graph, or a suitable amount of neutral sample solution. After dilution to 30 ml with water and thermostating for 5 min, the solution is adjusted to about pH 3.3 with 1 M NaOH from an Agla burette. The reaction is then started by injection of 0.5 ml of an aqueous solution of peroxydisulphate (20 mg ml^{-1}, adjusted to the working pH) from an Eppendorf pipette. The pH is kept

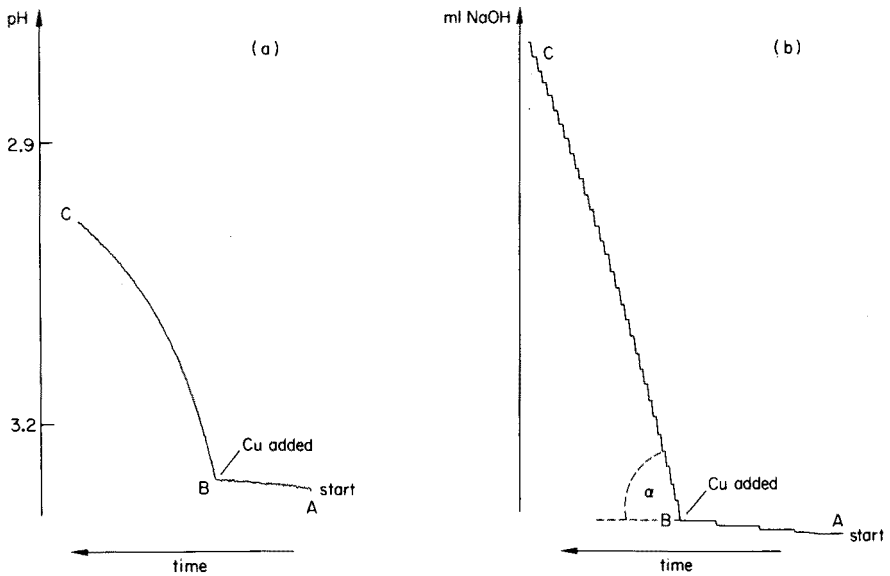

Fig. 3. Comparison of the copper-catalyzed oxidation of ascorbic acid with peroxydisulphate; pH is followed (a) in a closed system and (b) with the aid of the pH-stat method under the same conditions. Reaction is started by the addition of copper(II); $\overline{AB}$, uncatalyzed reaction; $\overline{BC}$, catalyzed reaction.

constant by stepwise Impulsomat-controlled addition of 0.05 M NaOH with the Multidosigraph. A recorder graph is shown in Fig. 2.

The calibration graph, drawn by plotting tan α (ordinate) vs. copper concentration, is linear between 1 and 10 μg Cu per 30.5 ml and goes through the ordinate.

Some results for the determination of copper are given in Table 1.

Other possible reactions

The following reductants were also examined for the determination of copper: hydrazine and hydroxylamine were tested as examples of inorganic substrates, and gluconic acid and glucose as examples of biochemically interesting ones. Hydrazine is oxidized to nitrogen:

$$N_2H_4 + 2S_2O_8^{2-} \rightarrow 4SO_4^{2-} + 4H^+ + N_2$$

The titration curve for the uncatalyzed system (Fig. 1b) shows that the most sensitive pH range is between 4 and 9; the catalyzed reaction is too slow at pH 4.0 and the uncatalyzed reaction is too fast at pH 5.0; consequently, the optimum value for the stat-method is pH 4.5. When 0.05 M NaOH was added automatically for the determination of copper, the recorder plots, calibration graph, results and reproducibility were similar to those obtained in the copper—ascorbic acid—peroxydisulphate system.

TABLE 1

Determination of copper(II) with the ascorbic acid—peroxydisulphate indicator reaction for microgram and nanogram amounts
(All results are given as the amount of copper(II) in 30.5 ml)

Given (μg)	Found (μg)	Error (μg)	Given (ng)	Found (ng)	Error (ng)
1.50	1.40	−0.10	18.0	18.5	+0.5
2.00	1.80	−0.20	31.0	30.5	−0.5
2.60	2.45	−0.15	64.0	63.5	−0.5
3.12	2.95	−0.17	87.0	90.0	+3.0
3.40	4.85	+1.45	107.0	110.0	+3.0
4.85	4.60	−0.25	110.0	108.0	−2.0
6.00	6.15	+0.15	110.0	113.5	+3.5
7.20	6.95	−0.25	117.0	120.0	+3.0
8.85	9.25	+0.40	118.8	124.5	+5.7
9.70	10.00	+0.30	118.0	117.5	−0.5

The optimum pH for the oxidation of hydroxylamine is also 4.5; the titration curve (Fig. 1c), however, shows that this pH is very unfavourable. The stat-method was tested with 0.05 M NaOH, but the single titration steps were very large, and this reagent cannot be recommended.

Gluconic acid is a very good substrate for the copper-catalyzed oxidation with peroxydisulphate. The optimal pH is pH 5.0, which is in agreement with the values of the titration curve (Fig. 1e). The copper determination with gluconic acid as substrate is done in the same way as described for ascorbic acid; the reproducibility and the range are similar. The copper-catalyzed oxidation of glucose itself with peroxydisulphate is sufficiently fast at pH 7.0, but during the course of the reaction the rate accelerates very considerably.

Determination of copper(II) in the nanogram range

The pH-stat method has the advantage over closed catalyzed systems that the pH value is kept constant over a markedly longer time; therefore the recorder plot for the volume of base added vs. time is almost linear. In closed systems, the changes of pH arising from the reaction cause relatively rapid changes in the speed of reaction, and the plot is distinctly curved. This can be seen in the example of the oxidation of ascorbic acid with peroxydisulphate. Figure 3 shows plots of both the closed and open systems under the same reaction conditions. Moreover, for open systems the concentration of reagent added from the burette can be chosen so that, for uncatalyzed relatively fast reactions, the speed of addition is relatively low. An example is given in Fig. 4: in the closed system, the uncatalyzed reaction at pH 5.0 proceeds so quickly that the curve angle after the addition of the catalyst cannot be evaluated, whereas in the pH-stat method the angle of climb can be measured without difficulties. This effect can be used for the determination of copper(II) in the nanogram range.

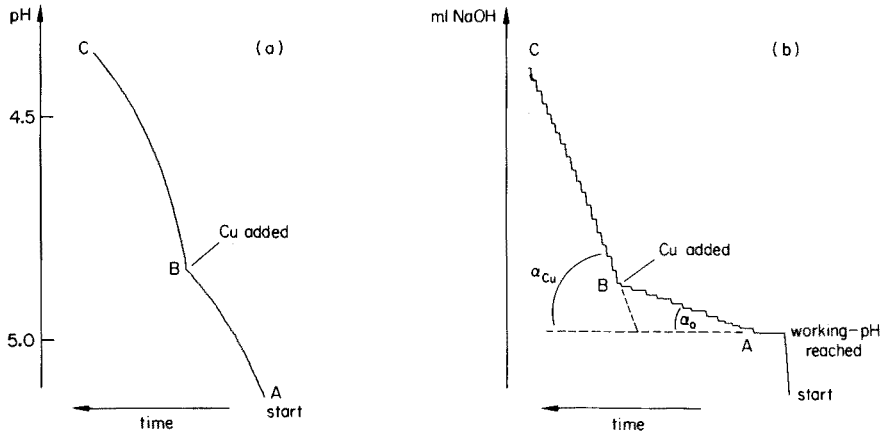

Fig. 4. Reaction and indication as in Fig. 3, but at a pH value such that the uncatalyzed reaction is already very fast: (a) closed system, (b) open system.

Procedure. To the measuring vessel are added 1 ml of an aqueous solution of ascorbic acid (10 mg ml^{-1}, adjusted to about pH 4.8) and 0.5 ml of a solution of potassium peroxydisulphate (20 mg $S_2O_8^{2-}$ ml^{-1}, adjusted to pH 4.8). The solution is diluted to 30 ml with water, all solutions are thermostated at 22.5°C before use. After adjustment to pH 5.0, the automatic burette is immediately started (0.05 M NaOH) and run for about 5 min, thus giving the blank for the test (α_0). Addition of 0.5 ml of copper standard solution (30—300 ng ml^{-1} for preparing the calibration graph) or the slightly acidic sample solution, and further addition of standard 0.05 M NaOH with the automatic Metrohm unit results in a new angle (α_{Cu}) for the catalyzed reaction (Fig. 4b).

For evaluation of the plot, the difference ($\tan \alpha_{Cu} - \tan \alpha_0$) is used. This has the advantage that the effect of traces of impurities which also may react with the catalyzed system, can be compensated because their contribution is included in α_0.

The calibration graph for 15—150 ng Cu/30.5 ml is linear when ($\tan \alpha_{Cu} - \tan \alpha_0$) is plotted against copper concentration, passing through the origin.

Some results for the determination of copper in this way are also given in Table 1.

OXIDATION REACTIONS WITH HYDROGEN PEROXIDE

Hydrogen peroxide is not such a good oxidizing reagent for pH-stat purposes as peroxydisulphate. However, one example should be mentioned, because of its rather unusual mechanism: the oxidation of thiosulphate, which is catalyzed by many metal ions, among them molybdenum(VI) [24].

Determination of molybdenum(VI)

In the absence of catalyst at pH 3.5—4.5, this reaction shows a slow, steady increase in basicity, expressed by the equation:

$$2S_2O_3^{2-} + H_2O_2 \rightarrow S_4O_6^{2-} + 2OH^-$$

After addition of molybdenum(VI), the reaction mixture becomes acidic

$$S_2O_3^{2-} + 4H_2O_2 \rightarrow 2SO_4^{2-} + 2H^+ + 3H_2O$$

Therefore, beneath a certain minimum concentration of the catalyst, no addition curve is observed with sodium hydroxide. The determination of molybdenum is best carried out at pH 3.5.

Procedure. To the reaction vessel are added 0.5 ml of 0.1 N sodium thiosulphate, 1 ml of molybdenum standard solution (6—60 μg Mo ml^{-1} as sodium molybdate) for preparing the calibration graph or an equivalent amount of neutralized sample solution, and enough water to give 25 ml. After thermostating for 5 min, the solution is adjusted to pH 3.5, and the catalyzed reaction is started by addition of 0.5 ml of hydrogen peroxide solution (10 mg ml^{-1}). The working pH is kept constant by automatic addition of 0.05 M NaOH from the Multidosigraph.

A calibration graph is drawn by plotting tan α (ordinate) vs. molybdenum concentration. It is linear within the range 6—60 μg Mo/25.5 ml and goes through the abscissa as postulated by the theory discussed above.

Some results for the determination of molybdenum are given in Table 2.

Determination of zirconium(IV)

It is, of course, possible to follow not only reactions producing protons by the pH-stat method but also catalyzed reactions consuming protons. In the latter case, a diluted acid, e.g. H_2SO_4, is added under pH control. This can be illustrated by the example of the zirconium(IV)-catalyzed oxidation of iodide by hydrogen peroxide [24]:

$$2I^- + H_2O_2 + 2H^+ \rightarrow I_2 + 2H_2O$$

The iodine formed during the reaction is removed by an excess of thiosulphate. It may be noted that in this example ascorbic acid cannot be used as the iodine-consuming reagent because its reaction with iodine itself forms protons

TABLE 2

Determination of molybdenum(VI) with the thiosulphate—hydrogen peroxide indicator reaction
(Results are given in μg Mo/25.5 ml)

Given	6.0	10.0	12.0	20.0	24.0	30.0	36.0	46.0	52.3	60.0
Found	4.5	11.2	13.2	20.5	24.2	31.3	34.5	43.5	52.0	59.2
Error (μg)	−1.5	+1.2	+1.2	+0.5	+0.2	+1.3	−1.5	−2.5	−0.3	−0.8

along with dehydroascorbic acid and iodide. The zirconium(IV)-catalyzed reaction is best carried out at pH 5.0.

Procedure. To the reaction vessel are added 0.5 ml of 0.1 M potassium iodide, 1 ml of hydrogen peroxide (1 mg ml^{-1}) and 0.5 ml of 0.1 N sodium thiosulphate, and the mixture is diluted to 25 ml with water. All solutions are thermostated at 22.5°C before use. Immediately after the reagents have been mixed, the pH is adjusted to 5.0 and the burette is started. After a 5-min run for the blank, the catalyzed reaction is started by addition of 0.5 ml of the zirconium standard solution (8—80 μg Zr ml^{-1}) for preparing the calibration graph, or the sample solution, acidified to about pH 5.5. Because zirconium forms polynuclear acids, it is necessary to store standard as well as sample solutions in acidic medium for some time [4]; a period of 24 h has proved to be sufficient for this purpose [25].

In the uncatalyzed period of reaction as well as in the catalyzed one, the pH is kept constant by automatic addition of 0.005 M H_2SO_4 from the Multidosigraph. The procedure is analogous to that described for copper in the ng-range (cf. Fig. 4). The calibration graph, drawn by plotting ($\tan \alpha_{Zr} - \tan \alpha_0$) vs. catalyst concentration, is almost linear in the given range. Some results for the determination of zirconium are given in Table 3.

Determination of vanadium(V)

Another example of proton consumption is the vanadium(V)-catalyzed oxidation of iodide with bromate to form iodine [26]. Again thiosulphate is used to consume the iodine formed during the reaction time. The vanadium(V) catalyst is activated by addition of pyrocatechol [27]. The working pH was 4.0.

Procedure. To the reaction vessel are added 3 ml of 0.1 M potassium bromate 1 ml of 0.1 N sodium thiosulphate, 1.5 ml of 0.1 M potassium iodide and 1 ml of an aqueous solution of pyrocatechol (1 mg ml^{-1}). The mixture is diluted with water to 25 ml. All solutions are thermostated at 22.5°C before use. Immediately after these reagents have been mixed, the pH is adjusted to 4.0 and the burette is started (0.005 M H_2SO_4). After a 5-min run for the blank, the catalyzed reaction is started by addition of 0.5 ml of vanadium(V) standard solution (8—80 μg V ml^{-1} as sodium vanadate, for preparing a calibration graph, or of the neutralized sample solution.

The recorder plots are evaluated as described above. Plotting ($\tan \alpha_V - \tan \alpha_0$ vs. catalyst concentration results in a linear calibration graph for the given range.

TABLE 3

Determination of zirconium(IV) with the iodide—hydrogen peroxide indicator reaction (Results are given in μg Zr/25.5 ml)

Given	5.0	6.0	12.0	15.5	20.0	22.0	25.3	30.0	37.0	42.5
Found	4.6	6.7	11.5	16.0	20.6	21.0	24.6	30.5	36.7	41.0
Error (μg)	−0.4	+0.7	−0.5	+0.5	+0.6	−1.0	−0.7	+0.5	−0.3	−1.5

TABLE 4

Determination of vanadium(V) with the iodide—bromate indicator reaction (Results are given in μg V/25.5 ml)

Given	5.0	7.0	10.0	12.5	16.5	22.5	24.0	27.1	32.7	36.0
Found	4.6	7.0	10.1	12.0	16.4	21.8	24.3	26.9	33.2	36.3
Error (μg)	−0.4	±0	+0.1	−0.5	−0.1	−0.7	+0.3	−0.2	+0.5	+0.3

Some results for the determination of vanadium in this way are given in Table 4.

REFERENCES

1 K. M. Møller, Biochim. Biophys. Acta, 16 (1955) 162.
2 H. V. Malmstadt and E. H. Piepmeier, Anal. Chem., 37 (1965) 34.
3 H. Weisz, D. Klockow and H. Ludwig, Talanta, 16 (1969) 921.
4 D. Klockow, H. Ludwig and M. A. Giraudo, Anal. Chem., 42 (1970) 1682.
5 H. Weisz, K. Rothmaier and H. Ludwig, Anal. Chim. Acta, 73 (1974) 224.
6 H. Weisz and K. Rothmaier, Anal. Chim. Acta, 75 (1975) 119.
7 S. Pantel and H. Weisz, Anal. Chim. Acta, 70 (1974) 391.
8 S. Pantel and H. Weisz, Anal. Chim. Acta, 74 (1975) 275.
9 C. F. Jacobsen, J. Leonis, K. Linderstrom-Lang and M. Ottesen in D. Glick (Ed.), Methods of Biochemical Analysis, Vol. IV, Interscience Publ., New York, 1957, p. 171.
10 G. G. Guilbault, Enzymatic Methods of Analysis, Pergamon Press, Oxford, 1970.
11 H. J. Schneider, H. Schneider-Bernlöhr and M. Hanack, Liebigs Ann. Chem., 722 (1969) 234.
12 R. E. Karcher and H. L. Pardue, Clin. Chem., 17 (1971) 214.
13 K. Tsuji, Microchem. J., 18 (1973) 163.
14 F. Malis and P. Fric, Arzneimittel-Forsch., 24 (1974) 499.
15 A. le Berre and A. Delacroix, Bull. Soc. Chim. Fr., 11 (1974) 2639.
16 S. Dupre, A. Antonucci, P. Piergrossi and M. Aureli, Ital. J. Biochem., 25 (1976) 229.
17 Gmelins Handbuch der Anorganischen Chemie, 8.Aufl., Bd.9, Tl.B 2, S.827 ff, Verlag Chemie, Weinheim, 1960.
18 D. A. House, Chem. Rev., 62 (1962) 185.
19 J. D. Miller, J. Chem. Soc. A, (1968) 1778.
20 M. G. R. Reddy, B. Sethuram and T. N. Rao, Z. Phys. Chem. Leipzig, 256 (1975) 875.
21 Y. K. Gupta and S. Ghosh, J. Inorg. Nucl. Chem., 11 (1959) 62.
22 R. Swaroop and Y. K. Gupta, J. Inorg. Nucl. Chem., 36 (1974) 169.
23 J. Bognar, L. Sipos and P. M. Szabo, Musz. Egy. Kozl. 2. Sorozat 22 (1975) 53; Chem. Abstr., 85 (1976) 86667.
24 K. B. Yatsimirskii, Kinetic Methods of Analysis, Pergamon Press, Oxford, 1966, pp. 83, 86.
25 J. Schlipf, Diploma Thesis, Freiburg i.Br., 1978.
26 K. B. Yatsimirskii and V. E. Kalinina, Zh. Neorg. Khim., 9 (1964) 1117.
27 A. K. Babko and L. V. Markova, Ukr. Khim. Zh., 32 (1966) 1106.

Analytica Chimica Acta, 104 (1979) 215—223

ANALYTICAL APPLICATION OF TRIETHYLENETETRAAMINEHEXA-ACETIC ACID

Part 2. Polarographic Investigation of the Reactions of TTHA at the Dropping Mercury Electrode+

STANISLAW RUBEL and MAREK WOJCIECHOWSKI*

Institute of Fundamental Problems in Chemistry, University of Warsaw, 02-093 Warszawa (Poland)

(Received 14th April 1978)

SUMMARY

TTHA gives an anodic d.c. wave and s.w. peak corresponding to oxidation of mercury at the d.m.e. surface with formation of a Hg(II)—TTHA complex. Similar processes are known for other ligands, e.g. EDTA and DCTA, but the greater stability of the Hg(II)—TTHA complex gives a significant improvement in the shapes of the anodic wave and s.w. peak. An increase in pH shifts the $E_{1/2}$ and E_p values towards more negative values because the conditional stability constant of the Hg(II)—TTHA complex is increased. Although the half-wave potentials of the reduction wave of Hg(II)—TTHA and of the anodic wave of TTHA, are the same, other criteria for the reversibility of polarographic reactions suggest that the anodic TTHA process at the d.m.e. is not completely reversible. The temperature coefficient of the wave and s.w. peak as well as the dependence of the wave height on the square root of the mercury head prove that the process is diffusion-controlled. Supporting electrolytes are given for which the d.c. wave and the s.w. peak of TTHA are well-shaped, with linear dependence between the wave or peak height and the concentration of TTHA in the ranges 5×10^{-5}—5×10^{-4} M (d.c.) and 1×10^{-5}—1×10^{-4} M (s.w.).

Dissolution of mercury limits the range of polarographically accessible anodic potentials with the dropping mercury electrode (d.m.e.). The potential at which dissolution starts depends on the kind and concentration of anion (A) present in the supporting electrolyte. The stronger the complex formed between the anion and Hg(II) or Hg(I) the more negative will be the depolarization potential. When the solution contains not only the complexing component A of the supporting electrolyte but also a more strongly complexing ligand X (10^{-3}—10^{-4} M) the d.c. polarographic curve shows an anodic wave which corresponds to the reaction: $Hg + nX^{m-} \rightleftharpoons HgX_n^{(2-mn)} + 2e^-$.

Matyska and Kösler [1] were the first to demonstrate such a process at the d.m.e. when EDTA is present. The anodic wave of EDTA is a two-electron, diffusion-controlled, nearly reversible process in which oxidation of mercury proceeds with formation of the Hg(II)—EDTA complex [2—7]. The $E_{1/2}$

+Part 1: Anal. Chim. Acta, 99 (1978) 105.

value of this wave depends on the pH of the solution and not on the EDTA concentration, whereas the diffusion current is proportional to EDTA concentration.

Anodic processes of DCTA [3], EGTA [8] and DTPA [9, 10] at the d.m.e. have also been investigated. Nakashima [6] stated that EDTA, HEDTA, DCTA and DTPA form well-defined square-wave peaks, the E_p values of which depend on the conditional stability constants of the respective mercury(II) complexes.

During titrations of metal ions which form sufficiently stable complexes with EDTA, the anodic current of EDTA at the d.m.e. appears after complete complexation of the metal ions present; this current is proportional to the concentration of free ligand in the solution. Anodic waves of EDTA and other complexing agents have been applied in end-point detection for amperometric titration of metals [4, 5, 10—12] as well as in the polarographic determination of calcium and magnesium with the use of EDTA and EGTA [13]. Alternating-current polarography has been used in the amperometric titration of metals with DTPA [14].

Triethylenetetraaminehexaacetic acid (TTHA), similarly to other ligands, reacts with Hg(II) ions formed by oxidation of mercury from the d.m.e. [15]. The potential at which this reaction occurs depends on the stability of the Hg(II)—TTHA complex in the solution investigated. If this complex is more stable than the mercury complexes of other components in the supporting electrolyte, the anodic d.c. wave or the s.w. peak will be connected with this complex formation. The more stable the Hg—TTHA complex compared to any other mercury complexes formed the more distinct will be the anodic TTHA wave or peak (Fig. 1, curve 4). The electrode process involves

$$Hg + H_nL^{n-6} \rightleftharpoons HgL^{4-} + nH^+ + 2e^- \qquad (1)$$

where H_nL^{n-6} is the protonated form of TTHA, the actual composition of which depends on pH. The concentration of unprotonated ligand can be calculated from $[L^{6-}] = C_L/\alpha_{L(H)}$, where C_L is the total concentration of the ligand and $\alpha_{L(H)}$ is the side-reaction coefficient for ligand protonation.

When the reaction is reversible, the diffusion coefficients of the HgL^{4-} complex and all forms of the ligand have similar values and the activity coefficients can be neglected; then, the $E_{1/2}$ value of the anodic wave of TTHA can be expressed by

$$E_{1/2} = E^0_{Hg} - (RT/2F) \ln K'_{HgL} \qquad (2)$$

where E^0_{Hg} is the standard potential of the Hg^{2+}/Hg system, and K'_{HgL} is the conditional stability constant of the complex, $K'_{HgL} = K_{HgL}/\alpha_{L(H)}$, K_{HgL} being the stability constant of the complex. This expression is valid when side-reactions of Hg(II) ions and the HgL^{4-} complex do not play a significant role.

TTHA is a more selective complexing reagent for metal ions in acidic solutions [17]. Accordingly, attempts were made to find a supporting

electrolyte of low pH with good buffering properties in which a well-defined polarographic wave of TTHA would be formed.

EXPERIMENTAL

Apparatus

The apparatus was the same as that described previously [16]. The solutions tested were placed in a 10-cm^3 thermostated (20.0 ± 0.1°C) polarographic cell and deaerated with argon for 15 min before measurement.

Reagents

The following solutions were prepared: 1.0×10^{-2} M solutions of triethylenetetraaminehexaacetic acid (TTHA; Fluka) [16] h, diaminocyclohexanetetraacetic acid (DCTA; Merck) and ethylenediaminetetraacetic acid (EDTA); 0.1 M solutions of perchloric acid (Riedel), sodium perchlorate (Merck) and sodium hydroxide. The buffers used were sodium citrate—perchloric acid, sodium formate—formic acid, sodium acetate—acetic acid, and ammonia—ammonium nitrate solutions. Methylcellulose (tylose; BDH) was used as a 0.5% (w/v) solution.

All reagents were of analytical grade (POCh, Poland except where indicated). Water was thrice-distilled from quartz apparatus.

RESULTS

Effect of pH on d.c. wave and s.w. peak of TTHA

The effect of pH was tested by recording polarographic curves for a series of solutions containing 5×10^{-4} M TTHA and 0.1 M $NaClO_4$; the pH was adjusted by adding 0.01 M $HClO_4$ or 0.01 M NaOH. The $E_{1/2}$ values of d.c. waves and E_p values of s.w. peaks evaluated are given in Table 1.

Above pH 6, the d.c. curve shows two overlapping waves; at increasing pH values, these waves move apart and are well separated at pH 8.0—9.5. The height of the first wave (more positive) decreases with increasing pH while the second one increases. Above pH 9.7 only the second wave exists. The total limiting current of the TTHA d.c. wave (or waves) is independent of pH.

At about pH 5, the s.w. curve shows a badly shaped TTHA peak, the width of which increases with increasing pH. In the pH range 6.5—9.5, two peaks occur; again the first decreases as the second increases with increasing pH, and above pH 9.5 only the second peak is present. The height of this peak does not change with further increase of pH.

Calculations done on the basis of the stability constants of HgH_4L, HgH_3L^-, HgH_2L^{2-}, $HgHL^{3-}$ and HgL^{4-} complexes showed that the first wave or peak corresponds to formation of the $HgHL^{3-}$ complex, whereas the second wave or peak corresponds to formation of the HgL^{4-} complex. In the pH range 6.5—9.5, $HgHL^{3-}$ and HgL^{4-} complexes are formed simultaneously.

The analytical applications of the anodic processes of TTHA depend on

TABLE 1

The dependence of $E_{1/2}$ and E_p values of TTHA (5×10^{-4} M) on the pH of 0.1 M $NaClO_4$ solution at 20°C

pH	$E_{1/2}$ (V)		E_p (V)	
	First wave	Second wave	First peak	Second peak
0.1 M $HClO_4$	—[a]	—	—	—
3.90	+0.145	—	*[a]	—
4.05	+0.14	—	*	—
4.96	+0.105	—	−0.07	—
5.04	+0.10	—	−0.07	—
5.70	+0.075	—	−0.08	—
6.11	+0.055	*	−0.105	—
6.80	+0.04	*	−0.065	−0.23
7.24	+0.035	*	−0.06	−0.23
8.15	+0.03	−0.13	−0.05	−0.25
8.59	+0.02	−0.16	−0.05	−0.255
9.50	*	−0.16	*	−0.28
10.34	—	−0.185	—	−0.30
10.83	—	−0.185	—	−0.30
0.1 M NaOH	—	−0.18	—	−0.29

[a](—) No wave or peak was observed. (*) The wave (or peak) was badly shaped and its $E_{1/2}$ or E_p value was not measurable.

using a suitable buffer solution as the supporting electrolyte. The behaviour of TTHA in several buffering supporting electrolytes of wide pH range was therefore studied. In buffer solutions of pH less than 4.5, neither d.c. wave nor s.w. peak was observed; among the acidic electrolytes, the sharpest wave or peak of TTHA was formed in acetate buffer pH 5.2. When alkaline buffers were used, the $E_{1/2}$ or E_p value became more negative and the height of the d.c. wave or s.w. peak of TTHA decreased (Fig. 1). The sharpest d.c. and s.w. signals for TTHA were obtained in ammoniacal buffer pH 9.3—10.1 and in 0.1 M NaOH.

Effect of the concentration of supporting electrolytes

Increasing the acetate buffer concentration (pH 5.2) improves the shape of the TTHA wave by eliminating the break at the foot of the wave (Fig. 1), and also makes the s.w. peak more symmetrical. At the same time, the $E_{1/2}$ value is shifted to more negative potentials whereas the E_p value changes to more positive potentials (Table 2). Similar behaviour was observed in chloroacetate buffers. The decreasing wave or peak height with increase in the acetate buffer concentration is connected with the increase of solution viscosity. At pH 5.2, the side-reaction coefficient of Hg(II) ions with acetate does not effect the conditional stability constant of the HgL^{4-} complex as much as the side-reaction coefficient with ammonia affects the constant at pH 10.1.

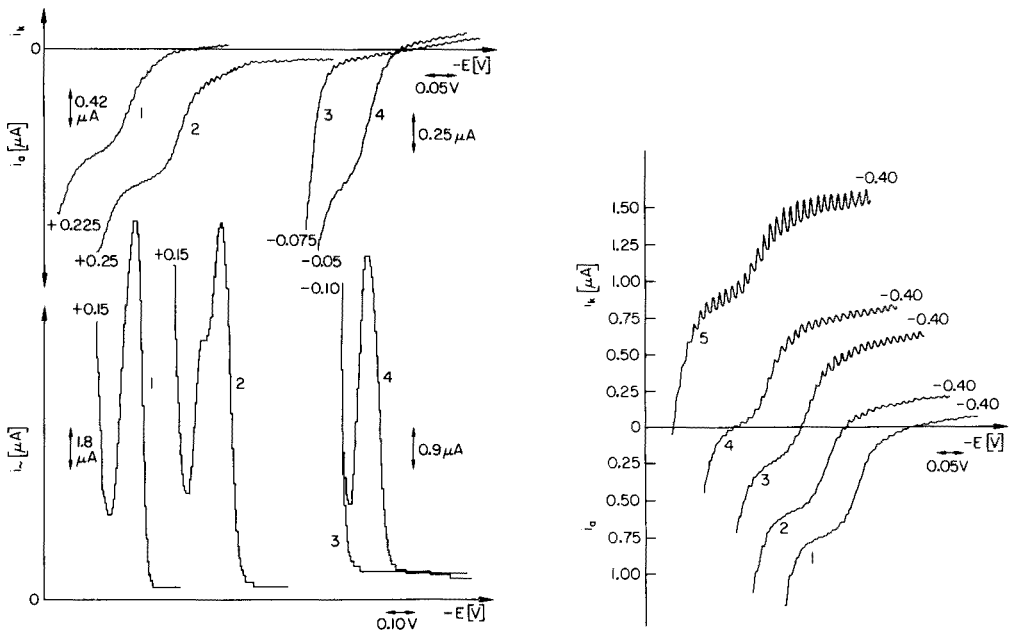

Fig. 1. The d.c. waves and s.w. peaks of TTHA recorded from different solutions: 1.0 M acetate buffer pH 5.2 + 1.5 × 10^{-4} M TTHA (curves 1); 0.2 M acetate buffer pH 5.2 + 1.5 × 10^{-4} M TTHA (curves 2); 0.25 M ammonia buffer pH 10.0 (curves 3); 0.25 M ammonia buffer pH 10.0 + 1.5 × 10^{-4} M TTHA (curves 4).

Fig. 2. The influence of Hg(II) ions on the anodic wave of 1.0 × 10^{-4} M TTHA in 0.1 M ammonia buffer pH 10.1. Concentration of $Hg(NO_3)_2$: 0.0 (curve 1); 0.2 × 10^{-4} M (curve 2); 0.5 × 10^{-4} M (curve 3); 1.0 × 10^{-4} M (curve 4); 2.0 × 10^{-4} M (curve 5).

TABLE 2

The influence of the supporting electrolyte on the height and the half-wave potential or peak potential of 1.0 × 10^{-4} M TTHA

Supporting electrolyte (M)		D.c.		S.w.	
		$E_{1/2}$ (V)	h(mm)	E_p (V)	h_p(mm)
Acetate buffer	0.2	+0.095	29.5	−0.04	124
	1.0	+0.085	25	0.00	114.5
	1.5	+0.085	25	+0.015	85
	2.0	+0.08	16.5	+0.015	85
Ammonia buffer	0.10	−0.19	48.5[a]	−0.27	206[a]
	0.25	−0.19	44	−0.24	135
	0.50	—[b]	—[b]	−0.22	51

[a]The d.c. and s.w. curves in ammonia buffer were recorded at higher sensitivity than in acetate buffer.
[b]Badly shaped wave with $E_{1/2}$ and h not measurable.

Increasing the ammonia concentration shifts the potential of anodic decomposition (oxidation of mercury with the formation of ammonia complex) of the supporting electrolyte towards negative potentials. Simultaneously, the conditional stability constant of HgL^{4-} decreases, so that the $E_{1/2}$ and E_p values for TTHA shift towards positive potentials. When the ammoniacal buffer reaches 0.75 M, neither a d.c. wave nor a s.w. peak can be observed.

These studies indicate that the best electrolytes are 1.0 M acetate buffer pH 5.2 and 0.1 M ammoniacal buffer pH 10.1. With these electrolytes, the curve shapes do not change for at least 60 min after solution preparation.

Comparison of anodic and cathodic processes of HgL^{4-} complex

The coincidence of the $E_{1/2}$ values of the reduction wave of the HgL^{4-} complex and of the anodic wave indicates that the latter corresponds to reaction (1). When the polarographic d.c. and s.w. curves were recorded for solutions containing constant concentrations of TTHA and increasing concentrations of Hg(II) ions, $E_{1/2}$ (an) and $E_{1/2}$ (cat) were found to be equal (Fig. 2). However, when the solutions contained constant concentrations of Hg(II) ions and increasing concentrations of TTHA (Fig. 3), there was a slight shift in the formation and reduction waves of the HgL^{4-} complex: e.g., in ammoniacal buffer $E_{1/2}$ (an) = —0.18 V; $E_{1/2}$ (cat) = —0.19 V. Both experiments were carried out in 1.0 M acetate buffer pH 5.2 and 0.1 M ammoniacal buffer pH 10.1. The presence of Hg(II) ions did not influence the curve shape or the E_p or i_p values for TTHA because currents of the same magnitude and character differing only in sign were recorded as identical peaks. These results confirmed that the Hg(II) complex with TTHA corresponds to 1:1 composition, unless an excess of Hg(II) is present so that the Hg_2L^{2-} complex may be formed.

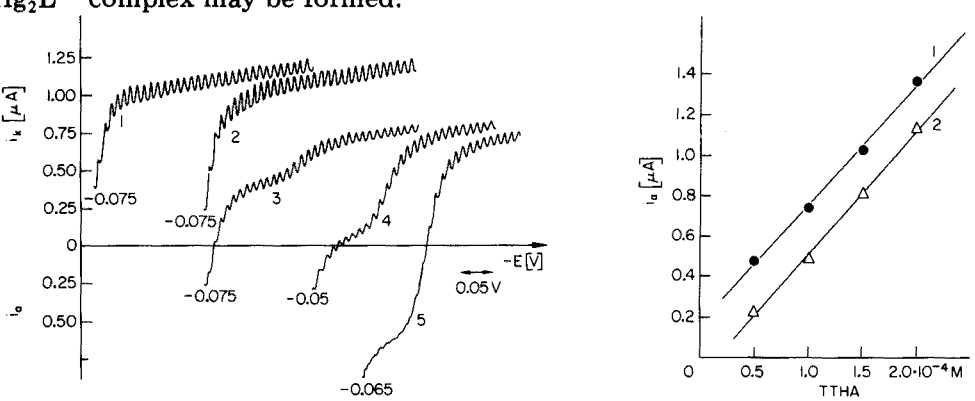

Fig. 3. The influence of TTHA on the reduction curve of Hg(II) (1.0×10^{-4} M $Hg(NO_3)_2$) in 0.1 M ammonia buffer pH 10.1. Concentration of TTHA: 0.0 (curve 1); 0.1×10^{-4} M (curve 2); 0.5×10^{-4} M (curve 3); 1.0×10^{-4} M (curve 4); 2.0×10^{-4} M (curve 5).

Fig. 4. The dependence of the limiting current of the anodic wave of TTHA on concentration in 1.0 M acetate buffer pH 5.2 (curve 1) and in 0.1 M ammonia buffer pH 10.1 (curve 2).

The equality of the $E_{1/2}$ values for the anodic TTHA wave and the cathodic HgL^{4-} wave indicates that the electrode process is reversible. Nevertheless, other experiments and criteria of reversibility led to opposite conclusions. The slope of the logarithmic curve of the anodic wave (Table 3) differed from the expected slope for a reversible 2-e electrode reaction. The difference $E_{1/2} - E_{3/4}$ for the TTHA wave was 40.5 mV in 0.1 M acetate buffer at pH 5.2 whereas, according to Tomeš criterion, it should be 27.5 mV at 20°C. The $E_{1/2}$ and E_p values of the TTHA wave decreased with the height of the mercury level.

In 0.1 M solutions of supporting electrolytes, two overlapping peaks were recorded for 1.0×10^{-3} M TTHA, and the E_p value differed significantly from $E_{1/2}$ for the anodic wave (Table 3). The peak width at half height (S) of the single peak recorded for 1.0 M acetate buffer solution at pH 5.2 was 65 mV, whereas for a reversible 2-e reaction S=44.5 mV at 20°C.

Cyclic voltammetric curves at the h.d.m.e. at low sweep rates showed one anodic and one cathodic peak. In 1.0 M acetate buffer pH 5.2, $E_{pa} = +72$ mV and $E_{pc} = +113$ mV; in 0.1 M ammonia buffer pH 10.1, $E_{pa} = -182$ mV and $E_{pc} = -220$ mV. The differences $E_{pa} - E_{pc}$ in these solutions were 41 mV and 38 mV, respectively; for a reversible 2-e process, the difference should be 29 mV. Those results show that the anodic reaction of TTHA at the d.m.e. is not fully reversible.

In 0.1 M acetate buffer at pH 5.2, the mean values of the temperature coefficient in the range 20—30°C were 1.6% per degree for the d.c. wave of TTHA and 1.7% per degree for the s.w. peak. The i_d of the TTHA wave was proportional to the square root of the mercury level. These results indicate that the anodic process of TTHA at the d.m.e. is diffusion-controlled.

The dependence of the wave and peak height on the TTHA concentration

In 0.2 M acetate buffer pH 5.2, a s.w. peak can be observed at —0.03 V even for 5×10^{-5} M TTHA solutions. Increase in the ligand concentration shifts the E_p value of this peak to slightly more negative potentials and the peak height increases. Simultaneously, a break appears on the rising part of

TABLE 3

Half-wave potentials of d.c. waves and peak potentials of s.w. peaks of 1.0×10^{-3} M TTHA and slopes of the logarithmic curve at 20.0 ± 0.1°C

Supporting electrolyte	pH	Slope of the log curve $\Delta E/\Delta \log$	$E_{1/2}$ (V)	E_p (V)
0.1 M Acetate buffer	5.2	46	+0.069	+0.02; —0.07
1.0 M Acetate buffer	5.2	47	+0.080	0.00
0.1 M Ammonia buffer	9.3	47	—0.161	—0.295
0.1 M NaOH		40	—0.181	—0.19; —0.29

the peak, and a new peak appears at TTHA concentrations above 2×10^{-4} M; when the concentration of TTHA is 2×10^{-4} M, the two peak potentials are +0.035 V and −0.045 V. In this supporting electrolyte, the height of the more negative peak is proportional to the TTHA concentration up to 1×10^{-4} M.

In 1.0 M acetate buffer pH 5.2 or in 0.1 M ammoniacal buffer pH 10.0, there is only one TTHA peak, the height of which is also proportional to the TTHA concentration up to 1×10^{-4} M. At higher concentrations, the increase of the peak height with concentration is slower. In contrast, the limiting current of the anodic wave of TTHA shows a linear dependence on concentration to well above 1×10^{-4} M in both supporting electrolytes (Fig. 4).

The influence of surface-active agent (tylose)

In 0.2 M acetate buffer pH 5.2, the TTHA wave ($E_{1/2}$ = +0.095 V) has a disadvantageous break at the foot. The presence of 0.015% tylose completely eliminates this break and improves the wave shape. The height and the half-wave potential of the anodic wave do not change.

In 1.0 M acetate buffer pH 5.2, the presence of surfactant affects the shape of the s.w. peak and decreases its height, although it has no effect on the shape, height and $E_{1/2}$ of the TTHA wave.

Effect of oxygen

Of the supporting electrolytes investigated, only in 0.1 M acetate buffer pH 5.2 is the anodic wave of TTHA distinctly separated from the first oxygen wave so that the limiting current can be measured in the presence of oxygen. However, especially at low concentrations of the ligand, removal of oxygen improves the shape of the anodic wave. In alkaline electrolyte solutions, the TTHA wave is visible only after deaeration. The presence of oxygen has no significant effect on the peak potential of TTHA, but the peak is slightly smaller.

CONCLUSIONS

The best shaped d.c. waves and s.w. peaks of TTHA are obtained in 1.0 M acetate buffer pH 5.2, 0.1 M ammoniacal buffer pH 9.3—10.1 or in 0.1 M NaOH. In these solutions, the limiting current of the d.c. wave is linearly dependent on the concentration in the range 5×10^{-5}—5×10^{-4} M TTHA, whereas the current of the s.w. peak shows a linear dependence in the concentration range 1×10^{-5}—1×10^{-4} M TTHA.

The heights of the TTHA wave and s.w. peak depend on the presence of metal ions forming stable complexes with TTHA. The addition of metal ions to the TTHA solutions reduces the TTHA current in proportion to the concentration of the added ions. During addition of TTHA solution to solutions containing suitable metal ions, the anodic wave and the s.w. peak of TTHA appear only when an excess of ligand is present. These results suggest the utilization of the anodic TTHA process in polarographic determinations of metals or in their amperometric titration.

REFERENCES

1 B. Matyska and I. Kösler, Chem. Listy, 45 (1951) 254. Collect. Czech. Chem. Commun., 16 (1951) 221.
2 J. Goffard, G. Michel and G. Duyckaerts, Anal. Chim. Acta, 9 (1953) 184.
3 B. Matyska, J. Doležal and D. Roubalova, Chem. Listy, 49 (1955) 1012; Collect. Czech. Chem. Commun., 21 (1956) 107.
4 C. N. Reilley, W. G. Scribner and C. Temple, Anal. Chem., 28 (1956) 450.
5 R. T. Campbell and C. N. Reilley, Talanta, 9 (1962) 153.
6 F. Nakashima, Rev. Polarogr. (Kyoto), 14 (1966) 74.
7 K. Niki, K. Suzuki, G. P. Sato and N. Mori, J. Electroanal. Chem., 49 (1974) 27.
8 B. Fleet, S. Win and T. S. West, J. Electroanal. Chem., 21 (1969) 541.
9 M. Kodama and A. Kimura, Bull. Chem. Soc. Jpn., 40 (1967) 1639.
10 G. Michel, Anal. Chim. Acta, 10 (1954) 87.
11 Y. K. Oong and M. C. Lee, Acta Pharm. Sinica, 7 (1959) 99, Anal. Abstr. 6 (1959) abstract 4673.
12 D. Roubalova and J. Doležal, Chem.-Anal., 49 (1960) 76.
13 B. Fleet, S. Win and T. S. West, Analyst, 94 (1969) 269.
14 M. Kodama and M. Murata, Bull. Chem. Soc. Jpn., 41 (1968) 2405.
15 M. Wojciechowski, Doctoral Thesis, Warsaw University, Warsaw, 1977.
16 S. Rubel and M. Wojciechowski, Anal. Chim. Acta, 99 (1978) 105.
17 L. Harju and A. Ringbom, Anal. Chim. Acta, 49 (1970) 221.

Analytica Chimica Acta, 104 (1979) 225–231

THE DETERMINATION OF EIGHT ELEMENTS IN HUMAN LIVER TISSUE BY FLAME ATOMIC ABSORPTION SPECTROMETRY IN SULPHURIC ACID SOLUTION

J. LOCKE

Home Office Central Research Establishment, Aldermaston, Reading, Berkshire RG7 4PN (Gt. Britain)

(Received 2nd August 1978)

SUMMARY

A flame atomic-absorption spectrometric method is detailed for the determination of Ca, Mg, Zn, Fe, Cu, Mn, Rb and Cd in human liver tissue. Metal losses for three alternative sample destruction procedures are discussed; in the recommended procedure, low-temperature ashing in an oxygen plasma is followed by dissolution in sulphuric acid and aspiration into an air—acetylene flame. The necessity of close matching of the K, Na, phosphate and sulphuric acid contents for samples and standards is demonstrated for several elements. The accuracy of the method was established by using NBS SRM Bovine Liver and carefully prepared synthetic standards. The relative standard deviation is typically 5%, although variations in the blood content between portions of liver tissue lead to poorer precision for iron.

The multi-element analysis of tissue is required in forensic toxicology for the investigation of suspicious death. Human livers have been analysed in this laboratory by spark-source mass spectrometry (s.s.m.s.), after sample ashing at low temperatures [1]. Good recoveries of many elements have been reported after low-temperature ashing [2, 3] but losses of selenium and arsenic were observed from doped liver tissue [1]. A possible loss of other elements on ashing required assessment and was investigated by comparing different sample destruction procedures: low-temperature ashing (oxygen plasma), high-temperature ashing (muffle furnace) and wet oxidation (nitric—sulphuric acid mixture). To permit ready comparison by flame atomic absorption spectrometry (a.a.s.), sulphuric acid was used for dissolving ashes or for wet oxidation.

In a.a.s., nitric or hydrochloric acid is often preferred for sample dissolution [4, 5], but high levels of sulphate are inevitably present in the final solutions from protein-rich tissue. A controlled excess of sulphate over that inherent in the sample should have a "levelling" effect and improve control over possible interferences.

Inter-elemental effects in the flame a.a.s. analysis of tissue and body fluids have been commonly overcome by the addition of lanthanum, e.g. for calcium in human serum [6] and for the physiologically important metals in human

tissue [4] and bovine liver [7]. Although sodium ions have been added to standards [8], the approach of matching phosphate levels in tissue solutions has not been described for flame a.a.s. despite the well established interaction of calcium and phosphate in air—acetylene flames. This paper therefore establishes the reliability of using phosphate-matched standards for the determination of eight elements in sulphuric acid solution with an air—acetylene flame. Elemental recoveries from the various sample destruction procedures are then compared.

EXPERIMENTAL

Instrumentation and technique

A Perkin-Elmer 303 atomic absorption spectrometer was fitted with a Boling three-slot 11-cm burner. Fuel-lean air—acetylene mixtures were used throughout. Instrument settings (height of beam centre above burner in mm/wavelength in nm) were: 12/285.2 for Mg, 8/422.7 for Ca, 6/279.5 for Mn, 6/248.3 for Fe, 6/324.7 for Cu, 6/213.8 for Zn, 4/780 for Rb and 6/228.8 for Cd.

Reagents and solutions

Where available, Hopkin and Williams standard solutions (1000 mg l^{-1}) were used. A stock solution of rubidium (1000 mg l^{-1}) was made by dissolving 0.3538 g of dried RbCl in 250 ml of water. A stock buffer solution was made by dissolving 20 g of KH_2PO_4 and 5 g of Na_2HPO_4 (A.R. grade, anhydrous salts) in 375 ml of (1 + 2) H_2SO_4—water followed by dilution to 500 ml. The mixture then contained 5% (w/v) phosphate and 25% (v/v) H_2SO_4.

A mixed stock solution containing 40 mg l^{-1} for Fe, Ca and Mg and 10 mg l^{-1} for Zn was made up in 0.05% (v/v) H_2SO_4, and 0, 5, 10, 15, 20, 25, 30 and 40-ml aliquots were pipetted into 100-ml flasks containing 1 ml of stock buffer solution. Dilution to volume with water gave solutions containing 0.05% (w/v) phosphate and 0.25% (v/v) H_2SO_4 with Fe, Ca and Mg in the range 0—16 mg l^{-1} and Zn in the range 0—4 mg l^{-1}. The mixed metal stock solution and the standards were stable for at least one month.

A mixed stock solution containing 10 mg Cd l^{-1}, 10 mg Rb l^{-1}, 20 mg Cu l^{-1} and 5 mg Mn l^{-1} was made up in 0.5% (v/v) H_2SO_4, and 0, 5, 10, 15, 20, 25, 30, 40, 50 and 60-ml aliquots were pipetted into 100-ml flasks containing 20 ml of stock buffer solution. Dilution to volume gave 1% (w/v) phosphate—5% (v/v) sulphuric acid solutions containing 0—6 mg Cd l^{-1}, 0—6 mg Rb l^{-1}, 0—12 mg Cu l^{-1} and 0—3 mg Mn l^{-1}. The mixed metal stock solution and the standards were stable for at least one month.

Sample preparation

Drained fresh human livers (5—20 g) were cut into small portions, care being taken to exclude major blood vessels and connective tissue. Homogenization, where required, was done with an MSE Atomic tissue macerator. Unless

otherwise stated, the tissue was dried at 120°C for 6 h in glass dishes and then ashed in a Tracerlab LTA 504 oxygen plasma asher (oxygen flow 50 ml min^{-1}, chamber pressure 0.5 torr). Approximately 60 h were required to convert 14 g of wet tissue to an ash but 4 samples could be handled simultaneously. Vitreosil crucibles were used for ashing tissue in a muffle furnace (overnight at 500°C plus 2 h at 550°C). The sample ashes (0.2 g) from either ashing method were dissolved in concentrated sulphuric acid (1 ml; analytical grade) by heating for 1 h on a steam bath. A few drops of 30% (w/v) hydrogen peroxide were added, the heating was continued for 1 h, and the mixture was diluted to 20 ml with water. Aliquots (2.5 ml) of these 1% ash solutions were further diluted to 50 ml, giving 0.05% (w/v) ash solutions.

For wet oxidations, 14 g of tissue were treated with 4 ml of concentrated sulphuric acid in a 100-ml round-bottomed flask fitted with a reflux condenser, warmed at ca. 80°C for 1 h, and then cooled to room temperature. Addition of 5 ml of concentrated nitric acid and standing for 15 min resulted in a vigorous reaction. When this reaction had subsided, the mixture was heated (electric mantle) under reflux, and 15 ml of concentrated nitric acid was added in small portions over 3 h. The mixture was then evaporated over a bunsen until charring began and, after cooling, 5 ml of hydrogen peroxide was added to clarify the solution. The whole was left overnight, the waxy residue (derived from fat) was filtered off, the filtrate and filter washings were made up to 20 ml with water, and a 2.5-ml aliquot was diluted to 50 ml. Standards for comparison with solutions derived from wet oxidations were made up in 20% or 1% (v/v) sulphuric acid to match the original or diluted solutions, respectively.

RESULTS AND DISCUSSION

The elements at sufficiently high levels in the ash for flame a.a.s. measurements were Mg, Ca, Mn, Fe, Cu, Zn, Rb and Cd. Sodium and potassium were considered to be at levels too high for accurate analysis. Other elements of interest, which were found in all livers examined by s.s.m.s. in this laboratory were Mo, Sn and Pb, but these were at insufficient concentrations for flame a.a.s. measurement.

Chemical composition of liver ash

Human liver ashed at low temperatures yielded a light brown, slightly hygroscopic powder; the average weight of ash from 15 livers was 1.48 ± 0.093%. Data from the literature together with preliminary s.s.m.s. and a.a.s. studies enabled the average composition of this ash to be estimated [1]. The most abundant elements, Na, K and P, were presumably present as alkali metal phosphates. The bulk of the chloride content (99%) was lost on ashing but some two thirds of the sulphur was retained, almost certainly as sulphate. Minor levels of Ca, Mg, Fe and Zn were present; the remainder of the ash consisted of trace elements, the elements detectable by s.s.m.s. being V, Cr, Mn, Co, Cu, Rb, Mo, Cd, Sn and Pb.

Calculation showed that a simple 4:1 mixture of anhydrous KH_2PO_4 and Na_2HPO_4 gave a good approximation to the major components of liver ash. The anionic species in the analytical solution were restricted to phosphate and sulphate by dissolving the ash in sulphuric acid. A stock solution of Na and K phosphates in sulphuric acid was used as a spectroscopic buffer, the stock and sample solutions being matched in total solid and acid content.

The trace elements (Mn, Rb, Cu and Cd) were at suitable levels for determination in a 1% (w/v) solution of the ash whereas for the minor elements (Ca, Mg, Fe and Zn) a 0.05% (w/v) ash solution was required.

Interference effects

Rather than carry out an extensive study on the effect of changes in fuel—air ratio and burner height, it was more appropriate to test the validity of the proposed spectroscopic buffer under standard operating conditions. Interferences , recoveries, accuracy and self-consistency were examined.

The effect of K and Na phosphates on the minor elements is shown in Table 1; Zn and Fe were unaffected by other components in the solution, whereas Ca and Mg were sensitive to the presence of phosphate. Doubling of the phosphate concentration in the buffer solution produced almost no change, which indicates a levelling effect of the phosphate. Calcium was the only metal substantially affected by the presence of the other minor elements. Thus one would expect changes in the ratios of the minor elements in actual samples to produce some interferences on calcium but not on Mg, Zn and Fe.

A mixed metal solution containing a Cu:Cd:Rb:Mn ratio of 4:2:2:1 suitably represented the relative metal concentrations in ash solutions from human liver. Phosphate added at the expected natural level produced a threefold increase in absorption for rubidium, indicating that matrix matching was essential. Small effects were seen with Mn and Cu (5% depression) whereas cadmium was unaffected. The minor elements gave no interference on the trace elements and were conveniently omitted from the standard solutions.

TABLE 1

Percentage interference on analytical signal from matrix constituents with 0.25% (v/v) H_2SO_4 present in all cases

Element	Single minor element solution		Four minor elements in mixed solution		
	Phosphate absent	0.05% Phosphate	Phosphate absent	0.05% Phosphate[a]	0.1% Phosphate
Mg	−12	−6	6	0	−1
Ca	30	25	50	0	−2
Fe	0	0	−2	0	0
Zn	0	0	0	0	0

[a]Defined as 100% signal and represents the metal standard as described in the proposed method (Ca, Mg, Fe = 8 mg l^{-1} and Zn = 2 mg l^{-1}). Enhancement or depression (negative values) are expressed as percentages.

Consistency, precision and accuracy

Additions of all eight metals were made to twelve separate sample solutions in amounts similar to those already present naturally. Except for calcium, the recoveries ranged from 98 to 101% with a maximum deviation of ±4%. The consistently low recovery for calcium (92 ± 3%) indicated that an empirical correction could be applied.

A complete breakdown of the sources of random error was not possible, but the precision was estimated under differing conditions (Table 2). Variations in the tissue sample were eliminated by using a pooled sample of liver ash; the solid was thoroughly mixed so that a 200-mg sub-sample was representative. Replicate determinations gave good precision, the poorest relative standard deviation (r.s.d.) being obtained for cadmium (4.7%).

The homogeneity of liver tissue was then investigated by sampling a complete organ at five separate points (Table 2). Only iron showed a marked increase in r.s.d., and this is attributable to the variable blood content of the samples (blood is rich in Fe in comparison with liver tissue). This was confirmed by homogenizing the tissue (Table 2). The results overall demonstrate that, except for iron, a 14-g sub-sample is representative of the complete organ.

The only commercially available liver standard is the National Bureau of Standards SRM 1577 Bovine Liver which differs somewhat in elemental composition from the human liver. Cadmium for example was at too low a concentration for application of the proposed method. Satisfactory agreement was found with the NBS values for Mg, Ca, Fe and Zn (Table 3). The only other materials of well-defined, similar composition were two synthetic samples made in this laboratory for reference purposes [1]. In general, good agreement was found with the known composition of these materials ("matrix ash" and "synthetic liver ash", Table 3). These results clearly show that the matrix matching of standards to samples as proposed in this work is entirely adequate. The only exception is calcium where a simple correction was successfully applied.

TABLE 2

Precision of tissue or ash analysis
(All values are relative standard deviations (%) from 5 replicates distributed over 5 separate analytical runs)

Element	Pooled ash	Homogeneous tissue	Complete organ
Mg	1.4	3.8	8.2
Ca	2.1	13	4.5
Mn	3.9	4.5	3.6
Fe	3.8	4.9	20.3
Cu	1.2	5.5	3.3
Zn	2.1	8.6	4.0
Rb	3.1	6.3	2.8
Cd	4.7	12	5.2

TABLE 3

Analysis of standard substances[a]

Element	NBS Bovine Liver (Dried material)		"Matrix ash"		"Synthetic liver ash"	
	Certified	Found	Weighed	Found	Weighed	Found
Mg	605[b]	567	11,360	11,640	11,430	11,900
Ca	123[b]	101[c]	3,685	3,720[c]	3,710	3,640[c]
Mn	10.3 ± 1.0	—[d]	23	25	125	121
Fe	270 ± 20	247.3	14,450	14,185	14,540	14,760
Cu	193 ± 10	—[d]	0	0	506	508
Zn	130 ± 10	128.6	4,030	3,696	4,055	3,936
Rb	18.3 ± 1	—[d]	0	0	311	301
Cd	0.27 ± 0.04	—[e]	0	0	117	116

[a]Single determinations throughout; results given as $\mu g\ g^{-1}$. [b]Not certified. Values for information purposes. [c]After correction for 92% recovery. [d]Insufficient material available. [e]Not determinable.

Alternative methods of sample destruction

Although low-temperature ashing was preferred for sample destruction, the alternatives of ashing at high temperatures or of wet oxidation were considered. The results from these alternatives applied to a homogenized liver (Table 4) show good agreement between high- and low-temperature ashing. An exception is copper where loss to the crucible probably occurred at high temperatures. With the remaining elements, the two results can be combined and classed as dry oxidation. Comparison with wet oxidation shows no significant differences for Mg, Fe, Zn and Rb. Discrepancies with calcium can be attributed to the

TABLE 4

Effect of ashing under different conditions
(Results are given as $\mu g\ g^{-1}$ in liver)

Element	Wet oxidation		Low temperature (oxygen plasma)		Muffle furnace (550°C)	
	Mean	S.d.[a]	Mean	S.d.[a]	Mean	S.d.[a]
Mg	131	4.3	133	4.3	131	1.9
Ca	56.9	4.4	47.9	4.0	45.9	1.9
Mn	1.52	0.06	1.31	0.04	1.30	0.03
Fe	121	3.5	114	1.7	121	1.5
Cu	10.3	0.37	9.0	0.10	7.9	0.29
Zn	46.5	1.2	47.9	1.0	47.8	1.1
Rb	6.69	0.20	6.09	0.12	6.17	0.14
Cd	1.34	0.04	1.10	0.09	1.13	0.03

[a]Standard deviation estimated from 4 results.

difficulty of matrix matching of samples and standards. Lower analytical signals and higher backgrounds (non-atomic absorption) were generally obtained with solutions from wet oxidations. These arose from the increased level of sulphuric acid present, an unavoidable consequence of wet oxidation, compared with solutions derived from ashed tissue.

No significant differences were observed between the various approaches to sample destruction, and it was deduced that no losses of any of the eight elements occurred on low-temperature ashing, the preferred method of sample preparation.

The method should be applicable to other tissues of animal or human origin if similar matrix-matching procedures are devised.

REFERENCES

1 J. Locke, D. R. Boase and K. W. Smalldon, Anal. Chim. Acta, 104 (1979) 233.
2 C. E. Gleit and W. D. Holland, Anal. Chem., 34 (1962) 1454.
3 T. H. Lockwood and L. P. Limtiaco, Am. Ind. Hyg. Ass. J., 36 (1975) 57.
4 G. E. Marks, C. E. Moore, E. L. Kanabrocki, Y. T. Oester and E. Kaplan, Appl. Spectrosc., 26 (1971) 523.
5 J. M. McKenzie, New Zealand Medical Journal, June 12 (1974) 1016.
6 J. P. Cali, G. N. Bowers and D. S. Young, Clin. Chem., 19 (1973) 1208.
7 P. F. Theron, R. Rimmer, H. A. Nicholls and W. J. Ehret, J. S. Afr. Vet. Ass., 44 (1973) 271.
8 C. A. Johnson, Anal. Chim. Acta, 81 (1976) 69.

Analytica Chimica Acta, 104 (1979) 233—244

THE QUANTITATIVE MULTI-ELEMENT ANALYSIS OF HUMAN LIVER TISSUE BY SPARK-SOURCE MASS SPECTROMETRY

J. LOCKE*, D. R. BOASE and K. W. SMALLDON

Home Office Central Research Establishment, Aldermaston, Reading, Berkshire RG7 4PN (Gt. Britain)

(Received 2nd August 1978)

SUMMARY

A procedure is described for the determination of 13 elements in human liver tissue by spark-source mass spectrometry. Spectral interferences are identified and calibration obtained by using carefully formulated synthetic standards. The relative standard deviation of this method is typically ±9% for replicate analyses of a pooled liver ash obtained by oxygen plasma ashing, and ±16% for replicate tissue samples taken through the whole analytical procedure. The accuracy of the method was checked by conducting complementary determinations by flame atomic absorption spectrometry. Results are presented for the multi-element analysis of 15 livers by both methods and compared with literature values.

In forensic toxicology the analysis of tissues and fluids is undertaken to investigate the possibility of accidental, suicidal or homicidal poisoning in cases of suspicious death. In this laboratory, there is a requirement for a general, multi-element screening technique for the initial analysis in such cases. If metallic poisoning is suspected but the nature of the poison is unknown, then an organ which generally tends to concentrate toxic elements is selected for study. In this work, the liver was selected as it is routinely available to the toxicologist, is conveniently sampled and has been shown to accumulate toxic metals [1]. However, healthy human liver also contains traces of metal either essential to the chemistry of the body or acquired cumulatively, but without apparent physiological importance. The distribution of these metals in the human population must be determined if case-work material is to be correctly interpreted.

Multi-element instrumental methods of analysis that have been described for the determination of ten or more elements in human tissue include neutron activation analysis [2, 3], x-ray fluorescence spectrometry [4], optical emission spectrometry [5, 6], proton-induced x-ray emission spectrometry [7] and spark-source mass spectrometry (s.s.m.s.). This last technique, with photoplates for recording the spectra, was considered appropriate for the present study since it provides a comprehensive analysis of inorganic systems [8]. Analyses of a range of body fluids and tissues have been reported including lung [9], hair [10], blood [11—13], cerebrospinal fluid [13], brain [14] and finger

nails [15]. An extensive range of metals was determined in human liver and other tissue after low-temperature ashing [16]. Other workers restricted the analysis to heavy metals as the samples were not ashed before analysis [17]. Ashed livers from pigs fed with cadmium have also been examined [18].

S.s.m.s. is not only a highly sensitive technique but the response is roughly uniform for most elements. Thus semi-quantitative analysis for most elements is feasible without recourse to chemical standards. Quantitative analysis requires standard samples so that appropriate sensitivity factors can be determined and potential interferences studied. The National Bureau of Standards Bovine Liver (SRM 1577) is the only liver tissue standard available and this does not closely resemble human liver tissue in elemental composition. Therefore in the present study specific chemical standards, not previously described in the literature, had to be prepared and their reliability demonstrated.

Electrodes are readily prepared from solid substances and thus low-temperature ashing was selected to minimize the loss of volatile elements. Ashed tissue has been found to give complex spectra although careful photoplate interpretation has allowed successful multi-element analysis of human kidney as well as sheep bone and lung [19]. A corresponding study on ashed human liver, an important pre-requisite in the preparation and application of chemical standards, has not previously been published.

EXPERIMENTAL

Vessels and reagents

Glassware and agate pestles and mortars were cleaned by soaking in concentrated nitric acid followed by thorough washing with water (distilled and demineralized). The acids and metal salts used were of analytical-reagent grade (BDH Chemicals). Sodium gold chloride and rhodium trichloride were obtained from Johnson Matthey Chemicals. In general, the metal solutions used as standards (1000 mg l^{-1}) were reagents for atomic absorption spectrometry (Hopkin and Williams). Spectrographically pure graphite (Ringsdorffe-Werke, Bonn-Bad Godesberg) was used.

Sampling of liver and ashing

Portions (5 g) of liver tissue were dried and ashed in a radio-frequency, oxygen plasma asher as described earlier [20].

Atomic absorption spectrometry (a.a.s.)

The elements Mg, Ca, Fe, Mn, Cu, Zn, Rb and Cd were determined as described previously [20].

Doping of electrode graphite

Stock solutions of gold and rhodium (ca. 1000 mg l^{-1}) were prepared in (1 + 1) hydrochloric acid by dissolving the appropriate weight of sodium gold chloride or rhodium trichloride. The precise metal content was determined

gravimetrically and the solution density by weighing 5 ml in a volumetric flask. Portions of these solutions were weighed to provide 1250 μg of each element and added to 25 g of graphite; 20 ml of redistilled acetone were added and the whole mixed to a paste in a shallow dish. The mixture was dried for 1 h under an infrared lamp, with occasional stirring with a glass rod. The resultant powder was further dried at 120°C overnight, cooled and reweighed. The powder was homogenized by vigorous shaking in a sealed container; the product contained 50 $\mu g\ g^{-1}$ each of Rh and Au.

Preparation of electrodes

Electrode material was prepared by mixing together 20 mg of doped graphite and 10 mg of ashed tissue in an agate pestle and mortar. Electrodes were formed by compressing this mixture in drilled polythene slugs in a steel die with standard accessories (AEI Scientific Apparatus Ltd., Manchester). A 5/16-in twist drill, with a modified tip [21] was used to produce electrodes with steeply conical ends. The graphite—ash mixture was used to form the tips of the electrode pair, the remainder of the electrodes consisting of pure graphite.

Mass spectrometer

Details of the instrument and ancillary equipment used are given in Table 1.

Interpretation and measurement of photoplate

Plates were interpreted by expanding the microdensitometer trace 100-fold along the mass scale with a ratio arm. The distances between peaks were plotted graphically against exact values of m/z for readily identifiable species such as Fe^+ or $C_4H_9^+$. Weak lines of doubtful origin, e.g., Co^+, Cr^+, were then identified from their isotopic weights, estimated to 0.02 of a mass number, read from the graph.

For plate measurement, unsaturated lines from singly charged ions were examined. Line densities were calculated by subtracting the background density in the inter-peak region from the maximum peak height. Data reduction followed a standard procedure [23] in which comparison was made between line densities of the isotope of unknown concentration and a suitable isotope of an internal standard element. Plate reading and data reduction were done automatically by using a computer program written in this laboratory [24]. Three elements (Zn, Rh and Au) were selected for calibration, with zinc as the primary means of calibration and Rh and Au used for checking purposes. Zinc already present in the samples at fairly consistent levels was conveniently and accurately determined by a.a.s., whereas Rh and Au were added via the electrode graphite. All five isotopes of zinc were used in constructing the emulsion calibration curve, and plates showing inconsistent data were rejected. By plotting logarithm (total ion exposure $\times$ isotopic abundance) against line density for each isotope, the ratio of the ion exposures to produce lines of equal density for the standard and analyte isotopes was determined.

TABLE 1

Equipment and general conditions of use

Mass spectrometer:		AEI MS702 double-focusing, modified Mattauch-Herzog geometry.
Vacuum conditions:	Magnetic analyzer	1×10^{-8} torr
	Source	3×10^{-6} torr during sparking
Electrode positioning:	Relative positions	End to end
	Alignment aids	Travelling microscope for linear arrangement of centre of electrode gap and slit system. Demountable jig for electrodes to first slit distance.
	Inter-electrode gap	0.4 mm maintained during sparking by using graticule of travelling microscope.
Instrument parameters:	Spark voltage	25 kV
	Accelerating voltage	20 kV
	Pulse duration	200 μs
	Pulse repetition rate	300 pulses s^{-1}
	Primary slit	0.002 in.
	Resolution	3000 at mass 208 by AEI definition [22]
	Detector	2 x 10 in. Ilford Q2 photoplate
	Photoplate exposure	18 exposures in 0.02—40 nC range
Developing conditions:	Developing	5 min Ilford Phenisol, 20°C
	Stop bath	Running water for 30 s
	Fixing	May—Baker Amfix high-speed fixer diluted 1:3 with water
	Washing	Running water for 5 min; wetting agent solution for about 20 s
	Drying	Warm air for 5 min.
Microdensitometer:		Joyce-Loebl Autodensidater Type CC with motor-driven specimen table; Hewlett Packard 2100A computer and 2752A teleprinter

Preparation of synthetic matrix ash

KH_2PO_4 (90 g), Na_2HPO_4 (10 g), Na_2SO_4 (20 g) and NaCl (0.2 g) were ground together to moderate fineness in an agate pestle and mortar. A mixture of salts of the minor elements, of known metal content, was similarly ground up from $FeSO_4 \cdot 7H_2O$ (10 g), $ZnSO_4 \cdot 7H_2O$ (2.5 g), $CaSO_4 \cdot 2H_2O$ (2.2 g) and $MgSO_4 \cdot 7H_2O$ (16 g). The matrix and minor element preparations were then mixed together by vigorous shaking in a large bottle and dried at 120°C for 2 h. The lumpy off-white solid produced was further ground, dried and weighed, yielding 139 g of matrix ash of composition ($\mu g\ g^{-1}$): Na 70,500; Mg 11,360; P 163,000; S 60,600; Cl 800; K 186,000; Ca 3685; Mn 23; Fe 14,450; Zn 4030. The slightly hygroscopic solid was stored in a well-stoppered container and sub-samples were finely ground after weighing before analysis.

Preparation of synthetic liver ash

The following weights of salts of accurately known metal content were added to 5 g of matrix ash and ground moderately finely: $KMnO_4$ (0.01456 g), $Pb(NO_3)_2$ (0.00515 g), $CuSO_4 \cdot 5H_2O$ (0.09924 g), RbCl (0.0220 g) and $3CdSO_4 \cdot 8H_2O$ (0.0132 g). These salts provided a convenient means of adding the metals that occurred in ashed liver within the approximate range 100—1000 $\mu g\ g^{-1}$. Below the 100-$\mu g\ g^{-1}$ level, small volumes of dilute solutions were more easily employed. Therefore, 10 ml of a solution containing 400 μg Mo, 140 μg Sn, 50 μg Co, 40 μg V and 40 μg Cr was added to the matrix ash—metal salt combination and the whole was stirred to dissolve and disperse as far as possible all the components of the mixture. The mixture was then evaporated in a shallow dish under an infrared lamp accompanied by continued stirring with a glass rod. Water loss continued until a very viscous syrup remained; on cooling in a desiccator a hard glassy solid resulted.

After standing for several hours to harden, the solid was thoroughly ground up in an agate pestle and mortar, combined with 45 g of matrix ash and vigorously shaken in a glass bottle to effect homogenization. The final product was 49.82 g of a pale brown, slightly hygroscopic solid of elemental composition ($\mu g\ g^{-1}$): Na 71,000; Mg 11,430; P 164,000; S 61,000; Cl 5000 max.; K 187,000; Ca 3710; V 8; Cr 8; Mn 125; Fe 14,540; Co 10; Cu 506; Zn 4055; Rb 311; Mo 80; Cd 117; Sn 28; Pb 65. A representative sub-sample of 50 mg was taken and finely ground to a fully homogeneous solid before analysis.

RESULTS AND DISCUSSION

Sample preparation and ashing

Liver tissue is sufficiently homogeneous that a sample weighing several grams is representative of the whole organ [20]. Low-temperature ashing produced a material suitable for electrode manufacture when a graphite-to-ash ratio of 2:1 was used to make it sufficiently electrically conducting. The resulting spectra recorded on photoplates as graded exposures showed a regular increase in line density for each isotope, indicating that sufficient mixing had

been achieved to overcome microscopic variations arising from the cellular nature of the original tissue.

Losses of Mg, Ca, Mn, Fe, Cu, Zn, Rb and Cd do not occur on low-temperature ashing [20] but with some other elements, losses are possible. This aspect was investigated by doping tissue samples and ashing at low temperatures followed by comparison with suitable standards representing full recovery. All elements were added in the region commonly observed in acute poisoning cases (50 $\mu g\ g^{-1}$ in the liver) which for Pb and As (seen as traces in normal liver) represented a large excess over normal levels. The elements Se, Te, Tl, Bi and Ba were not generally observed in ash samples from normal liver. The recovery of Sb, Ba, Tl, Bi or Pb was greater than 90%, but was 64% for As, and only 18% for Se and 15% for Te. This is in contrast to the good recovery of selenium reported for ashing alfalfa in similar low-temperature equipment [25].

During the analysis no trace of mercury isotopes was seen on the photoplate even in doped samples, presumably because of loss from the highly reducing electrodes during sparking so that the metal did not enter the spark plasma. Thus mercury is excluded from the proposed method and good quantitative results are unlikely to be obtained for As, Se or Te.

Interpretation of spectra

An examination was made of the atomic and molecular species generated by mixtures of salts which represented the basic composition of liver ash. Literature values for the alkali metals and phosphorus were used to calculate the basic matrix [26, 27] with the assumption that no phosphorus was lost on ashing the tissue. Preliminary s.s.m.s. data for the sulphur and minor element (Zn, Ca, Mg, Fe) content of ash samples were used to estimate the average chemical composition. The minor elements were conveniently added as sulphate to the phosphate matrix and the balance of sulphate supplied as sodium sulphate. Use of this "matrix ash" as a standard led iteratively to a more accurate estimate of these elements in the sample ashes and to an improved formulation for matrix ash.

When the trace elements were discounted, a close resemblance was seen between the final matrix ash and ashed livers. The spectra were complex but many features were readily identifiable. The regularly spaced pattern of lines from graphite was seen together with many weak lines of hydrocarbon origin, possibly from residual pump oil vapour of the type $C_xH_y^+$ ($x = 4—6$, $y = 3—9$). The combination of the Na and K phosphates of the matrix with sulphate and carbon produced a large number of molecular ions particularly at the low mass range. Table 2 lists the degree of interference seen for the elements of interest by comparing matrix ash with sample ashes. With nickel and magnesium, the severe interferences found could not be resolved. The first-row transition elements, unless present at very low levels, were only slightly affected and the heavy metals Mo, Cd, Sn and Pb suffered no measurable interference. Generally no interference was seen for the isotopes of Sb, Ba, Tl, Bi and Th, which are elements of interest to the forensic toxicologist. The elements V, Cr, Co,

TABLE 2

Interfering species in the mass spectrum of ashed liver tissue for normal elemental levels

Isotope	Potential interferences[a]	Percentage interference in liver ash—graphite[b]	Analytical status of isotope in liver ash
^{24}Mg	C_2	100	c, d
^{25}Mg	^{13}CC	100	c, d
^{26}Mg	CN	100	c, d
^{40}Ca	MgO, CN_2	1	c, e
^{42}Ca	CNO	5	c, e
^{51}V	CK, C_4H_3	100	f
^{52}Cr	CCa, ^{13}CK, C_2N_2	50	f
^{53}Cr	—	100	f
^{55}Mn	NaS, C_2P	resolved doublet	e
$^{54,56,57}Fe$	—	<1	c, e
^{59}Co	—	up to 30	f
^{58}Ni	Fe	>100	d
^{60}Ni	$Na^{37}Cl$, C_5	400	d
^{63}Cu	PS	5	e
^{65}Cu	$P^{34}S$	5	e
$^{64,66,68}Zn$	—	<1	c, e
^{67}Zn	SCl	2	c, e
^{70}Zn	Cl_2	<10	c, e
^{87}Rb	—	<2	e
^{98}Mo	—	<2	e
^{112}Cd	—	<2	e
^{118}Sn	—	<2	e
^{208}Pb	—	<2	e

[a]Singly charged species and most abundant isotope unless otherwise indicated, based on ref. 11. [b]100% interference represents equal line densities for element of interest in liver ash and line seen in matrix ash. [c]Interference estimated by comparison between KH_2PO_4/Na_2HPO_4 and liver ash. [d]Element not determinable. [e]Element present at determinable level, interference 10% or less. [f]Element determinable as maximum concentration only.

and to a lesser extent manganese, were at such low levels that interference was likely but not easily quantified because of the difficulty of obtaining reagents pure enough for the manufacture of matrix ash. The largest impurity introduced was manganese, because even analytical-reagent grades of $FeSO_4$ contain appreciable levels of this element. A.a.s. determinations agreed with s.s.m.s. measurements, which confirms that the spectral line seen at the exact mass for manganese in matrix ash did not contain an appreciable contribution from molecular species. With Co, Cr and V present at only 1 or 2 $\mu g\ g^{-1}$ in the ash, if at all, the situation was less clear. However, no species were seen that would completely overwhelm spectral lines from these elements and thus prevent one from making a useful estimate of their upper concentration limit.

The resolution of the instrument used in this work was insufficient to permit certain identification of the interfering species observed but possible

candidates are listed in Table 2, based on a high-resolution study of blood [11]. The presence of many metals at higher levels in liver compared with blood leads to a reduction in the degree of interference observed for liver, and for almost all of the elements of interest, spectral interference presented little difficulty.

Synthesis of chemical standards

Without the use of chemical standards for calibration purposes, the concentration of an unknown element can be determined only to within a factor of three for most elements [28]. The relative sensitivity factor (RSF) for each element, is defined as the concentration of an element derived by s.s.m.s. divided by the true concentration in the sample. A chemical standard of similar composition to the matrix under examination must be available for RSF determination and therefore a suitable material was synthesized by an extension of the process used for matrix ash. Typical samples of ashed human liver were analysed for trace elements (assuming unit sensitivity) and a provisional doped matrix ash was prepared on the basis of the data obtained. This standard provided working RSF values and so permitted a more accurate formulation and manufacture of a synthetic standard closely resembling ashed human liver "synthetic liver ash" (SLA).

The SLA thus prepared permitted the determination of RSF values for the elements Ca, V, Cr, Mn, Fe, Co, Cu, Rb, Mo, Sn and Pb. Where only a trace of an element was observed in normal ashed samples (V, Cr, Co), its concentration was raised in the standard to improve the estimate of the RSF. The SLA was subsequently used for calibration purposes and for routine monitoring of instrument stability.

Precision and accuracy

An attempt was made as far as possible to isolate the various random sources of error in the proposed method. The most important factors contributing to the variance in the final analytical result were thought to be sample preparation, variable source behaviour (changing ratio of ion production between standard and analyte) and variable emulsion response of the photoplate. Table 3 lists the relative standard deviations (r.s.d.) calculated at various stages of the method. Most readily determined was the precision of reading the photoplate by the microdensitometer and the subsequent data reduction involving the whole procedure of line density determination, calibration curve construction and unknown element calculation. The good precision (r.s.d. of about 5%) was a result of the automated plate reading and computerized data reduction.

Comparison of the precision of photoplate measurement with repeat analyses on a pooled ash sample indicated variations caused by changing electrode/plasma behaviour during sparking and the non-uniformity of emulsion response within and between photoplates. The average r.s.d. of 9% observed for the total of these effects was in the region generally asssociated with Ilford Q2

TABLE 3

Relative standard deviations of photoplate reading, repeat analysis of liver ash and repeat analysis of liver tissue
(All values are relative standard deviations (%) of concentration estimated from 6 replicates. Zn used for calibration except for Mo, Cd and Sn (Rh used) and Pb (Au used).)

Isotope	Photoplate reading and data reduction[a]	Repeat analysis pooled ash	Repeat analysis same tissue[b]	RSF[c]
^{42}Ca	3.4	14	27	1.41
^{51}V	7.5	14	30	0.78
^{52}Cr	3.4	16	30	2.00
^{54}Fe	6.5	9.5	26	1.49
^{57}Fe	4.2	2.5	17	1.51
^{55}Mn	3.1	7.2	20	1.95
^{59}Co	1.5	6.5	19	1.64
^{63}Cu	4.5	10.2	13	1.82
^{65}Cu	4.2	10.2	12	1.79
^{66}Zn	2.5	3.6	3.7	1.02
^{68}Zn	4.9	2.8	4.3	1.00
^{70}Zn	5.7	3.0	4.5	0.99
^{87}Rb	19	12	13	3.84
^{98}Mo	3.0	10	15	0.77
^{112}Cd	1.8	14	22	0.35
^{118}Sn	2.3	6	11	1.37
^{208}Pb	2.6	9.2	19	0.45

[a]Includes re-setting of instrument daily. [b]Samples taken separately from right lobe of wet tissue. [c]RSF values contain no correction for the mass response of the photoplate or for line width variation.

photoplates [28] indicating that the contribution from variation of the spark plasma was limited.

Variations in the emulsion response along the length of the photoplate were suspected from the inconsistency of the two methods of calibration based on either zinc, a minor element, or the added trace elements rhodium and gold. Thus on repeat analysis of a standard with zinc for calibration, a greater spread was seen in the results for Cd, Mo, Sn and Pb than when Au or Rh was used for calibration. Conversely, a greater spread in the results for elements situated at masses close to zinc (at both minor and trace levels, e.g. Fe, Mn, Co) was seen when Rh or Au calibration was used. Thus for elements of mass less than 90, zinc was used for calibration; for elements above mass 90 (Sn, Cd, Mo) rhodium was selected, with gold being specifically used to calibrate for lead, a nearby element on the mass scale. On average, these corrections decreased the r.s.d. of the analytical result by approximately one third.

As expected, a noticeable decrease in precision occurred on passing to repeat determination of the same liver tissue, where an average precision of some 16% was seen for most elements (Table 3). This additional variability

probably arose from a combination of sampling errors, weighing errors (hygroscopic solids), handling losses, introduction of minor contamination and small concentration variations within the tissue. The variation in metal content of the liver in the human population is much greater than the variation in the results obtained here, thus the method can be used for studies of metal distribution in various populations.

Since suitable reference materials were not available to assess the accuracy of the method, comparison was made with a.a.s. data. Tissue metal contents for fifteen subjects from England, who died suddenly from accidents, are given in Table 4. For comparison, the results were combined for each technique and the results expressed as a mean and standard deviation. The agreement between a.a.s., s.s.m.s. and published values is considered acceptable in view of the many possible sources of error; only cadmium showed a significant difference in the mean values.

Contamination problems

Stainless steel knives and scissors are routinely used by the pathologist for taking tissue samples at a post-mortem examination and are a potential source of contamination by Fe, Cr and Ni. Large quantities of iron are present in liver and the introduction of a further trace would be insignificant. The levels of Cr and Ni expected in cases of acute poisoning would be very much higher than the contamination introduced during handling of normal tissue.

TABLE 4

Metal concentrations ($\mu g\ g^{-1}$) in 15 liver samples[a] by s.s.m.s. and a.a.s.

Isotope	Ashed liver[b]		Liver as received (wet tissue)					
	S.s.m.s.		S.s.m.s.		A.a.s.		Literature[c]	
	Mean	S.d.	Mean	S.d.	Mean	S.d.	Mean	Ref.
Mg	—[c]	—	—	—	173	16	172	[26]
^{42}Ca	2570	730	38	11	41	8	50	[26]
^{51}V	3.0	0.86	0.044	0.014	—	—	0.04	[16]
^{52}Cr	3.0	1.4	0.045	0.059	—	—	0.08	[16]
^{54}Fe	16,020	5530	237	95	238	91	180	[26]
^{55}Mn	101	50	1.50	0.79	1.4	0.35	1.4	[26]
^{59}Co	3.4	1.2	0.05	0.02	—	—	0.061	[26]
^{63}Cu	494	234	7.3	3.7	7.1	3.7	6.7	[26]
^{68}Zn	4310	1190	63.8	19.1	63.8	19.1	47; 75.8	[26; 16]
^{87}Rb	440	161	6.5	2.6	6.9	1.8	3.9	[26]
^{98}Mo	48	21	1.30	0.32	—	—	1.0	[26]
^{112}Cd	63	43	0.93	0.59	1.50	0.71	2.2	[26]
^{118}Sn	28	12	0.42	0.16	—	—	0.32	[26]
^{208}Pb	45	28	0.67	0.39	—	—	2.3	[16]

[a]Males, mean age 25 years, sudden accidental death. [b]Mean ash weight obtained from wet tissue = 1.48 ± 0.093%. [c]Not determined.

Routine analysis

The practical application of the method described here in casework and research requires good instrumental stability over a period of months. A stability test was carried out in which a standard was analysed in quadruplet and the process repeated three months and six months later, yielding 3 sets of 4 photoplates in all. The mean and standard deviations of the elemental concentrations were calculated for each set and examined for significant differences (Student's t-test). Only in two instances (Cr and Mn) was a significant difference seen at the 5% level. In both cases agreement was seen between two sets of data but not with the third. When the data that agreed were combined, there was no significant difference from the remaining four results, in spite of the fact that two different batches of photoplates were used and one batch showed only one third of the ion sensitivity of the other.

Conclusions

This study has successfully demonstrated the use of s.s.m.s. for detecting abnormalities in the minor and trace element levels in human liver tissue. After suitable chemical standards had been prepared accurate quantitative results were obtained for 13 elements. Normal levels were established from 15 tissue samples and the detection of many toxic metals, not usually seen, was shown to be feasible with elemental coverage for most of the periodic table. The proposed method is therefore considered suitable for routine analysis of liver for population studies and in forensic toxicology. Further samples need to be analysed to determine elemental variations associated with sex, environment and other factors, so that accurate interpretation of liver analyses can be made.

REFERENCES

1 E. Berman, in A. Stolman (Ed.), Progress in Chemical Toxicology, Vol. 4, Academic Press, New York and London, 1969, p. 155.
2 Trace Elements in Relation to Cardiovascular Diseases, Report No. 157, International Atomic Energy Agency, Vienna, 1973 (papers presented at Research Co-ordination Meeting, Vienna, 19—23 Feb. 1973).
3 H. Smith, Second International Conference on Activation Analysis, Glasgow, 27—29 Sept. 1972. Texts of papers, No. 8.
4 A. Forssen, Ann. Med. Exp. Biol. Fenn., 50 (1972) 99.
5 R. L. Dahlquist and J. W. Knoll, Appl. Spectrosc., 32 (1978) 1.
6 H. J. Koch, E. R. Smith, N. F. Shimp and J. Connor, Cancer, 9 (1956) 499.
7 K. Kemp, F. P. Jensen, J. T. Møller and N. Gyrd-Hansen, Phys. Med. Biol., 20 (1975) 834.
8 J. Roboz, in G. H. Morrison (Ed.), Trace Analysis: Physical Methods, Interscience, New York, 1965, p. 435.
9 R. Brown, M. L. Jacobs and P. G. T. Vossen, Accu-labs Research Corp. Inc. Report, Wheat Ridge, Colorado, March 1971.
10 J. P. Yurachek, G. G. Clemena and W. W. Harrison, Anal. Chem., 41 (1969) 1666.
11 N. L. Gregory, Anal. Chem., 44 (1972) 231.
12 D. F. Ball, M. Barber and P. G. T. Vossen, Biomed. Mass Spectrom., 1 (1974) 365.
13 W. Gooddy, T. R. Williams and D. Nicholas, Brain, 97 (1974) 327.

14 W. Gooddy, E. I. Hamilton and T. R. Williams, Brain, 98 (1975) 65.
15 W. W. Harrison and G. G. Clemena, Clin. Chim. Acta, 36 (1972) 485.
16 E. I. Hamilton, M. J. Minski and J. J. Cleary, Sci. Total Environ., 1 (1972/1973) 341.
17 A. W. Fitchett, R. P. Buck and P. Mushak, Anal Chem., 46 (1974) 710.
18 S. Wong, Ph.D. Thesis, Cornell University, 1973, Diss. Abstr. Int., B, 34 (11), p. 5361, B, (1974).
19 C. A. Evans and G. H. Morrison, Anal. Chem., 40 (1968) 869.
20 J. Locke, Anal. Chim. Acta, 104 (1979) 225.
21 Technical Information Sheet No. A2014, AEI Scientific Apparatus Ltd., Manchester, England.
22 Operating Instructions for MS 702, Vol. 1, AEI, p. 66.
23 G. D. Nicholls, A. L. Graham, E. Williams and M. Wood, Anal Chem., 39 (1967) 584.
24 J. Locke, unpublished work.
25 C. E. Gleit and W. D. Holland, Anal. Chem., 34 (1962) 1454.
26 Ref. (1). p. 144. Data used are mainly taken from International Commission on Radiological Protection, Report of the Task Group on Reference Man for Purposes of Radiological Protection.
27 W. Niedermeier, J. H. Griggs and J. Webb, Appl. Spectrosc., 28 (1974) 1.
28 H. Farrar, in A. J. Ahearn (Ed.), Trace Analysis by Mass Spectrometry, Academic Press, New York and London, 1972, p. 239.

Analytica Chimica Acta, 104 (1979) 245—252

NITROGEN GAS PREPARATIVE SYSTEM FOR ISOTOPE-RATIO ANALYSIS BY MASS SPECTROMETRY

C. J. SMITH and P. M. CHALK*

School of Agriculture and Forestry, University of Melbourne, Parkville, Victoria 3052 (Australia)

(Received 1st June 1978)

SUMMARY

An apparatus and procedure are described for preparing nitrogen gas samples for precise ^{15}N: ^{14}N measurement. Gas is generated by reaction of ammonium sulphate with alkaline hypobromite in an evacuated system. The design of the apparatus and its recommended mode of operation overcome the problem of air contamination of samples. The gas is cleaned by liquid nitrogen freezing and is transferred to a sample tube with a Toepler pump, so that it can be analysed quickly and conveniently on a mass spectrometer.

The stable isotope ^{15}N is often used as a tracer in the biological sciences [1]. Isotope ratios are measured on nitrogen gas, usually by mass spectrometry. The preparation of the nitrogen gas usually involves oxidation of ammonium ions by alkaline hypobromite in an evacuated system [2]. During this stage of the analysis, contamination with atmospheric nitrogen can occur, either through incomplete degassing or air leakage into the apparatus [3, 4]. This is a serious problem because correction for air contamination, based on the measurement of the oxygen or argon peaks, has proved to be unsatisfactory [3—5].

Several nitrogen gas preparative systems have been described. Most have employed ground-glass joints and high-vacuum stopcocks which require greasing [2, 6—10]. These are troublesome and liable to leak. In some instances this problem is accentuated by the use of manifolds which allow for evacuation of several samples at one time [2, 7, 9, 11]. Evacuation has been achieved with a mechanical pump [10], or a mechanical pump coupled with a mercury diffusion pump [6, 7] or an oil diffusion pump [2, 9, 11, 12]. Pump specifications have not been stated, but pressures (torr) of 1×10^{-2} [7], 1×10^{-3} [2], 1×10^{-4} [10] and 1×10^{-6} [9, 12] have been reported.

After preparation, the nitrogen gas is either kept in the Rittenberg tube [2, 5, 7, 11, 12], or transferred to a sample tube [6, 8—10] before coupling to the mass spectrometer. Occasionally, the preparative system is attached to the mass spectrometer [2, 13, 14]. Transfer of gas to an evacuated sample tube has been accomplished with [6, 8, 9] or without [10] a Toepler pump. Storage of gas in the Rittenberg tube is not desirable because of the likelihood

of air leakage [2, 6, 7]. Sample tubes with greased stopcocks [6, 8, 9] can also leak, and so break-seal tubes have been employed [10].

Details are given in this paper of the design and operation of a system which facilitates the preparation of ^{15}N-labelled gas samples free of air or other contaminants.

EXPERIMENTAL

Apparatus

Glass assembly and accessories (Fig. 1). The glass assembly consists of a Rittenberg tube connected to a Toepler pump, which is joined to the high-vacuum pump assembly through a liquid nitrogen trap. Tapered joints with unground cones and sockets are employed. The socket is fitted with a partly recessed O-ring of Viton A. Although the joints are greaseless, the O-ring of the horizontal ORB 19 cone is lightly greased with Apiezon M so that the Rittenberg tube can be rotated. Greaseless high-vacuum taps of 6 mm internal bore, which incorporate O-rings of polytetrafluoroethylene and Viton A, are used. Sample tubes are also made from these taps, which are guaranteed to hold a vacuum of 1×10^{-6} torr. One arm of the tap is fitted with an ORB 10 cone, while the other arm is closed to give a sample volume of 3 ml. Taps and joints were obtained from Young Scientific Glassware, London.

Vacuum is measured by a Penning gauge head connected to a control unit with a range of 1×10^{-2} to 1×10^{-7} torr. The head is joined to the glassware by a quick-release vacuum coupling with a nitrile O-ring seal. These high-

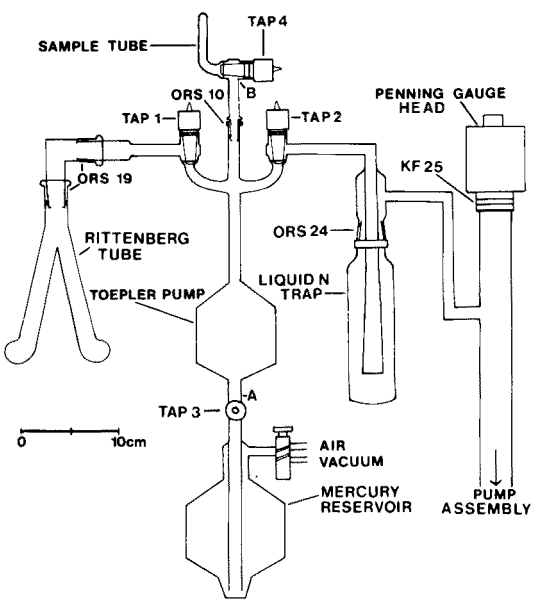

Fig. 1. Glass assembly and accessories.

vacuum accessories were obtained from Edwards High Vacuum, Crawley, England.

A pump capable of reducing the pressure to 4×10^{-1} torr is required to lower the mercury in the Toepler pump. A 700-ml Dewar flask is required for the liquid nitrogen trap, and a Dewar flask of at least 5 l is required at the assembly for liquid nitrogen storage. The assembly is clamped to a bench-mounted, steel frame with a baseplate which supports the mercury reservoir.

Pump assembly (Fig. 2). All components were obtained from Edwards High Vacuum. The assembly consists of a Diffstak pumping system (Model 63/150M) connected to a floor-mounted rotary pump (Model EDM 6). The Diffstak system consists of a water-cooled oil diffusion pump which can be by-passed by means of an in-built isolation valve and a backing/roughing valve. The backing/roughing valve is connected to the rotary pump via an SC 10 alloy crosspiece which allows insertion of a Pirani gauge head and an air admittance valve. The Pirani gauge head is connected to a control unit with a range of 3 to 1×10^{-3} torr. The rotary pump has a displacement of 7 m^3h^{-1} and can give an ultimate vacuum of 1×10^{-4} torr. The Diffstak can give an ultimate vacuum of 2×10^{-8} torr. The Diffstak is mounted under the bench below the glass assembly, and is connected to it through the bench via stainless steel flexible bellows. Quick-release vacuum couplings sealed with nitrile O-rings are used in the assembly.

Mass spectrometer. Isotope ratios (mass 28/mass 29) were determined on

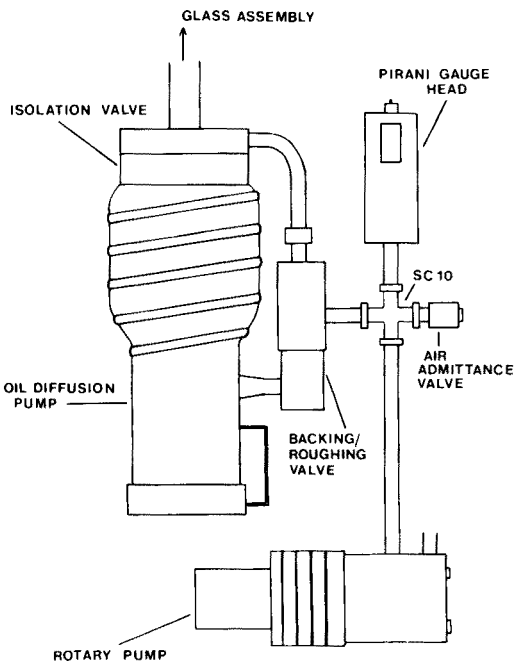

Fig. 2. Pump assembly.

a Micromass 602C double-collector mass spectrometer, equipped with a digital multimeter for display of the ion currents.

Reagents

Sodium hypobromite solution, ca. 1.4 M. This solution was prepared as described by Edwards [14], but with 18 ml of bromine instead of 15 ml.

Ammonium sulphate solutions, ^{15}N-labelled. Solutions containing ca. 2.0 atom-% ^{15}N (1000 μg N ml^{-1}), ca. 1.0 atom-% ^{15}N (1000, 500 and 250 μg N ml^{-1}), and ca. 0.4 atom-% ^{15}N (1000 μg N ml^{-1}) were prepared from stock solutions containing 20, 99 and 1.0 atom-% ^{15}N respectively, by adding weighed amounts of analytical-reagent ammonium sulphate (natural ^{15}N abundance = 0.366 atom-%).

Procedure

Nitrogen gas preparation. Transfer 1 ml of ammonium sulphate solution to one bulb of the Rittenberg tube. (Normally, ^{15}N-labelled samples would consist of 1—2 ml of acidified ammonium distillates containing up to 2 mg of nitrogen [2, 9].) Transfer 2 ml of sodium hypobromite solution to the other bulb of the Rittenberg tube, and attach it to the glass assembly, being careful to keep the tube vertical at all times to prevent mixing of the contents.

Prepare the liquid nitrogen trap and attach a sample tube to the assembly. With taps 1, 2 and 4 (Fig. 1) open and the oil diffusion pump isolated, begin evacuation of the system with the rotary pump. Tap the Rittenberg tube between the arms, to aid degassing of the solutions. When the pressure displayed on the Pirani gauge reaches 1×10^{-1} torr, engage the oil diffusion pump. Continue tapping the arms of the Rittenberg tube until the solutions begin to freeze. When the pressure reaches 4×10^{-4} torr, as shown on the Penning gauge, immerse the bulbs of the Rittenberg tube in liquid nitrogen, and continue evacuation to a pressure of 4×10^{-5} torr. Close tap 1, and slowly thaw the frozen solutions.

Repeat the evacuation, freezing and thawing cycle twice. During the last period of freezing, maintain a pressure of 1×10^{-5} torr for at least 3 min. Before final thawing, close taps 1 and 2, and isolate both pumps by closing the isolation valve. Mix the sodium hypobromite and ammonium sulphate solutions by rotating the Rittenberg tube several times in the vertical plane perpendicular to that shown in Fig. 1. Equalize the solution volume in each bulb, warm and beat the tube to ensure complete oxidation of ammonium. When gas evolution has ceased, freeze the bulbs by immersion in liquid nitrogen. Heat the glassware with a stream of warm air to speed the removal of condensate, and continue to freeze for 4 min following removal of all obvious traces of condensation.

Open tap 1 to allow clean nitrogen gas to expand into the Toepler pump. Close tap 1, and carefully regulate tap 3 to allow mercury to rise slowly from level A to level B (Fig. 1) of the Toepler pump. Close tap 4, apply a vacuum to the mercury reservoir, and slowly lower the mercury to below the ORS-10

socket by carefully regulating tap 3. Remove the sample tube, and allow the mercury to fall to level A. Open tap 1 to release the vacuum in the Rittenberg tube, and remove it from the assembly.

Mass spectrometer. An instrument correction factor is used for standard atmospheric nitrogen and unknowns. This enables all measured isotope ratios to be related to the currently accepted value of 0.3663 ± 0.0004 atom-% ^{15}N for atmospheric nitrogen [4]. Results are calculated from the equation: atom-% $^{15}N = 100/2R' + 1$, where the adjusted isotope ratio $R' = RF$, and R is the measured ratio. The correction factor $F = 136.1/R_a$, where R_a is the ratio for atmospheric nitrogen.

RESULTS AND DISCUSSION

Sample precision is an important criterion by which the efficacy of the preparative system can be judged. Good precision is obtained when the bulbs of the Rittenberg tube are frozen in liquid nitrogen for 4 min after all obvious traces of condensation have been removed (Table 1). Nitrous oxide, carbon dioxide and water vapour formed during hypobromite oxidation interfere with nitrogen isotope-ratio analyses by the mass spectrometer, and are removed by liquid nitrogen freezing [2, 3].

Liquid nitrogen or liquid air [2, 8—10, 12—14], and a dry ice—alcohol mixture [6, 7, 11] have been used to clean samples, but the last is considered to be ineffective [2, 3]. Samples have been cleaned by freezing the sample tube, and/or passing the gas through a capillary U-tube or helix immersed in the liquid. However, capillary tubes must be frequently cleaned, otherwise blockage will occur and the sample will be lost. This, as well as freezing of the sample tube, will increase analysis time on the mass spectrometer. This is avoided in the procedure described, as is the additional problem of memory effects in capillary-type liquid nitrogen traps [15].

Precision is markedly affected by sample size (Table 2), and decreases as the amount of nitrogen used to prepare the sample decreases. Poor precision

TABLE 1

Effect of time of freezing in liquid nitrogen on precision

Time[a] (min)	Mean[b] atom-% ^{15}N	Standard deviation	Coefficient of variation (%)
0	0.905	0.035	3.90
0	1.911	0.073	3.84
4	0.939	0.004	0.43
4	2.026	0.009	0.42

[a]Time elapsed after all obvious traces of condensation removed from glassware.
[b]Six replicates; samples prepared from 1000 μg N.

TABLE 2

Effect of sample size on precision

N used to prepare sample (μg)	Replicates	Mean atom % ^{15}N	Standard deviation	Coefficient of variation (%)
250	6	0.913	0.017	1.81
500	9	0.931	0.007	0.75
1000	9	0.943	0.005	0.48

with low nitrogen content is reported for another preparative system [9]. Precision is good when at least 500 μg of nitrogen is used, and could be improved for smaller samples if more gas were transferred to the sample tube. This is possible through a slight modification to the glass assembly. When the mercury rises in the Toepler pump, pockets of gas are trapped at the bases of taps 1 and 2. The significance of this loss would be reduced if the expansion bulb of the Toepler pump were placed above the taps rather than below them. It is estimated that one stroke of the pump would then effectively transfer 75% of the gas generated, and a second stroke would ensure that at least 90% was transferred to the sample tube. For efficient transfer of the sample to the mass spectrometer, the volume of the sample tube is made small in comparison with the expansion volume of the mass spectrometer.

Precision is unaffected by the abundance of ^{15}N in the range 0.4—2 atom-% ^{15}N (Table 3). The majority of samples generated in biological tracer studies would normally fall within this range. Standard deviations of ±0.001 and ±0.005 atom-% ^{15}N, for samples near 0.4 and 1 atom-% ^{15}N, respectively, are in close agreement with data given for another preparative system [13]. The coefficients of variation of less than 1% are lower than the 1—3% reported for several other studies [15].

Several factors influenced the design and operation of the preparative system. Because it is unlikely that many researchers will have a mass spectrometer exclusively for their own use, the unit is designed to operate independently, and to provide samples which can be rapidly and conveniently analysed. Even if it is possible to have a sample preparative unit attached to a mass spectrometer, it is still desirable to employ a pumping system separate from that of the instrument [9, 14]. Another advantage of a remote system with an efficient Toepler pump and a small sample tube, is the ability to transfer more of the sample generated to the mass spectrometer.

The pump assembly is designed to allow for complete and rapid degassing of the glass assembly. This is achieved through a combination of pumps of specified low ultimate pressure, and high pumping speed in relation to glass assembly volume. The glass assembly is designed to be free of leaks through the use of greaseless taps and joints with O-ring seals. Apart from the sample

TABLE 3

Effect of sample ^{15}N abundance on precision

Mean[a] atom-% ^{15}N	Replicates	Standard deviation	Coefficient of variation (%)
0.392	8	0.001	0.33
0.943	9	0.005	0.48
2.026	9	0.008	0.40

[a]Samples prepared from 1000 μg N.

tubes, the number of these is kept to a minimum, and the O-rings should be replaced following prolonged usage. The sample tubes are far more convenient than non-reusable break-seal tubes, and, unlike Rittenberg tubes with greased caps or taps, they do not leak.

Sample preparation technique is also an important consideration. Hypobromite is prepared by a simple procedure, other methods [2, 7] being unnecessarily tedious and complex. Freezing, thawing and agitation during evacuation aid in degassing the liquid sample and hypobromite [5, 12]. Random checks of the oxygen peak at mass 32 have indicated a consistently low level of air contamination of samples. Unlike another procedure proposed [13], care is taken to ensure that complete oxidation of the sample and release of nitrogen occurs. Failure to do so can result in isotopic fractionation [3, 4, 12].

The authors thank the Glaciology Section, Antarctic Division, Department of Science, for use of their mass spectrometer, and Mr. V. Morgan for technical advice. This work was supported by a grant from the J. M. Higgins Research Foundation, and a Commonwealth Postgraduate Research Award to the senior author.

REFERENCES

1 R. D. Hauck and M. Bystrom, ^{15}N - A selected Bibliography for Agricultural Scientists, Iowa State University Press, Ames, 1970.
2 J. M. Bremner, in C. A. Black et al. (Eds.), Methods of Soil Analysis, Part 2, Am. Soc. Agron. Inc., Madison, Wisconsin, 1965, pp. 1256—1286.
3 J. M. Bremner, H. H. Cheng and A. P. Edwards, in The Use of Isotopes in Soil Organic Matter Studies, Report of FAO/IAEA Tech. Meeting, Pergamon Press, Oxford, 1966, pp. 429—442.
4 R. D. Hauck and J. M. Bremner, Adv. Agron., 28 (1976) 219.
5 C. Balestrieri, Life Sci., 7 (1968) 269.
6 D. Rittenberg, in D. W. Wilson, A. O. C. Nier and S. P. Reimann (Eds.), Preparation and Measurement of Isotopic Tracers, J. W. Edwards, Ann Arbor, Michigan, 1948, pp. 31—42.
7 D. B. Sprinson and D. Rittenberg, J. Biol. Chem., 180 (1949) 707.
8 R. F. Glascock, Isotopic Gas Analysis for Biochemists, Academic Press Inc., New York, 1954, pp. 195—201.

9 C. M. Cho and E. Haunold, in The Use of Isotopes in Soil Organic Matter Studies, Report of FAO/IAEA Tech. Meeting, Pergamon Press, Oxford, 1966, p. 443—445.
10 A. S. J. Reid, G. L. Cumming and G. R. Webster, Pl. Soil, 26 (1967) 196.
11 J. H. Smith, J. O. Legg and J. N. Carter, Soil Sci., 96 (1963) 313.
12 G. B. Shearer, D. H. Kohl and B. Commoner, Soil Sci., 118 (1974) 308.
13 P. J. Ross and A. E. Martin, Analyst, 95 (1970) 817.
14 A. P. Edwards, J. Environ. Qual., 2 (1973) 382.
15 A. E. Martin and P. J. Ross, in Transactions of the 9th International Congress of Soil Science, Vol. 3, International Society of Soil Science and Angus and Robertson, Sydney, 1968, pp. 521—529.

Analytica Chimica Acta, 104 (1979) 253—266

THE ISOLATION AND IDENTIFICATION OF POLYCHLORO-2-(CHLOROMETHYLSULPHONAMIDE) DIPHENYL ETHER ISOMERS AND THEIR METABOLITES FROM EULAN WA NEW AND FISH TISSUE BY GAS CHROMATOGRAPHY—MASS SPECTROMETRY

DAVID E. WELLS

Freshwater Fisheries Laboratory, Pitlochry (Gt. Britain)

(Received 24th July 1978)

SUMMARY

The active ingredients of Eulan WA New have been isolated and identified by nuclear magnetic resonance and mass spectrometry. The gas chromatography thermal decomposition products of the polychloro-2-(chloromethylsulphonamide) diphenyl ether isomers have been monitored and the chromatogram of Eulan WA New has been characterized. A method for the extraction, clean-up, and analysis of the isomers and their metabolites in fish tissue by g.c.—m.s. has been developed.

Polychloro-2-(chloromethylsulphonamide) diphenyl ethers (PCSD) (IIa, IIb, IIc) used as mothproofing agents in the textile industry, are the active ingredients in the formulation [1] of Eulan WA New. These materials have been introduced in a number of countries [2, 3] as an alternative to dieldrin because of their lower toxicity to fish [2]. Wrabetz et al. [4] have determined Eulan WA New in waste water by gas—liquid chromatography (g.l.c.) and thin-layer chromatography (t.l.c.), but did not isolate or identify any of the PCSD isomers or their metabolites. More recently, Westöö and Noren [3] have identified two polychloro-2-aminodiphenyl ethers (PADs) (VI, VIII) in fish; they attributed these to the main metabolites of Eulan WA New. They analysed the fish extracts by g.c.—m.s. and compared the spectra of the metabolites with model compounds made from known starting materials. The PADs, which also occur as impurities in the Eulan WA New formulation, are the precursors in the manufacture as well as the primary metabolites formed by the biodegradation of the PCSDs.

In this work the PCSD isomers and their metabolites have been isolated from Eulan WA New by column chromatography and characterized by m.s. and n.m.r. A thermal rearrangement reaction of the PCSDs at the g.c. injection port was identified by m.s. with electron impact (e.i.) and chemical ionization (c.i.) sources and a pathway has been assigned to the rearrangement. A clean-up technique, which separates both the PADs and the PCSDs from the co-extracted lipid material from fish tissue and analysis by g.c.—mass fragmentography, is also described.

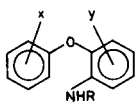

I	R = H	a 4
II	R = SO_2CH_2Cl	b 5
III	R = CH_2Cl	c 6

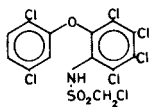

IV

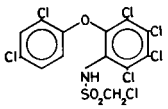

V

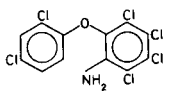

VIII

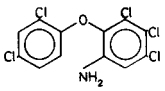

VI

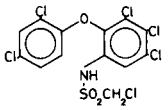

VII

EXPERIMENTAL

Materials

A sample of the mixed PCSD isomers (Farbenfabriken Bayer AG) was used as a starting material for the isolation of the individual isomers and the preparation of the PAD metabolites. The Eulan WA New formulation (Bayer (U.K.) Ltd., Shipley), used in the textile industry was used for comparison with fish extracts suspected to contain PCSD and PAD isomers.

The organic solvents (Rathburn Chemicals (Walkerburn) Ltd.), supplied as glass distilled grade, were used without further purification. The alumina (Reeve Angel Scientific grade A11 0 col.) used for the separation of the isomers and clean-up, was sieved and the 64—125-μm particle band-size was retained. This was fired at 800°C for 4 h to remove organic impurities, cooled and deactivated to 4% with distilled water. The pH of the supernate from a 10% (w/v) slurry of this basic alumina was 11. Acidic alumina was prepared by washing the basic oxide with 1 M hydrochloric acid. The slurry was filtered, dried at 150°C for 4 h, and deactivated to 4% with distilled water. The pH of the supernate from a 10% (w/v) slurry of the acidic alumina was 3.6. All other reagents were AnalaR grade (BDH) and were used as supplied.

Extraction and clean-up of the fish tissue

Samples of pike (*Esox lucius*), perch (*Perca fluviatilis*) and brown trout (*Salmo trutta*) were taken from an area where Eulan WA New was known to be used as a mothproofing agent. Sub-samples of the tissue were weighed, ground with anhydrous sodium sulphate, transferred quantitatively to a Soxhlet

and exhaustively extracted with n-hexane (100 ml). The final volume was adjusted to 100 ml with n-hexane and a suitable aliquot was taken for the analysis.

The micro-columns (200 mm × 6 mm i.d.) were filled with acidic alumina (2 g) followed by an upper charge of basic alumina (1 g). The tissue extract, concentrated to 1 ml, was pipetted onto the column head followed by a charge of n-hexane (25 ml). The collection tubes were replaced and the charge was renewed with diethyl ether (30%) in n-hexane (20 ml). The collection tubes were again replaced and glacial acetic acid (15%) in n-hexane (1 ml) was added to the column head, followed by diethyl ether (30%) in n-hexane. The first and third eluates were recombined for analysis by g.c.—m.s.

Separation of the PCSD isomers. A borosilicate glass preparative column (200 mm × 22 mm i.d.) was dry-packed with the prepared acidic alumina. The mixed PCSD isomers (1 g) were dissolved in diethyl ether (2 ml), pipetted onto the column, and eluted with 30% diethyl ether in n-hexane (100 ml). The eluant was collected in 10-ml portions and each fraction was analysed by g.c.—m.s. to determine its purity. The first 20 ml contained trace quantities of the PAD isomers (Ib and Ic). The major PCSD isomer, IIb, was eluted in the range 40—100 ml, after which the column was recharged with pure diethyl ether and IIc was collected in the range 110—150 ml. The individual fractions containing the same isomer were added together and the isomer was isolated by evaporation of the solvent.

Preparation of the PAD isomers. The mixed PCSD isomers (2 g) were refluxed with 70% sulphuric acid (50 ml) for 3 h. The resultant liquor was cooled in an ice bath and slowly diluted with distilled water (200 ml). The solution was made alkaline with 40% (w/v) potassium hydroxide and the aqueous phase was extracted with 2 × 50 ml of n-hexane. The n-hexane extract was evaporated to 1 ml and chromatographed on a similar column to that used for the PCSD isomers; a column charge of basic alumina (30 g) and n-hexane as the eluant were used. The two PAD isomers isolated were Ib and Ic.

Instrumentation

The mass spectra were obtained with a Finnigan 3200F g.c.—m.s. (quadrupole) system. The spectra were recorded with a Bell and Howell 525150 oscillograph and the signal generated was monitored either in the total ion mode (t.i.m.) or selected ion mode (s.i.m.) with the Programmable Multiple Ion Monitor. The g.c. was interfaced to the m.s. via a single-stage glass jet separator which was housed in its own oven line-of-sight to the ion source. The Finnigan 9500 chromatograph was fitted with a 6.25 m × 1.5 mm U-glass column containing 3% Dexsil 300 as the liquid phase on a solid support of Chromosorb W-HP. High-grade helium was used as the carrier gas. The c.i. spectra of the mass chromatogram of Eulan WA New were obtained on a similar system with a Finnigan 6000 Data system. Methane was used as the make-up and reagent gas.

The n.m.r. spectra of the PCSD isomers were obtained on a Perkin—Elmer R32 instrument at 90 MHz. The compounds were dissolved in deuteromethanol and spiked with tetramethylsilane (TMS) as a reference and lock-in standard.

RESULTS AND DISCUSSION

The initial total ion mass chromatogram (Fig. 1) of Eulan WA New indicated that the mixture contained a series of PCSD isomers with the chlorine content of the phenyl rings increasing from 3 to 6 chlorine atoms, and the majority of the mixture being divided between IIb and IIc. A similar series of the PAD isomers was also identified as impurities in the formulation. Before any further detailed analysis was made, the major PCSD isomers were isolated by column chromatography, and the corresponding PAD isomers were generated by the hydrolysis of Eulan WA New.

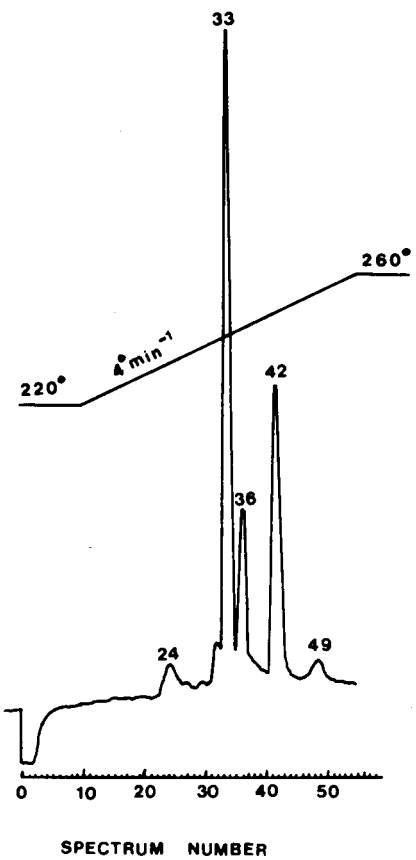

Fig. 1. Total ion mass chromatogram (70—550 a.m.u.) of Eulan WA New. Column — 3% Dexsil 300 on Chromosorb W HP. Injector temperature, 240°C; separator temperature, 250°C; carrier gas — helium at 15 ml min^{-1}. Spectrum No. 33 = VII, 42 = V, 49 = VIII.

N.m.r. spectra of PCSD isomers

The aromatic regions of the n.m.r. spectra of the PCSD isomers IIb and IIc are given in Fig. 2(a), and an expanded scale (10 Hz) spectrum for IIb is given

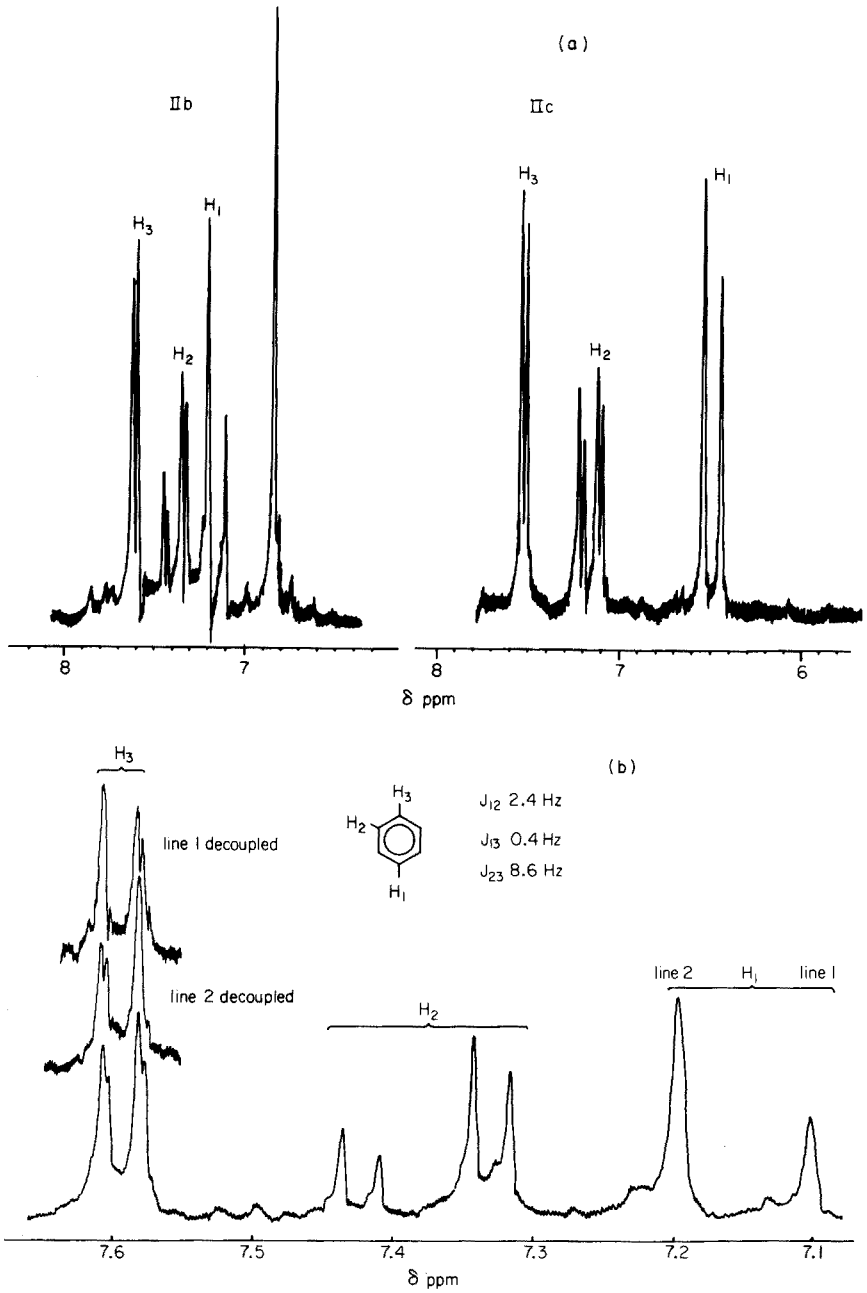

Fig. 2. Limited n.m.r. spectra of the aromatic region of the PCSD isomers. (a) IIb and IIc at 90 MHz; sweep, 10 ppm; reference, TMS. (b) IIb with 10 MHz sweep *o—m* coupling.

in Fig. 2(b). Both isomers exhibited an *o—m* coupling of the protons on one aromatic nucleus. The isomer IIb gave a singlet at $\delta = 6.83$ from the second aromatic ring, indicating a lone proton. There was no other signal in the aromatic region from IIc. The spectra also confirmed that the two samples were single isomers and that the level of impurity was probably not greater than 5%.

There are four possible isomeric configurations that can be deduced from the n.m.r. spectrum for IIc. However, the mass spectrum indicated that the structure was either IV or V, with the majority of chlorine atoms on the same phenyl ring as the sulphonamide group. This basic structure has been confirmed for the corresponding PAD isomer (VIII) [3] which is a precursor of the PCSD and is present as an impurity in Eulan WA New.

Solid probe mass spectra of PCSD isomers

The e.i. solid probe mass spectra of IIb and IIc over the mass range 240—520 amu at 30 eV are given in Fig. 3. The fragmentation pathways of both isomers were very similar, differing by 34 amu because of the replacement of a proton by a chlorine atom. Therefore only the more abundant IIb isomer will be reported in detail. The molecular ion (^{35}Cl) at *m/e* 467 displayed an isotopic cluster at *m/e* 467—475 of six chlorine atoms, and agreed with the empirical

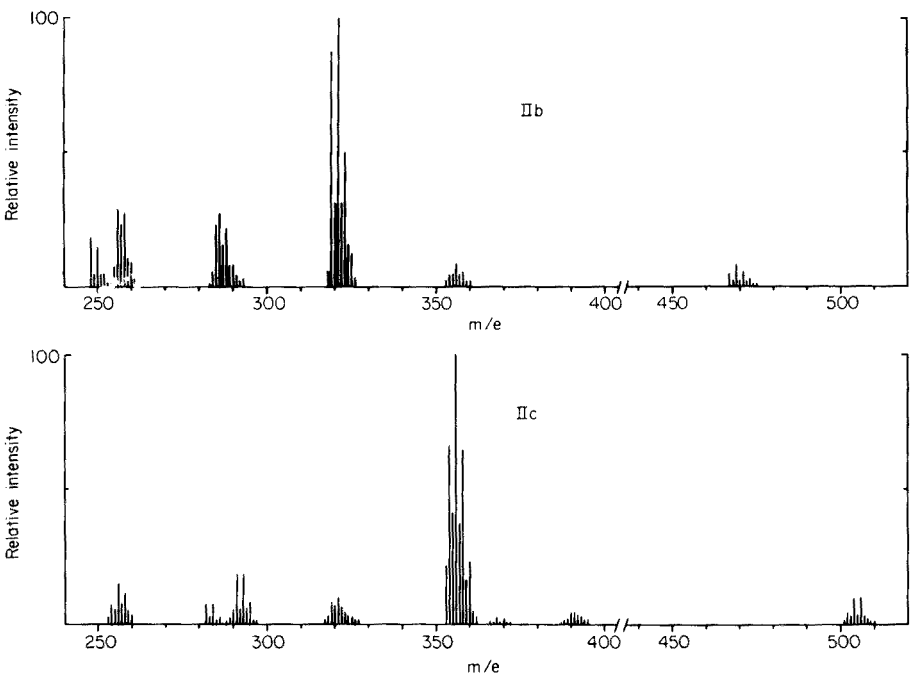

Fig. 3. Solid-probe mass spectra of penta-(IIb) and hexa-(IIc) 2-(chloromethylsulphonamide) diphenyl ether isolated from Eulan WA New. Electron energy, 30 eV; probe temperature, 180°C.

formula $C_{13}H_7NO_3SCl_6$. Moving to lower mass, the fragments at *m/e* 353—360 formed two groups, each containing five chlorine atoms, at *m/e* 353 and *m/e* 354. Further loss of chlorine yielded the base peak at *m/e* 319 containing four chlorine atoms.

Initially the decomposition was thought to be a straightforward sequential bond fission by loss of the sulphonamide group followed by the chlorine atoms of the aromatic ring. However, the formation of the odd electron fragment (*m/e* 319) as the base peak, and difficulty in assigning a route to ions *m/e* 256—260 and *m/e* 290—294 by simple fragmentation, precluded such a simple explanation. A metastable scan was obtained for the major fragments above *m/e* 256 with a JEOL D100 high-resolution m.s. The results indicated that the *m/e* 256 ion was obtained from *m/e* 284 and the *m/e* 290 ion from *m/e* 318. The loss of a neutral species of 28 mass units strongly suggested that carbon monoxide was eliminated. If so, the two phenyl groups of the fragments at *m/e* 284 and *m/e* 318 must be linked via the nitrogen as well as the oxygen in order to sustain the loss of carbon monoxide alone. The parent ion of the daughter at *m/e* 319 was predominantly the molecular ion at *m/e* 467 with a small contribution from *m/e* 354. The explanation for this loss involves a synchronous removal of $-SO_2CH_2Cl$ and a chlorine atom from the second phenyl ring of the molecular ion, and a cyclic rearrangement to form the odd electron species at *m/e* 319. The proposed fragmentation scheme for the PCSD isomer IIb is given in Scheme A.

Thermal rearrangement of the PCSD isomers

The isolated PCSD and PAD isomers were chromatographed individually to obtain their g.c. characteristics and to identify the components within the mass chromatogram of Eulan WA New. The mass spectra of the PCSD isomers obtained from the mass chromatogram were different from those obtained from the solid probe; evidently a rearrangement or decomposition reaction had taken place. The e.i. (30 eV) spectrum of the chromatographed PCSD isomer IIb is given in Fig. 4(a).

Assuming that the reaction was intramolecular rather than intermolecular, the highest mass detected (*m/e* 366) could not be the molecular ion unless the nitrogen atom had been removed in the rearrangement. However, as no reaction could account for the removal of the nitrogen from the PCSD to give a more stable molecule at *m/e* 366, this indicated that the molecular ion was at a higher mass. Spectra obtained at 20 eV and 15 eV did not show ions above *m/e* 366.

The c.i.-methane spectra of the chromatographed PCSD isomer IIb displayed an intense ion at *m/e* 402 ($M + 1$) with satellites at *m/e* 430 ($M + 29$) and *m/e* 442 ($M + 41$), and major fragments at *m/e* 366 and *m/e* 332 (Fig. 4b). Although this indicated that the molecular ion was at *m/e* 401 and contained 6 chlorine atoms, it was not possible to account for the loss of 2 chlorine atoms (70 amu) from this mass to form the cluster at *m/e* 332, containing 4 chlorine atoms, in the e.i. spectra. Therefore the molecular ion of the g.c.

Scheme A

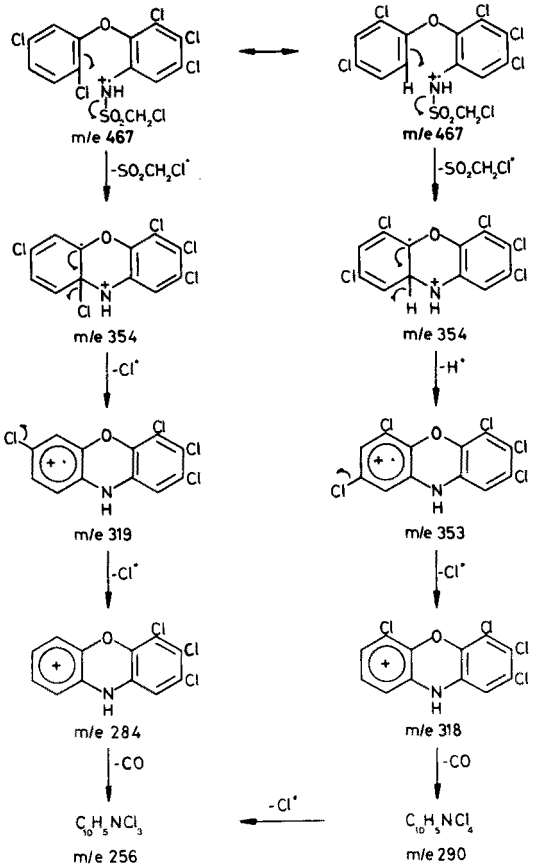

thermal decomposition product, when operating in the e.i. mode with helium as a carrier gas must be greater than *m/e* 401.

The most likely thermal reaction is the expulsion of SO_2 (64 amu) from the PCSD IIb isomer *m/e* 467 to form the *N*-chloromethyl derivative IIIb at *m/e* 403 (Scheme B), which equally accounts for the decomposition and the fragmentation of the product (Scheme C). The fragmentation is similar to the PCSD IIb with a ring closure rearrangement to form the more stable fragments at *m/e* 366 and *m/e* 332. This ring closure also accounts for the loss of carbon monoxide from *m/e* 297 and *m/e* 269. The pyrolysis of the PCSD takes place in the injection port. This was confirmed by altering the injection port temperature from 190°C to 250°C intervals of 20°C. A very broad, poorly resolved chromatogram was obtained below 230°C which reverted to a well-defined pattern (Fig. 1) above this temperature. There was no variation in the chromatogram at different separator temperatures, whether the glass surface was silanized or not. The decomposition was quantitative and it was possible to

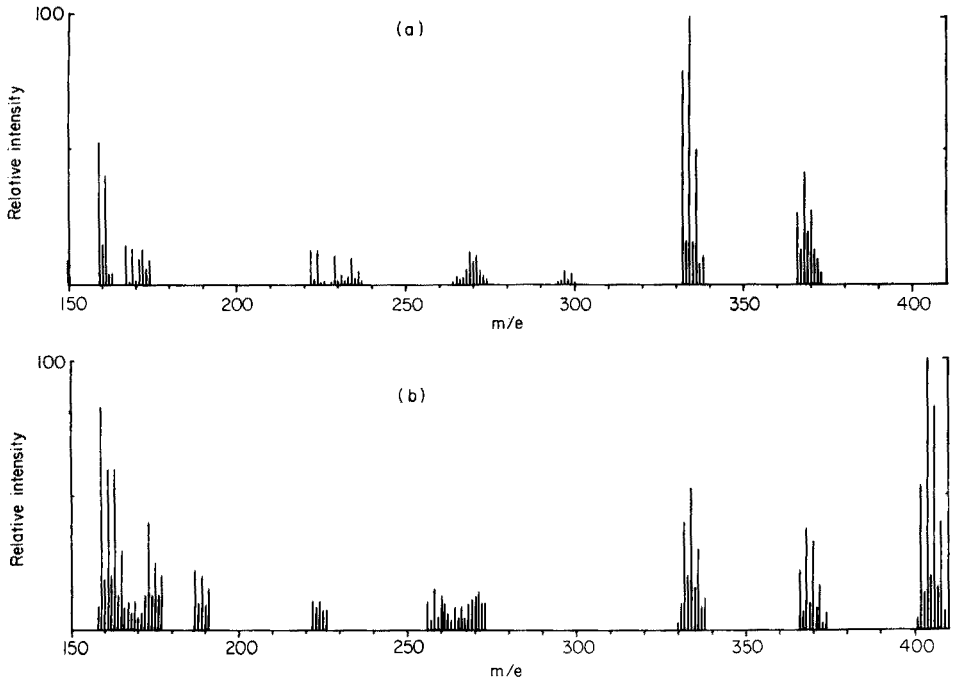

Fig. 4. Mass spectra of the g.c. thermal decomposition product of the PCSD isomer IIb. (a) E.i. spectrum at 30 eV; (b) c.i.—methane spectrum.

Scheme B

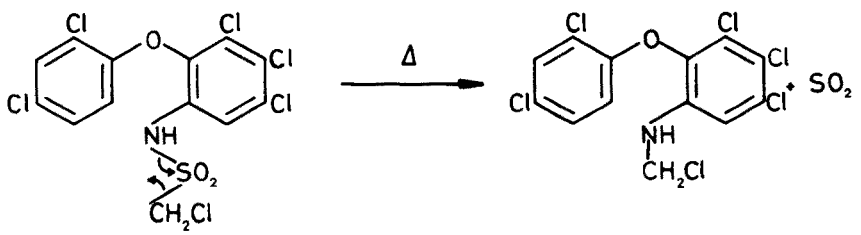

IIb IIIb

obtain a reproducible calibration curve for the PCSD isomer by monitoring the decomposition product.

Mass spectra of the polychloro-2-amino diphenyl ether isomers

There was no thermal decomposition or rearrangement of the PAD isomers Ia, Ib, Ic in the g.c., and the mass spectra were the same for each isomer whether obtained via the solid probe or the g.c. inlet. As with the PCSD isomers the spectra were similar, differing predominantly by 34 amu caused by the substitution of a proton by a chlorine atom. The e.i. (30 eV) and

Scheme C

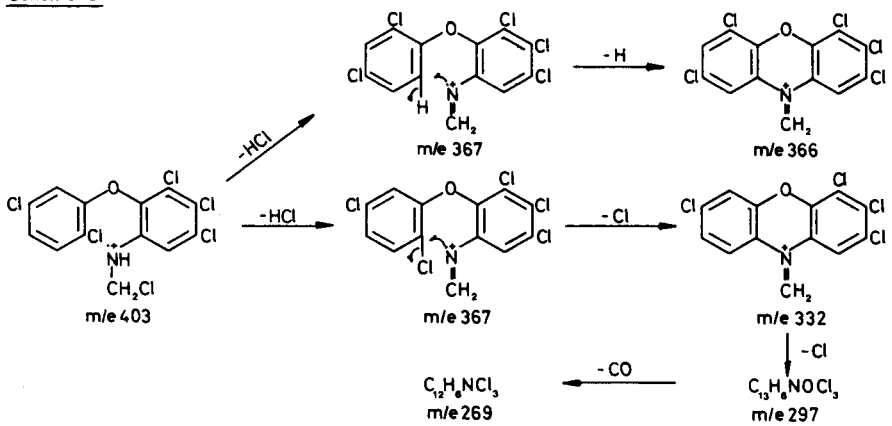

c.i.—methane mass spectra of the predominant PAD isomer (Ib) in Eulan WA New and the main metabolite from the PCSD (IIb), are given in Fig. 5.

The fragmentation pattern follows three possible pathways with (M—Cl), (M—HCl) and (M—$C_6H_2Cl_2$) ions being formed at *m/e* 320, *m/e* 319 and *m/e* 220, respectively. Further losses of Cl, C_6H_3 and CO lead to *m/e* 182, which in turn can

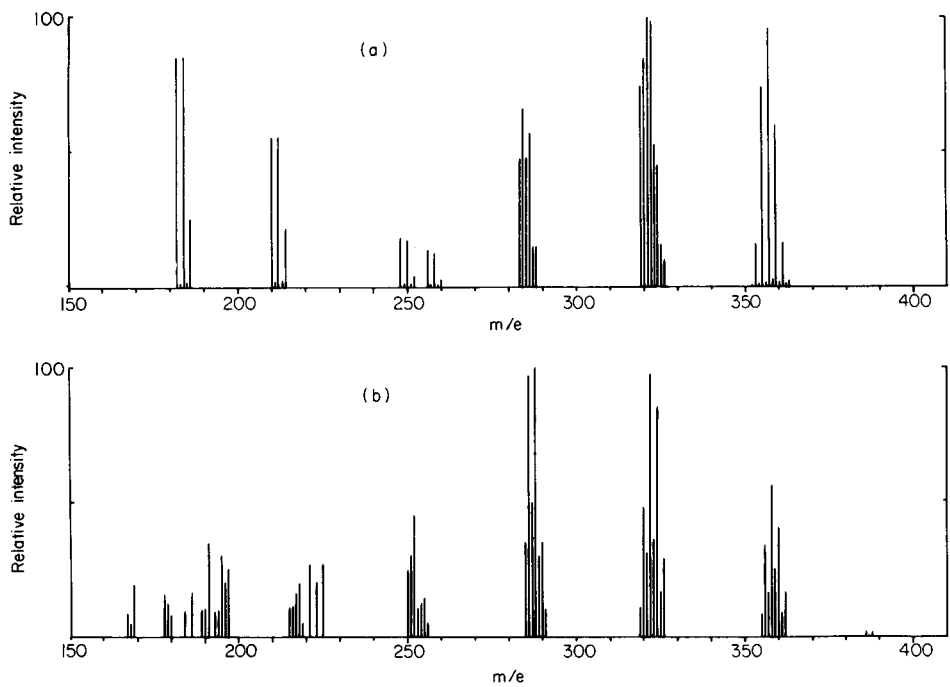

Fig. 5. Mass spectra of pentachloro-2-aminodiphenyl ether isolated from the acidic hydrolysis of Eulan WA New. (a) E.i. spectrum at 30 eV; (b) c.i.—methane spectrum.

lose HCl to give *m/e* 146. One of the pathways is likely to go via a tricyclic series of fragments at *m/e* 319 and *m/e* 284, similar to the PCSD IIb fragmentation, to account for the loss of CO from *m/e* 284 to yield *m/e* 256. The fragmentation pathway is given in Scheme D. The c.i.—methane spectrum of the PAD isomer Ib (Fig. 5(b) displays an (M + H) ion with a lower intensity than the molecular ion in the e.i. spectrum and a weak ($M + C_2H_5$) ion.

Identification of the PCSD and PAD isomers in the chromatogram of Eulan WA New

The mass spectra of the PCSD and PAD isomers were used to identify each of the major peaks in the chromatogram of Eulan WA New. Westöö and Noren [3] confirmed the isomeric configurations of two PADs with an LKB 2091 m.s. at 70 eV; the results obtained in this work agree with their conclusions. The n.m.r. and mass spectra of the two main PCSD isomers indicate that the sulphonamides have the same configuration of the chlorine atoms on the phenyl nuclei as the corresponding amine, confirming the relationship between the PCSD (VII and V) and PAD (VI and VIII) isomers, respectively.

Analysis of PCSD and PAD isomers in fish tissue

After the major components of Eulan WA New had been characterized it was possible to develop a method to detect and determine the levels of the PCSD and PAD isomers in fish tissue.

Clean-up of PCSD and PAD isomers

Lipid material extracted into the n-hexane is usually removed prior to g.c. or g.c.—m.s. analysis to prevent degradation of the g.c. column and to minimize the interference on the chromatograms of the compounds of interest [5]. An initial attempt to clean-up fish tissue extracts spiked with Eulan WA New by means of a micro-column charged with basic alumina (3 g) and n-hexane as an eluant was unsuccessful. The PADs were eluted between 10 and 20 ml

Scheme D

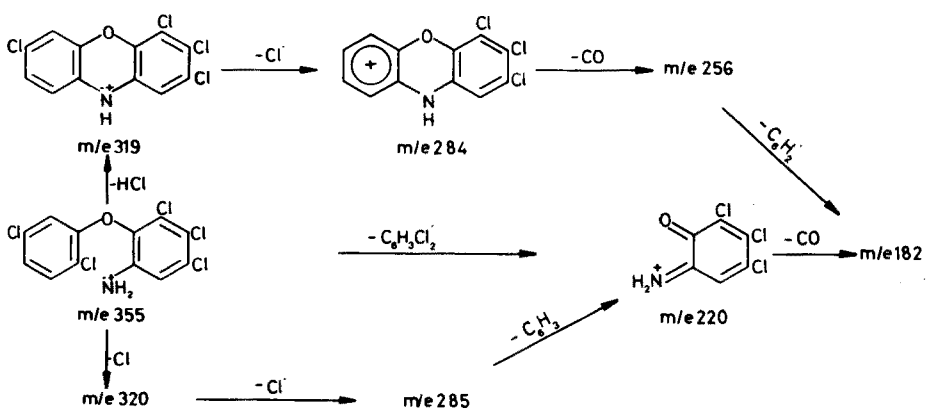

but the PCSDs remained on the column regardless of the polarity of the solvent used. The use of acid alumina was also unsuccessful because, although the PCSDs were removed from the column with 30% diethyl ether in n-hexane, they were not separated from the lipid material which also eluted with the more polar solvent. The difference in behaviour of the PCSD isomers on the acid and basic alumina can be explained by considering the different possible configurations of the compounds (Scheme E). The PCSD isomers can exist equally as the tautomer (IX) which under basic conditions will form the cationic species (X). This can occur at the adsorbent surface when the basic alumina is used. The isomers are ionically bonded and not removed by organic solvents. The acid alumina however, keeps the PCSD isomers in the protonated form (X) which is more easily chromatographed. Once this equilibrium was appreciated it was possible to devise a novel combination of an upper basic and lower acidic alumina column to effect the desired separation of the PCSD isomers and the co-extracted polar material. During the first elution with n-hexane the PAD isomers are chromatographed and the lipid residues and the PCSD isomers are retained at the head of the column. After the PADs have been eluted, the lipid resides are removed by increasing the polarity of the solvent with diethyl ether (30%). The PCSDs retained at the head of the column on the basic alumina are released by acidifying with a solution of glacial acetic acid (15%) in n-hexane, and continuing to elute with the diethyl ether in n-hexane.

Mass fragmentography of PCSD and PAD isomers

The cleaned-up samples were analysed by g.c.—m.s. in the s.i.m. mode with the multiple ion monitor. The advantages of this technique were the increased sensitivity over the t.i.m. mode and the inherent selectivity displayed by resultant fragmentograms. The specific ion selected for the PAD isomers was *m/e* 321, the major ion from the *m/e* 319—326 isotopic cluster (Fig. 5). The PCSD isomers were monitored by *m/e* 334 from the *m/e* 332—338 isotopic cluster and by *m/e* 370 from the *m/e* 368—374 isotopic cluster (Fig. 4a) of the thermal decomposition product.

The mass fragmentogram of the PAD and PCSD isomers in perch liver extract is given in Fig. 6 and examples of the concentrations of these materials found in the fish tissue are given in Table 1.

CONCLUSIONS

The active ingredients of Eulan WA New have been isolated and identified as pentachloro-2-(chloromethylsulphonamide) diphenyl ether and hexachloro-2

Scheme E

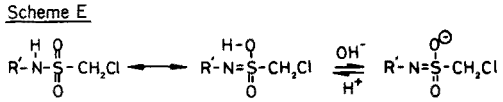

IX X

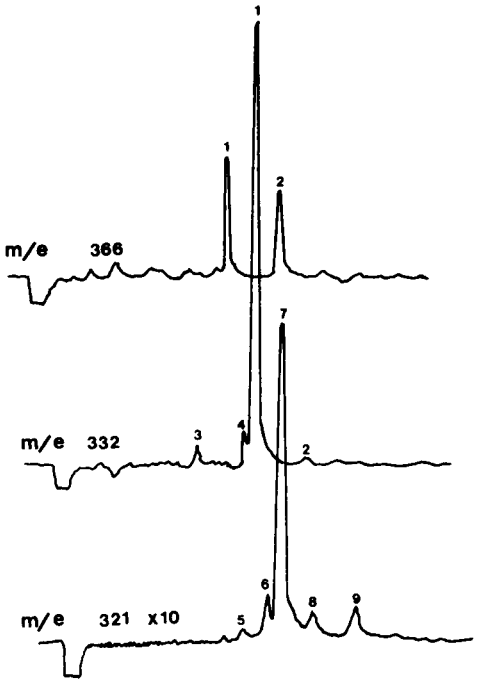

Fig. 6. Mass fragmentogram of a perch liver extract for PCSD and PAD isomers. PCSD isomers analysed as the PCD decomposition product. *m/e* 366 and *m/e* 332: peak 1, pentachloro-2-(chloromethylsulphonamide) diphenyl ether; peak 2, hexachloro-2-(chloromethylsulphonamide) diphenyl ether; peaks 3 and 4, unknown. *m/e* 321: peaks 5, 6, 8 unknown; peak 7, pentachloro-2-aminodiphenyl ether; peak 9, hexachloro-2-aminodiphenyl ether.

TABLE 1

Analysis for PCSD and PAD isomers in fish tissue (Results are given in mg kg^{-1})

	PCSDs		PADs		t-PCSD/t-PAD
	VII	V	VI	VIII	(VII + V)/(VI + VIII)
Pike (Muscle)	0.26	0.10	0.98	0.11	0.33
(Liver)	0.10	0.02	3.72	2.16	0.02
Perch (Muscle)	0.58	0.04	0.01	0.01	31.00
(Liver)	5.28	0.44	0.48	0.48	6.22
Trout (Muscle)	0.30	0.16	0.01	0.01	23.00
(Liver)	1.92	0.28	0.34	0.42	2.89

(chloromethylsulphonamide) diphenyl ether. The configurations of the chlorine atoms on these diphenyl ether nuclei gave every indication of being identical to those on the pentachloro- and hexachloro-2-aminodiphenyl ethers, which are present as impurities, or which occur as metabolites in natural samples.

The PCSD isomers have been shown to decompose within the injection port of the g.c. to form the penta- and hexachloro-2-(*N*-chloromethylamino) diphenyl ether by a three-centred elimination of sulphur dioxide. This decomposition product then gives a reproducible chromatographic response which can be related directly to the PCSD isomer.

The method clean-up developed with mixed acid and basic alumina has enabled the PCSD and PAD isomers to be separated from the coextracted lipid material as well as being recovered quantitatively. The initial results (Table 1) from the analysis of fish tissue show that it is possible to obtain the concentrations of the individual isomers and metabolites and to monitor the parent/metabolite ratios.

The author wishes to thank Dr. R. Tranter, University of Stirling, for the metastable analysis of the PCSD isomers, and Dr. S. Evans, Finnigan Instruments, for obtaining the c.i.—methane spectra of the components of the Eulan WA New chromatogram.

REFERENCES

1 Farbenfabriken Bayer AG, private communication.
2 The Non-Agricultural Use of Pesticides in Great Britain, Pollution Paper No. 3, HMSO (London), 1974.
3 G. Westöö and K. Noren, Ambio, 6 (1977) 232.
4 K. Wrabetz, H. Scheiter and D. Meek, Fresenius Z. Anal. Chem., 271 (1975) 272.
5 D. E. Wells and S. J. Johnstone, J. Chromatogr., 140 (1977) 17.

Analytica Chimica Acta, 104 (1979) 267—278

CONSTRUCTION AND PERFORMANCE OF A TIME-MULTIPLEX MULTIPLE-SLIT FLAME ATOMIC FLUORESCENCE SPECTROMETER FOR MULTI-ELEMENT ANALYSIS

ERIC D. SALIN** and J. D. INGLE, JR.*

Department of Chemistry, Oregon State University, Corvallis, Oregon 97331 (U.S.A.)

(Received 6th June 1978)

SUMMARY

The design and performance characteristics of a new multi-element flame atomic fluorescence spectrometer are presented. Radiation from four hollow-cathode tubes is directed onto an unsheathed air—hydrogen flame. The resulting atomic fluorescence is viewed by a special monochromator with a separate exit slit for each element. The light exiting from all slits is directed to a single photomultiplier tube. The fluorescence signals from different elements are distinguished by a time multiplex approach. Single-element detection limits for ten elements and multi-element detection limits for four elements are presented. The degradation of detection limits by flame background emission noise and effect of flame composition on performance are discussed. Better than 1% precision is obtained for moderate analyte concentrations.

Atomic fluorescence (a.f.) potentially offers many advantages for multi-element analysis [1] and has attracted numerous workers in this field [2—16] in attempts to exploit these advantages with a very diverse set of approaches. While a flame emission or hollow-cathode lamp spectrum contains many lines, an a.f. spectrum usually only contains one or a few lines so that lower resolution monochromators and large spectral bandpasses may be employed. Other advantages include linear calibration graphs over several orders of magnitude, simple source alignment and the ability to use line or continuum sources. The simplest approaches to multi-element a.f.s. are those of Palermo et al. [4] and Walsh [7]. Neither of these systems used a monochromator of any type. Instead a solar-blind photomultiplier tube was employed.

Palermo et al. [4] introduced the "time division multiplex" mode of operation in which the pertinent data are separated by temporal division. This mode requires that each hollow-cathode lamp is pulsed at a different time and that the collection electronics be co-ordinated with the pulsing electronics. Demultiplexing of a time multiplex signal is considerably easier than demultiplexing signals from other domains such as frequency. The pulsing of the

**Present Address: Department of Chemistry, University of Alberta, Edmonton, Alberta T6G 2G2 (Canada).

hollow-cathode lamps and data acquisition were controlled by a computer. The hollow-cathode lamps were operated in a low-duty cycle (turned on for a small fraction of the total time) and high-intensity mode (pulsed at higher currents) so that the lamp intensity per unit time was equivalent to a 50% duty cycle and no signal-to-noise disadvantages resulted. However, operation was limited to the u.v. region where the solar-blind tube has a measurable response and the flame background is low. The resonance wavelengths of the elements studied were all below 260 nm. Both flame and electrothermal atomization were employed.

Chester and Winefordner [14] described a multi-element frequency-multiplex non-dispersive a.f.s system with a solar-blind photomultiplier tube in which two electrodeless discharge lamps are chopped at different frequencies and each signal is discriminated with a separate lock-in amplifier. Also a multi-element Fourier transform non-dispersive a.f. spectrometer [15] and a multi-element Hadamard transform a.f. spectrometer [16] have been described. Another system used a rotating filter wheel instead of a monochromator which placed appropriate broadband filters in sequence in the optical path between the flame and a photomultiplier tube [2, 3, 9]. The pulsing of the hollow-cathode lamps was co-ordinated with the rotation of the wheel so that the lamps were pulsed only when the appropriate filter was in place. The filters could be large and were placed close to the flame, thus allowing a high light-collection efficiency.

Most workers have used dispersive systems and a sequential analysis approach implemented with a programmable monochromator [3, 5, 6, 8, 10—12]. The more modern systems utilize computer control [5, 6, 8] allowing great versatility and speed in wavelength selection and optimization. Because large slits are used, wavelength selection is simplified because precise positioning is unnecessary. For sources in sequential dispersive systems, hollow-cathode lamps [3, 5, 9, 10—12], electrodeless discharge lamps [3], and EIMAC xenon lamps [5] have been employed.

Chester et al. [13] used a silicon-intensified target (s.i.t.) multichannel detector and a monochromator with an EIMAC xenon arc lamp for simultaneous multi-element a.f.s. and found that detection limits were worse than with a programmable monochromator system.

Recently, a modified multi-element atomic absorption (a.a.) spectrometer has been described [17, 18]. It employs a multiple-exit slit monochromator, one photomultiplier tube and no moving parts; it does not require computer control, distinguishes among signals with a time-multiplex approach, and can monitor a spectral range of 200 nm. The instrument can easily be converted to a multi-element a.f. spectrometer by changing to a different burner and flame and by changing the orientation of the hollow-cathode lamps. This paper is concerned with a preliminary evaluation of this new multi-element dispersive time-multiplex a.f. spectrometer. The spectrometer has the advantages of both the speed and simplicity of non-dispersive systems and the wide wavelength operating range and background discrimination of programmable monochromator systems.

EXPERIMENTAL

Instrumentation

The instrumentation is a modification of a previously described time-multiplex multiple-slit flame a.a. spectrometer [17, 18]. Hence the basic instrumentation and operation of the system will be briefly reviewed and only the differences will be described in detail.

A block diagram of the instrument is presented in Fig. 1. It is optically similar to a conventional single-element a.f. spectrometer in many respects. The radiation from four single-element hollow-cathode lamps is directed at the flame. The resulting a.f. signals are collected by a lens and directed into the medium-resolution ($f/8$) monochromator entrance slit (1.2 mm wide). The normal single-exit slit is replaced by a multiple-exit slit which has 1.2-mm wide exit slits at the locations necessary to transmit the desired resonance radiation for each element. The radiation exiting from all slits is directed with a high-efficiency mirrored photon funnel to the photocathode of one photomultiplier tube. The photo-anodic current is converted to a voltage with a current-to-voltage (I—V) converter with a 0.1-ms time constant and then converted by a voltage-to-frequency (V—F) converter to a pulse train.

The signals from each element are distinguished with the time-multiplex approach previously used for a multi-element non-dispersive system [4]. The clock and control circuit, which consists of a crystal clock, counters, demultiplexers and monostables [17, 18], supplies 10-ms logic signals to turn each lamp on and off sequentially one at a time and to direct the V—F pulse train at the proper time to a separate up-down counter for each element. For this work, the pulsing frequency was 12.5 Hz and the duty cycle 12.5%, so that in an 80-ms period each lamp is on for 10 ms with a 10-ms off-time between lamp pulses from different lamps.

At the beginning of the cycle, lamp 1 is pulsed on and after a 0.7-ms delay to allow for the rise time of the lamp pulse, the V—F pulse train is directed

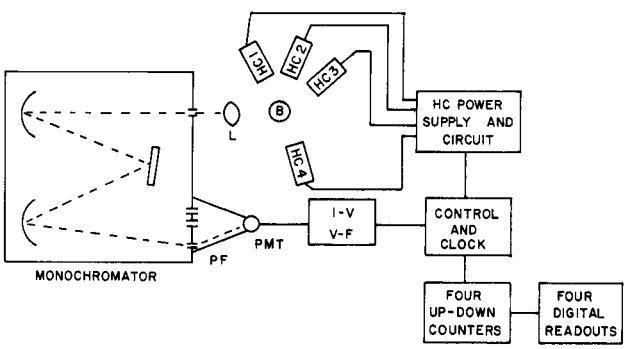

Fig. 1. Block diagram of instrument. PMT, photomultiplier tube; I—V, current-to-voltage converter; V—F, voltage to frequency converter; HC, hollow cathode tube; L, focusing lens; B, burner; PF, photon funnel. Lenses not shown.

into the up input of up-down counter 1 for 9.3 ms. After lamp 1 has been turned off and an identical 0.7-ms delay time, the V—F pulse train is directed to the down input of up-down counter 1 for 9.3 ms. This addition—subtraction performed in the first 20 ms by the up-down counter provides a number displayed on the digital readout for which the contribution from the steady-state dark current and flame background signals has been subtracted. This sequence is repeated for the other three lamps; there is a separate up-down counter and digital readout for each element. After each lamp has been pulsed on once and one background signal has been subtracted for each lamp, a single "lap" has been completed. The electronics allow collection of 1—256 laps.

The lamp-pulsing and data-acquisition electronics are identical to the previously described flame a.a. spectrometer [17]. The primary differences are the arrangement of the hollow-cathode lamps, the type of burner and flame, and the construction of the multiple slit mask.

Figure 2 is a photograph showing the arrangement of the optical and atomization components. The lamps are arranged around the flame in a semicircle; lenses (1 in. diameter $f/3$ focal length) are used to focus the radiation from each lamp into a beam with a cross-section of approximately 0.5 in. diameter. A Meker-type burner head, constructed from aluminium, is installed on the Jarrell-Ash nebulizer-chamber assembly in place of the normal slot burner head. The Meker head has a 16-hole pattern of holes (0.040 in. diameter) spaced uniformly in a circular area 0.5 in. in diameter.

To minimize lamp radiation scatter, all exposed surfaces which could reflect radiation into the monochromator are blackened. To reduce scatter further, two tubes of 1 in. diameter were made from black construction paper. The first tube (5.5 in. long) is placed around the optical axis between the entrance

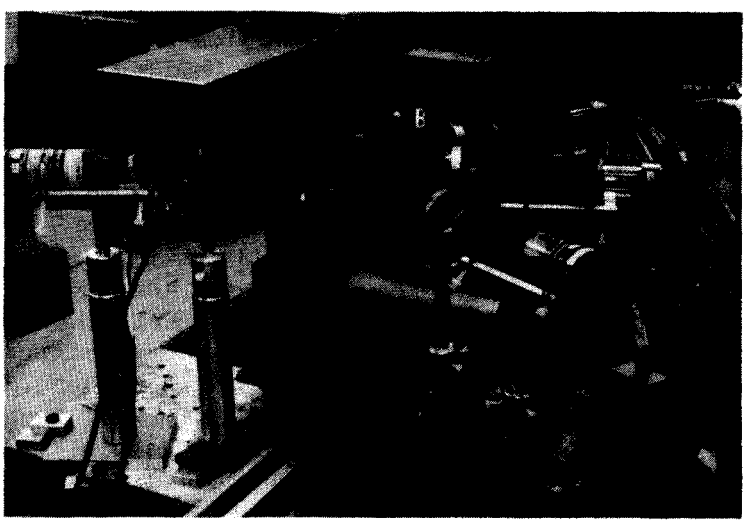

Fig. 2. Photograph of optical components. (A) Meker Burner; (B) Light Tube.

lens and the entrance slit. The second tube (3 in. long) is fixed to the other side of the entrance lens and pointed down the optical axis toward the flame.

The entrance slit (1.2-mm wide) and the slits on the multiple-exit array are of the same size, to yield a 4.2-nm spectral bandpass. The construction of the multiple-exit slit array is simpler than that used for a.a.s. [17]. For a.a.s., higher resolution is required and 85-μm slits have to be placed with an accuracy of ± 10 μm by using elaborate photoreduction and etching techniques. For a.f.s. 1.2 ± 0.1-mm slits need only be placed within $\pm$ 0.1 mm of the correct position.

The correct slit positions (distances between the centers of the slits) were previously determined photographically [17]. The a.f.s. multiple exit slit mask is made by placing a piece of black electrical tape on a 1×3 in. quartz slide which is placed on top of the previously prepared [17] multiple-exit slit mask. A razor blade is used to cut out slits (1.2 mm wide and 13 mm high) centered at the positions indicated by the mask for a.a.s. The slide is placed in a slit array holder and aligned in front of a 1×3 in. slot cut in the focal plane of the monochromator, as previously described [17]. Slits were made for Cu (324.7 nm), Mn (279.5 nm), Au (267.6 nm), Fe (248.6 nm), Co (240.7 nm) and Zn (213.9 nm). The Mg (285.2 nm) and Pb (283.3 nm), and Ni (232.0 nm) and Cd (228.8 nm) line pairs were so close that a single 1.2-mm slit was used for each pair. It is possible to make a multiple slit mask for any group of elements as long as the wavelength spread is 200 nm or less.

Operation

In each experiment, all unused slits were blocked with tape. For most experiments the IP28 photomultiplier tube was operated at 1000 V. The gain on the *I—V* converter was varied from 10^5 to 10^7 V A^{-1} as necessary, to prevent readout resolution limitations. All data were collected over 100 laps to provide signal averaging. Ths corresponds to a total measurement time of 8 s for four elements in which the atomic fluorescence and background signals for each element are each measured for 1 s.

The system was normally operated with the burner head 2 cm below the optical axis. Hydrogen was used as the fuel, and the flow rate was varied from 0.6 to 5.0 l min^{-1}. Air flow was maintained at a constant 4.8 l min^{-1} with a resultant sample flow rate of 4 ml min^{-1}.

The hollow-cathode lamps were normally operated at 50—75% of their maximum rated r.m.s. current to achieve high intensity (see Table 1). The lamp current during a pulse is eight times the r.m.s. value. Lamp positions were optimized by aspirating an appropriate standard (high range) and adjusting the lamp position for maximum peak signal while monitoring the signal output of the *I—V* converter with an oscilloscope.

All standards were prepared from reagent-grade metal salts and distilled, deionized water. The detection limits determined are defined as the concentration yielding an analytical signal twice the r.m.s. noise in the blank signal.

TABLE 1

Data for Single-element determinations

Element	λ (nm)	Detection limits				Lamp			
		A(ppb)[a]	B(ppb)[b]	C(ppm)[c]	D(ppm)[d]	H_2 Flow ($l\ min^{-1}$)	Current (mA)[e]	Noise[f]	Slope[g]
Au	242	300	—	9	—	2.6	12	4 (0.5)	2.4
Au	267	200	50	100	—	2.6	12	2 (0.5)	2.0
Cd	283	20	8	1	20	0.4	6	0.8 (0.8)	7.9
Co	241	60	40	2	—	4.4	15	0.4 (0.5)	1.3
Cr	358	200	—	40	—	5.2	15	1 (0.5)	1.3
Cu	325	7	5	0.3	—	0.4	13	2 (0.8)	48
Fe	248	300	60	0.6	—	4.4	15	8 (0.5)	5.4
Mg	285	40	2	0.1	—	5.2	8	60 (0.25)	300
Mn	280	50	5	0.5	—	5.2	16	10 (0.5)	4.
Ni	232	100	50	1	—	5.2	15	4 (0.5)	8.5
Pb	283	7,000	50	1000	20,000	0.7	6	16 (2)	0.4
Pb	217	35,000	—	—	—	2.8	6	8.4 (0.5)	0.0
Zn	214	30	20	1	500	3.2	13	0.3 (0.5)	2.0

[a]Determined under optimal single-element conditions by the time-multiplex a.f.s. method.
[b]Determined under multi-element conditions [17] by the time-multiplex a.a.s. method.
[c]Best reported values for atomic fluorescence with hollow-cathode lamps [19].
[d]Multi-element values reported for time-multiplex non-dispersive system [4].
[e]For time-multiplex method.
[f]Single-element photocathodic rms noise $\times 10^{18}$ A in blank signal: the dark current and readout noise, in the same units, are in parentheses.
[g]Photocathodic current per ppb $\times 10^{20}$ A.

RESULTS AND DISCUSSION

Single element determinations

The time-multiplex multi-element a.f.s. detection limits for single elements and other data obtained with only one slit open are presented in Table 1. Since the detection limits were observed in some cases to vary by over an order of magnitude with hydrogen flow rate, the values reported are for the optimum conditions. For comparison purposes, the values obtained with the instrument in the flame a.a.s. mode with the same integration time (100 laps) are presented. The best single-element a.f.s. detection limits [19] for hollow-cathode sources are also reported. These values are not necessarily obtained with the same flame used in this work, nor are they necessarily obtained with an instrument suitable for multi-element analysis. The detection limits reported by Palermo et al. [4] under compromise multi-element conditions are also reported these data are of interest because the system operates in the time-multiplex mode (although it is non-dispersive) and uses a sheathed air—hydrogen flame. Sheathing the flame improves detection limits by reduction of the flame background and noise. The present burner was not sheathed, but the detection

limits obtained for single-element analysis are the same or much better than those obtained by Palermo et al [4]. In all cases except gold, the single-element detection limits are considerably worse than those obtained with a.f.s. by other workers, with hollow-cathode lamps, but are within a factor of 5 of those obtained with the t.m.m.s. instrument in the flame a.a.s. mode (except for Mg, Mn and Pb).

Unlike the flame work previously carried out with the air—acetylene flame [17], for a.f.s. with the air—hydrogen flame the slope of calibration plots the detection limits and signal-to-noise ratios can vary considerably with flame composition. The atomization efficiency and/or fluorescence quantum efficiency appear to vary more with composition in the cooler air—hydrogen flame and so affect calibration curve slopes. In addition, the flame background and noise increase with the fuel-to-oxidant ratio and, from Table 1, background emission noise is usually the limiting noise at the detection limit. As an example, when the fuel flow for a 20-ppm copper solution is changed from 3.0 to 5.2 l min^{-1} (air = 4.6 l min^{-1}), the signal-to noise ratio drops by a factor of 8. The most severe case was that of magnesium. The signal from a 10-ppm magnesium solution is reduced to an undetectable level under the conditions that are optimal for copper, but under optimal conditions, magnesium generates the largest signal per unit weight.

Multi-element determinations

To test the multi-element performance of the instrument, cadmium, copper, magnesium and zinc were determined simultaneously in tap water under compromise flame conditions. These conditions (see footnotes to Table 3) were selected with two considerations in mind: (a) obtaining a measurable signal from magnesium at the ppm level, and (b) obtaining a good detection limit for copper, which was at the 50-ppb level. These two goals are opposed, but the compromise conditions selected met the requirements.

Calibration curves are shown in Fig. 3, the dependence of precision on analyte concentration is indicated in Table 2 and the detection limits and analytical data are presented in Table 3. The concentrations of Zn, Cu and Mg in tap water were also determined by flame a.a.s. on a Varian AA-6 spectrophotometer. Cadmium was determined with the time-multiplex multiple-slit instrument by a.a.s. with carbon rod atomization [20].

At concentrations well above the detection limit, the signal-to-noise ratio is limited by signal shot noise, analyte fluorescence flicker noise and lamp flicker noise [21]. Table 2 shows the relative standard deviation in the fluorescence signal for Cd, Cu, Au, and Mg determined simultaneously. The precision at high concentrations is better than 1%, which is better than that previously reported for single-element a.f.s. measurement made on the Varian AA-6 [21]. At high concentrations, the precision decreases for some elements. This has been observed previously and has been ascribed to fluctuations in the inner filter effect [21].

The a.a.s. and a.f.s. analyses for zinc in tap water agree well, but cadmium was below the a.f.s. detection limit. The error for copper is within the experimental

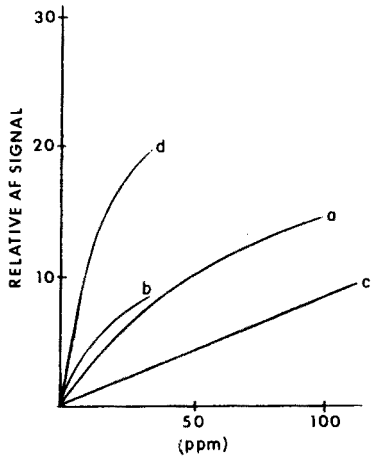

Fig. 3. Calibration curves. (a) Cu; (b) Zn; (c) Mg; (d) Cd.

TABLE 2

Relative standard deviations (%) for the time-multiplex multiple-slit a.f.s. method (All data recorded under multi-element conditions for the analysis of tap water; values were obtained from ten 100-lap determinations).

Conc. (ppm)	Relative standard deviation (%)			
	Zn	Cd	Cu	Mg
0.1	20	12	12	—
0.25	10	4	3	12
1	3	2	2	3
2.5	1.7	1.1	1.2	1.2
10	0.7	0.6	0.4	—
25	1.6	1.2	0.7	1.5
100	2	—	0.9	0.7
250	—	—	2	0.8

error; the value is near the detection limit of the present a.f.s. system under these conditions. The magnesium value by a.f.s. is low, probably because of incomplete atomization in the cooler air—hydrogen flame. The value determined by a.f.s. varied with flame composition. Evidently, compounds in tap water bind with magnesium and reduce its atomization. EDTA was added to the sample in an attempt to bind magnesium preferentially, but this did not alleviate the problem.

Compared to single-element a.f.s., multi-element detection limits are expected to be worse for several reasons. This was observed (Table 3). The data in Table 4 demonstrate some of the basic problems. The background noise was measured under identical gain conditions with the flame off, and

TABLE 3

Tap water analysis by the proposed a.f.s. method[a]

Element	Detection limits		Amount found (ppm)		Ratio[e]
	(ppm)[b]	(ppm)[c]	A.a.s.	A.f.s.[d]	
Zn	0.2	0.03	0.48	0.45	0.78
Cu	0.05	0.007	0.083	0.065	2.3
Mg	0.1	0.04	5.6	3.4	0.13
Cd	0.09	0.02	0.007	not detected	0.70

[a]Photomultipler tube gain = 2×10^6, $R_f = 10^7\ \Omega$, H_2 = 3.0 l min^{-1}, air = 4.6 l min^{-1}.
[b]Under the compromise conditions of the multi-element a.f.s. method.
[c]Single-element values from Table 1.
[d]Time-multiplex multiple-slit multi-element determination.
[e]Ratio of multi-element calibration slope to best single-element slope.

TABLE 4

Background emission noise dependence on slits
All noise expressed in terms of cathodic current $\times 10^{18}$ A. Photomultiplier tube gain = 3×10^6 and $R_f = 10^7\ \Omega$.

Slits	H_2 Flow (l min^{-1})			
	0 (no flame)	0.7 (lean)	2.8 (rich)	4.9 (very rich)
All ten	2	4	14	50
Top four	2	2	3	12
Bottom four	2	3	13	50

with different flame compositions for different sets of slits open. The "top" four slits consist of the Zn, Cd, Ni and Co slits and range from 214 to 241 nm. The "bottom" four slits include the Cu, Mg, Pb and Mn slits and range from 280 to 325 nm. The bottom set of slits encompass the OH bandhead observed in all analytically-used combustion flames.

Several important observations can be made based on the data in Table 4. First, as expected, the noise increases with the fuel richness and hence the luminosity of the flame. Secondly, also as expected, the absolute background signal and noise are greater for the bottom (higher wavelength) slits that coincide with the OH emission; the absolute noise with all slits open does not differ appreciably from that with just the bottom four slits open. This implies that the background noise for a determination of all ten elements is not significantly greater than that observed for Cu, Mg, Pb and Mn. This does not mean that the detection limits will be the same as those for single-element analysis, but that the addition of another element to a multi-element analysis scheme does not necessarily mean a substantial increase in background noise.

The higher background emission signal and noise with multi-element a.f.s. is more of a problem for elements with short wavelength resonance lines, such

as Zn, Cd, Ni, Co and Fe, whose flame emission background is low, if they are determined with elements like Cu, Mg, Mn and Pb (283 nm) which have high flame emission background levels. Also with a compromise flame composition, the background noise can be higher and the calibration slope less than for the optimal composition for single-element determinations.

For the test multi-element analysis (see Table 3), the magnesium calibration slope is about 1/8 of its optimal value. The slopes for cadmium and zinc are changed only slightly. However, the background flame emission from the copper and magnesium slits has substantially degraded the detection limit for these elements. The copper slope is increased, and the detection limit is reduced from that for single element measurement obtained under very lean flame conditions. The best magnesium signal-to-noise ratio is obtained for richer flames where the ratio of calibration slope to background emission noise is greater.

One other difficulty caused by the multiple-slit design is a potential spectral problem. This problem is due to radiation from one hollow-cathode lamp passing through a slit other than the desired slit. This is much less of a problem than in the a.a.s. mode [17] where the monochromator directly views the entire lamp output. In the a.f.s. mode, the excess of radiation could result from either scattering of non-resonance lines or from fluorescence from other elements caused by other resonance lines from a hollow-cathode lamp. The former type of spectral problem will only affect the magnitude and noise of the blank signal, and the problem was not found with the sources employed. The latter type of spectral problem can cause errors in analysis since the fluorescence signal observed in one electronic channel can be due to two or more elements. For instance, for the simultaneous determination of copper and zinc, the copper line from the zinc lamp would cause copper fluorescence in the sample, and this would result in an enhanced signal in the zinc channel. Previous work [17] indicates that problems will exist in determinations of Zn with Cu, Mn with Cu, Fe with Cu, Co with Mg, Ni with Mn, and Zn with Pb. In some cases the secondary resonance lines are relatively weak, so that each situation must be evaluated individually.

Certainly zinc with copper is one of the most difficult problems because the copper line is much more intense than the zinc line. Filters can be used to eliminate or minimize this problem; however, in this case an "interference" calibration was made for the signal that a given concentration of copper would produce in the zinc channel. The concentration of copper was determined and the appropriate correction from the "interference" calibration curve was made for the data in Table 3. The use of filters should generally be avoided while measuring atomic fluorescence near the detection limit, because the signal attenuation directly affects the signal-to-noise ratio and therefore the detection limit. The detection limit is raised by exactly the amount that the signal is attenuated. The best interference filters available in this laboratory have a 20% throughput and will raise the detection limit by a factor of 5. For zinc, the filter has a throughput of 10%; this would raise the detection limit to 2 ppm, which is above the zinc concentration in tap water.

CONCLUSIONS

The time-multiplex multiple-slit spectrometer is a viable approach to multi-element analysis. It costs little more than a single-element a.f. spectrometer because it requires only one photomultiplier tube and associated power supply, a medium-resolution monochromator, and one hollow-cathode lamp power supply. The simple electronics, photon funnel and multiple slit array add little to the cost. Computer control is not required as with sequential programmable monochromator systems. The effective focal plane coverage is greater than with electronic multichannel detectors. The spectral range covered is larger than possible with non-dispersive systems with a solar blind photomultiplier tube.

Changing to another set of elements is rapid because of the ease of lamp alignment and of the multiple exit-slit array manufacture. Extension to simultaneous analysis of more than four elements is possible.

The detection limits, though sub-ppm, are considerably worse than the best single-element values reported because of the low-intensity sources employed. However, they are adequate for many samples. Improvements would result from optimization of slit width, lamp duty cycle and pulsing frequency, and the use of a different flame and more intense sources (e.g. electrodeless discharge tubes). The air—hydrogen flame was limiting because of its poor atomization characteristics and the dependence of fluoresence signal and detection limits on flame composition. Hotter flames, sheathing, and better burner design would minimize many of these problems. It would also be possible to carry out simultaneous atomic absorption and fluorescence measurements, which have previously not been demonstrated.

The basic instrumental design could be used to construct a sequential dye laser-excitation atomic fluorescence spectrometer. Only the dye laser wavelength need be programmed. The multiple-slit array could be constructed for specific elements as was shown in this paper or a mask could be constructed which only blocked radiation at wavelengths where the flame exhibited intense band emission.

REFERENCES

1 J. D. Winefordner, J. J. Fitzgerald and N. Omenetto, Appl. Spectrosc., 29 (1975) 369.
2 D. Mitchell and A. Johansson, Spectrochim. Acta., Part B, 25 (1970) 175; 26 (1971) 677.
3 J. D. Norris and T. S. West, Anal. Chem., 45 (1973) 226; Anal. Chim. Acta, 55 (1971) 359; 59 (1972) 474.
4 E. G. Palermo, A. Montaser and S. R. Crouch, Anal. Chem., 46 (1974) 2154.
5 D. J. Johnson, F. W. Plankey and J. D. Winefordner, Anal. Chem., 47 (1975) 1739.
6 R. W. Spillman and H. V. Malmstadt, Anal. Chem., 48 (1976) 303.
7 A. Walsh, Pure Appl. Chem., 23 (1970) 1.
8 R. W. Spillman and H. V. Malmstadt, Am. Lab., March (1976) 89.
9 R. M.Dagnall G. F. Kirkbright, T. S. West and R. Wood, Anal. Chem., 43 (1971) 1765; 97 (1972) 245.
10 A. Fulton, K. C. Thompson and T. S. West, Anal Chim. Acta, 51 (1970) 373.

11 G. B. Marshall and T. S. West, Anal. Chim. Acta, 51 (1970) 179.
12 M. S. Cresser and T. S. West, Anal. Chim. Acta, 51 (1970) 530.
13 T. L. Chester, H. Haraguchi, D. O. Knapp, J. D. Messman and J. D. Winefordner, Appl. Spectrosc., 30 (1976) 410.
14 T. L. Chester and J. D. Winefordner, Spectrochim. Acta, Part B, 31 (1976) 21.
15 S. J. Martin and H. V. Malmstadt, Pittsburg. Conf. Anal Chem. and Appl. Spectrosc., Cleveland, Ohio, 1975.
16 F. W. Plankey, T. H. Glenn, L. P. Hart and J. D. Winefordner, Anal. Chem., 46 (1974) 100
17 Eric D. Salin and J. D. Ingle, Jr., Anal. Chem., 50 (1978) 1737.
18 Eric D. Salin, Ph.D. Thesis, Oregon State University, 1978.
19 V. Sychra, V. Svoboda and I. Rubeska, Atomic Fluorescence Spectroscopy, Van Nostrand Reinhold, 1975, pp. 187—299.
20 E. Salin and J. D. Ingle, Jr., Appl. Spectrosc., in press (Vol. 32).
21 N. W. Bower, Ph.D. Thesis, Oregon State Univ., 1977.

Analytica Chimica Acta, 104 (1979) 279—284

MERGING ZONES IN FLOW INJECTION ANALYSIS
Part 2. Determination of Calcium, Magnesium and Potassium in Plant Material by Continuous Flow Injection Atomic Absorption and Flame Emission Spectrometry

E. A. G. ZAGATTO, F. J. KRUG, H. BERGAMIN F°*, S. S. JØRGENSEN** and B. F. REIS
Centro de Energia Nuclear na Agricultura CEP. 13.400 Piracicaba, S. Paulo (Brasil)
(Received 25th August 1978)

SUMMARY

A flow-injection analysis system is described for the automatic determination of calcium, magnesium and potassium in plant material by atomic absorption and flame emission spectrometry. Flow rates and damping factors were studied; the sample undergoes a dispersion of ca. 40-fold with automatic incorporation of lanthanum when necessary. The proposed method allows 300 determinations per hour with a typical relative standard deviation of 0.5% and a reagent consumption of only 500 μg of lanthanum per determination, which is about 1% the usual amount. The results for plant digests agree with those obtained by the standard a.a.s. procedure.

The flow injection approach [1] has been successfully applied to many analytical procedures with spectrophotometric [2, 3], potentiometric [4, 5] and turbidimetric [6] measurements. The technique requires precise sample dispersion control associated with reproducible injection and timing, which are usually easily achieved [7]. Sample dispersion, which is sometimes a drawback in flow injection analysis, can be a very useful experimental variable when concentrated samples have to be analysed or when reagents must be added to the samples.

The determination of calcium and magnesium in plant digests by atomic absorption spectrometry (a.a.s.) is usually done after appropriate dilution of the sample with addition of a lanthanum or strontium salt to prevent phosphate, sulphate and aluminium interferences [8]. If many plant samples have to be analysed, sample preparation is often the limiting factor in the analytical capacity of the laboratory.

This paper deals with a flow injection procedure for the determination of calcium, magnesium and potassium by a.a.s., where the required sample dilution and reagent addition are done automatically. The utilization of merging zones [9] and small sample volumes minimizes the consumption of masking agent.

**Present address: Chemistry Department, Royal Veterinary and Agricultural University, 40 Thorvaldsenssvej, DK-1871 Copenhagen V, Denmark.

The required sample dispersion is achieved by using the confluence configuration [4] associated with appropriate system dimensions [7].

EXPERIMENTAL

Apparatus

A Technicon AAII peristaltic pump furnished with suitable tygon pumping tubes was employed. Preliminary experiments indicated that the aspiration capacity of the spectrometer alone was not enough to provide an adequately constant flow rate for precise results.

The double proportional injector [9] used permits the utilization of merging zones. A low sample volume (20 μl) was chosen in order to save reagents and to obtain the required degree of sample dispersion. The injected volume of reagent was 50 μl.

The Perkin-Elmer model 306 atomic absorption spectrometer used was connected to an ECB (Equipamentos Cientificos do Brasil Ltda., Sao Paulo) recorder. The spectrometer was operated in accordance with the Perkin-Elmer standard procedures for maximum sensitivity with air—acetylene flames. Conventional hollow-cathode lamps were used for calcium and magnesium; potassium was measured by emission spectrometry. The dispersion coil (Fig. 1) was connected to the aspiration tubing of the spectrometer.

Samples, standards and reagents

Wet digestion with nitric—perchloric acid [6] was employed for mineralization of the plant leaves from *Sorghum spp.* These digests were used without treatment in the proposed method. For conventional a.a.s., 0.5 ml of each digest was mixed with 2.5 ml of a 5% (w/v) lanthanum solution and the volume was made up to 25 ml with demineralized water.

Working standards for flow injection analysis contained 0.4 M perchloric acid and covered the ranges 0—350 ppm (Ca and K) and 0—80 ppm (Mg).

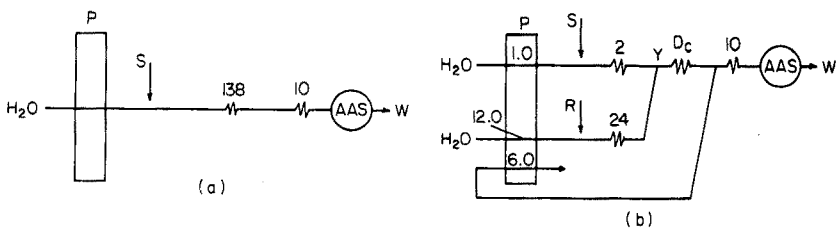

Fig. 1. Flow diagrams of (a) the system used to investigate flow rate through the burner and damping factor (for a 150-ppm Ca standard), and (b) the system used for analysis. In the analytical system, 20 μl of sample, S, and 50 μl of reagent, R (1% La solution for calcium and magnesium or distilled water for potassium) are injected into water carrier streams. The corresponding sample and reagent zones merge at point Y and are directed to a dispersion coil, D_C (230 cm long for K and Mg, or 99 cm for Ca). P is the peristaltic pump; AAS is the spectrometer; W denotes waste. The numbers under P represent pumping rates in ml min^{-1}; the numbers on the coils are coil lengths in cm. For details, see text.

These standards were diluted in the same way as the samples for the manual a.a.s. method.

All reagents used were of analytical grade and demineralized water was used in all experiments.

The lanthanum reagent used in the manifold was a 0.1 M HNO_3 solution containing 31.2 g of $La(NO_3)_3 \cdot 6H_2O$ per liter (1% La). With the system shown in Fig. 1(b), the quantity of lanthanum added to each ml of sample was 25 mg, which is slightly more than the recommended amount [8].

Manifold

The manifold was made entirely of polyethylene tubing (0.86 mm i.d.). The injector and all connectors were made from perspex. Details of the system build-up have already been described [3, 6]. The flow rate through the burner was fixed after preliminary experiments with the system shown in Fig. 1(a) and utilization of a 150 ppm Ca standard. Flow rates of 6.7, 7.8, 9.2, 12.1 and 15.3 ml min^{-1} were tested. Under normal conditions, the aspiration rate of the spectrometer is about 6 ml min^{-1}; therefore when the flow rate through the burner was below this amount erratic results were obtained mainly because of air entering the flow injection system through the connectors. Different damping factors (0.5, 1.2, 4.5 and 15.8 s, experimentally measured) were also tested for each flow rate.

In the proposed system (Fig. 1b), the sample and lanthanum reagent were injected simultaneously into water carrier streams which merged at point Y, giving good overlap of the sample and reagent zones, as indicated in Fig. 2. After the dispersion coil, the stream was split, and one branch was directed to measurement. A damping factor of 1.2 s was employed.

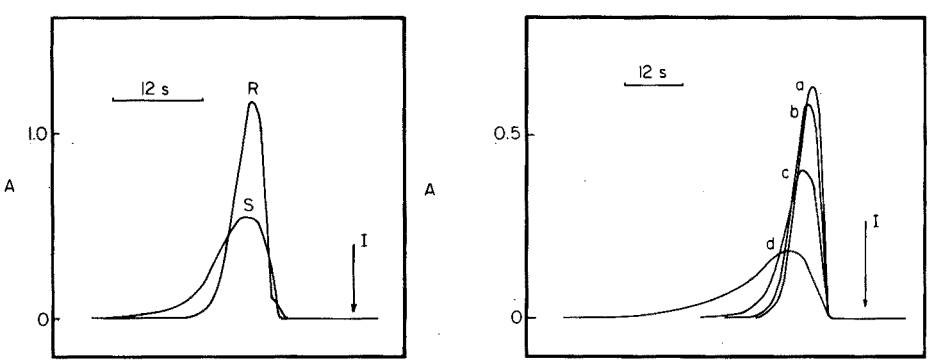

Fig. 2. Recorded high-speed peaks for calcium in the analytical system (Fig. 1b). Both sample (S) and reagent (R) were replaced by a 200-ppm Ca solution injected at time I.

Fig. 3. Influence of the damping factor on the recorded peak shape, for a 150-ppm Ca standard injected into the system (Fig. 1b) at instant I. a, b, c and d correspond to damping factors of 0.5, 1.2, 4.5 and 15.8 s, respectively.

RESULTS AND DISCUSSION

Damping factors and flow rates

Attenuation of the recorded peak height (Fig. 3) and improved reproducibility (Table 1) were achieved by using higher damping factors, but the sampling rate decreased. It is important to note that when high damping factors are employed, the sampling rate depends basically on the damping factor and not on the flow injection system. Accordingly, a damping factor of 1.2 s was chosen.

Increasing the flow rate through the burner decreased the recorded peak height (Fig. 4) and increased the sampling rate. Decreases in the signal happen mainly because, when the flow rate through the burner increases, the instrumental response is not fast enough to collect the entire pulse generated by the flow injection—burner system. The signals also decreased when the time constant of the amplifier was increased (Fig. 4). It is concluded, therefore, that all curves of Fig. 4 should have the same origin, because when the flow rate tends to zero, the absorbance to be measured can be fully detected.

A 7 ml min^{-1} flow rate through the burner was chosen. Higher flow rates were not used because the peak attenuation achieved would not be useful from the analytical view point, and flow rates below 6 ml min^{-1} could not be employed (see above). The desired signal attenuation was then achieved through sample dispersion, with consequent lowering of reagent consumption.

Sample dispersion

The dispersion of the sample was achieved by combining three procedures: (a) by making the injected volume as small as possible [7]; (b) by using a low

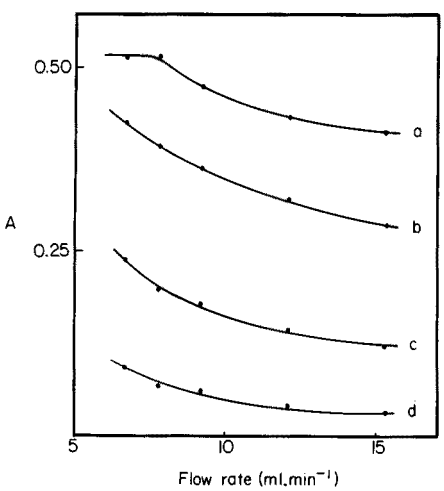

Fig. 4. Dependence of the recorded peak height on the flow rate through the burner and on the damping factor. a, b, c and d correspond to damping factors of 0.5, 1.2, 4.5 and 15.8 s, respectively.

ratio between sample and reagent carrier streams (thus at point Y (Fig. 1b) the sample zone underwent a 1:13 dilution); and (c) by splitting the flow before measurement, directing only a fraction of the sample zone to the burner. Larger system volumes, i.e. longer dispersion coils or wider tubing were not employed for dispersion, because this would have decreased the sampling rate.

It was not possible to design a single system to determine the three cations studied, because of their different concentrations in the digests and the sensitivity of the spectrometer. For calcium determinations, the dispersion coil was replaced by a smaller one (Fig. 1b), with consequent increase in sampling rate.

Analytical characterstics

The proposed system is suitable for determining potassium, calcium and magnesium in plant digests without pretreatment, at a typical sampling rate of 300 samples per hour, after adequate sample dispersion and incorporation of lanthanum (500 μg of lanthanum per sample) when necessary. In all cases the signal is measured in the most useful part of the calibration curve, with a typical standard deviation better than 1% (Table 1).

Table 2 indicates the comparative results obtained by the proposed system and by the conventional a.a.s. procedure.

TABLE 1

Influence of the damping factor on the reproducibility and sampling rate. The data were obtained with the system shown in Fig. 1b and refer to a 150-ppm Ca standard.

Damping factor (s)	0.5	1.2	4.5	15.8
Sampling rate[a] (samples/h)	360	320	200	100
R.s.d. (n = 10)	2.6	0.8	0.4	0.4

[a]As described earlier.

TABLE 2

Comparative results obtained by the proposed method (A) and by the conventional a.a.s. procedure (B). Data refer to the element content (%) in dry matter.

Sample	K		Mg		Ca	
	A	B	A	B	A	B
1	2.78	2.77	0.48	0.47	0.86	0.75
2	2.55	2.55	0.35	0.36	1.78	1.75
3	1.85	1.95	0.27	0.25	0.57	0.50
4	2.31	2.39	0.60	0.60	1.92	1.80
5	1.84	2.00	0.47	0.47	0.92	0.90
6	1.99	2.08	0.62	0.60	1.80	1.80
7	3.32	3.49	0.14	0.15	0.45	0.46
8	2.45	2.57	0.35	0.35	1.80	1.70

The proposed system can also be used when the double proportional injector is not available. The reagent carrier stream (Fig. 1b) is then replaced by a 0.1% lanthanum (or the equivalent amount of strontium) solution, which meets the sample carrier stream at point Y. This procedure is suggested when only a single injector is available, or when the lanthanum or strontium salt to be employed as masking agent has a high calcium content which would give a blank value in the proposed system. In the confluence configuration, the consumption of reagent would be increased, but the blank would be eliminated [10].

Peter B. Vose is thanked for his assistance in the preparation of this manuscript.

REFERENCES

1 J. Růžička and E. H. Hansen, Anal. Chim. Acta, 78 (1975) 145.
2 J. Růžička and E. H. Hansen, Anal. Chim. Acta, 79 (1975) 79.
3 H. Bergamin F°, J. X. Medeiros, B. F. Reis and E. A. G. Zagatto, Anal. Chim. Acta, 101 (1978) 9.
4 J. Růžička, E. H. Hansen and E. A. G. Zagatto, Anal. Chim. Acta, 88 (1977) 1.
5 E. H. Hansen, F. J. Krug, A. K. Ghose and J. Růžička, Analyst, 102 (1977) 714.
6 F. J. Krug, H. Bergamin F°, E. A. G. Zagatto and S. S. Jørgensen, Analyst, 102 (1977) 503.
7 J. Růžička and E. H. Hansen, Anal. Chim. Acta, 99 (1978) 37.
8 C. Riandey, in M. Pinta (Ed.), Atomic Absorption Spectrometry, Adam Hilger, Bristol, (1975), p. 74.
9 H. Bergamin F°, E. A. G. Zagatto, F. J. Krug and B. F. Reis, Anal. Chim. Acta, 101 (1978) 17.
10 H. Bergamin F°, B. F. Reis and E. A. G. Zagatto, Anal. Chim. Acta, 97 (1978) 427.

Analytica Chimica Acta, 104 (1979) 285—291

AUTOMATIC METHOD FOR THE DETERMINATION OF TOTAL MERCURY IN FRESH AND SALINE WATERS AND SEDIMENTS

HAIG AGEMIAN* and J. A. DaSILVA

Canada Centre for Inland Waters, Water Quality Branch, 867 Lakeshore Road, P.O. Box 5050, Burlington, Ontario (Canada)

(Received 29th May 1978)

SUMMARY

Acid—dichromate and ultraviolet digestion are used sequentially in an automated system to extract mercury from particulate matter and oxidize organomercurials in briny waters and sediments. Mercury is then determined by reduction with tin(II) and cold-vapor atomic absorption spectrometry. The flow-through system is completely automatic and can accommodate samples with particulate solids up to 1 g l^{-1}. The detection limit is 0.02 μg Hg l^{-1} in water or 20 μg Hg kg^{-1} in sediments. Both waters and sediments with high chloride levels can be analysed without interference at a rate of 30 samples per hour.

Agemian and Chau [1] used an automatic u.v. digestion method to oxidize dissolved organomercury compounds in fresh and saline waters; the u.v. irradiation prevented interference from chloride. Sulfuric acid—u.v. digestion [1] effectively oxidizes dissolved organomercurials but only partially digests samples of high particulate matter, because u.v. rays do not penetrate turbid waters completely. For high-particulate waters, an acid digestion under oxidizing conditions would be more effective. Jirka and Carter [2] used sulfuric acid—persulfate for automatic digestion of particulate matter, but this digestion is unsuitable for saline waters as discussed earlier [1]. Thus automatic methods [2—7] in which strong oxidants such as persulfate or permanganate are used, cannot provide reliable results on sets of samples including saline waters or high varying levels of chloride.

The present paper reports an extension of the sulfuric acid—u.v. digestion technique [1] to include a sulfuric acid—dichromate digestion step which extracts mercury efficiently from particulate matter; this is followed by u.v. photo-oxidation to oxidize organomercurials in turbid waters. The upper limit for particulate matter in solution (1 g l^{-1}) allows the analysis of sediments if they are first slurried in distilled water and then treated like water samples. Dichromate is essential in the preservation of low levels of mercury in natural waters [8], and the present method is completely compatible with it. In essence, a concentrated form of the preservative system is used to leach mercury from the particulate matter, followed by u.v. photo-oxidation. Neither the dichromate

nor the u.v. radiation affects chloride, and total mercury can therefore be determined in water or sediments with varying salinities, from fresh to marine systems.

EXPERIMENTAL

Apparatus

The manifold (Fig. 1) consisted of the following conventional parts: (a) an automatic stirring sampler (Technicon AutoAnalyzer 11 sampler with 30-2/1 cam; alternatively, a magnetic stirring bar may be put in the sample bottle and sampling done manually while stirring; (b) proportioning pump (Carlo Erba, Model 08-59-10202); (c) oil bath set at 95°C with a Technicon heating coil (170-G060-01); (d) u.v. digestor [1, 9]. The gas separator (Fig.2) is an improved version of the one already reported [10], with a wider entrance and a much larger separation chamber to prevent suspended solids from entering the mercury cell. The original separator works well with clear waters only, whereas the new design can be used for both clear and turbid waters and for frothing and bubbling solutions; the separation efficiency of the two designs gave exactly the same calibration curves for clear solutions.

The mercury monitor (Pharmacia Fine Chemicals) has a 30-cm long cell and no background correction; mercury was determined at the 253.7-nm line. A Hewlett-Packard Model 7101B strip-chart recorder was used. A Polytron homogenizer (Brinkman Instruments) served for sample pretreatment of sediments.

All tubing used in the manifold (Fig. 1) was clear standard Technicon tubing except for the sulfuric acid line, which was Acidflex tubing. The two points

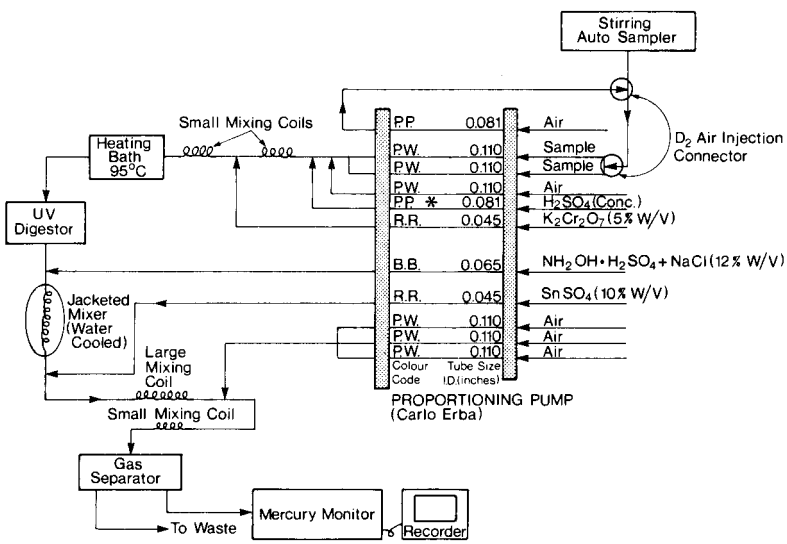

Fig. 1. Mercury manifold.

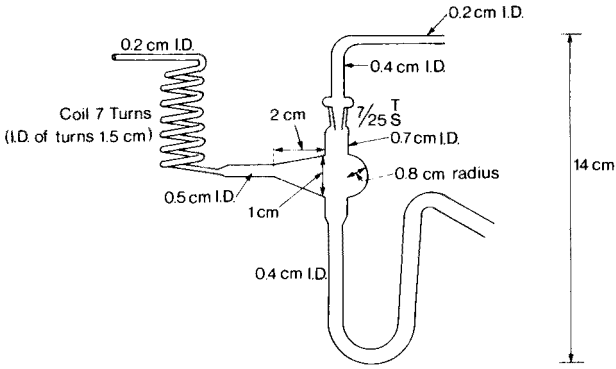

Fig. 2. Modified gas separator made of Pyrex tubing.

in Fig. 1 where the sample is injected into the manifold should be D2 air-injection connector glass fittings to scrub the tubes of particles.

Reagents and solutions

High-purity certified reagents (Fisher Scientific Company) were used. The reagent solutions were 5% (w/v) potassium dichromate in water, 10% (w/v) tin(II) sulfate in 1 M sulfuric acid, and 12% (w/v) hydroxylammonium sulfate in 12% (w/v) sodium chloride solution.

Mercury stock solutions were prepared from mercury(II) chloride (1000 mg Hg l^{-1}) and methylmercury(II) chloride (500 mg Hg l^{-1}).

Preservation

For the preservation of water samples (100 ml) in glass bottles, 1 ml of 18 M sulfuric acid and 1 ml of 5% (w/v) potassium dichromate were added [8]. For sediments, samples were obtained wet [11]; after homogenization, samples equivalent to about 100 mg (dry weight) were weighed into 250-ml plastic bottles, the above amounts of sulfuric acid and dichromate were added, and the mixtures were made up to 100 ml with distilled water. The samples were treated as turbid water samples.

Procedure

Before samples could be analysed in the flow-through system, the particulate matter in the water samples and sediment slurries had to be ground to give a fine suspension. Samples were therefore homogenized and pulverized in a Polytron Homogenizer. Suspended sediment samples were then aspirated into the system by the stirring technique described under Apparatus. Sampling was done for 30 s with wash periods of 90 s. The analytical system shown in Fig. 1 allows a sample rate of 30 per hour.

The blank value of the preservative is the only blank encountered in the method and is usually lower than 0.02 μg Hg l^{-1}. Some grades of dichromate

may contain high mercury blanks but this could be removed either by extraction of the 5% (w/v) dichromate solution with a solution of dithizone in chloroform (0.01% w/v) at pH 1.4—2.0, or by heating the $K_2Cr_2O_7$ crystals in a muffle furnace at 300—350°C.

DISCUSSION

The classical sulfuric acid—dichromate digestion method for organic matter has been used extensively for the determination of organic matter in soils [12]. As discussed earlier [1], this system does not react appreciably with chloride under the conditions of the mercury manifold and is compatible with the chemistry. The use of dichromate is advantageous in many respects. Its solutions are stable, do not have solid intermediate decomposition products (such as for $KMnO_4$), and are compatible with the preservative system used. Furthermore, as it can be used as quite concentrated solutions (5% w/v) it is valuable in the oxidation of large amounts of organic matter such as in soils and sewage samples, and is suitable for the routine monitoring of large numbers of samples.

In this study, the u.v. photo-oxidation (Fig. 1), gave good recoveries of organomercurials similar to that obtained by Agemian and Chau [1]. The sulfuric acid—dichromate digestion extracted mercury efficiently from sediment particles. The efficiency of the automatic extraction depended on the sample preparation for particulate samples and on the amount of sediment in the sample. The practical working limit for sediment was about 1 g l^{-1}, provided that an ultrasonic homogenizer such as the "Polytron" was used. With these precautions and the D2 air-injection glass fittings at the spots indicated on the manifold (Fig. 1), efficient movement of the sample slurry and suspension was obtained. Stirring of the sample during sampling and its homogeneous flow in the manifold are essential, because the preservative system extracts the mercury only slightly from the sediment particles. When sediments were stored under the preservative conditions for a week and then the supernatant solutions analysed, only about 1% of the mercury present was recovered. When the solution was stirred and the slurry was analysed automatically, 100% of the mercury was extracted.

Table 1 provides satisfactory comparative data for this method and a semi-automatic method for mercury in sediments [7, 13]. The latter is a comprehensive method, involving manual digestion with H_2SO_4—HNO_3 and a trace of hydrochloric acid at 60°C for 2 h, oxidation with $KMnO_4$—$K_2S_2O_8$, tin(II) reduction and cold-vapor measurement. In the present method, about 0.1 g (dry weight) of sediment is used, compared to about 1 g in the semi-automatic method [7, 13], yet the detection limits are the same, i.e. about 20 μg Hg kg^{-1}. The blank of the present method is due only to the preservative system (about 0.01 μg l^{-1}) whereas the blank from all the digestion acids and oxidants used in the semi-automatic method is 0.1—0.2 μg l^{-1}.

To check if the turbidity of the samples affected the u.v. photo-oxidation, several sediment slurry solutions were spiked with methyl-mercury(II) chloride.

TABLE 1

Comparison of semi-automatic method [13] and the present method for the determination of mercury in sediments

Sample location[a] and description	Hg in sediment ($\mu g\ kg^{-1}$)		Recovery by present method (%)
	Semi-automatic method	Present method	
1. Calgary, Alberta-Clay	1079	995	92
2. Ottawa River-Silty Clay	1619	1380	85
3. Rideau River-Silt	754	700	93
4. Rideau River-Sandy Clay	79	81	103
5. Rideau River-Clay	90	87	97
6. Rideau River-Sandy Silt	250	230	92
7. Rideau River-Red Silt	208	204	98
8. Rideau River-Clay	65	62	95
9. Rideau River-Silty Clay	88	88	100
10. Lake Ontario-Silty Clay	638	641	100
11. Lake Ontario-Silty Clay	618	623	101
12. Lake Superior-Red Sandy Silt	100	100	100
13. Lake Erie-Silt	210	230	109
14. Lake Erie-Silt	188	179	95

[a]All locations in Canada.

TABLE 2

Recovery of mercury as CH_3HgCl from solution containing 0.1 g of sediment per 100 ml of solution

Sample	Total amount of Hg in sample (ng)	Amount of Hg + 50 ng of spike (ng)	Recovery (%)
1	101	153	106
2	141	198	114
3	68	118	100
4	4	52	96
5	7	53	92
6	15	65	100
7	12	60	96
8	6	56	100

Table 2 shows that the particulate matter (equivalent to 1 $g\ l^{-1}$) did not affect the oxidation of methylmercury(II). Standard additions plots for methylmercury(II) added to a typical sediment were linear for the range 0—1.0 $\mu g\ Hg\ l^{-1}$. To check the recoveries with the present method further, samples used in a Water Quality Branch [14] Interlaboratory study were analysed. Table 3 shows the satisfactory agreement of this method.

Besides chloride, sulfide may occur in varying amounts in natural waters and sediments, and may tie up mercury as HgS. The u.v. photo-oxidation

TABLE 3

Comparison of data generated by this method to an interlaboratory quality control study [14]

Sediment sample	Present method (±0.01 mg kg^{-1}) (mg kg^{-1})	Results of quality control study (28 Labs) (mg kg^{-1})	
		Mean	Acceptable range [14]
1. Lake Superior Sediment	0.10	0.09	0.06—0.11
2. Lake Erie Sediment 1	0.19	0.18	0.13—0.23
3. Lake Erie Sediment 2	0.21	0.23	0.17—0.29
4. Lake Ontario Sediment 1	0.64	0.67	0.52—0.82
5. Lake Ontario Sediment 2	0.62	0.63	0.50—0.75

prevents any interferences from sulfide (spiked as Na_2S) as high as 100 mg l^{-1} [1]. In the present method, varying sulfide concentrations as high as 500 mg l^{-1} did not affect the mercury signal from 1 μg Hg^{2+} l^{-1}.

The accuracy of the method was checked again by analysing the National Bureau of Standards (NBS) Reference Material for Mercury in Water No. 1642A. Duplicate analyses gave results of 1.09 and 1.14 μg l^{-1} (certified level, 1.10 ± 0.06 μg l^{-1}). The precision of the method with sediment suspensions of 1 g l^{-1} was tested at two levels of mercury. The relative standard deviations at levels of 0.114 and 0.874 mg Hg kg^{-1} were 10 and 4%, respectively.

The authors thank C. Pacenza for secretarial help.

REFERENCES

1 H. Agemian and A. S. Y. Chau, Anal. Chem., 50 (1978) 13.
2 A. M. Jirka and M. J. Carter, Anal. Chem., 50 (1978) 91.
3 B. W. Bailey and F. C. Lo, Anal. Chem., 43 (1971) 1525.
4 T. B. Bennett, Jr., W. H. McDaniel and R. N. Hemphill, Advances in Automated Analysis, 1972 Technicon International Congress, Vol. 8, Mediad, Inc., Tarrytown, N.Y.
5 A. A. El-Awady, R. B. Miller and M. J. Carter, Anal. Chem., 48 (1976) 110.
6 Methods for Chemical Analysis of Water and Wastes, Environmental Protection Agency Publication No. EPA-625/6-74-003, U.S. Environmental Protection Agency, Office of Technology Transfer, Washington, D.C. 20460.
7 Analytical Methods Manual, Inland Waters Directorate, Water Quality Branch, Ottawa, 1974.
8 J. Carron and H. Agemian, Anal. Chim. Acta, 92 (1977) 61.
9 B. K. Afghan, P. D. Goulden and J. F. Ryan, Water Res., 6 (1972) 1475.
10 P. D. Goulden and B. K. Afghan, in Advances in Automated Analysis, 1970, Technicon International Congress, Vol. 2, Mediad, Inc., Tarrytown, N.Y.

11 H. Agemian and A. S. Y. Chau, Anal. Chim. Acta, 75 (1975) 297.
12 C. A. Black, D. D. Evans, J. L. White, L. F. Ensminger and F. E. Clark, Methods for Soil Analysis, Part 2, Chemical and Microbiological Properties, American Society of Agronomy, Inc., Madison, Wisconsin, 1965.
13 H. Agemian and A. S. Y. Chau, Analyst, 101 (1976) 91.
14 K. I. Aspila and J. M. Carron, Inter-Laboratory Quality Control Study No. 18, Total Mercury in Sediments, Report Series, Inland Waters Directorate, Water Quality Branch, Special Services Section, Department of Fisheries and Environment, Burlington, Ontario.

Analytica Chimica Acta, 104 (1979) 293—297

ATOMIC ABSORPTION SPECTROMETRY OF GERMANIUM WITH A TUNGSTEN ELECTROTHERMAL ATOMIZER

KIYOHISA OHTA and MASAMI SUZUKI*

Department of Chemistry, Faculty of Engineering, Mie University, Kamihama-cho, Tsu, Mie-ken 514 (Japan)

(Received 19th June 1978)

SUMMARY

The electrothermal atomization of germanium in a metal micro-tube atomizer is described. Tungsten is preferable to other metals for the atomizer. Hydrogen lowers the atomization temperature of germanium, and improves the sensitivity for germanium significantly when the optimum flow rates are applied. There are pronounced interferences from diverse elements and acids on the atomization of germanium. A procedure which involves carbon tetrachloride extraction of germanium tetrachloride and back-extraction of germanium into water avoids many of the interferences and is recommended for rock samples.

Little information is available about the flameless atomic absorption spectrometry of germanium. Johnson et al. [1] compared the graphite tube with the carbon filament as the atomizer for atomic absorption of germanium, and showed that the tube would facilitate the formation of germanium atoms by retaining the GeO species within the tube until the temperature had risen sufficiently for breakage of the Ge—O bond to occur. The filament technique was not applicable, probably because of loss of the sample as a volatile oxide species.

The electrothermal atomic absorption spectrometry of germanium with a metal micro-tube atomizer is described in this paper. Atomic absorption characteristics were studied with this atomizer and a fast-response amplifier system. The usefulness of this method of electrothermal atomization was demonstrated for geological samples.

EXPERIMENTAL

Apparatus

The monochromator, photomultiplier and signal control unit were the same as used previously [2]. The output signal from the signal control unit was displayed on a Memoriscope (Iwatsu MS-5021).

The atomizer was a tungsten micro-tube (17 mm long, 0.5 mm bore) mounted in the absorption chamber (300-ml volume) which was purged with

argon and hydrogen. Tungsten micro-tubes were made from tungsten sheet (0.05 mm thick). The method of measuring the tube temperature has been described [3].

The source of resonance radiation was a germanium hollow-cathode lamp (Hamamatsu TV Co.). The analytical wavelength used was 265.12—265.16 nm. Background absorption was corrected with a deuterium lamp (Original Hanau D200F). All sample solutions were injected with glass micropipettes.

Reagents

Germanium stock solution was prepared by dissolving germanium dioxide in the minimum of sodium hydroxide solution, acidifying with hydrochloric acid, and diluting with deionized water. Arsenic solution was prepared by dissolving arsenic(III) oxide in sodium hydroxide; antimony solution was prepared from potassium antimony tartrate. Other metal ions were used as their chloride or nitrate salts. All reagents were of analytical-reagent grade.

RESULTS AND DISCUSSION

Atomization characteristics of germanium

Germanium was atomized from various samples to clarify its atomization characteristics. Aqueous germanium solution, germanium tetrachloride extracted into carbon tetrachloride, germanium back-extracted into water from a carbon tetrachloride extract, and the germanium—phenylfluorone complex in butanol were compared. Figure 1 shows the Memoriscope traces of the germanium absorption. The sample solution (1 μl) was placed in the micro-tube and dehydrated at 50°C, and germanium was atomized by heating so as to give a final temperature of 2100°C. The absorption at the lower temperature (1350°C) during atomization from aqueous germanium solution originated from sodium chloride which was present in the germanium solution. Sodium chloride appears to affect the germanium absorption in atomization from aqueous solutions. The germanium absorption was lower in atomization from carbon tetrachloride extract, probably because germanium chloride volatilized without formation of free atoms; germanium tetrachloride has a lower boiling point than the oxide. The temperature giving maximum absorption was shifted to higher regions for atomization from the phenylfluorone complex. Satisfactory atomization was possible for germanium from the back-extract.

Johnson et al. [1] reported that germanium atoms were not produced below ca. 3000°C and that the time taken for the graphite tube temperature to rise should be as short as possible to prevent loss of sample as germanium oxide. With the present atomization device, the temperature giving maximum absorption was about 1950°C. Furthermore, this device permitted rapid increase of the tube temperature. Only 0.35 s was needed to raise the tube temperature from 700 to 2100°C. The germanium absorption commenced 0.2 s after the power was switched on and reached a maximum after 0.33 s when germanium

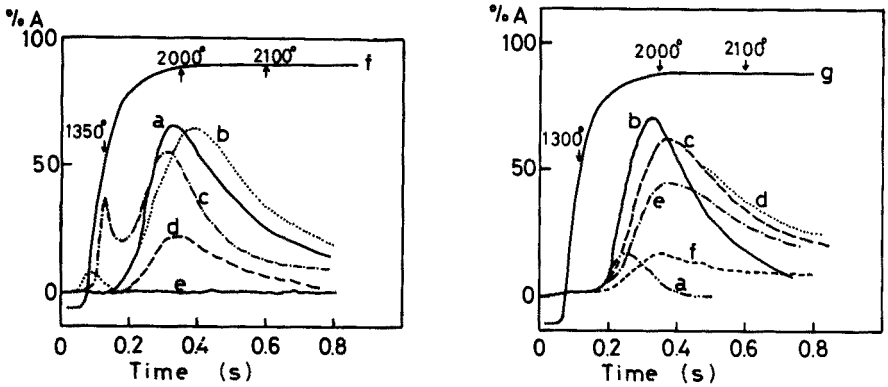

Fig. 1. Memoriscope traces of germanium atomization in the tungsten micro-tube atomizer. (a) Ge (20 ng) back-extracted from the carbon tetrachloride extract; (b) Ge (20 ng) as the phenylfluorone complex; (c) Ge (25 ng) in aqueous solution; (d) Ge (20 ng) extracted into carbon tetrachloride; (e) background; (f) curve of temperature increase. Gas flow rates, 400 ml Ar min^{-1} and 100 ml H_2 min^{-1}.

Fig. 2. Memoriscope traces of germanium atomization at different gas flow rates. (a) 480 ml Ar min^{-1} and 20 ml H_2 min^{-1}; (b) 400 ml Ar min^{-1} and 100 ml H_2 min^{-1}; (c) 300 ml Ar min^{-1} and 200 ml H_2 min^{-1}; (d) 200 ml Ar min^{-1} and 300 ml H_2 min^{-1}; (e) 100 ml Ar min^{-1} and 400 ml H_2 min^{-1}; (f) 500 ml H_2 min^{-1}; (g) curve of temperature increase. Ge (20 ng) back-extracted from carbon tetrachloride extract was used in all cases.

from the back-extract was atomized. The lower atomization temperature of germanium with the present atomization device may result from the presence of hydrogen.

Although molybdenum micro-tubes are preferable for the atomization of most elements, tungsten micro-tubes are recommended for germanium. Lower sensitivity was obtained for the atomization of germanium with a molybdenum atomizer, probably because of some interaction of germanium with the tube.

Effect of hydrogen flow rate

Hydrogen had a large effect on the atomization of germanium (Fig. 2). Maximum absorption for germanium was found with a hydrogen flow rate of 100 ml min^{-1} provided that the total flow rate of argon and hydrogen was 500 ml min^{-1}. The increased absorption is probably due to more effective formation of germanium atoms through the reaction $GeO_2 + 2H_2 \rightarrow Ge + 2H_2O$, which is known to proceed at about 650°C. As the flow rate of hydrogen exceeded the optimum, the sensitivity tended to decrease. The thermal properties of hydrogen seem to play a significant role in the loss of sensitivity at higher flow rates. Hydrogen has a higher specific heat (3.42 cal g^{-1} at 25°C) and higher thermal conductivity (471.11 cal s^{-1} cm^{-2}) than argon. At flow rates of 100 ml min^{-1}, the reducing effect of hydrogen will be more important than the decreased sensitivity caused by its thermal effect, but latter effect predominates with increase in the hydrogen flow rate.

Sensitivity and reproducibility

The absolute sensitivity under optimized conditions was found to be 2×10^{-10} g (for 1% absorption). The precision of the determination with the tungsten micro-tube atomizer was evaluated by making repeated measurements on 20 ng of germanium. The coefficient of variation was found to be 5.4% (n = 10).

Interferences

The effects of some foreign elements and acids were investigated. Figure 3 shows the Memoriscope traces for atomization of germanium from aqueous solutions containing antimony and magnesium. As can be seen, antimony and magnesium seriously affected the germanium absorption. Gallium also showed pronounced interference. High background absorption was recorded for arsenic (Fig. 4). Johnson et al. [1] reported that the germanium absorption signal was superimposed on an irregular background absorption caused by either molecular absorption or light scatter by the interfering species in atomization in a graphite tube atomizer; they stated that the germanium absorption peak could not be resolved from the background absorption. Other elements interfered in the same way as magnesium. The interferences from acids were serious, the germanium absorption being appreciably suppressed even by 0.1 M acids. The atomization of germanium in the presence of foreign elements and acids is therefore not viable analytically.

Fortunately, germanium can be separated from interferences, except arsenic(III), by extraction into carbon tetrachloride from 9 M hydrochloric

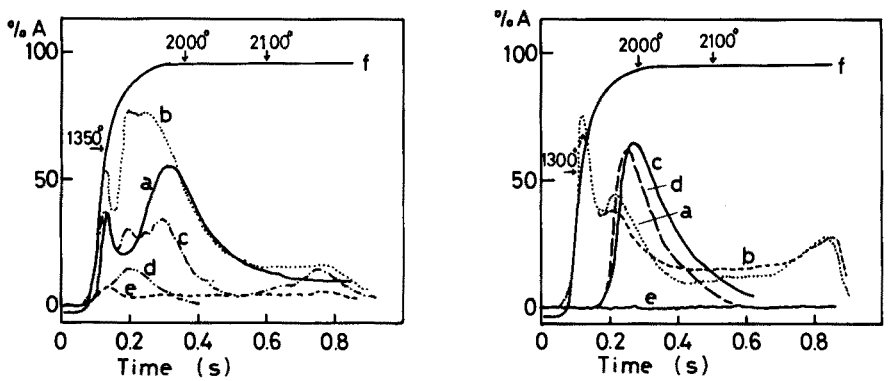

Fig. 3. Memoriscope traces of interferences on the germanium absorption. (a) Ge (25 ng); (b) Ge (25 ng) and Sb (2.5 μg); (c) Ge (25 ng) and Mg (2.5 μg); (d) Sb (2.5 μg); (e) Mg (2.5 μg (f) curve of temperature increase. Ge aqueous solution was used. Gas flow rates were the same as in Fig. 1.

Fig. 4. Memoriscope traces of interferences on germanium absorption. (a) Aqueous solution of Ge (25 ng) and As (2.5 μg); (b) As (2.5 μg) in aqueous solution; (c) Ge (25 ng) back-extracted from carbon tetrachloride extract; (d) Ge (25 ng) and As (2.5 μg) back-extracted from carbon tetrachloride extract; (e) As (2.5 μg) back-extracted from carbon tetrachloride extract; (f) curve of temperature increase. Gas flow rates were the same as in Fig. 1.

acid solution and washing the organic phase with 9 M hydrochloric acid. Figure 4 shows the Memoriscope traces for atomization of germanium which had been extracted from solutions containing 100-fold amounts of arsenic(III). Although the temperature giving maximum absorption of germanium shifted to a somewhat lower temperature region, marked interference was not observed. This extraction process was effective for determining germanium in complex samples.

Determination of germanium in rocks

The electrothermal atomization of germanium with a tungsten micro-tube after carbon tetrachloride extraction allows the determination of germanium in complex samples such as rocks. Arsenic is the only element which is extracted with germanium, but it is not back-extracted to a significant extent.

Procedure. Decompose 2—3 g of rock sample with 4 ml of concentrated nitric acid and 4 ml of hydrofluoric acid (40%) in a Uni-Seal decomposition vessel by heating at 100°C in an electric oven for 3 h. After decomposition, transfer the solution to a Teflon separatory funnel and add hydrochloric acid to make the acidity 9 M. Extract germanium tetrachloride with 1 ml of carbon tetrachloride. Rinse the organic phase with 5 ml of hydrochloric acid (9 M). Then shake the carbon tetrachloride extract vigorously with 1 ml of water for 10 min to strip the germanium. Transfer the aqueous back-extract to the micro-tube and atomize germanium. Prepare a calibration curve by treating standard solutions as above.

Analytical results obtained from the determination of germanium in rock samples are given in Table 1, together with the published data. The results demonstrate the usefulness of the electrothermal atomization with a tungsten micro-tube.

We are grateful to Dr. A. Ando, Geological Survey of Japan, for the rock samples.

TABLE 1

Determination of germanium in rock samples

Sample	Amount taken (g)	Ge (ppm)	
		Found[a]	Reported[b]
JG-1	2	1.7 ± 0.5	1.2
JB-1	3	0.22 ± 0.03	<0.7

[a]Mean of three or four determinations with average deviation. [b]Ref. [4].

REFERENCES

1 D. J. Johnson, T. S. West and R. M. Dagnall, Anal. Chim. Acta, 67 (1973) 79.
2 K. Ohta and M. Suzuki, Anal. Chim. Acta, 96 (1978) 77.
3 K. Ohta and M. Suzuki, Anal. Chim. Acta, 83 (1976) 381.
4 A. Ando, H. Kurasawa, T. Ohmori and E. Takeda, Geochem. J., 8 (1974) 175.

Analytica Chimica Acta, 104 (1979) 299—306

COMPLEXATION EN SOLUTION AQUEUSE DES IONS MAGNESIUM(II), MANGANESE(II), NICKEL(II), CUIVRE(II) ET PLOMB(II) AVEC LA *S*-CARBOXYMETHYL-L-CYSTEINE

M. CROMER-MORIN et J. P. SCHARFF*

Laboratoire de Chimie Minérale, Université Claude Bernard Lyon I, 43 Boulevard du 11 Novembre 1918, 69621 - Villeurbanne (France)

M. CLAUDE et M. R. PÂRIS

Laboratoire de Chimie de Coordination, Faculté des Sciences de l'Université de Dijon, 21000 - Dijon (France)

(Reçu le 2 août 1978)

RESUME

La formation des complexes de la *S*-carboxyméthyl-L-cystéine (H_2A) avec les ions Mg(II), Mn(II), Ni(II), Cu(II) et Pb(II) est étudiée par protométrie à 25°C et à force ionique 1 M $NaClO_4$. Sauf dans le cas des ions Mg(II) où aucune interaction notable n'est détectée, divers complexes sont mis en évidence: MnA; $CuHA^+$; CuA; CuA_2^{2-}; $NiHA^+$; NiA; NiA_2^{2-}; $PbHA^+$; PbA et $PbA(OH)^-$. Les constantes de stabilité ionique globales de tous ces complexes sont calculées et affinées. Les résultats permettent d'obtenir la répartition des différentes espèces en fonction du pH et suggèrent quelques interpretations d'ordre structural concernant les complexes métalliques en solution.

SUMMARY

Complex formation of magnesium(II), manganese(II), nickel(II), copper(II) and lead(II) with S-carboxymethyl-L-cysteine in aqueous solution.

The complex formation between Mg(II), Mn(II), Ni(II), Cu(II), Pb(II) ions and *S*-carboxymethyl-L-cysteine (H_2A) has been studied by measurement of pH at 25°C and constant ionic strength (1 M $NaClO_4$). Although no interaction occurs with Mg(II), this work provides evidence for a variety of complexes: MnA; $CuHA^+$; CuA; CuA_2^{2-}; $NiHA^+$; NiA; NiA_2^{2-}; $PbHA^+$; PbA and $PbA(OH)^-$. The overall formation constants of all these species are computed and refined. The results allow the determination of the distribution of the complexes as a function of pH; some structural features of the metal complexes in solution are indicated.

La fonction thioéther intervient dans la structure de nombreux composés biologiquement actifs. Cette activité est d'ailleurs souvent spécifiquement liée à la présence d'ions métalliques [1]. Parmi ces composés, les amino acides soufrés sont très importants et nous avons abordé dans ce travail l'étude des complexes formés par la *S*-carboxyméthyl-L-cystéine avec les ions Mg(II), Mn(II), Ni(II), Cu(II) et Pb(II). Le coordinat envisagé que l'on trouve par exemple dans l'urine de patients atteints de cystathioninurie [2] est un

antiséborrhéique [3] utilisé également dans le traitement de l'acné [4] et dans d'autres buts thérapeutiques sous diverses appellations commerciales (Thiodril, Rhinathiol).

A notre connaissance seules deux études antérieures sur la complexation de ce coordinat ont été réalisées concernant la coordination des ions Cu(II), Ni(II), Zn(II) et Co(II) [5] et l'étude des complexes du nickel(II) avec la *S*-carboxyméthyl-L-cystéine et la *S*-carboxyéthyl-L-cystéine [6].

PARTIE EXPERIMENTALE

Réactifs

La *S*-carboxyméthyl-L-cystéine (Laboratoires Joullié) est utilisée sans purification supplémentaire. Le produit est anhydre (analyse thermogravimétrique) et sa pureté est vérifiée par dosage potentiométrique. Les perchlorates métalliques sont soit des produits commerciaux ($NaClO_4 \cdot H_2O$, Merck p.a.; $Mg(ClO_4)_2 \cdot 2\ H_2O$, Fluka puriss; $Mn(ClO_4)_2 \cdot 6\ H_2O$, Fluka purum; $Pb(ClO_4)_2 \cdot$ ac Fluka purum en solution aqueuse à 50%), soit obtenus dans le cas du nickel et du cuivre à partir de sulfates, nitrates ou chlorures par la technique d'échange d'ions sur résine Dowex 50-X8 (20—50 mesh) et recristallisés dans l'eau. Dans tous les cas, l'acidité libre des solutions utilisées est déterminée par la méthode de Gran et leur titre en ion métallique est obtenu par titrage à l'EDTA avec détection visuelle ou potentiométrique sur électrode de mercure.

Technique expérimentale

L'étude des complexes formés a été réalisée par une méthode protométrique. Les mesures de pH ont été effectuées en cellule étanche sous atmosphère d'azote suivant le processus déjà décrit [7] en milieu de force ionique 1 M, maintenue constante par du perchlorate de sodium et à la température de 25 ± 0,1°C.

INTERACTIONS PROTON—COORDINAT

Les valeurs de pK_1^H, pK_2^H et pK_3^H (voir Tableau 1) ont été obtenues par titrage par la soude ou l'acide perchlorique de quatre solutions où c_A = 4,800; 5,000; 5,976 et 7,968 $\times 10^{-3}$ M (la solubilité du coordinat dans nos conditions expérimentales étant de l'ordre de 8×10^{-3} M). L'exploitation des courbes de titrage permet le tracé de la courbe $\bar{q}_0 = f(-\log h)$ (Fig. 1). La valeur de pK_1^H peut être calculée facilement dans la zone de pH comprise entre 7,50 et 10,50 où seul l'équilibre $HA^- \rightleftharpoons H^+ + A^{2-}$ intervient. Le calcul effectué pour divers points de la courbe conduit à $pK_1^H = 9{,}01 \pm 0{,}02$.

En milieu plus acide (pH 1,70—4,50), compte tenu des valeurs respectives de pK_2^H et pK_3^H, nous avons traité la courbe $\bar{q}_0 = f(-\log h)$ par la méthode des moindres carrés permettant d'obtenir $pK_2^H = 3{,}33 \pm 0{,}03$; $pK_3^H = 1{,}91 \pm 0{,}01$.

La comparaison avec les constantes de dissociation de la *S*-méthylcystéine [8] et des acides thiodiacétique [9] et dithiodiacétique [10] permet d'attribuer

TABLEAU 1

Liste des symboles

H_2A	: *S*-carboxyméthyl-L-cystéine
c_M, c_A	: Concentrations totales des constituants M et A
c_H	: Concentration totale des protons neutralisables
m, a, h, oh	: Concentrations des constituants libres, des ions H^+ et OH^-
β_{pqr}	: Constante de stabilité ionique globale de l'espèce $M_pH_qA_r$ formée d'après l'équilibre $pM + qH + rA \rightleftharpoons M_pH_qA_r$; $\beta_{pqr} = [M_pH_qA_r]/m^p h^q a^r$.
$K_q^H = [H_{q-1}A]\cdot h/[H_qA]$	: Constante de dissociation du coordinat H_qA
$\bar{r}$	: Nombre moyen de coordinats A fixés par atome métallique M
$\bar{q} = (c_H - h + oh)/c_A$	: Nombre moyen de protons fixés par mole de coordinat A.

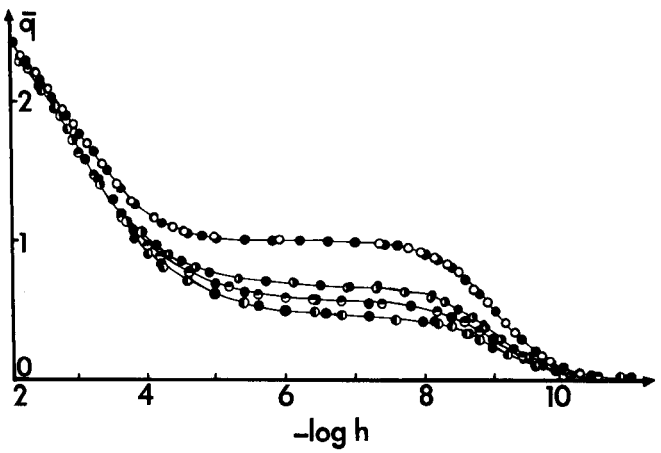

Fig. 1. Courbes de titrage normalisées du système Cu(II)—*S*-carboxyméthyl-L-cystéine. (○) $\bar{q}_0$ ($c_M = 0$); (◐) $R \simeq 4$; (◑) $R \simeq 5$; (◕) $R \simeq 6{,}5$; (●) points recalculés.

la valeur de K_1^H à la dissociation du groupement $-NH_3^+$, celle de K_2^H au groupement carboxylique $-SCH_2COOH$ et K_3^H à la dissociation du groupement carboxylique de la partie cystéine du coordinat.

INTERACTIONS M(II)—*S*-CARBOXYMETHYL-L-CYSTEINE

Méthode d'investigation

Nous avons utilisé conjointement l'exploitation classique des courbes de formation $\bar{r} = f(-\log a)$ où $\bar{r} = (\Sigma r\beta_{10r}a^r)/(1 + \Sigma\beta_{10r}a^r)$ (ces courbes sont calculées dans chaque cas pour différents rapports $R = c_A/c_M$ et la méthode est valable uniquement dans le cas de la formation exclusive de complexes simples mononucléaires du type MA_r) et l'exploitation des données $\bar{q} = f(-\log h)$ déjà décrite dans plusieurs publications [11—13]. Rappelons qu'il s'agit de rendre minimum la somme $U = \Sigma(\bar{q}_{exp.} - \bar{q}_{calc.})^2$, où $\bar{q}_{exp.} = (c_H - h + oh)/c_A$ et $\bar{q}_{calc.} = (\Sigma q\beta_{pqr}\, m^p h^q a^r)/c_A$, les variables m et a étant calculées à partir du système d'équations

$c_M = m + \sum p\beta_{pqr}\, m^p h^q a^r$ et $c_A = a + \sum r\beta_{pqr}\, m^p h^q a^r$

Les constantes β_{pqr} vérifiant la condition "U minimum" sont déterminées par la technique du "pit-mapping" à l'aide de notre programme de calcul ACREF 3 AM [14]. Cette méthode peut s'appliquer dans le cas général de complexes du type $M_pH_qA_r$ incluant les espèces hydroxydées ($q < 0$) et protonées ($q > 0$).

Résultats

Dans tous les cas, nous avons neutralisé par la soude des solutions correspondant à différents rapports $R = c_A/c_M$ de réactifs. Les concentrations utilisées sont indiquées dans le Tableau 2.

En ce qui concerne le système Mg(II)—H_2A, les courbes de neutralisation obtenues en présence de l'ion métallique et du coordinat coïncident pratiquement avec celles du coordinat seul et aucun phénomène significatif de complexation ne peut être détecté. La même conclusion a été obtenue par Lenz et Martell [8] lors de l'étude des interactions de Ca(II), Mg(II) et Sr(II) avec la méthionine, l'éthionine, la cystéine, la *S*-méthylcystéine et la pénicillamine.

Le manganèse(II) complexe la *S*-carboxyméthyl-L-cystéine pour des pH supérieurs à 7. Cette complexation est relativement faible et on constate sur la courbe de formation (Fig. 2) que $\bar{r}$ reste largement inférieur à 1. Nous

TABLEAU 2

Compositions des solutions étudiées ($R = c_A/c_M$)
(Dans le cas des complexes des ions Cu(II) et Ni(II), toutes les solutions étudiées contiennent une quantité totale d'acide perchlorique de $1{,}006 \times 10^{-2}$ M)

M(II)	R	c_A ($\times 10^{-3}$ M)	c_M ($\times 10^{-3}$ M)
Mg(II)	1	5,000	4,975
	2,5	5,000	1,990
Mn(II)	1,5	6,040	3,984
	2	6,060	2,988
	2,5	5,030	1,992
Ni(II)	3	5,990	2,080
	3	7,188	2,496
	4	3,944	1,040
	5	4,992	1,040
	6,5	6,989	1,040
Cu(II)	3	5,760	2,000
	3	7,200	2,500
	4	3,963	1,032
	5	4,954	1,032
	6,5	6,935	1,032
Pb(II)	2	6,000	3,120
	2,5	4,970	2,080
	3	6,000	2,080
	4	8,360	2,080

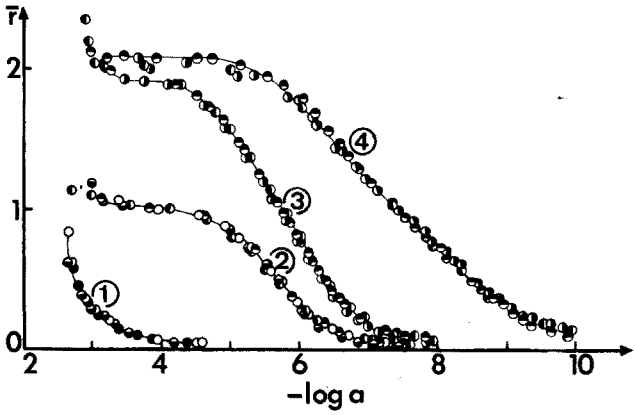

Fig. 2. Courbes de formation des systèmes M(II)—*S*-carboxyméthyl-L-cystéine. (1) Mn(II); (2) Pb(II); (3) Ni(II); (4) Cu(II) (•) $R \simeq 1{,}5$: (○) $R \simeq 2$; (⊖) $R \simeq 2{,}5$; (⊖) $R \simeq 3$; (◐) $\simeq 4$; (◑) $R \simeq 5$.

n'avons donc considéré que l'espèce MnA et affiné sa constante de stabilité ionique β_{101} dans le domaine de pH 7—9. Nous avons introduit dans nos calculs la constante d'hydrolyse de $MnOH^+$ déterminée par Fontana et Brito [15] mais cette espèce hydroxydée demeure négligeable puisque à pH 9 et dans le cas de $R = 2$, sa concentration reste inférieure à 1% de la concentration totale c_M en manganèse(II) alors que la concentration de MnA est de l'ordre de 50% de c_M. L'affinement portant sur les trois solutions examinées conduit à $\log \beta_{101} = 2{,}58$ (déviation standard: 0,01) pour 81 couples de données expérimentales $\bar{q}$; —log h exploités.

Dans le cas des complexes du cuivre(II), les calculs effectués pour les différents rapports envisagés donnent des couples de valeurs $\bar{r}$: —log a qui se répartissent sur une courbe unique (Fig. 2) pour des valeurs de —log a comprises entre 4 et 9. Cette courbe de formation tend vers 2 indiquant la formation probable de CuA et CuA_2^{2-} à l'exclusion d'espèces polynucléaires ou hydroxydées. Les courbes de titrages montrent d'ailleurs la libération de quatre protons par atome métallique ce qui confirme la fixation de deux moles de coordinat par atome métallique. Par contre la dispersion des points devient non négligeable lorsque —log $a > 9$, c'est-à-dire pour pH 2—4. L'affinement par la méthode du pit-mapping montre que l'introduction d'une constante β_{111} relative à l'espèce protonée $CuHA^+$ améliore nettement les résultats dans cette zone (Fig. 1). Finalement on est conduit aux valeurs suivantes

$$\log \beta_{111} = 11{,}76(0{,}03); \log \beta_{101} = 8{,}60(0{,}05); \log \beta_{102} = 15{,}24(0{,}06)$$

obtenues pour 88 couples de données $\bar{q}$; —log h.

Pour les complexes du nickel(II), le processus est identique et là encore outre les espèces NiA et NiA_2^{2-}, nous détectons une espèce protonée $NiHA^+$. Le traitement de 88 couples de données conduit aux valeurs

$\log \beta_{111} = 10{,}70(0{,}19)$; $\log \beta_{101} = 6{,}44(0{,}04)$; $\log \beta_{102} = 11{,}70(0{,}03)$

Cette espèce protonée se forme en quantité relativement faible par rapport aux espèces mononucléaires prépondérantes (Fig. 3) et ceci peut expliquer la valeur plus élevée de la déviation standard associée à la détermination de β_{111}.

Enfin dans le cas du plomb(II), la courbe de formation obtenue tend vers 1 indiquant la formation de PbA. Pour les faibles valeurs de $\bar{r}$, la dispersion des points est importante et nous avons envisagé la formation de $PbHA^+$. Pour $\bar{r} > 1$, les courbes montrent un aspect caractéristique de la formation d'espèces hydroxydées ce qui est confirmé par l'examen des courbes de titrage. Nous avons donc considéré les complexes $PbHA^+$, PbA et PbA(OH) dont les constantes de stabilité sont affinées. Lors des calculs nous avons introduit les valeurs des constantes d'hydrolyse des ions plombeux déterminées par Lee [16] mais là encore ces espèces demeurent négligeables. L'affinement porte sur 179 couples de données. Les constantes obtenues ainsi que tous les résultats de ce travail sont rassemblés dans le Tableau 3.

A l'aide de ces données nous pouvons calculer les courbes de répartition des différentes espèces complexes en fonction du pH et la Fig. 3 montre le cas des complexes du nickel(II), du cuivre(II) et du plomb(II) pour $R = 4$.

Discussion

Les résultats ci-dessus conduisent aux remarques suivantes. Dans le cas du complexe MnA, la valeur originale de β_{101} se place tout à fait normalement dans la série d'Irving-Williams. Pour les complexes cuivriques, nous indiquons pour la première fois la valeur de β_{102}. L'ensemble de nos résultats est en accord avec les conclusions de Nakon et al. [5] en ce qui concerne la structure

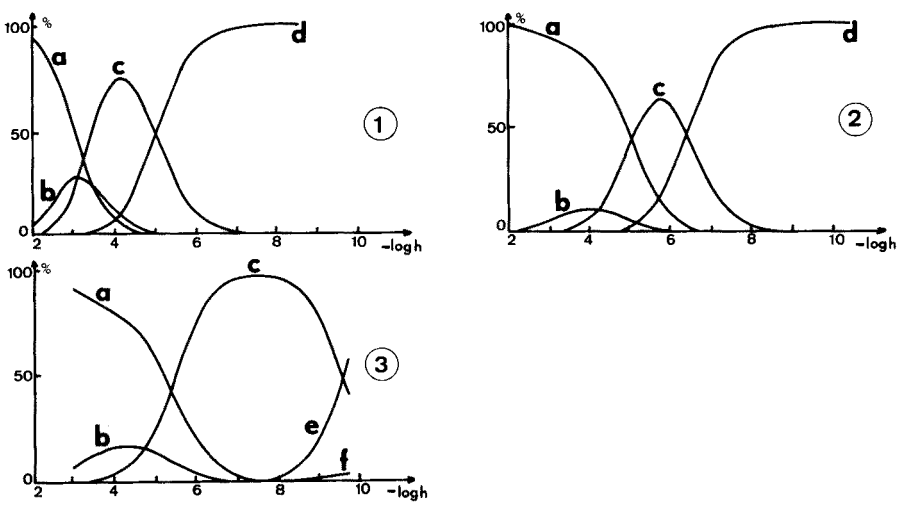

Fig. 3. Répartition des différents complexes en fonction du pH dans les systèmes M(II)—*S*-carboxyméthyl-L-cystéine pour $R \simeq 4$. (1) Cu(II); (2) Ni(II); (3) Pb(II) (a) M; (b) MHA; (c) MA; (d) MA_2; (e) MA(OH); (f) MOH).

TABLEAU 3

Constantes de stabilité ioniques ($NaClO_4$ M; 25°C)

M(II)	*pqr*	Nos valeurs	Autres auteurs	
		$\log \beta_{pqr}$ (déviation standard)	[KNO_3 0,1 M; 25°C) [5]	($NaClO_4$ 2 M; 25°C) [6]
Mg(II)		Aucun complexe détecté		
Mn(II)	101	2,58(0,01)		
Cu(II)	111	11,76(0,03)	11,12 ± 0,02	
	101	8,60(0,05)	8,15 ± 0,01	
	102	15,24(0,06)	—	
Ni(II)	111	10,70(0,19)	—	—
	101	6,44(0,04)	6,22 ± 0,02	6,40 ± 0,03
	102	11,70(0,03)	11,16 ± 0,02	11,65 ± 0,05
Pb(II)	111	10,48(0,01)		
	101	5,78(0,01)		
	1 − 11	−3,82(0,01)		

du complexe $CuHA^+$ (où l'ion cuivre(II) est complexé par la structure terminale "type amino acide", le groupement carboxylique $-SCH_2COOH$ étant protoné) et celle de l'espèce CuA_2^{2-}. Par contre pour le complexe CuA, nos résultats ne suggèrent pas une coordination de l'atome de soufre avec un comportement tétradenté du coordinat indiqué par Nakon et al. [5]. Nous pensons que la structure de $CuHA^+$ est conservée avec uniquement une déprotonation du groupement carboxylique terminal. En effet, d'après nos valeurs, la constante de l'équilibre $CuHA^+ \rightleftharpoons CuA + H^+$ est $\log K = -3{,}16$, valeur voisine de celle correspondant à la dissociation de $-SCH_2COOH$ ($\log K_2^H = -3{,}33$). D'autre part, Nakon et al. [5] indiquent un maximum d'absorption de l'espèce CuA à 710 nm alors que dans le cas du complexe Cu(glycine)$^+$ des travaux [12] montrent une valeur très voisine du maximum d'absorption situé à 714 nm. Enfin si l'on compare pour les mêmes conditions expérimentales ($NaClO_4$ 0,5 M; 25°C), les constantes de CuA ($\log \beta_{101} = 8{,}37$) et CuA_2^{2-} ($\log \beta_{102} = 14{,}78$) [17] avec celles des complexes Cu(alanine)$^+$ ($\log \beta_{101} = 8{,}21$) et Cu(alanine)$_2$ ($\log \beta_{102} = 15{,}00$) [18], on constate que les valeurs sont du même ordre alors que dans le cas d'une coordination tétradentée, il faudrait s'attendre à une valeur beaucoup plus élevée de β_{101} (espèce CuA).

L'espèce protonée $NiHA^+$ est signalée pour la première fois. Dans le cas des complexes du nickel(II), les constantes β_{101} et β_{102} sont très différentes de celles obtenues pour Ni(alanine)$^+$ ($\log \beta_{101} = 5{,}39$) et Ni(alanine)$_2$ ($\log \beta_{102} = 9{,}91$) [11]. D'autre part, le fait qu'il n'existe pas d'espèce NiA_3^{4-} suggère la chélation tridentée de la *S*-carboxyméthyl-L-cystéine. La coordination du soufre et de l'azote a d'ailleurs été démontrée par spectroscopie puisque pour la bande $^3A_{2g}$ (F) → $^3T_{1g}$ (F), on observe un maximum d'absorption à 615 nm pour NiA et 579 nm pour NiA_2^{2-} [5], valeurs nettement différentes de celles observées

avec des coordinats comme l'alanine (atomes donneurs O,N) [11] ou l'acide thiodiacétique (atomes donneurs S,O)[6, 9].

Enfin les résultats concernant les complexes du plomb(II) sont originaux. Des espèces analogues ont été détectées dans divers cas de complexes Pb(II)—amino acides [19—21]. La valeur de $\log \beta_{101} = 5{,}78$ doit être remarquée car des travaux récents [21] montrent que pour le complexe Pb(glycine)$^+$, $\log \beta_{101} = 5{,}46$. Or d'une manière générale on observe une diminution de la stabilité ionique avec l'augmentation du nombre d'atomes de l'amino acide [22]. Dans le cas présent, l'augmentation de stabilité observée devra être expliquée à l'aide d'informations structurales précises.

Nous remercions très vivement Monsieur C. Warolin (Laboratoires Joullié) qui a attiré notre attention sur l'importance thérapeutique de la *S*-carboxyméthyl-L-cystéine et qui a bien voulu nous fournir les échantillons de ce coordinat.

BIBLIOGRAPHIE

1 D. B. McCormick, R. Griesser et H. Sigel dans H. Sigel (Ed.), Metal Ions in Biological Systems, Vol. 1, M. Dekker, New York, 1973.
2 H. Kodama, M. Ohmori, M. Suzuki et S. Mizuhara, Physiol. Chem. Phys., 2 (1970) 287.
3 G. Kalopissis (Oreal, SA), German Patent, 2.023.159.
4 G. Kalopissis (Oreal, SA), German Patent, 1.930.023.
5 R. Nakon, E. M. Beadle et R. J. Angelici, J. Am. Chem. Soc., 96 (1974) 719.
6 M. Aplincourt et R. Hugel, Bull. Soc. Chim. Fr., 11—12 (1976) 1793.
7 M. Morin, M. R. Pâris et J. P. Scharff, Anal. Chim. Acta, 57 (1971) 123.
8 G. R. Lenz et A. E. Martell, Biochemistry, 3 (1964) 745.
9 M. Aplincourt, D. Noizet et R. Hugel, Bull. Soc. Chim. Fr., 1 (1972) 26.
10 K. Suzuki, C. Karaki, S. Mori et K. Yamasaki, J. Inorg. Nucl. Chem., 30 (1968) 167.
11 R. P. Martin et L. Mosoni, Bull. Soc. Chim. Fr., 8—9 (1970) 2917.
12 R. P. Martin, L. Mosoni et B. Sarkar, J. Biol. Chem., 246 (1971) 5944.
13 M. Morin et J. P. Scharff, Anal. Chim. Acta, 66 (1973) 113.
14 M. Cromer-Morin, R. P. Martin et J. P. Scharff, Compt. Rend., 277 (1974) 1339.
15 S. Fontana et F. Brito, Inorg. Chim. Acta, 2 (1968) 179.
16 Y. H. Lee, Acta Chem. Scand., A 30 (1976) 593.
17 M. Claude, M. R. Pâris, M. Cromer-Morin et J. P. Scharff, résultats non publiés.
18 M. M. Ramel et M. R. Pâris, Bull. Soc. Chim. Fr., 4 (1967) 1359.
19 A. M. Corrie, G. K. R. Makar, M. L. D. Touche et D. R. Williams, J. C. S. Dalton Trans., (1975) 105.
20 A. M. Corrie et D. R. Williams, J. C. S. Dalton Trans., (1976) 1068.
21 Y. Khayat, M. Cromer-Morin et J. P. Scharff, J. Inorg. Nucl. Chem., à paraître.
22 M. Morin et J. P. Scharff, Bull. Soc. Chim. Fr., 7—8 (1973) 2198.

Analytica Chimica Acta, 104 (1979) 307—317

METHODE D'ELUTION SELECTIVE POUR L'EXTRACTION DES METAUX LOURDS DE L'EAU DE MER SUR RESINE CHELATANTE

JANINE LAMATHE

Service de Chimie, Laboratoire Central des Ponts et Chaussées, 58, Boulevard Lefèbvre, 75732 Paris Cedex 15 (France)

(Reçu le 15 juin 1978)

RESUME

On a expérimenté l'extraction des métaux lourds de l'eau de mer sur résine chélatante Chelex 100 en vue de leur dosage par spectrométrie d'absorption atomique (s.a.a.) sans flamme. Le maximum de rétention des métaux lourds n'est pas obtenu avec la résine sous la forme H^+ qui se transforme progressivement au contact de l'eau de mer par fixation de cations alcalins et alcalino-terreux. Ces cations, élués simultanément avec les métaux lourds, provoquent des interférences importantes sur les dosages par s.a.a. sans flamme. La séparation des métaux lourds est quantitative sur la résine Chelex 100 sous la forme Ca^{2+}; par traitement à l'acide acétique 1:100, on élimine totalement les alcalins et les alcalino-terreux fixés sur la résine avant de procéder à l'élution des métaux lourds. L'élution par l'acide nitrique 1 M permet de récupérer Cu, Pb, Ni, Zn, Cd et Co globablement et quantitativement, et une élution intermédiaire avec de l'acide nitrique 0,01 M permet d'isoler Zn, Cd et Co de Cu et de Pb qui sont élués ensuite par l'acide nitrique 1 M.

SUMMARY

A selective method of elution for the extraction of heavy metals from sea waters on a chelating resin.

The extraction of heavy metals in sea water with Chelex 100 prior to their determination by atomic absorption spectrometry (a.a.s.) with electrothermal atomization is discussed. Maximum retention of heavy metals is not obtained with the resin in the H^+ form, because it is gradually transformed in contact with sea water by the fixation of alkali and alkaline-earth cations which are eluted simultaneously with the heavy metals and interfere during a.a.s. The separation of heavy metals is quantitative on Chelex 100 in the Ca^{2+} form; treatment with dilute acetic acid (1 + 99) eliminates the alkali and alkaline-earth metals fixed on the resin before elution of the heavy metals. Elution with 1 M nitric acid gives simultaneous and quantitative recovery of Cu, Pb. Ni, Zn, Cd and Co; intermediate elution with 0.01 M nitric acid isolates Zn, Cd and Co from Cu and Pb, which are subsequently eluted with 1 M nitric acid.

La détermination de teneurs de l'ordre de quelques microgrammes de métaux lourds par litre d'eau de mer, est rendue difficile par la présence des quantités importantes de sels contenus dans le milieu. Les possibilités du dosage direct par spectrométrie d'absorption atomique (s.a.a.) sans flamme ont été étudiées

récemment pour le zinc [1], le cadmium, le cuivre, le fer et le manganèse [2], le cadmium et le zinc [3]. D'après ces auteurs, le dosage direct peut être réalisé dans certaines conditions d'instrumentation.

Lorsqu'on atomise de l'eau de mer dans un four graphite on obtient des signaux importants d'absorptions non spécifiques qui masquent les absorptions spécifiques notamment pour Cd, Zn et Pb. Par ailleurs, on connaît mal les interférences possibles entre les constituants de la matrice et les métaux lourds. Pour diminuer ces interférences, d'ordre physique et chimique, Campbell et Ottaway [3] diluent avec de l'eau distillée les échantillons d'eau de mer et analysent ces derniers suivant la technique des ajouts. Ce procédé abaisse considérablement la sensibilité des dosages et rend, entre autres, celui du plomb impossible. Le dosage direct des métaux lourds dans l'eau de mer étant difficile, voire impossible, de nombreux chercheurs ont étudié des techniques de séparation et de concentration des métaux lourds.

Les méthodes les plus couramment utilisées sont: (a) la complexation des métaux lourds par l'ammonium pyrrolidine dithiocarbamate (APDC) et extraction des complexes organo-métalliques formés par la méthylisobutylcétone (MIBK) [4]; (b) la séparation des métaux lourds par chromatographie sur résine chélatante Dowex A1 (Chelex 100), ceux-ci étant ensuite dosés par diverses techniques: s.a.a. avec flamme [5, 6], s.a.a. sans flamme [7], voltamétrie par redissolution anodique [8, 9], activation neutronique [10, 11], fluorescence-x [12—14]. Davey et Soper [15] ont mis au point un appareillage permettant de réaliser, en mer, la concentration des métaux lourds par utilisation de la résine Chelex 100.

La méthode de séparation sur résine chélatante paraîssant simple et permettant d'obtenir un facteur de concentration très supérieur à celui obtenu par la méthode à l'APDC—MIBK, nous avons étudié la séparation du cuivre, du plomb, du zinc et du cadmium sur la résine Chelex 100.

La résine Chelex 100 (Bio-Rad Laboratories) qui correspond à la résine Dowex A1 purifiée, est constituée d'une matrice d'un copolymère de styrène—divinylbenzène sur laquelle sont greffés des groupements amino—diacétate qui lui confèrent la propriété de former des complexes stables avec les cations métalliques suivant l'ordre de sélectivité: métaux lourds > alcalino-terreux >> alcalins. Le passage d'une forme ionique à une autre provoque de grandes variations de volumes. Rosset [16, 17] a donné les hauteurs relatives d'une colonne de résine sous diverses formes par rapport à la forme sodium choisie comme référence. On remarque que plus l'affinité de la résine pour un cation est grande, plus le volume de la résine sous cette forme est petit. C'est pour éviter des variations importantes du volume de la colonne de résine, au cours des différentes phases de la séparation des métaux lourds, que la résine Chelex 100 est généralement utilisée sous la forme hydrogène. Lee et al. [10] préconisent même un mélange avec de la poudre de verre pyrex de même granularité.

L'application de la méthode décrite par Riley et Taylor [5] nous a conduit à constater que par passage de 50 ml d'une solution de NaCl (30 g l^{-1}), 5 g de résine Chelex 100 forme H^+ retiennent environ 6 mg de sodium. Cette

quantité est insignifiante comparée à celle présente dans les 50 ml de solution saline passés sur la colonne. Cependant, si l'on respecte les conditions de concentration finale de l'éluat, soit 10 ml, la concentration en sodium au moment du dosage est égale à 600 mg l^{-1}. Cette quantité, relativement importante, peut provoquer des interférences au moment du dosage des métaux lourds, surtout si l'on veut augmenter la limite de sensibilité par utilisation de la s.a.a. sans flamme.

Depuis 1968, la méthode de Riley et Taylor [5] a été utilisée par de nombreux chercheurs, cependant ce n'est que dans des articles récemment publiés que se trouve signalé cet inconvénient. Ainsi, Abdullah et al. [9] de même que Florence et Batley [8] indiquent qu'il se produit une rapide conversion de la forme H^+ en forme Na^+ et même Mg^{2+} et Ca^{2+} au contact de l'eau de mer. Enfin, Van Grieken et al. [14] mentionnent que l'emploi de la résine Chelex 100 est limité aux solutions renfermant de faibles concentrations en alcalins et alcalino-terreux.

ETUDE DE LA RETENTION DES ALCALINS ET ALCALINO-TERREUX PAR PASSAGE D'EAU DE MER SUR LA RESINE CHELEX 100

Effet du pH de l'eau de mer

Le pH le plus fréquemment utilisé est le pH 7,6 indiqué par Riley et Taylor [5]. Il correspond au pH naturel de l'eau de mer (entre 7,5 et 8). Bury et Levert [11] préconisant un pH de 6 et Evrard et al. [7] un pH de 8,6, la rétention des métaux alcalins et alcalino-terreux a été étudiée à ces trois pH par passage de 50 ml d'eau de mer sur 5 g de résine Chelex 100 sous forme H^+ (colonne de résine, h = 4 cm, diam. 1 cm). Les pH ont été obtenus par ajout, soit d'acide nitrique dilué, soit d'ammoniaque diluée. Les métaux alcalins et alcalino-terreux fixés sur la résine ont été élués par de l'acide nitrique 2 M et dosés par s.a.a. avec flamme (Tableau 1). On voit que la variation du pH joue peu sur les quantités respectivement retenues de Mg, Ca, Na et K.

Effet du volume de l'eau de mer

A pH 7,6, par passage de 50 ml, 500 ml et 1 l d'eau de mer, sur 5 g de résine Chelex 100 sous forme H^+, on retient les quantités indiquées dans le Tableau 2.

TABLEAU 1

Quantités des cations retenues sur la résine à pH 6; 7,6; 8,6

Cations	Quantités retenues (mg)		
	pH 6	pH 7,6	pH 8,6
Mg	3,72	3,84	4,44
Ca	2,16	2,31	2,66
Na	2,44	2,56	2,88
K	0,14	0,13	0,12

TABLEAU 2

Effet du volume de l'eau de mer à pH 7,6

Cations	Quantités retenues (mg)		
	50 ml	500 ml	1 l
Mg	3,84	19,60	13,45
Ca	2,31	16,00	8,22
Na	2,56	5,10	16,60
K	0,13	0,18	0,41

Si l'on calcule le nombre de milliéquivalents (méq) de cations fixés sur la résine, on remarque que 1 g de résine sèche fixe 0,45 méq pour 50 ml, 2,18 méq pour 500 ml et 1,70 méq pour 1 l d'eau de mer. Ces résultats donnent l'impression que la rétention de Ca, Mg, Na et K passe par un maximum. La capacité d'échange de la résine étant de 2,9 méq g^{-1}, la quantité théorique d'eau de mer pour saturer la colonne se situerait donc vers 300 ml.

On observe également une variation entre les quantités de Mg, Ca, Na et K respectivement retenues pour 500 ml et 1 l d'eau de mer. Ceci peut, sans doute, s'expliquer par la modification progressive du pH de l'effluent qui passe de 2,1 pour les 100 premiers ml à 3,3 pour les 100 derniers ml, le pH étant voisin de 3 après le passage de 500 ml d'eau de mer. Ce pH de 3 favorise probablement la fixation de Na au détriment de Ca et Mg. On constate d'ailleurs une augmentation de la hauteur du lit de résine qui passe de 4 à 5 cm. Florence et Batley [8] ont observé également cette modification du pH de l'effluent et indiquent que le pH de celui-ci atteint 7,4 après passage de 4 l d'eau de mer sur une colonne de résine H^+ de 10 × 0,8 cm.

Enfin, on constate un ralentissement très net de la vitesse d'écoulement de l'effluent. A vitesse constante, 1 l d'eau de mer devrait passer sur la colonne de résine (4 × 1cm) en 3 h, or le temps réel est de 5 h. Ce ralentissement est dû au remplacement des ions H^+ de la résine par des ions de rayons atomiques plus grands, ce qui diminue le volume interstitiel de la colonne de résine et cela sans changement du volume apparent.

Nous avons également mis en évidence que la rétention de Ca et Mg n'est pas due au fait que la résine est sous forme H^+. En effet, si l'on fait passer 500 ml d'eau de mer sur la résine forme Na^+, on constate immédiatement une contraction du lit de résine dont la hauteur diminue de moitié. Après passage de 500 ml d'eau de mer sur 3 g de résine forme Na^+, on trouve fixés sur la résine: 15,0 mg Mg; 12,0 mg Ca; 2,7 mg Na. Etant donné que les 3 g de résine renfermaient au départ 48 mg de Na, il y a donc déplacement de Na par Ca et Mg. Par contre, on ne constate pas de ralentissement de la vitesse d'écoulement et le pH de l'effluent reste toujours voisin de 7.

ETUDE DE LA FIXATION DU CUIVRE, DU PLOMB, DU CADMIUM ET DU ZINC SUR LA RESINE CHELEX 100 FORME H^+ ET Ca^{2+}

L'étude de la séparation de Cu, Pb, Cd et Zn par chromatographie sur Chelex 100 a été réalisée sur des solutions synthétiques en se plaçant à une concentration telle que l'éluat final renferme 1 mg l^{-1} de chaque métal afin de pouvoir effectuer les dosages par s.a.a. avec flamme. La résine (100—200 mesh) a été utilisée sous les formes H^+ et Ca^{2+}. La forme H^+ est obtenue par traitement de la forme Na^+ par de l'acide nitrique 2 M. La forme Ca^{2+} est obtenue par passage, sur le lit de résine forme H^+, d'une solution d'acétate de calcium 0,5 M. Le lit de résine est ensuite lavé à l'eau distillée jusqu'à absence d'ions Ca^{2+} dans l'effluent. Pour le passage sur la résine H^+, les solutions synthétiques ont été préparées avec trois matrices différentes: eau distillée, solution de NaCl à 30 g l^{-1}, eau de mer. Pour le passage sur la résine Ca^{2+}, seule la solution synthétique dans l'eau de mer a été utilisée. Pour tous ces essais, le pH des solutions était amené à 7,6. Les dosages des métaux lourds élués par HNO_3 2 M ont été effectués par s.a.a. avec flamme. Les résultats exprimés en mg l^{-1} sont indiqués dans le Tableau 3. On constate que la séparation de Zn et de Cd n'est pas quantitative en solution saline avec la résine forme H^+, alors que cette séparation est quantitative avec la résine forme Ca^{2+}.

Il faut remarquer que la séparation est quantitative avec la résine forme H^+ lorsque la solution synthétique est dans de l'eau distillée. Après passage sur la résine H^+, le pH des solutions effluentes étaient respectivement de 3,2 pour l'eau distillée, 2,3 pour la solution NaCl, 2,2 pour l'eau de mer. Ce pH très bas pour les solutions de NaCl ou d'eau de mer passées sur résine H^+ est peut-être la cause de la mauvaise séparation du zinc et du cadmium. En effet, Florence et Batley [8] indiquent que l'on obtient 98% de rétention pour Cd et Zn lorsque le pH de la résine est supérieur à 2,9 pour Cd et à 2,5 pour Zn. Par ailleurs, Bury et Levert [11] ont montré que la rétention de Cd est favorisée par la présence de calcium. Nous avons constaté que le pH de l'eau de mer passée sur la résine Ca^{2+} reste voisin de 7.

La première conclusion que l'on peut tirer de cette étude est la nécessité d'utiliser la résine Chelex 100 sous la forme Ca^{2+} si l'on veut séparer quantitativement le zinc et le cadmium présents dans l'eau de mer. Si l'on ne veut

TABLEAU 3

Quantités (mg l^{-1}) des cations eluées par HNO_3 2 M

Cations	Résine forme H^+			Résine forme Ca^{2+}
	Eau distillée	NaCl à 30 g l^{-1}	Eau de mer	Eau de mer
Zn	1,000	0,900	0,826	0,994
Cd	0,992	0,452	0,352	0,992
Cu	0,960	0,972	0,967	0,960
Pb	1,000	1,000	1,000	1,000

doser que le cuivre et le plomb, les formes H^+ ou Ca^{2+} peuvent être utilisées indifféremment.

Cependant, il faut tenir compte des quantités de Ca, Mg et Na fixées sur la résine et qui, éluées avec les métaux lourds, se retrouveront dans l'éluat final. Par passage de 50 ml d'eau de mer, 5 g de résine retiennent pour la forme H^+: 3,70 mg Mg; 2,10 mg Ca; 2,05 mg Na, et pour la forme Ca^{2+}: 18,10 mg Mg, 37,00 mg Ca et 2,80 mg Na. On remarque que pour la résine forme Ca^{2+} qui renfermait 70 mg de calcium, les ions Ca^{2+} ont été remplacés partiellement par Mg et Na. Ce phénomène, en contradiction avec l'ordre d'affinité de la résine pour ces cations, peut s'expliquer par une modification des constantes apparentes d'échanges d'ions. Celles-ci dépendent de la force ionique de la solution et varient par conséquent avec la concentration de la solution en équilibre avec la résine.L'objectif de cette étude étant le dosage des métaux lourds par s.a.a. sans flamme, nous avons contrôlé l'action éventuelle de Ca, Mg et Na sur ces dosages.

DOSAGES PAR S.A.A. AVEC FOUR GRAPHITE DE Cu, Pb ET Cd, EN PRESENCE DE Mg, Ca ET Na

Tenant compte des quantités de Mg, Ca et Na pouvant être retenues sur la résine, les courbes d'étalonnage en milieu HNO_3 0,1 M ont été établies en présence de 50, 200 et 1000 mg par litre de Mg, Ca et Na qui ont été introduits dans les solutions étalons sous forme de nitrates (qualité suprapur).

Nous avons constaté, pour les trois métaux étudiés, des interférences importantes à partir de 50 mg l^{-1} de Mg, Ca et Na seuls ou en mélange. A titre d'exemple la Fig. 1 représente les courbes d'étalonnage obtenues pour le cuivre. Les interférences observées avec 200 et 1000 mg sont sensiblement identiques, mais les dosages deviennent très difficiles à réaliser avec 1000 mg. Ces interférences sont variables mais toujours très importantes. L'action de Ca sur Pb est très intense et semble provoquer en outre un effet de mémoire. En établissant une courbe d'étalonnage avec des solutions de Pb pur, après une série de dosage de solutions de Pb renfermant 50 mg l^{-1} de Ca, on constate une diminution importante de l'absorbance par rapport à la droite d'étalonnage préalablement établie et on obtient une droite très proche de celle obtenue en présence de 50 mg l^{-1} de Ca (Fig. 2).

Cette observation pose le problème de la justesse du dosage, dans le four graphite, du plomb et de certains métaux lourds dans les eaux douces, celles-ci renfermant fréquemment des quantités de calcium supérieures à 50 mg l^{-1}.

ETUDE DES POSSIBILITES D'ELUTION SELECTIVE

L'acide nitrique fortement concentré (2 M et même 4 M) est généralement utilisé pour l'élution des métaux lourds fixés sur la résine Chelex 100 forme H^+. Le sodium, le calcium et le magnésium formant des complexes moins stables que Cu, Pb, Cd et Zn, un essai a été réalisé en effectuant des élutions

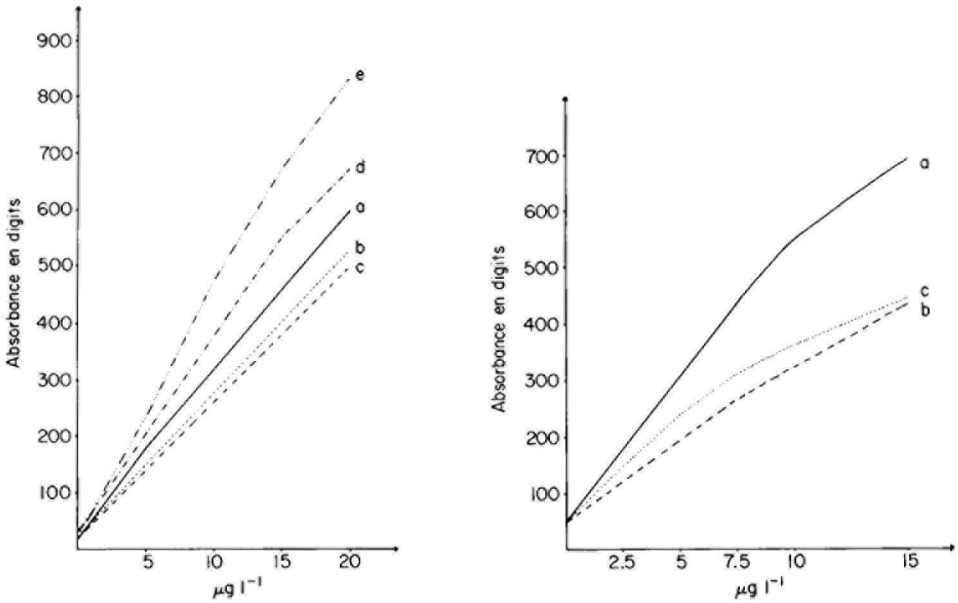

Fig. 1. Courbes d'étalonnage du cuivre par s.a.a. sans flamme en présence de 50 mg l^{-1} de Mg, Ca, Na, seuls ou en mélange. (a) Cu seul; (b) Cu + 50 mg Ca l^{-1}; (c) Cu + 50 mg Na l^{-1}; (d) Cu + 50 mg Mg l^{-1}; (e) Cu + mélange.

Fig. 2. Courbes d'étalonnage du plomb par s.a.a. sans flamme en présence de 50 mg Ca l^{-1} en milieu acide nitrique 0,1 M. (a) Pb seul; (b) Pb + 50 mg Ca l^{-1}; (c) Pb seul après série en presence de Ca.

en cascade avec des solutions d'acide nitrique de concentrations croissantes. Un mélange (50 ml) renfermant 10 mg l^{-1} de Cu, de Pb, de Cd et de Zn dans l'eau de mer, amenés à pH 7,6, ont été passés sur une colonne de 5 g de résine forme H^+. Les éluats ont été recueillis dans des fioles jaugées de 500 ml (de manière à avoir une solution renfermant 1 mg l^{-1} de chacun des métaux lourds) et de l'acide nitrique 2 M a été ajouté aux éluats nitriques (10^{-4}, 10^{-3}, 10^{-2} et 10^{-1} M) en quantité suffisante pour amener les solutions en milieu acide 10^{-1} M. Les dosages ont été effectués par s.a.a. avec flamme (Tableau 4).

On constate que Ca et Mg sont élués en même temps que Zn et Cd par HNO_3 10^{-2} M, de même que la quasi totalité de Na. Par contre, Pb peut être élué par HNO_3 10^{-1} M et Cu n'est élué totalement qu'avec HNO_3 1 M. Il ne semble donc pas nécessaire d'utiliser des acides fortement concentrés. Ces résultats montrent qu'il est possible d'isoler Cu et Pb en effectuant une élution préalable par HNO_3 10^{-2} M qui élimine Na, Ca et Mg, suivie d'une élution par HNO_3 N qui élue Cu et Pb. En ce qui concerne Zn et Cd, qui sont élués en même temps que Na, Ca et Mg par HNO_3 10^{-2} M, nous avons recherché une autre possibilité d'élution sélective pour ces deux métaux.

La technique décrite par Brajter et Grabarek [18] qui ont étudié la séparation de Ca en présence de Cu et de Mg en présence de Pb par elution avec une

TABLEAU 4

Quantités (mg l^{-1}) des cations eluées par les éluants nitriques

Cations	Eluant HNO_3						Total mg l^{-1}
	100 ml 10^{-4} M	100 ml 10^{-3} M	100 ml 10^{-2} M	50 ml 10^{-1} M	50 ml M	25 ml 2 M	
Na	0,438	0,927	0,627	0,158	néant	néant	2,15
Ca	néant	néant	3,77	néant	néant	néant	3,77
Mg	néant	0,014	6,86	néant	néant	néant	6,874
Zn	néant	néant	0,754	0,044	néant	néant	0,798
Cd	néant	néant	0,302	0,034	néant	néant	0,336
Pb	néant	néant	néant	0,950	néant	néant	0,950
Cu	néant	néant	néant	0,668	0,294	néant	0,962

solution de nitrate de potassium 0,5 M à pH 2,5 permet d'éliminer totalement Na et partiellement Ca et Mg, mais présente l'inconvénient de remplacer ces cations par une quantité importante de potassium qui provoque de fortes interférences lors des dosages par s.a.a. Nous avons alors envisagé l'utilisation d'un acide faible pour déplacer les alcalins et les alcalino-terreux. Etant donné que les métaux se fixent sur les atomes d'oxygène des groupements amino-diacétate de la résine, nous avons choisi l'acide acétique pour des raisons d'affinité chimique. Afin de maintenir la résine à un pH voisin de 2,9, pour ne pas provoquer une désorption partielle du cadmium, l'acide acétique a été dilué au 1:100. Les courbes d'élution des alcalins et alcalino-terreux ont été réalisées avec 5 g de résine forme calcium après passage de 50 ml d'eau de mer. Le sodium et le potassium sont élués totalement dès le début du passage de l'acide acétique au 1:100. Le magnésium s'élue beaucoup plus rapidement que le calcium, mais après passage de 250 ml d'acide acétique l'élution du calcium est totale (Fig. 3).

Au cours de l'élution des alcalins et des alcalino-terreux par l'acide acétique au 1:100, on constate une accélération de l'écoulement. Si l'on trace la courbe du volume élué en fonction du temps, on s'aperçoit que l'accélération se produit après les cent premiers ml d'acide acétique, c'est-à-dire lorsque le magnésium est presque totalement élué ainsi que la majeure partie du calcium. Ceci confirme donc l'hypothèse précédemment émise, de la variation du volume interstitiel du lit de résine en fonction du rayon ionique des ions fixés. Nous avons vérifié sur des mélanges de métaux lourds dans l'eau de mer que l'acide acétique 1:100 élimine totalement les alcalins et les alcalino-terreux sans entraîner les métaux lourds. Ces derniers sont ensuite isolés sélectivement à l'aide d'élutions en cascade par l'acide nitrique 10^{-2} M et 1 M [19]. Les résultats des dosages effectués par s.a.a. avec flamme sont indiqués dans le Tableau 5. On voit que dans le cas d'un mélange très complexe, on peut éluer quantitativement Zn, Cd et Co par HNO_3 10^{-2} M, et Cu et Pb par HNO_3 1 M. Par contre, Ni et Cr^{3+} se retrouvent partagés entre les deux éluats. On remarque

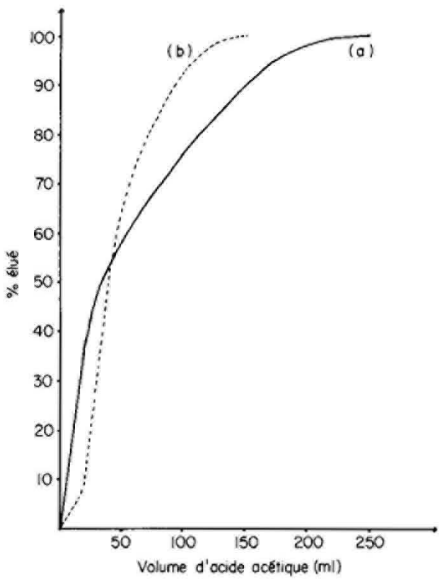

Fig. 3. Courbes d'élution de Ca et Mg par l'acide acétique dilué (1 + 99). (a) Ca; (b) Mg.

TABLEAU 5

Quantités (mg l^{-1}) des cations éluées en cascade par l'acide nitrique 10^{-2} M et 1 M

Cations	Elution HNO_3 10^{-2} M	Elution HNO_3 1 M
1°- Mélange Cu, Pb, Zn, Cd[a]		
Zn	0,92	0,01
Cd	0,97	0,03
Pb	0,08	0,91
Cu	néant	0,96
Mg, Ca, Na, K	néant	néant
2°- Mélange Cu, Pb, Zn, Cd, Ni, Co, Cr^{3+}[a]		
Zn	0,95	—
Cd	0,96	—
Co	0,94	—
Ni	0,46	0,60
Cr^{3+}	0,55	0,30
Cu	—	1,02
Pb	—	0,90
Mg, Ca	néant	—

[a] 1 mg l^{-1} de chaque élément dans l'eau de mer.

également que pour le Cr^{3+} la séparation n'est pas quantitative, une partie restant adsorbée sur la résine. L'utilisation d'acide nitrique très concentré ne permet pas de le désorber totalement. Enfin, un essai qualitatif nous a permis de confirmer que le chrome(VI) n'est pas retenu sur la résine Chelex 100.

SEPARATION DE MICROGRAMMES DE METAUX LOURDS DANS L'EAU DE MER

La technique de séparation des métaux lourds, mise au point sur des solutions renfermant 1 mg l^{-1} de chaque métal, a été expérimentée sur une solution renfermant 10 μg de Cu, 10 μg de Pb, 10 μg de Zn et 2 μg de Cd par litre d'eau de mer. L'eau de mer utilisée pour réaliser cette solution synthétique a été préalablement passée sur résine sous forme Ca^{2+} afin d'en éliminer les métaux lourds éventuellement présents, que l'on désignera "eau de mer purifiée". Le mélange des métaux lourds a été obtenu à partir de solutions étalons à 1 g l^{-1}, par dilution avec l'eau de mer purifiée.

La séparation a été effectuée avec 100 ml du mélange synthétique selon le mode opératoire suivant. Sur une micro-colonne de résine Chelex 100, (100—200 mesh), forme Ca^{2+} (diamètre 1 cm, hauteur 4 cm), on fait passer 100 ml d'eau de mer amenés à pH 7,6. Après lavage à l'eau distillée déionisée jusqu'à absence d'ions chlorures dans l'effluent, on élue les alcalins et alcalino-terreux par passage de 250 ml d'acide acétique (1 + 99). Cet éluat est rejeté. On lave la résine avec 25 ml d'eau distillée déionisée afin d'éliminer l'acide acétique restant dans le volume interstitiel du lit de résine.On élue ensuite successivement par 100 ml d'acide nitrique 10^{-2} M le zinc et le cadmium, puis par 10 ml d'acide nitrique 1 M le cuivre et le plomb (cet éluat est dilué à 100 ml afin d'avoir une concentration en acide nitrique égale à 10^{-1} M au moment du dosage). Un essai à blanc a été réalisé parallèlement avec 100 ml d'eau de mer purifiée.

Les quantités de métaux lourds élués ont été déterminées, par s.a.a. en four graphite, à partir de courbes d'étalonnages établies en milieu acide nitrique 10^{-1} M pour Cu et Pb, et 10^{-2} M pour Cd. Pour les dosages du cadmium et du plomb, les éluats ont été dilués au demi avec respectivement HNO_3 10^{-2} M pour Cd et HNO_3 10^{-1} M pour Pb afin de se situer dans la partie linéaire des courbes d'étalonnages. Les résultats sont indiqués dans le Tableau 6 à l'exception de Zn en raison des difficultés rencontrées pour le dosage de cet élément à ces teneurs. Ces résultats peuvent être considérés comme satisfaisants, les dosages par s.a.a. sans flamme comportant pour ces teneurs une imprécision qui influe sur l'estimation du rendement.

TABLEAU 6

Rendements pour Cu, Pb et Cd

Métal	Quantité dans le mélange (μg l^{-1})	Quantité éluée (μg l^{-1})			Rendement
		1er essai	2ème essai	3ème essai	
Cu	10	9,00	8,20	7,80	78 à 90%
Pb	10	7,60	7,30	7,70	73 à 77%
Cd	2	1,54	1,50	1,46	73 à 77%

CONCLUSIONS

Par utilisation d'acide acétique (1:100) on peut éluer totalement les alcalins et les alcalino-terreux, qui se fixent sur la résine Chelex 100, avant de procéder à l'élution sélective des métaux lourds. Ce traitement, qui permet d'éliminer les interférences importantes provoquées par les alcalins et les alcalino-terreux sur les dosages des métaux lourds par s.a.a. sans flamme, rend possible l'utilisation de la résine sous forme Ca^{2+} pour obtenir des séparations quantitatives des métaux lourds dans l'eau de mer et les solutions salines.

BIBLIOGRAPHIE

1 A. Le Bihan et J. Courtot-Coupez, Analusis, 3 (1975) 559.
2 D. A. Segar et A. Y. Cantillo, Analytical Methods in Oceanography, Advances in Chemistry series 147, American Chemical Society, Washington D.C., 1975.
3 W. C. Campbell et J. M. Ottaway, The Analyst, 102 (1977) 495.
4 Norme expérimentale AFNOR T 90-112, avril 1976, Dosage de 10 éléments métalliques par spectrophotométrie d'absorption atomique.
5 J. P. Riley et D. Taylor, Anal. Chim. Acta, 40 (1968) 479.
6 M. Satake, T. Asano, Y. Takagi et T. Yonekubo, Nippon Kagaku Kaishi, Jpn., 5 (1976) 762.
7 M. Evrard, G. Michard et D. Renard, C. R. Acad. Sci., Ser. C, 281 (1975) 681.
8 T. M. Florence et G. E. Batley, Talanta, 23 (1976) 179.
9 M. I. Abdullah, O. A. El-Rayis et J. P. Riley, Anal. Chim. Acta, 84 (1976) 363.
10 C. Lee, N. B. Kim, I. C. Lee et K. S. Chung, Talanta, 24 (1977) 241.
11 F. Bury et J. M. Levert, Bull. Soc. Chim. Belg., 84 (1975) 663.
12 C. W. Blount, D. E. Leyden, T. L. Thomas et S. M. Guill, Anal. Chem., 45 (1973) 1045.
13 D. E. Leyden, T. A. Patterson et J. J. Alberts, Anal. Chem., 47 (1975) 733.
14 R. E. Van Grieken, C. M. Bresseleers et B. M. Vanderborght, Anal. Chem., 49 (1977) 1326.
15 E. W. Davey et A. E. Soper, Limnol. Oceanogr., 20 (1975) 1019.
16 R. Rosset, Bull. Soc. Chim. France, 8 (1964) 1845.
17 R. Rosset, Bull. Soc. Chim. France, 1 (1966) 59.
18 K. Brajter et J. Grabarek, Talanta, 23 (1976) 676.
19 J. Lamathe, C. R. Acad. Sci., Ser. C, 286 (1978) 393.

Analytica Chimica Acta, 104 (1979) 319—326

ETUDE PHOTOELECTRONIQUE DE LA SEPARATION DU PLOMB ET DU CADMIUM PAR ECHANGE IONIQUE SUR LE PHOSPHATE DE HAFNIUM**

LUCETTE R. BALSENC* et MARCO G. SIMONA

Département de chimie minérale, analytique et appliquée de l'Université, 1211- Genève-4 (Suisse)

(Reçu le 5 mai 1978)

RESUME

La séparation des ions de plomb(II) et de cadmium(II) sur le monohydrogenophosphate de hafnium monohydrate [$Hf(HPO_4)_2 \cdot H_2O$] utilisé comme échangeur de cations a été étudiée à divers pH et en présence de divers agents complexants. La spectroscopie photoélectronique (x.p.s. ou e.s.c.a.) a permis de montrer que le plomb pénètre dans les couches profondes de l'échangeur alors que le cadmium se fixe de préférence à la surface de celui-ci. Cette propriété a été mise à profit pour améliorer la sélectivité de la méthode en masquant le cadmium par un ligand de grandes dimensions (1, 10-phénanthroline) qui empêche le cadmium de se fixer sans nuire à la fixation du plomb.

SUMMARY

X-ray photoelectronic study of the separation of lead and cadmium ions on crystalline hafnium phosphate used as a cation exchanger

Crystalline hafnium monohydrogenphosphate monohydrate [$Hf(HPO_4)_2 \cdot H_2O$] is a useful cationic exchanger for separating lead(II) and cadmium(II) ions. Studies have been carried out at various pH and in the presence of various ligands. X-ray photoelectron spectroscopy has shown that lead diffuses into the deeper layers of the exchanger while cadmium remains near the surface. This property can be used to improve the selectivity of the method by masking cadmium with a large ligand (1,10-phenanthroline), which prevents the metal from adsorbing without any effect on lead fixation.

Si le phosphate de zirconium en tant qu'échangeur d'ions a retenu l'attention de nombreux chercheurs [1—4], le phosphate de hafnium en revanche n'a pas connu la même popularité; il nous a donc semblé intéressant d'étudier en détail les propriétés de ce composé [5]. Nous décrivons ici une application du phosphate de hafnium à la séparation de deux cations bivalents de propriétés chimiques à maints égards relativement proches, le plomb(II) et le cadmium(II). Ces deux métaux toxiques sont couramment utilisés dans l'industrie et sont présents en quantités relativement importantes dans les eaux résiduaires.

**Dédié au professeur Denys Monnier à l'occasion de son 75e anniversaire.

La sorption des ions métalliques sur le phosphate cristallin de hafnium [$Hf(HPO_4)_2 \cdot H_2O$] que nous abrégeons en HfP dans la suite de ce travail, dépend de plusieurs facteurs eux-mêmes tributaires du mode de préparation: cristallinité, dimension des grains et contenu en eau. Par conséquent, nous nous sommes tout d'abord attachés à préparer du HfP dont les caractéristiques soient reproductibles. Les résultats de ce travail ainsi que les propriétés d'échangeur envers les ions alcalins ont été présentés [6]. L'échangeur utilisé possède une structure en couches. Les atomes de hafnium sont coplanaires, le plan des hafniums se trouve pris en sandwich entre deux couches de groupements PO_4H; chaque hafnium est coordonné à six oxygènes, chacun des oxygènes appartenant à un groupement PO_4H différent; dans ces groupements, l'oxygène porteur de l'atome d'hydrogène est dirigé vers la couche adjacente. Les atomes de hafnium et de phosphore sont disposés de telle manière qu'ils forment un cycle à six éléments en forme de chaise. Une telle répartition des éléments a pour résultat de former des cavités de type zéolitique; il existe une cavité par unité de formule et la molécule d'eau y réside.

HfP est un échangeur cationique chargé en ions H^+; l'échange peut être schématisé de la manière suivante

$$HfPHH \cdot H_2O + M^{2+} + n\ H_2O \rightleftharpoons HfPMe\ (n+1)\ H_2O$$

où $3 \leqslant n \leqslant 7$. En règle générale, le cation échangé n'est pas distribué uniformément dans la masse de l'échangeur mais pénètre lentement depuis la surface couche après couche.

La fixation des ions Pb^{2+} et Cd^{2+} sur HfP a été effectuée par la méthode discontinue (batch method) car notre échangeur, constitué de microcristaux, ne se prêtait pas à la formation d'une colonne chromatographique. Nous avons tout d'abord étudié la fixation séparée du Pb^{2+} et du Cd^{2+} puis la fixation simultanée des deux cations; l'influence du pH sur le taux de partage a été examinée.

Pour tenter d'améliorer la sélectivité de la méthode, nous avons eu recours à des agents de masquage, c'est-à-dire à des anions susceptibles de former avec Pb^{2+} et Cd^{2+} des complexes de stabilité différente; nous avons choisi de masquer le cadmium et de fixer le plomb. Premièrement, nous avons introduit dans le milieu à analyser des ligands simples, tels que chlorure, iodure, perchlorate, thiosulfate et salicylate. Secondement, nous avons joué sur les dimensions des complexes formés en utilisant un ligand de volume relativement important, la 1,10-phénanthroline, de telle manière que l'ion complexé ne puisse plus pénétrer, par empêchement stérique, à l'intérieur de l'échangeur.

La quantité de métal restant en solution a été déterminée pour chaque échantillon par deux méthodes différentes: par comptage de traceurs radioactifs et par spectrometrie d'absorption atomique (s.a.a.). La concentration moyenne du métal fixé sur l'échangeur a été déterminée par comptage direct du traceur radioactif tout d'abord, puis par s.a.a. après élution; dans la suite de ce travail nous désignerons cette concentration par [A]. En outre, la phase solide a été soumise à l'analyse par spectrométrie photoélectronique (x.p.s. ou

e.s.c.a.), ce qui nous a permis de déterminer la quantité de métal fixé à la surface de l'échangeur.

En effet, cette technique permet d'analyser qualitativement et semi-quantitativement les couches superficielles sur une profondeur moyenne de 2 nm environ [7] ; nous avons désigné la concentration superficielle ainsi mesurée par le symbole [B].

Si le rapport [B]/[A] est supérieur à 1, ce qui est le cas le plus fréquent, le cation demeure en surface; ceci se produit généralement pour de faibles concentrations ou pour des cations hydratés de grandes dimensions qui diffusent lentement à l'intérieur de la cavité zéolitique. Si le rapport [B]/[A] est proche de 1 le cation est distribué uniformément dans l'échantillon. Finalement, si le rapport [B]/[A] est inférieur à 1, le cation se fixe en profondeur, sans former de film sur la surface; un tel comportement est observé dans le cas où la fixation n'obéit plus aux lois de l'échange ionique. Le cas du plomb à pH 2 examiné ci-après, en est un exemple typique.

La spectrométrie photoélectronique permet non seulement d'identifier les éléments présents à la surface de l'échantillon mais encore de déterminer l'environnement chimique et l'état d'oxydation de l'atome considéré [8].

PARTIE EXPERIMENTALE

Tous les réactifs utilisés sont de qualité puriss., pro analysi ou AnalaR. Le HfP a été préparé dans nos laboratoires; nous avons déterminé une capacité de 5,08 méq g^{-1}, en bon accord avec la valeur théorique de 5,15 méq g^{-1}.

Une solution 10^{-3} M du métal en milieu nitrate—acide nitrique (10 ml) est mise en contact avec 100 mg de phosphate de hafnium et soumise à l'agitation magnétique à une température de 22 ± 1°C. Le temps de contact est fixé à 1 h. Des essais préliminaires s'étendant sur une période de 20 h ont montré que l'équilibre était atteint après 1 h pour le plomb et 15 min pour le cadmium. Les deux phases sont ensuites séparées par centrifugation et leur contenu en cation analysé. Les solutions et éluats ont été analysées par s.a.a. et comptage de traceurs radioactifs, la phase solide par comptage de traceurs radioactifs avant et après élution, et e.s.c.a. L'élution se fait au moyen d'une solution d'acide nitrique 6 M.

Pour les essais effectués en présence d'électrolytes et de 1,10-phénanthroline, le pH de la solution de départ a été fixée à 5,2; après échange le pH de la solution variait entre 2,9 et 5.

Chacun des résultats ci-après est la moyenne de cinq mesures à l'exception des expériences effectuées avec l'iodure de sodium et le salicylate qui sont la moyenne de trois mesures.

RESULTATS ET DISCUSSION

Fixation du plomb et du cadmium

Plomb. La Fig. 1 montre les nombres de milliéquivalents (méq) de plomb fixés et d'hydrogène libérés par 100 mg d'échangeur. Nous constatons que, si

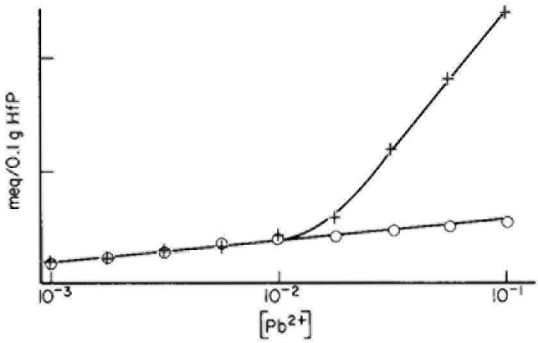

Fig. 1. Fixation du plomb sur l'échangeur en milieu NO_3^- en méq par 100 mg d'échangeur. pH (initial) = 5.0. (+) Pb^{2+} fixé; (○) H^+ libéré.

pour des concentrations de plomb inférieures à $7{,}5 \times 10^{-3}$ M, le phénomène obéit aux lois de l'échange ionique, il s'en écarte résolument pour des concentrations plus importantes. Lorsque la concentration du Pb^{2+} dans la solution à analyser est égale à 5×10^{-2} M, par exemple, l'échangeur ne libère que 1 méq de H^+ pour 2,5 méq de Pb^{2+} fixé.

Deux mécanismes peuvent être envisagés; nous pouvons supposer que pour des concentrations importantes un excès de plomb est adsorbé à la surface de l'échangeur, ou, alternativement, que le plomb diffuse à l'intérieur de l'échangeur où il pourrait précipiter.

A l'évidence des spectres photoélectroniques nous avons retenu la seconde hypothèse car les valeurs déduites de ces spectres nous permettent de calculer un rapport [B]/[A] égal à 0.60, ce qui signifie que le plomb n'est pas réparti uniformément dans l'échangeur mais qu'il a pénétré dans les couches profondes; en revanche, l'état chimique dans lequel se trouve le plomb à l'intérieur de l'échangeur ne peut être déduit des spectres photoélectroniques puisque cette technique ne permet d'examiner que les couches superficielles. Toutefois, comme la concentration des ions NO_3^- est relativement élevée dans la solution de départ, on pourrait envisager qu'une partie du plomb se trouve sous forme de complexe du type $Pb(NO_3)_x(H_2O)_n^{2-x}$ [9, 10] bien que les constantes de formation du complexe soient faibles [11].

Cadmium. En milieu nitrique Cd^{2+} se fixe moins bien que le Pb^{2+} (Fig. 2a); on pourrait attribuer cette affinité moindre au fait que la cadmium est susceptible, en milieu nitrate, de former l'ion $CdNO_3^+$ [12]. Nous avons toutefois calculé que, dans nos conditions d'expérience, la concentration du complexe nitrato simple n'excède pas 1,5% de la concentration totale du métal [13]. En revanche, la formation d'une paire ionique $Cd_2NO_3^{3+}$.aq. pourrait être envisagée, les dimensions de cet ion seraient suffisantes pour rendre difficile la diffusion à l'intérieur de l'échangeur. De fait, la spectrométrie photoélectronique nous montre un rapport [B]/[A] supérieur à 4 ce qui signifie que la plus grande partie du Cd^{2+} est retenue à la surface de l'échangeur. De plus, ces

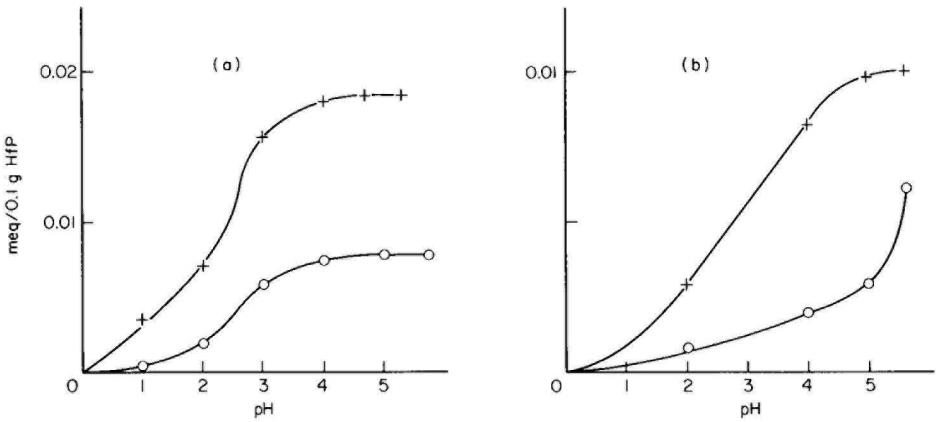

Fig. 2. Fixation du plomb et du cadmium en fonction du pH. (a) Fixation individuelle; (b) fixation simultanée. (+) Pb^{2+}; (○) Cd^{2+}.

mêmes spectres nous montrent un pic de l'azote que l'on peut raisonnablement attribuer au nitrate (410 ev); le rapport des intensités est d'un atome d'un d'azote pour deux atomes de cadmium. Toutefois comme les pics du cadmium et de l'azote se recouvrent partiellement et que la déconvolution est peu aisée, ces valeurs sont à considérer avec prudence.

Fixation simultanée du plomb et du cadmium. La Fig. 2(b) montre la fixation de Pb^{2+} et Cd^{2+} sur l'échangeur à partir d'une solution renfermant un mélange des deux cations en concentration équimoléculaire, ceci à différents pH. Il est intéressant de noter que le taux de fixation de Pb^{2+} ne varie que très peu en présence de Cd^{2+}; à pH 5 par exemple la valeur passe de 98% de métal fixé (Pb seul) à 92% (en présence de Cd) alors que le taux de fixation du cadmium, dans les mêmes conditions, tombe de 35 à 15%. C'est au pH 5 que le rapport des coefficients de partage Pb/Cd est le plus favorable. Toutefois si la concentration du cadmium est très supérieure à celle du plomb (10—50 fois), on n'obtient une séparation satisfaisante qu'en abaissant le pH jusqu'à 1.5 ou 2.

Nous avons tenté d'augmenter ce rapport en ajoutant à la solution des électrolytes; quelques résultats caractéristiques sont présentés dans le Tableau 1. Malgré l'avantage apparent d'un degré de complexation plus élevé pour le cadmium, la diminution simultanée des coefficients de partage des deux éléments par rapport au milieu nitrate rend le rapport Q (coefficient de partage du plomb/coefficient de partage du cadmium) nettement défavorable. Ceci est dû à la superposition de deux effets; d'une part l'effet complexant de l'anion conduisant à la diminution effective de la concentration des cations Pb^{2+} et Cd^{2+} et d'autre part la compétition pour les sites d'échange entre les cations bivalents et les ions Na^{+} provenant de la dissociation de l'agent complexant.

Nous avons alors choisi de masquer le cadmium en formant un complexe de dimension suffisamment importante pour qu'il ne puisse pas pénétrer à

TABLEAU 1

Coefficients de partage du plomb et du cadmium en présence de divers ligands à pH (initial) 5,2.

	Sans complexant	ClNa 10^{-1} M	INa 10^{-3} M	ClO_4Na 10^{-1} M	$S_2O_3Na_2$ 10^{-2} M	Salicylate 10^{-1} M
P_{Pb}	4900	250	900	355	47	1900
P_{Cd}	53	5	24	19	11	1570
Q^a	92	50	38	19	4	1

$^aQ = P_{Pb}/P_{Cd}$.

l'intérieur de l'échangeur. La 1,10-phénanthroline (L) forme avec le Cd^{2+} des complexes beaucoup plus stables qu'avec le Pb^{2+} ($\beta_3(Cd) = 10^{15,8}$; $\beta_3(Pb) = 10^9$), en outre elle présent l'avantage de ne pas libérer dans la solution de cations susceptible d'entrer en compétition avec le Pb^{2+} pour les sites d'échange.

Les résultats obtenus sont les suivants (Tableau 2). En l'absence de 1,10-phenanthroline (L), le plomb se fixe en plus grande proportion que le cadmium; toutefois les deux métaux sont présents en même quantité à la surface de l'échangeur, ce qui signifie que la plus grande partie du plomb a migré vers les couches intérieures. Par adjonction d'une quantité modérée du ligand telle que le rapport des concentrations soit [L] = [M] ([M] = concentration totale du plomb et cadmium), la quantité totale de plomb fixé sur l'échangeur ($[Pb]_E$) diminue à peine (2%) alors que la quantité totale de cadmium fixé ($[Cd]_E$) décroît considérablement (30%); à la surface en revanche les quantités de métal fixées augmentent du simple au double. Si nous augmentons encore la concentration du complexant telle que le rapport soit 10 [L]: 1[M], $[Pb]_E$ demeure approximativement constant alors que $[Cd]_E$ diminue encore; en revanche la concentration superficielle des deux cations augmente. Finalement, en ajoutant un grand excès de complexant (100[L]: 1[M]) $[Pb]_E$ augmente légèrement (5%) alors que $[Cd]_E$ tombe au tiers environ de sa valeur précédente, les concentrations superficielles suivent la même évolution. La majeure partie du cadmium se trouve alors sous forme

TABLEAU 2

Coefficients de partage du plomb et du cadmium en présence de 1,10-phénanthroline (L)

P_M	[L]:[M]			
	Sans L	1:1	10:1	100:1
P_{Pb}	5000	4900	4800	5000
P_{Cd}	65	41	15	4,5
Q^a	77	119	320	1111

$^aQ = P_{Pb}/P_{Cd}$.

de complexe, la surface est saturée et il ne peut plus se fixer. En revanche $[Pb]_E$ augmente car un certain nombre de sites ont été libérés à l'intérieur de l'échangeur par le masquage du cadmium.

En présence de 1,10-phénanthroline, la spectrométrie photoélectronique présente deux pics pour l'azote, l'un situé à 410 eV (nitrate) dont l'intensité diminue lentement lorsque [L] augmente, et l'autre situé à 406,5 eV qui peut être attribué avec certitude à 1,10-phénanthroline liée au métal [14] ; son intensité augmente parallèlement à la concentration du ligand. La 1,10-phenanthroline protonnée reste en solution et ne s'adsorbe pas sur HfP.

En présence de 1,10-phénanthroline les conditions expérimentales doivent être légèrement modifiées en particulier la valeur du pH initial qui est ajustée en fonction du rapport des concentrations [Cd]/[Pb] dans la solution. Si ce rapport est inférieur à 10, il est possible, en fixant le pH entre 7 et 8, d'extraire totalement le plomb en laissant pratiquement tout le cadmium en solution, ceci en une seule opération. Si le rapport des concentrations est supérieur à 10, on ne peut éviter la fixation de traces de cadmium qu'en abaissant le pH à une valeur de 5,5 environ; toutefois, dans ces conditions on ne parvient à fixer que 70% du plomb en une seule opération.

Interférences

En appliquant la méthode de séparation du plomb et du cadmium en présence de 1,10-phénanthroline au dosage de ces éléments dans les eaux résiduaires nous avons constaté que, si les interférences des ions bivalents tels que Mg^{2+}, Ba^{2+}, Fe^{2+}, Co^{2+} et Ni^{2+} étaient négligeables, les ions monovalents, lorsqu'ils étaient présents en concentration élevée, interféraient par adsorption compétitive; toutefois leur effet n'est pas entièrement négatif. Tout comme le phosphate de zirconium [15], HfP renferme un certain nombre de sites de très haute réactivité; ce nombre est estimé à 0,1—0,2% du total des groupements phosphates monohydrogénés. Les ions monovalents bloquent ces emplacements réactifs, augmentant ainsi la sélectivité de la méthode. Dans notre cas particulier, en l'absence d'ions monovalents, le cadmium vient s'adsorber sur les sites réactifs rendant pratiquement impossible une séparation totale des deux éléments. En présence d'ions Na^+ (10^{-2} à 10^{-1} M), seul le plomb se fixe sur l'échangeur, le coefficient de partage du cadmium tombant à 0.

Les essais ont été effectués avec des concentrations de plomb de l'ordre de 10^{-4} M, les concentrations de cadmium variant de 10^{-4} à 5×10^{-3} M.

Précision

En régle générale la précision des mesures photoélectroniques est faible. Si l'on désire déterminer la concentration d'un élément dans un environnement inconnu, la méthode est au mieux semi-quantitative (± 50%). Il a été établi par exemple que l'intensité relative d'une transition photoélectronique d'un métal complexé varie avec la nature du ligand et la structure cristalline du composé [16] ; de plus le facteur de proportionalité varie d'un élément à l'autre. Dans le cas présent, la sensibilité de la méthode est élevée pour le plomb et le

cadmium et ces deux éléments produisent des pics bien résolus de grande dimension. D'autre part, le dosage du phosphate de hafnium échangé est devenu un exercice de routine et des courbes d'étalonnage précises ont été établies. Des essais ont montré que la reproductibilité était satisfaisante (± 5%) et que la précision des analyses photoélectroniques se trouvait comprise entre 10 et 15%. Cette précision peut sembler dérisoire, toutefois il est bon de garder présent à l'esprit que ces résultats sont obtenus en mesurant des quantités de matière extrêmement faibles, typiquement de l'ordre de 10^{15} atomes.

Conclusion

Le phosphate cristallin de hafnium s'est révélé un matériel de choix pour la fixation sélective du plomb en présence de cadmium. Divers essais ont montré que, par un ajustement judicieux du pH, il était possible d'extraire sélectivement le plomb en présence de cadmium même si ce dernier se trouve en quantité 50 fois supérieure.

Nous remercions le Fonds national suisse de la recherche scientifique (projet 2.253 074) qui nous a permis d'entreprendre ce travail.

BIBLIOGRAPHIE

1 C. B. Amphlett, L. A. McDonald et M. J. Redman, J. Inorg. Nucl. Chem., 6 (1958) 220.
2 A. Clearfield et J. A. Stynes, J. Inorg. Nucl. Chem., 26 (1964) 117.
3 S. E. Horsley et D. V. Nowell, J. Colloid Interface Sci., 49 (1974) 394.
4 J. P. Gupta, N. J. Manning et D. V. Nowell, J. Inorg. Nucl. Chem., 40 (1978) 87.
5 C. K. Jørgensen, L. Balsenc et H. Berthou, Chimia, 27 (1973) 384.
6 M. G. Simona, L. R. Balsenc et C. K. Jørgensen, Helv. Chim. Acta, 61 (1978) 1984.
7 D. E. Eastman et M. I. Nathan, Physics Today, 28 (1975) 44.
8 C. K. Jørgensen, Fresenius Z. Anal. Chem., 288 (1977) 161.
9 A. I. Biggs, H. N. Parton et R. A. Robinson, J. Am. Chem. Soc., 77 (1955) 5844.
10 V. E. Mironov, Russ. J. Inorg. Chem., 6 (1961) 336.
11 R. Hugel, Bull. Soc. Chim. Fr., (1965) 971.
12 H. E. Hellwege et G. K. Schweitzer, J. Inorg. Nucl. Chem., 27 (1965) 99.
13 A. R. Davis et R. A. Plane, Inorg. Chem., 7 (1968) 2565.
14 C. K. Jørgensen et H. Berthou, Mat. Fys. Medd. Dan. Vid. Selsk., 38 (1972) 000.
15 J. Albertsson, Acta Chem. Scand., 20 (1966) 1689.
16 D. M. Wyatt, J. C. Carver et D. M. Hercules, Anal. Chem., 47 (1975) 1297.

Analytica Chimica Acta, 104 (1979) 327—336

NEW RADIOANALYTICAL METHODS OF HIGH SELECTIVITY

V. I. SHAMAEV

Mendeleev Institute of Chemical Technology, Miusskaja Square 9, Moscow A-47 (U.S.S.R.)

(Received 27th February 1978)

SUMMARY

Two new radioanalytical methods, characterized by high selectivity — close to that of the calibration curves method but much simpler experimentally — have been developed. In combination with preliminary substoichiometric concentration steps, both methods allow micro amounts of one element to be determined in the presence of macro amounts of other elements with similar chemical properties. The methods have been verified through the determination of cesium in the presence of 4000-fold quantities of potassium.

Of the various radioanalytical methods, the Method of Calibration Curves (m.c.c.) [1] gives the highest selectivity; direct determinations of a labelled element are possible in the presence of quantities of an interfering element which exceed the quantities permissible in substoichiometric variants of isotope-dilution and radiometric correction methods by a factor of 50—200. The need to plot these calibration curves experimentally with samples (or solutions) of known composition, however, makes m.c.c. too tedious for use in single analyses; only in continuous routine analyses can the time involved in plotting a calibration curve be justified.

In this report, two new radioanalytical methods which allow determinations to be made more simply and quickly without loss of the high selectivity of m.c.c., are described.

COMPARATIVE METHOD IN THE ANALYSIS OF TWO-COMPONENT SYSTEMS OF SIMILAR ELEMENTS

In this method, a fraction of the labelled and unlabelled elements is isolated from a solution (labelled with a radioisotope of the element to be tested) by means of a reagent which is added in an amount substoichiometric with respect to the sum of the two elements: $m_R/n < m_0$ and $m_0 = m_M + m_B$, where m_R is the molar amount of the reagent, n is the stoichiometric ratio in the compound formed, m_M is the molar amount of the labelled element (element to be determined) and m_B is the molar amount of the unlabelled (interfering) element.

The non-isolated fraction of the labelled element is determined radiometrically: $\alpha_x = A_{\text{non-is}}/A_{\text{in}}$, where $A_{\text{non-is}}$ and A_{in} are the radioactivities of

the non-isolated fraction and the initial (total) radioactivity of the labelled element.

A standard solution with the same total mass (m_0) of the two elements and an arbitrary (but, if possible, close to the assumed) ratio of the elements is prepared. The two elements are isolated from the standard solution with the same quantity (m_R) of the reagent as was used for the sample solution. The non-isolated fraction of the labelled element in the standard solution (α_{st}) is determined radiometrically. From these data, the quantity of labelled element in the sample solution can be calculated.

The method of calculation can be derived from the equation for the exchange constant, reported previously [2]:

$$\beta = \frac{1-\alpha}{\alpha} \times \frac{m_B - (m_R/n) + m_M(1-\alpha)}{(m_R/n) - m_M(1-\alpha)} \qquad (1)$$

where β is the exchange constant, i.e. the ratio of the equilibrium constants for the labelled and unlabelled elements in the given process, and α is the non-isolated fraction of the labelled element after the separation with a sub-stoichiometric quantity of the reagent, from the solution containing both elements.

As the quantities m_0 and m_R/n are the same for both standard and sample solutions and $m_B = m_0 - m_M$, eqn. (1) gives $m_0 - m_R/n = \text{const.} = m_M\,\alpha\,(1-\beta) + (m_R/n)\,(\beta/D)$, which converts to $m_M\,\alpha_x\,(1-\beta) + (m_R/n)\,(\beta/D_x) = m_{st}\,\alpha_{st}\,(1 - + (m_R/n)\,(\beta/D_{st})$ where $D = (1-\alpha)/\alpha$. After some transformations,

$$m_M = m_{st} \times \frac{\alpha_{st}}{\alpha_x} + \frac{m_R}{n} \frac{\beta}{\beta - 1} \times \frac{1}{\alpha_x}\left(\frac{1}{D_x} - \frac{1}{D_{st}}\right) \qquad (2)$$

or

$$m_M = m_{st} \times \frac{\alpha_{st}}{\alpha_x} + \frac{m_R}{n} \times \frac{\beta}{\beta - 1} \times \frac{1 - \alpha_{st}/\alpha_x}{(1-\alpha_x)\,(1-\alpha_{st})} \qquad (3)$$

The value of β can be calculated as the ratio of the corresponding equilibrium constants (e.g. the ratio of the extraction constants of the elements) but it is recommended that this constant be determined directly by the method described earlier [2]. Because eqns. (2) and (3) involve the ratio $\beta/\beta - 1$, the influence of any inaccuracy in the values of β on the error of an analysis is small.

Table 1 gives the results of model calculations. The theoretical values were calculated by means of eqn. (1) of a previous paper [1]. The standard amount of the labelled element was taken as $m_{st} = 0.3$ mmol ($\alpha_{st} = 0.753$). The results of the calculations (Table 1) show that, with an increase in the difference $m_{st} - m_M$, the relative importance of the second term in eqn. (3) increases but this does not influence the error of the determinations, which depends only on the precision with which the different values of eqn. (3) are calculated. Thus calculations according to eqn. (3) do not lead to any systematic error. But in actual analyses, the values α_x and α_{st} can only be determined with a

TABLE 1

Model calculations for the comparative method for two-component systems ($\beta = 25$; $m_0 = 10$ mmol; $m_R/n = 0.2$ mmol)

m_M (mmol)	$\frac{m_B}{m_M}$	$m_{st}\frac{\alpha_{st}}{\alpha_x}$	$\frac{m_R}{n} \times \frac{\beta}{\beta-1} \times \frac{1-\alpha_{st}/\alpha_x}{(1-\alpha_x)(1-\alpha_{st})}$	m_M calc.	Relative error (%)
0.1	99.0	0.324	−0.221	0.103	3
0.2	49.0	0.310	−0.103	0.207	3.5
0.3	33.3		(standard)		
0.4	24.0	0.291	+0.113	0.404	2.2
0.5	19.0	0.284	+0.2185	0.5025	0.5
0.6	15.7	0.279	+0.3197	0.5987	0.3
0.7	13.3	0.274	+0.427	0.701	0.15
0.8	11.5	0.270	+0.529	0.799	0.12
1.0	9.0	0.263	+0.748	1.011	1.1
2.0	4.0	0.247	+1.760	2.007	0.35

certain error; the influence of these errors on the total error increases with an increase in the absolute value of the second term of eqn. (3). The minimum error is attained if $\alpha_x = \alpha_{st}$, when the second term of eqn. (3) becomes zero, and $m_x = m_{st}$.

To obtain optimum results, the method of successive approximations is recommended. The separation with the substoichiometric quantity of reagent (m_R) is carried out, and with the theoretical curve [1] (for the given β and m_R/nm_0) a first approximation (m_{M_1}) for the labelled element is determined.

A standard solution (labelled with radioisotope of the element M) is prepared with the same m_0 and $m_{st} \simeq m_{M_1}$. The separation from this standard solution is done with the same quantity of reagent (m_R), and α_{st_1} is determined radiometrically. If $\alpha_{st} > \alpha_x$, the next standard solution is prepared with a smaller quantity of the labelled element ($m_{st_2} < m_{st_1}$), and vice versa.

As there is no necessity to attain full coincidence of α_{st} with α_x, the whole analysis (with the use of theoretical calibration curves) can be completed in one or two stages.

Obviously, the same factors as in the m.c.c. influence the precision of determinations [1], i.e. the radiometric error in the determination of α, the slope of the calibration curve at the point required (it is preferable to use a quantity of reagent stoichiometric for the amount of the labelled element, i.e. $m_R/n \simeq m_M$), the relative content of the (labelled) element to be determined in the sample solution, and the absolute value of α.

As in m.c.c. there is no need to meet the conditions of substoichiometry in order to obtain a single-valued dependence for $\alpha = f(m_M/m_0)$ which is realized when the unlabelled element influences the degree of isolation of the labelled element. Therefore the factor $\beta\, m_R/n\ (\beta - 1)$ in eqn. (3) has a rather formal meaning; for "non-substoichiometric" reagents, this factor can be determined by two special experiments with two different standard solutions (m_0 and m_R — const., $m_{st_1} \neq m_{st_2}$):

TABLE 2

Determination of cesium in the presence of potassium
(m_0 = 27.5 μmol; m_{st} = 1.31 μmol; m_{TPB} = 1.474 μmol)

Cs taken			Cs found			
m_{Cs} (μmol)	$\frac{m_K}{m_{Cs}}$	α	m_{Cs} Eqn. (3) (μmol)	Relative error (%)	m_{Cs} Eqn. (5) (μmol)	Relative error (%)
2.48	10:1	0.63	2.413	−2.7	1.97	−20.5
1.70	15:1	0.57	1.649	−3.0	1.47	−13.5
1.31	20:1	0.54	(standard)			
1.06	25:1	0.51	0.987	−6.9	0.996	−6.4
0.89	30:1	0.51	0.987	+10.9	0.996	+11.9
0.89	30:1	0.50	0.881	−1.0	0.923	+3.7
0.67	40:1	0.48	0.606	−9.4	0.770	+14.9
0.67	40:1	0.49	0.749	+11.8	0.847	+21.9
0.54	50:1	0.45	0.359	−33.5	0.535	−1.0
0.54	50:1	0.46	0.463	−14.2	0.611	+13.0

$$\frac{\beta}{\beta - 1} \times \frac{m_R}{n} = (m_{st_1}\,\alpha_{st_1} - m_{st_2}\,\alpha_{st_2}) \frac{(1 - \alpha_{st_1})(1 - \alpha_{st_2})}{\alpha_{st_1} - \alpha_{st_2}} \qquad (4)$$

Application of the method

The method was applied to the determination of cesium in the presence of potassium with extraction of the tetraphenylborate complexes into nitrobenzene. The results of the analyses are given in Table 2 (left part).

The left part of Table 3 is based on data from the determination [3] of vanadium in the presence of chromium by m.c.c. The interfering element (chromium) is not extracted by the reagent used (cupferron); its interference is caused by reduction of vanadium and formation of chromium vanadate. Table 3 shows that this method can be used for analyses of alloys containing 5—30% of vanadium. The left part of Table 4 presents the data [4] obtained for the determination of hafnium in the presence of zirconium by extraction of the thiocyanate complexes of these elements into tributyl phosphate (50% in dibutyl ether). For m_{st} = 1.5% (w/w), determinations are possible for 0.2—5% of hafnium in zirconium. In these cases, the values of the factor $\beta\, m_R/n\ (\beta - 1)$ were calculated from eqn. (4).

THE INTERPOLATION METHOD BASED ON LINEARITY OF THE INITIAL PARTS OF CALIBRATION CURVES

If the relative amount of the reagent used is low enough, the initial parts of the theoretical (Fig. 1) and experimental (Fig. 2) calibration curves are linear and this fact can be used for analytical purposes.

In this method, as in the previous method, fractions of the two elements are isolated from a labelled solution and from a standard solution; the same

TABLE 3

Analysis of chromium—vanadium alloys by extraction with cupferron into chloroform (5-mg samples, $m_{cupf.}$ = 8.69 μmol, pH 2.45; α_0 = 0.21, $m_R/n \times \beta/\beta - 1$ = 9.16)

Amount of V taken		Amount of V found				
m_V (μmol)	V (% w/w)	α	m_V Eqn. (3) (μmol)	Relative error (%)	m_V Eqn. (5) (μmol)	Relative error (%)
0.96	1.0	0.231	—	—	0.896	6.7
1.92	2.0	0.258	1.51	21.3	2.05	6.8
4.80	5.0	0.322		(standard)		
7.20	7.5	0.376	7.14	0.83	7.32	1.6
9.60	10.0	0.430	9.43	1.87	9.41	2.2
14.4	15.0	0.551	15.06	4.6	14.57	1.2
19.2	20.0	0.596	20.4	6.2	16.5	14.2
28.8	30.0	0.740	30.8	7.3	22.7	21.3

TABLE 4

Determination of hafnium in zirconium—hafnium alloys by extraction of thiocyanate complexes with a 50% solution of tributyl phosphate into dibutyl ether, saturated with thiocyanate
(250-mg samples, 2 M H_2SO_4; α_0 = 0.196; $m_R/n \times \beta/\beta - 1$ = 0.12 μmol)

Hf taken		Hf found				
m_{Hf} (μM)	Hf (% w/w)	α	m_{Hf} Eqn. (3) (μmol)	Relative error (%)	m_{Hf} Eqn. (5) (μmol)	Relative error (%)
1.68	0.1	0.200	—	—	—	—
2.80	0.2	0.200	2.6	7.1	2.9	5.0
7.28	0.5	0.208	7.0	5.3	8.8	20.8
10.0	0.7	0.2083	8.4	16.0	9.05	9.5
14.0	1.0	0.214	13.2	5.7	13.3	5.0
21.3	1.5	0.225		(standard)		
28.0	2.0	0.237	30.6	9.3	30.0	7.1
71.7	5.1	0.281	63.0	12.1	62.5	12.0
139.4	10.1	0.291	65.0	60.2	70.5	55.2
168.0	12.2	0.298	70.0	58.3		

quantity of reagent is used in each case. The standard solution must be of known composition with the same total quantity of both elements (m_0) as the labelled solution.

In both cases, the non-isolated fractions of the labelled element (α_x and α_{st}) are determined radiometrically and the amount of the required element is calculated from

$$m_M = m_{st} (\alpha_x - \alpha_0)/(\alpha_{st} - \alpha_0) \quad (5)$$

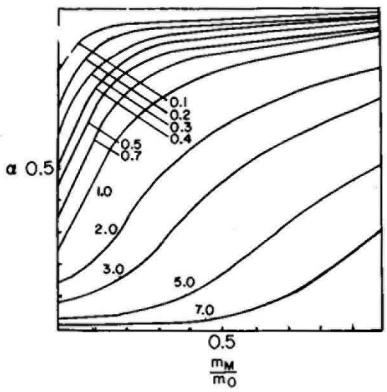

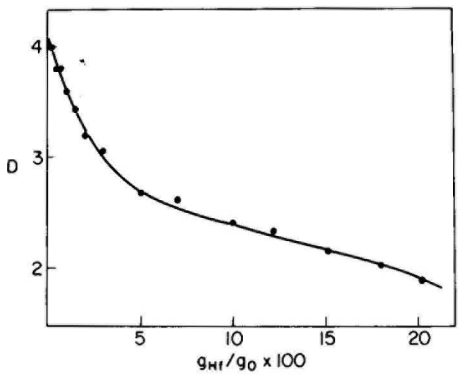

Fig. 1. The theoretical calibration curves $\alpha = f(m_M/m_0)$ for $\beta = 25$. The numbers on the curves are the relative quantities of reagent, $10 \times m_R/nm_0$.

Fig. 2. The calibration curve $D = f(g_{Hf}/g_0)$ for the determination of hafnium in zirconium—hafnium alloys by extraction of thiocyanate complexes with a solution of TBP in dibutyl ether.

where α_0 is the non-isolated fraction of the labelled element when its quantity tends to zero (i.e. $m_M \to 0$ and $m_B \to m_0$) for the same quantity of the reagent. The value of α_0 can be calculated theoretically, if the value of β is known and if substoichiometric separation conditions are met, from eqn. (10) of a previous paper [2]:

$$\beta_{(m_M \to 0)} = \frac{1-\alpha_0}{\alpha_0} \frac{m_B - m_R/n}{m_R/n} \tag{6}$$

Hence

$$\alpha_{0(m_M \to 0)} = \frac{\lambda - 1}{\lambda + (\beta - 1)} \tag{7}$$

where ($\lambda = 1/h_0 = nm_0/m_R$). Experimentally, the value of α_0 can be found by isolation of the fraction, with the same quantity of the reagent, from a solution labelled with a radioisotope of element M and containing a suitable amount of the unlabelled element such that $m_B = m_0$.

For the system Cs — K—TPB with extraction into nitrobenzene, for which the exchange constant β is 25, calculation from eqn. (7) for $\lambda = 18.7$ gives $\alpha_0 = 0.412$; experimentally, the non-isolated fraction from micro amounts of ^{137}Cs, for the same λ, is $\alpha_0 = 0.38$.

Table 5 gives the results of model calculations according to eqn. (5). These results and analogous calculations for different values of β and λ show that this method possesses a systematic error, which can be explained by deviation of the function $\alpha = f(m_M/m_0)$ from linearity. When $m_{st} \geqslant m_R/n$, the error of an analysis changes in the following way with increase in the ratio m_M/m_0:

TABLE 5

Model calculations for two-component systems by the comparative method with use of the linear dependence $\alpha = f(m_M/m_0) = 0.432$
($\beta = 25$, $\lambda = 20$, $(m_M)_{st} = 0.5$ mmol, $m_0 = 10$ mmol, $m_R/n = 0.5$ mmol)

m_M (mmol)	$\frac{m_B}{m_M}$	α_x	$\alpha_x - \alpha_0$	$m_{calc.}$ (mmol)	Relative error (%)
0.1	99.9	0.458	0.026	0.097	−3.0
0.2	49.0	0.488	0.056	0.211	+5.5
0.3	32.3	0.514	0.082	0.306	+0.5
0.4	24.0	0.541	0.109	0.407	+1.7
0.5	19.0	0.566	0.134	(standard)	
0.6	15.7	0.590	0.158	0.589	−1.8
0.7	13.3	0.613	0.181	0.675	−3.6
0.8	11.5	0.634	0.202	0.754	−5.7
0.9	10.1	0.654	0.222	0.828	−8.0
1.0	9.0	0.672	0.240	0.895	−10.5
1.5	5.7	0.744	0.312	1.164	−22.4
2.0	4.0	0.792	0.360	1.343	−33.0
3.0	2.3	0.850	0.418	1.560	−50.0

at first it has a positive value, then goes through the zero point at $m_M = m_{st}$, and with further increase in m_M, becomes increasingly negative. When $m_{st} < m_R/n$, the error has a negative value which after the point $m_M = m_{st}$, becomes positive. The calculated errors are shown in Fig. 3 for $\beta = 25$ and $h_0 = 0.05$ for different ratios of m_{st}/m_0. The optimum results of an analysis can be achieved if $m_{st} = m_R/n$, but for each value of m_{st} the region of minimum error is situated in the region $m_M \simeq m_{st}$. In Fig. 4, the calculated errors are shown for $\beta = 25$ and $m_{st} = m_R/n$; the optimum regions of the ratios m_M/m_0 for each value of $h_0 = m_R/nm_0$ are obvious.

The most suitable range for the substoichiometric fraction of a reagent is $h_0 = 0.04$—0.07. Similar results were obtained for systems with other values of β.

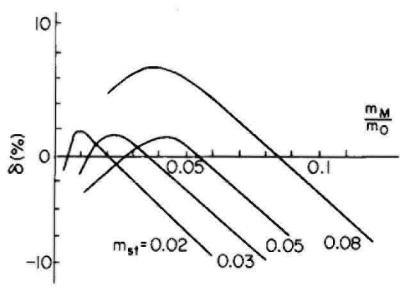

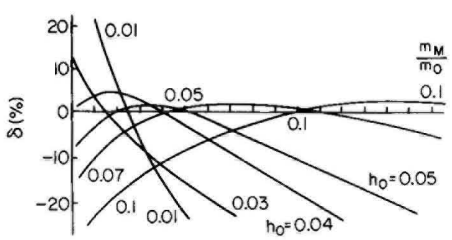

Fig. 3. The theoretical error for determinations by the interpolation method for $\beta = 25$ and $h_0 = 0.05$ for different ratios of m_{st}/m_0.

Fig. 4. The theoretical error for determinations by the interpolation method for $\beta = 25$ and $m_{st} = m_R/n$ for different values of h_0.

Approximate limits of the applicability of the method, for theoretical errors of less than 10%, obtained in model calculations are given in Table 6. If the β-values are low enough, the lower limits of the determinable relative quantity of a labelled element (less than 1%) can be realized only for systems with $\beta > 10$ to 15.

Experimental verifications of this method were carried out with the systems used in the comparative method (right-hand columns of Tables 2—4). The data show that, in most cases of low relative contents of the labelled element, this method gives better results than the previous one.

In another variant of the interpolation method based on the linear dependence $\alpha = f(m_M/m_0)$, two aliquots of the sample solution are used; to one of these a known quantity (m_{ad}) of the element to be determined is added. From both aliquots, isolation with the same substoichiometric quantity of reagent is carried out and the non-isolated fraction of the labelled element (α_x and α_{ad}) is determined radiometrically. The unknown quantity of the labelled element in the first aliquot is calculated from:

$$m_M = m_{ad}\,(\alpha_x - \alpha_0)/(\alpha_{ad} - \alpha_x) \qquad (8)$$

APPLICATION OF THE METHODS IN COMBINATION WITH PRELIMINARY SUBSTOICHIOMETRIC CONCENTRATION OF THE ELEMENT TO BE DETERMINED

In the methods described above, it is necessary to know the total quantity (m_0) of both elements in the solution. This value can be determined best by preliminary isolation of a fraction of both elements with a substoichiometric quantity (with respect to m_0) of a reagent. If the conditions of substoichiometric separation are met, the value of m_0 in the resultant solution will equal the quantity of reagent used: $m_0 = m_R/n$. At the same time, the concentration (enrichment) of a labelled element (with regard to an interfering element) is realized. This opens the way to relatively simple determinations of micro amounts of one element in the presence of macro amounts of elements with similar chemical properties.

Figure 5 shows the calculated enrichment factors (κ) as a function of a substoichiometric fraction of a reagent (h_0) for different values of the exchange constants (β). The calculations were carried out for $m_M \to 0$ ($m_B \gg m_M$). In the same figure, isolated fractions ($1 - \alpha$) of the labelled element are shown by broken lines. The losses of a labelled element in preliminary substoichiometric concentration operations can be corrected by means of the equation [5] (m_M)

TABLE 6

The approximate limits of applicability of the interpolation method with use of the linear dependence $\alpha = f(m_M/m_0)$

h_0	0.01	0.02	0.03	0.04	0.05	0.07	0.1
$(m_M/m_0) \times 100$ (%)	2—3	1—3	0.5—5	0.3—7	0.3—10	1—15	5—20

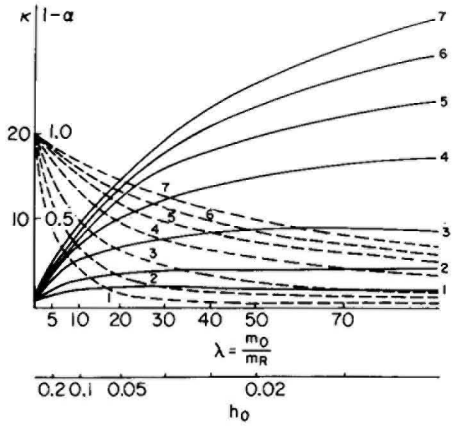

Fig. 5. The dependence of the enrichment factors (unbroken lines) and the isolated fractions of the micro amounts of labelled element (broken lines) on the substoichiometric fraction of a reagent. (1) $\beta = 2$; (2) $\beta = 5$; (3) $\beta = 10$; (4) $\beta = 20$; (5) $\beta = 30$; (6) $\beta = 40$; (7) $\beta = 50$.

initial = $m_M/(1-\alpha)$. The possibility of combining both these methods with preliminary substoichiometric concentrations was verified for the determination of small quantities of cesium in the presence of potassium with extraction by TPB into nitrobenzene. Two samples containing mixtures of cesium and potassium salts were analysed. In the first sample, $m_K/m_{Cs} = 400$; in the second $m_K/m_{Cs} = 4000$. Substoichiometric concentration (one-stage in the first case, and two-stage in the second) was carried out with a nitrobenzene solution of TPB. The results of this preliminary concentration are shown in Table 7. The quantity of cesium in the solutions was determined by the methods described above; the results are given in Table 8. For the given ratio m_K/m_{Cs}, the results given by the interpolation method are superior.

TABLE 7

Results of the preliminary substoichiometric concentration of cesium (partial separation of cesium and potassium)

Initial composition of mixtures (μmol)	Quantity of reagent at each stage of concentration (μmol)	$(1-\alpha)_{Cs}$	Enrichment factor	$\frac{m_K}{m_{Cs}}$ [a]
$m_K = 524$ $m_{Cs} = 1.31$	2.63	0.62	12.3	32.4
$m_K = 1440$ $m_{Cs} = 0.366$	(1) 72.4 (2) 3.62	0.58 0.46	(1) 11.5 (2) 9.2	(1) 341 (2) 37.1

[a]Ratio of the elements in the resultant solution.

TABLE 8

Determination of cesium in the presence of large amounts of potassium

Composition of standard solution. (μmol)	α_x	α_{st}	α_0	Amount of cesium found		
				$(m_{Cs})_{fin.}$ (μM)	$(m_{Cs})_{in.}$ (μM)	Relative error (%)
$(m_K/m_{Cs})_{init.}$ = 400; $(m_{Cs})_{init.}$ = 1.31 μmol						
m_K = 25.4				0.938[a]	1.51[a]	15.2
m_{Cs} = 0.772	0.570	0.555	0.430			
m_{TPB} = 1.313				0.862[b]	1.39[b]	6.1
$(m_K/m_{Cs})_{init.}$ = 3935; $(m_{Cs})_{init.}$ = 0.366 μmol						
m_K = 3.5				0.0871[a]	0.328[a]	10.4
m_{Cs} = 0.117	0.465	0.490	0.360			
m_{TPB} = 0.181				0.0945[b]	0.354[b]	3.3

[a]From eqn. (3). [b]From eqn. (5).

The technical assistance of V. G. Djatchkova is gratefully acknowledged.

REFERENCES

1 V. I. Shamaev, Zh. Anal. Khim., 27 (1972) 48.
2 V. I. Shamaev, Zh. Anal. Khim., 30 (1975) 2069.
3 M. E. Savkin, Nguen-Dyk-Ngia and V. I. Shamaev, Zh. Anal. Khim., 28 (1973) 1732.
4 V. I. Shamaev and G. K. Garbauskas, Radiokhimiya, 15 (1974) 132.
5 V. I. Shamaev, Zh. Anal. Khim., 22 (1967) 988.

Analytica Chimica Acta, 104 (1979) 337—343

DETERMINATION OF COPPER AND MANGANESE IN SEA WATER BY NEUTRON ACTIVATION ANALYSIS AND ATOMIC ABSORPTION SPECTROMETRY

H. V. WEISS and P. R. KENIS

Naval Ocean Systems Center, San Diego, CA 92152 (U.S.A.)

J. KORKISCH* and I. STEFFAN

University of Vienna, Institute for Analytical Chemistry, Währingerstrasse 38, A-1090 Vienna (Austria)

(Received 22nd June 1978)

SUMMARY

Two methods are compared for the determination of copper and manganese in sea water; the methods have been developed independently at two laboratories. One method is based on the simultaneous isolation of the two elements from sea water by co-crystallization with 8-quinolinol. The crystals are irradiated with neutrons, and after simple purification steps radio-induced ^{64}Cu and ^{56}Mn are quantified by γ-ray spectrometry. The other method involves chloroform extraction of the diethyldithiocarbamates of copper and manganese and subsequent determination of the two elements by atomic-absorption spectrometry. Both methods provide reliable measurements of copper and manganese concentrations at natural levels in sea water.

For the determination of copper and manganese in sea water, a variety of different methods has been used [1—26]; analytical techniques based on neutron activation analysis, following the preconcentration of these two elements by co-crystallization, have not been described in the literature. The present paper reports a method based on these analytical principles and also describes a technique of enrichment by liquid—liquid extraction followed by atomic-absorption measurement of extracted copper and manganese.

EXPERIMENTAL

Samples

Sea water was collected on two occasions at a depth of 20 ft. below the surface of the end of the pier at the Scripps Institution of Oceanography, La Jolla, California. One collection took place on 2 July 1976 while the other was not dated. At the time of collection the samples were acidified — the undated with nitric acid and the dated with hydrochloric acid (10 ml l^{-1} of sea water), filtered through a 0.45-μm membrane (Millipore membrane) and stored in acid-leached polyethylene containers.

Neutron-activation analysis procedure (n.a.a.)

Chemicals. The reagent 8-quinolinol "Baker Analyzed" was used in powder form. Manganese and copper carrier solutions contained 10 mg ml^{-1} of cation in distilled water. Comparators contained 1 and 4 μg of manganese and copper respectively, per ml. Hydrogen sulfide gas was of CP quality, while other chemicals were of AR grade.

Isolation of copper and manganese from sea water. Sea water was acidified with concentrated hydrochloric or nitric acid to a final concentration of 1% (v/v). Aliquots (250 ml) were transferred to containers and received 10^{-2} μCi of a high specific activity ^{64}Cu (10^2 mCi g^{-1} Cu) or 0.1 ml of a carrier-free ^{54}Mn. The solution was warmed for one hour on a hot-plate to approximately 80°C to equilibrate the radio-element with its counterpart in the sample. After cooling, 250 mg of 8-quinolinol was stirred into the sample and ammonia solution was added until the pH of the solution attained a value of 7—8. Crystallization was encouraged by agitation with a rod. After the solution had stood for 1—2 h, the crystals were collected on sintered glass of medium porosity. The isolated crystals, together with those adhering to the container walls, were dissolved in dilute acid (1.6 M). The γ-ray activity of the solution was measured in a well-type NaI (Tl) detector and compared with a tracer standard.

Treatment of sea water samples. Aliquots (250 g) were transferred to plastic beakers; Mn (0.2 μg) and Cu (2.0 μg) were added to some aliquots. ^{54}Mn tracer was then added, and the elements were co-crystallized. The solution was passed through a sintered glass disc of medium porosity. The crystals were transferred to a 7-ml polyethylene, snap-top irradiation vial. The ^{54}Mn γ-ray activity of the separated crystals was measured and compared with a standard to correct for the fraction of oxine that adhered to the walls of the sample container.

Blanks. The copper and manganese content was determined at least in duplicate, for oxine (250 mg), and ammonium hydroxide solution (2.5 ml). These reagents were used in these amounts in the pre-irradiation processing. For future reference, these elements were also quantified in 2.5-ml aliquots of high-purity nitric acid (Ultrex, J. T. Baker).

A procedural blank was determined in quadruplicate on 250-ml aliquots of sea-water filtrates freed of copper and manganese by previous co-crystallization with 8-quinolinol. The filtrates were acidified with 1 ml of Ultrex nitric acid, spiked with ^{54}Mn and the elements were co-crystallized as described above.

Comparators. Each comparator solution (1 ml) was irradiated separately.

Irradiation. Samples, comparators, and blanks were irradiated for two hours at full power in the TRIGA Reactor, University of California, Irvine, California. The flux was 1×10^{12} ncm^{-2} s^{-1}, and the specimens were rotated about the reactor core at 1 rev./min.

Radiochemical purification and measurement. After irradiation the sample or blank was quantitatively transferred with 50 ml of 3 M hydrochloric acid to a vessel that contained 1 and 2 ml of copper and manganese carriers, respectively. All blanks received a standard quantity of ^{54}Mn and, except for the 8-quinolinol blank, they also received 250 mg of 8-quinolinol. Hydrogen

sulfide gas was bubbled for 30 s through the solution, and the resultant CuS precipitate was collected by filtration. The CuS was dissolved in about 10 drops of freshly prepared aqua regia, evaporated to dryness and then diluted to 30 ml with water. The solution was filtered through a sintered glass disc to separate insoluble matter. Then 10 ml of concentrated hydrochloric acid were added to the filtrate, and CuS was precipitated and separated. The filtrate from the initial copper separation was made ammoniacal, and the precipitated oxinate was collected and then dissolved in 50 ml of concentrated nitric acid. The solution was heated over a flame for several minutes to degrade the oxine, while hot solid potassium bromate was added to precipitate manganese dioxide. After cooling in an ice-bath, the precipitate was separated by filtration.

The corresponding carrier was added to the comparator. Copper was precipitated singly as described above; the manganese comparator was brought to 50 ml with concentrated nitric acid, heated, and then treated with potassium bromate.

All precipitates to be measured were collected on membrane filters, covered with a complementary paper disc and bagged in polyethylene.

The induced radioactivities were measured flat against the surface of a 38-cm Ge (Li) detector coupled to a 4096-channel pulse-height analyzer. The γ-ray pulses were accumulated for 10—20 min under live-time counting conditions. The pulse-height data were fed into a computer which provided the net counting rate for the 511- and 847-keV photopeaks of ^{64}Cu and ^{56}Mn. The count rate was normalized for the ^{54}Mn yield determined prior to irradiation and for the lapse of time from the end of the irradiation.

Carrier yield determinations. The filter membrane containing the precipitated copper and manganese was folded and inserted into 1.3-ml, snap-top, polyethylene vial to which 0.6 ml of distilled water was added. Standards (0.6 ml of carrier solution) placed in similar vials also received a blank filter membrane to reproduce volume and geometric conditions. Samples and standards were irradiated for precisely 60 s in a pneumatic tube facility with the reactor at full power. The 511-keV photopeak of ^{64}Cu and 847-keV photopeak of ^{56}Mn were measured in the manner described for the sample. After correction for decay from the end of the irradiation, comparison of the re-irradiated samples with standards allowed calculation of the copper carrier yield.

The normalized ^{56}Mn and ^{64}Cu of the original irradiation were corrected for these yields. Upon comparison of fully normalized samples and comparator photopeaks, the weight of element in the sample was computed.

Atomic-absorption procedure (a.a.s.)

The diethyldithiocarbamates of copper and manganese are isolated from 1-l samples of sea water by means of chloroform—acetone extraction under exactly the same experimental conditions as described earlier [1]. Prior to the extraction from sea water, the separatory funnels to be used are purified by extracting successively two 1-l samples of twice-distilled water employing the same extraction technique and discarding both the aqueous and organic phases.

The organic extract obtained after the extraction of 1 l of sea water is carefully evaporated to dryness on a steam bath and organic matter is destroyed by treatment of the residue with 10 ml of a freshly prepared solution of aqua regia. The solution is evaporated to dryness, the residue is dissolved in 10 ml of 6 M hydrochloric acid and after evaporation to dryness the residue is again taken up in 10 ml of 6 M hydrochloric acid. In this solution copper and manganese are determined by atomic-absorption spectrometry [1].

RESULTS

In at least four assays during the co-crystallization step, the recoveries of manganese and copper were 99.8 ± 1.3 and 100.4 ± 1.4%, respectively.

The concentrations of these elements in the reagents used in the pre-irradiation processing were measured; the data showed that following the initial acidification 0.002 ± 0.001 and 0.015 ± 0.004 μg of manganese and copper were added to the sample by way of 8-quinolinol and the ammonium hydroxide solution. If nitric acid of the quality analyzed had been used in the acidification process, an additional 0.003—0.001 and 0.005 ± 0.001 μg of the respective elements would have been introduced. The procedural blanks for manganese and copper were 0.010 ± 0.001 and 0.035 ± 0.010 μg, respectively.

The average copper and manganese concentrations and standard deviations (6 determinations) for the undated sea-water sample appear in Table 1. The data for the six aliquots that were spiked with manganese and copper are also included. The elements added were recovered quantitatively

Table 2 shows the average of six assays for the sample analyzed by both procedures. From these data it is evident that the two methods can be employed

TABLE 1

The concentrations (μg/250 g) of copper and manganese found in the undated sea-water sample and in spikes of the same sample

Element	Unspiked concentration	Spike concentration	Quantity of spike (μg)
Cu	0.291 ± 0.021	2.300 ± 0.092	2.0
Mn	0.158 ± 0.005	0.357 ± 0.007	0.20

TABLE 2

Results of determinations of copper and manganese in sea-water samples obtained by both analytical procedures

Element	Concentrations (μg kg^{-1})	
	N.a.a.	A.a.s.
Mn	0.96 ± 0.04	1.00 ± 0.05
Cu	1.98 ± 0.12	2.20 ± 0.09

effectively to determine copper and manganese in sea water with reasonably high accuracy. Comparison of these average values with values obtained by other investigators (see Table 3) shows that a relatively good agreement of the data is obtained, especially with respect to the copper content, which has been determined in samples of sea water much more frequently than manganese.

DISCUSSION

In the crystallization step, copper and manganese are carried quantitatively with the solid phase. However, in subsequent processing the 5—10% of the oxine that adhered to the container walls was not transferred to the irradiation vial. A quantitative transfer was effected expeditiously by dissolution with

TABLE 3

Copper and manganese contents (in $\mu g\ l^{-1}$) of sea water

Contents		Analytical method	Ref.
Copper	Manganese		
1.98 ± 0.12	0.96 ± 0.04	Co-crystallization—n.a.a.	This paper
2.20 ± 0.09	1.00 ± 0.05	Extraction—a.a.s.	
2.2	4.0	Extraction—ion exchange—a.a.s.	[1]
0.8—5.7	2.5—9.1	Extraction—a.a.s.	[2]
1.5—19.8	1.4—20.7	A.a.s.	[3]
0.7—1.5	—	A.a.s.	[4]
1.3	—	A.a.s.	[5]
0.57	—	A.a.s.	[6]
4.8	—	Ion exchange—a.a.s.	[7]
1.12; 1.37	—	Extraction—a.a.s.	[8]
6.06	—	Ion exchange—a.a.s.	[9]
1.12—1.92	—	Coprecipitation—n.a.a.	[10]
1.49—3.35	—	Coprecipitation—n.a.a.	[11]
8.2; 9.0	—	Polarography[a]	[12]
20	—	Ring-oven method	[13]
2.4; 3.2	—	Extraction spectrophotometry	[14]
26.0—28.0	—	Extraction spectrophotometry	[15]
0.8	—	Flotation[b] spectrophotometry	[16]
2.5; 6.47	—	Extraction spectrophotometry	[17]
2.6	—	Electron spin resonance	[18]
0.48—1.6	—	Ion exchange—x.r.f.	[19]
2.22; 3.80	—	Anodic stripping voltammetry	[20]
0.38	—	Isotope dilution m.s.	[21]
9.8; 1.75; 0.93	—	Anodic stripping voltammetry	[22]
—	4.1—6.4	Coprecipitation[c]	[23]
1—20[d]	0.5—3.0[d]	—	[24]
3.0[e]	2.0[e]	—	[25, 26]

[a]Single-sweep polarography and anodic stripping voltammetry. [b]Adsorption colloid flotation. [c]Coprecipitation followed by extraction and spectrophotometry. [d]Range of values reported. [e]Mean of reported values.

acid. However, this treatment was precluded, because dissolved oxinate underwent degradation during the neutron bombardment, and this complicated the subsequent precipitation of the oxinate in the radiochemical purification of manganese.

The loss of metal-carrying oxine was corrected by measurement of the ^{54}Mn yield after transfer to the irradiation vial. Since manganese and copper were completely co-crystallized, this yield also applied to copper. Furthermore, by not adding additional reagents before the irradiation, the blank was also minimized.

At the end of a 2-h irradiation period, 2.5×10^3 and 6.0×10^4 photopeak counts per minute were accumulated per microgram of copper and manganese. Thus, submicrogram amounts of these elements were quantifiable with acceptable counting statistical errors. As the usual concentrations of copper and manganese in sea water center around the ppb level for copper and tenths of a ppb for manganese, even the modest irradiation schedule adopted provides adequate sensitivity.

The radiochemical purity for both elements is such that they would be susceptible to reliable quantification with the inherently more efficient Ge (Li) detector, were greater sensitivity required.

This research was sponsored by the Fonds zur Förderung der wissenschaftlichen Forschung, Vienna, Austria and by the U.S. Office of Naval Research under Contract No. NR 683-301. The generous support from these sources is gratefully acknowledged.

REFERENCES

1 J. Korkisch and A. Sorio, Anal. Chim. Acta, 79 (1975) 207.
2 D. L. Zalev, I. P. Alimarin and C. I. Neuman, Zh. Anal. Khim., 27 (1972) 1223.
3 D. C. Burrell, Anal. Chim. Acta, 38 (1967) 447.
4 R. R. Brooks, B. J. Presley and I. R. Kaplan, Anal. Chim. Acta, 38 (1967) 321.
5 T. H. Donnelly, J. Ferguson and A. J. Eccleston, Appl. Spectrosc., 29 (1975) 158.
6 L. L. Edwards and B. Oregioni, Anal. Chem., 47 (1975) 2315.
7 J. P. Riley and D. Taylor, Anal. Chim. Acta, 40 (1968) 479.
8 D. W. Spencer, D. E. Robertson, K. K. Turekian and T. R. Folsom, J. Geophys. Res., 75 (1970) 7688.
9 R. A. A. Muzzarelli and R. Rocchetti, Anal. Chim. Acta, 69 (1974) 35.
10 T. Fujinaga, Y. Kusaka, M. Koyama, H. Tsuji, T. Misuji, S. Imai, J. Okuda, T. Takematsu and T. Ozaki, J. Radioanal. Chem., 13 (1973) 301.
11 S. Gohda, Bull. Chem. Soc. Jpn., 45 (1972) 1704.
12 G. C. Whitnack and R. Sasselli, Anal. Chim. Acta, 47 (1969) 267.
13 R. W. Frei and C. A. Stockton, Mikrochim. Acta, (1969) 1196.
14 J. Abraham, M. Winpe and D. E.. Ryan, Anal. Chim. Acta, 48 (1969) 431.
15 J. P. Riley and P. Sinhaseni, Analyst, 83 (1958) 299.
16 Y. S. Kim and H. Zeitlin, Sep. Sci., 7 (1972) 1; Chem. Commun., (1971) 672.
17 B. G. Stephens, H. L. Felkel and W. M. Spinelli, Anal. Chem., 46 (1974) 692.
18 Y. P. Virmani and E. J. Zeller, Anal. Chem., 46 (1974) 324.
19 D. E. Leyden, T. A. Patterson and J. J. Alberts, Anal. Chem., 47 (1975) 733.

20 W. Lund and M. Salberg, Anal. Chim. Acta, 76 (1975) 131.
21 M. Murozumi and Y. Abe, Jpn. Anal., 24 (1975) 337.
22 T. M. Florence, J. Electroanal. Chem., 35 (1972) 237.
23 S. M. Shah and S. R. Rao, Current Science (India), 41 (18) (1972) 659.
24 J. P. Riley and G. Skirrow, Chemical Oceanography, Vol. 2 Academic Press, New York, 1965, pp. 295—424.
25 J. L. Mero, The Mineral Resources of the Sea, Elsevier, Amsterdam, 1964, pp. 26—27.
26 E. D. Goldberg, in J. P. Riley and G. Skirrow (Eds.), Chemical Oceanography, Academic Press, New York, 1965, p. 163.

Analytica Chimica Acta, 104 (1979) 345—353

AN INVESTIGATION OF QUENCHING EFFECTS IN THE DIRECT FLUORIMETRIC DETERMINATION OF URANIUM IN MINERALS†

JOHANNES C. VESELSKY* and YVONNE RATSIMANDRESY**

International Atomic Energy Agency, Laboratory Seibersdorf, A-2444 Seibersdorf (Austria)

(Received 8th May 1978)

SUMMARY

A semilogarithmic dependence of the reduction of uranium fluorescence intensity on the concentration of Fe(III), Cr(III) or Mn(II) in the flux was established which enables the quenching power to be defined in terms of the characteristic half-concentration, $c_{1/2}$, i.e. that concentration which reduces uranium fluorescence to half its original value. A similar dependence holds for unknown mixtures of quenchers in minerals; this makes possible a simple direct determination of uranium without spiking, by extrapolation of the quenching function to sample weight zero. The dependence of the results by the spike method on the degree of quenching was determined and two improved analytical procedures are proposed for the determination of about 20—5000 ppm of uranium in minerals.

Several elements cause partial quenching of the uranium fluorescence excited by ultraviolet radiation in various fluxes and interfere in the fluorimetric determination of uranium. This interference can be eliminated in three ways: by dilution, by purification of the uranium by extraction, ion-exchange or other methods, and by correction of the quenching effect by means of an internal uranium standard ("spike" method); a detailed review of this subject has been published [1]. The dilution method has its limitations [1] while purification of the uranium requires elaborate processing. Both methods include an initial leaching or dissolution step, which is unnecessary when the mineral is simply fused and measured in the flux, if a spike is added (direct method).

Comments on such a direct fluorimetric determination of uranium have been published [2—4]. Grimaldi, et al. [3], who used a carbonate flux, claimed to have observed no quenching effects. This is difficult to understand. In addition, the authors of [1] have observed that a flux composed of a mixture of alkali metal carbonates frequently does not decompose samples completely. Pure sodium fluoride — historically the first fluorimetric flux — has been used by Price et al. [2], but this substance was abandoned because

---

** On leave of absence from Laboratoire d'analyse Minerales et d'Essais Industriels, Ampandrianomby, Tananarive, Madagascar.

†Presented at Euroanalysis III, Dublin, 1978.

of some practical disadvantages and replaced by a mixture of 98% NaF and 2% LiF, which has a lower melting point, higher sensitivity and better surface properties (see review [1]). Vozella, et al. [4] used 400-mg pellets prepared from this material, but the direct method described was applied only to a highly specialized problem, i.e. the determination of uranium in zirconium.

A more generally applicable method based on the use of 400-mg NaF/LiF pellets has already been described [1]. A small portion (0.4 mg) of the finely powdered (< 400 mesh) mineral is weighed onto a fused 400-mg NaF/LiF pellet in a special small platinum dish. After fusion and measurement of the partially quenched uranium fluorescence, a spike is added and the pellet fused a second time, followed by another measurement of the fluorescence. The absolute amount of uranium present on the pellet is calculated from the formula: $U_{sa} = F_1 \cdot U_{sp}/(F_2 - F_1)$, where U_{sa} = μg of uranium in the sample on the pellet, gU_{sp} = μg of spike uranium, F_1 = intensity of fluorescence before spiking, and F_2 = intensity of fluorescence after spiking.

The method has certain disadvantages, the most serious being the possibility of errors because of the difficulty of obtaining representative samples and the necessity of using a microbalance to measure the small sample weights. When this method was used, even for reference samples of high homogeneity (IAEA uranium standards), repeatedly erroneous results were obtained. In practically all these cases results were low, sometimes by 20—30%. This must be a consequence of the spiking step because other possible sources of error such as incomplete sample decomposition were ruled out. Consequently, the behaviour of some of the more important quenchers was investigated. For simplicity, the preliminary experiments were carried out with 400-mg pellets; later interest was focused on considerably heavier pellets, thus permitting larger sample weights.

Other investigations of the quenching effect have been published [2, 5, 6] but there seems to be no exact quantitative classification of quenching behaviour; definitions such as "very strong", "weak", etc. [6] are unsatisfactory. The degree of quenching is usually expressed as a percentage by Q, which is given by: $Q = 100\,(1 - F/F_0)$ where F_0 is the uranium fluorescence intensity in the absence of a quencher and F is the fluorescence intensity of the same quantity of uranium in the presence of a certain amount of quencher. A theoretical study of quenching in fluorimetry of uranium was carried out by Price et al. [7]; these authors introduced the important parameter "half-concentration" ($c_{1/2}$), which will be discussed below.

The purposes of the work described in this paper were:

1. to investigate the dependence of the quenching on the concentration of uranium and of quenchers (Fe(III), Mn(II) and Cr(III) in flux pellets of two different sizes (400 mg and 2.5 g NaF/LiF) and to derive from the results a numerical value suitable for the classification of the quenchers;
2. to investigate the spiking step in the direct determination of uranium in minerals (with 2.5 g pellets) in detail and to develop an improved procedure. This part of the work included a check of the dependence of the analytical results on the degree of quenching and the amount of spike added.

EXPERIMENTAL

The experimental technique with 400-mg pellets has been described [1]; truncated cone-shaped dishes made of 0.4-mm platinum sheet holding 2.5 g of flux mixture were used throughout for the experiments with heavier pellets. The fluorescence measurements were carried out with a Galvanek-Morrison fluorimeter (Jarrell-Ash Co.). The dimensions of the dishes and the platinum tray used for their introduction into the furnace (Simon-Mueller furnace model 3A, operated with a slight overvoltage to achieve and maintain about 1000°C) permitted the simultaneous fusion of ten 400-mg or four 2.5-g pellets. The details of the experimental technique used for the heavy pellets are given below (Procedure 1).

Uranium solutions were prepared by dissolution of very pure U_3O_8 in (1 + 1) nitric acid and suitable dilution, the usual concentrations being 100 and 10 μg U ml^{-1}.

The quencher solutions were prepared by suitable dissolution of reagent-grade Fe_2O_3, $MnSO_4 \cdot H_2O$ and Na_2CrO_4; the standard concentration was always 1.0 mg Me ml^{-1}. Chromium(VI) had to be reduced to chromium(III) by hydrogen peroxide in sulphuric acid; excess of peroxide was removed by boiling.

The flux mixture was prepared by intimately mixing reagent-grade NaF (98%) and LiF (2%) (in batches of about 2 kg); sometimes commercially available 200-mg pellets (Opto-Electronics (W.Zeh), Wiesbaden) were used.

The various amounts of quencher as well as the uranium were transferred to the pellets by means of Eppendorf micropipettes, up to 20 μg of quencher per 400-mg pellet and up to 250 μg per 2.5-g pellet. The dependence of the fluorescence intensity on the amount of quencher was investigated for two different uranium concentrations (1.0 and 0.1 μg U/pellet).

RESULTS

Definition of "quenching power"

A plot of uranium fluorescence from a given uranium concentration in a pellet in the presence of different concentrations of Cr(III), Fe(III) and Mn(II) is shown in Fig. 1. The plot is linear on a semi-logarithmic scale, in good agreement with an exponential dependence on quencher concentration: $I = I_0 e^{-kc}$ where I is the intensity of fluorescence at a quencher concentration c, I_0 is the intensity of fluorescence with no quencher, and k is a constant.

The "quenching power" of an individual element can conveniently be expressed by the "half-concentration" $c_{1/2}$, which is that concentration of quencher in the pellet which reduces uranium fluorescence intensity to one half of its value in the absence of the quencher: $I_0/2 = I_0\, e^{-kc_{1/2}}$, i.e. $c_{1/2} = \ln 2/k$. Quenching may be understood as an optical absorption effect obeying Lambert's equation [2], and the empirical equation above can be related to the Lambert–Beer relationship: $I = I_0\, e^{-\epsilon cl}$ where the terms have their conventional meanings. The constant k would be formally equal to ϵl and a simple

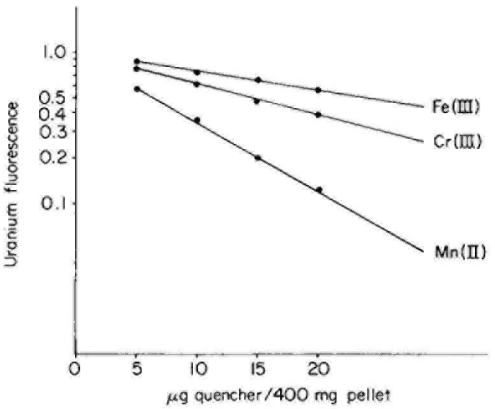

Fig. 1. Quenching of the fluorescence of uranium (0.1 or 1.0 μg) in 400-mg pellets by Mn(II), Cr(III) and Fe(III).

semilogarithmic dependence is valid as long as k does not depend on the quencher concentration. At relatively high quencher concentrations in the 2.5-g pellets (Figs. 2—4) k varies with the quencher concentration; here the linear part of the relationship, for smaller quencher concentrations, can be used for the definition of $c_{1/2}$.

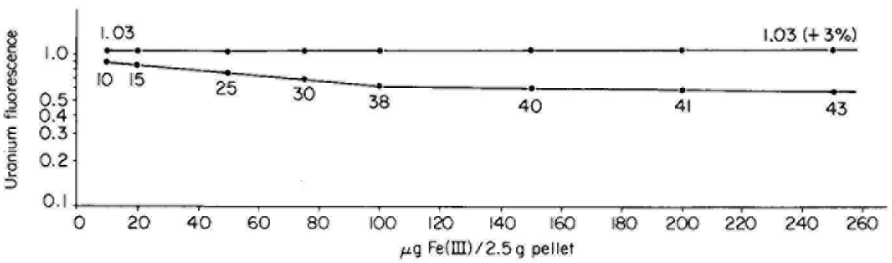

Fig. 2. Quenching of the fluorescence of uranium (1.0 μg) in 2.5-g pellets by Fe(III): numbers under points indicate % quenching. Upper curve is after correction with a uranium spike.

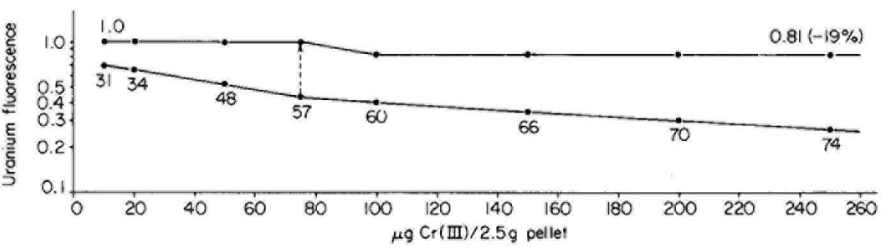

Fig. 3. Quenching of the fluorescence of uranium (1.0 μg) in 2.5-g pellets by Cr(III): numbers under points indicate % quenching. Upper curve is after correction with a uranium spike.

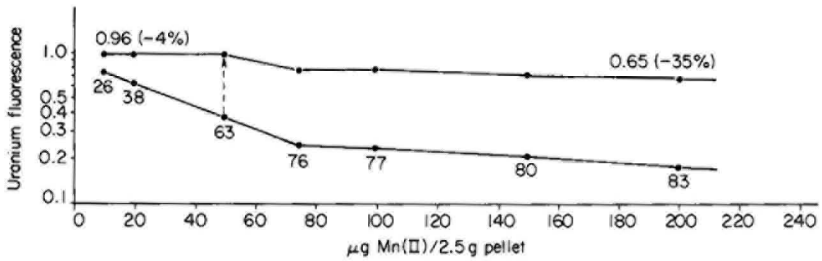

Fig. 4. Quenching of the fluorescence of uranium (1.0 μg) in 2.5-g pellets by Mn(II): numbers under points indicate % quenching. Upper curve is after correction with a uranium spike.

Numerical values of $c_{1/2}$ were measured for Fe(III), Cr(III) and Mn(II). The values obtained (Table 1) show that Mn(II) is the most powerful quencher of those investigated, followed by Cr(III) then Fe(III). A similar sequence has been reported [5] and possibly also holds for other flux mixtures [6]. It appears from Table 1 that a reasonably reproducible numerical characterization of the quenching power of an element is possible for a given experimental set-up; quantitative examination of the quenching power of other elements is therefore desirable and will be carried out later.

The values of $c_{1/2}$ (in ppm) do not depend on the pellet size or the uranium concentration; the validity of the semilogarithmic dependence is more extensive for the small pellets, which is possibly due to the greater sample thickness in the case of the heavier fluxes. The quenching curve of Cr(III) shows a definite blank at $c = 0$ (see Fig. 3) for reasons which are not yet understood.

Problems with internal standards

Individual quenchers. An attempt was made to correct every individual point in Figs. 2—4 to the theoretical value by addition of a suitable amount

TABLE 1

Values of $c_{1/2}$ for 400-mg pellets containing 0.1 (or 1.0) μg U and 2.5 -g pellets containing 1.0 μg U

Element	400-mg pellets		2.5-g pellets	
	$c_{1/2}$ (μg of element in flux)	$c_{1/2}$ (ppm)	$c_{1/2}$ (μg of element in flux)	$c_{1/2}$ (ppm)
Fe(III)	25.0 ± 0.5[a]	62.5 ± 1.3	165 ± 5[b]	66.0 ± 2
Cr(III)	16.0 ± 0.5[a]	40 ± 1.3	100 ± 5[b]	40.0 ± 2
Mn(II)	6.9 ± 0.2[a]	17.2 ± 0.5	38 ± 2[b]	15.2 ± 0.8

[a]Mean and standard deviation for 5 analyses. [b]Mean and deviation for 2 analyses.

of uranium spike and applying the formula given above for U_{sa}; the numbers under the points show the degree of quenching Q. The figures show that such corrections yield good results only up to a certain value of Q, above which the corrected value is low; this Q limit appears generally to be around 60% (see Figs. 3 and 4, vertical dotted line). For iron(III) this limit is not reached, so that a low uranium value resulting from the presence of only iron(III) can always be satisfactorily corrected, within the investigated concentration range (Fig. 2). The upper lines in Figs. 2—4 show the results of the correction: for Cr(III) and Mn(II), up to a Q limit of about 60% the corrected results are within a few % of the theoretical value, above 60% they become abruptly lower.

Mixed quenchers. The quenching effect of mixtures of elements cannot be regarded as an additive phenomenon [6] so that it was impossible to predict whether the regularity in the behaviour of individual quenchers would hold for the more complicated systems of quenchers which are present in natural minerals. Consequently, the dependence of fluorescence reduction on sample weight was investigated. For this purpose, various amounts of mineral (1—6 mg) were weighed into the platinum dishes, covered with 2.5 g of flux mixture and fused; the fluorescence was measured against a suitable uranium standard. The quantity of uranium per mg of sample was calculated and plotted against the total sample weight on semilogarithmic paper. The graphs obtained (Fig. 5, for example) are very similar to those in Figs. 2—4. The values of Q were calculated for the individual points and the samples were subjected to the spiking procedure mentioned in the previous paragraph. The results were practically the same as for single quenchers, as can be seen from the upper line in Fig. 5: correct results were obtained up to Q about 60% (vertical dotted line); at higher Q values they were low.

The linearity of the quenching function in the semilogarithmic plot in Fig. 5 suggests a novel method for obtaining correct analytical results without spiking. The extrapolation of the quenching function to sample weight zero

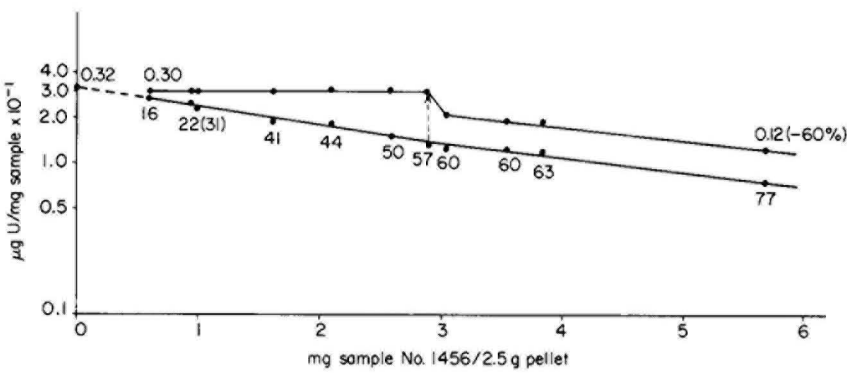

Fig. 5. Quenching of the uranium fluorescence in 2.5-g pellets by a mixed quencher for various weights of sample: numbers under points indicate % quenching. Upper curve is after correction with a uranium spike.

must intersect the ordinate at a position corresponding to the true value of the amount of uranium per mg of sample. The dotted extrapolation of the quenching function in Fig. 5 yields a result very close to that obtained by the spiking technique at low Q values (0.32 μg U mg^{-1} for extrapolation, and 0.30 μg U mg^{-1} for spiking).

Dependence of results on the quantity of uranium spike. A satisfactory direct determination of uranium in minerals may depend strongly on the amount of uranium spike added. The optimum quantity of internal standard to be added depends on the fluorescence of the original quenched sample. When three standard minerals of very different compositions were analyzed by using increasing amounts of spike, the results listed in Table 2 were obtained. The results appear to be either independent of the quantity of spike (standard 1) or they pass through a maximum, which represents the correct analytical result (standards 2 and 3), at a spike/sample fluorescence ratio of 2.5:1. All the spike experiments described in the previous sections utilized this number. The test minerals were all well defined standards, namely monazite (standard 1), torbernite (standard 2) and uraninite (standard 3), which had previously been homogenized and analyzed spectrophotometrically.

Procedures

The results given above led to the development of the following procedures.

Procedure 1. (Direct determination of uranium by the spike method). Weigh 1—2 mg of the finely powdered sample into a platinum fusion dish on a conventional analytical balance. Add 2.5 g of flux mixture. Prepare a suitable standard for instrument calibration and a reagent blank in the same way. Fuse in a muffle furnace at 1000° C. Continue heating for 10 min after melting to achieve total sample decomposition. Open the furnace and allow to cool for 5 min. Remove the sample tray from the furnace with platinum-

TABLE 2

Dependence of results on spike addition (2.5-g pellets)

Standard 1 (0.04% U)		Standard 2 (0.26$_5$% U)		Standard 3 (0.31$_8$% U)	
nx[a]	U found (%)	nx	U found (%)	nx	U found (%)
1.25	0.039	0.56	0.05	0.36	0.097
2.1	0.046	0.77	0.16	0.97	0.15
3.6	0.038	1.2	0.20	1.5	0.26
5.1	0.041	1.7	0.20	2.5	0.31
Average	0.041 ± 0.001$_8$	2.1	0.22	3.5	0.20
		2.5	0.26	5.7	0.10
		2.9	0.21		
		4.5	0.18		

[a] nx = ratio of fluorescence intensity with spike to that in absence of spike.

tipped crucible tongs and wait for 1 min before putting the sample holder onto an asbestos tray. Leave it there for another 2 min and transfer to a desiccator. Allow to cool for 15 min. Adjust the zero point and the maximum reading of the instrument with blank and standard pellets. Measure the fluorescence of the sample pellet. Calculate the apparent amount of uranium in the pellet by comparison of the fluorescence of sample and standard. Add the uranium spike (2.5 × the apparent uranium content in the sample) in the form of a suitably concentrated uranium standard solution, dry under a heat lamp and fuse once more. Allow to cool and measure the fluorescence as described above. Calculate the absolute amount of uranium in the pellet by using the formula for U_{sa} given above.

Procedure 2. (Direct determination of uranium by extrapolation of the quenching function). Weigh 3 or 4 samples (1—4 mg) of the mineral to be analyzed into the fusion dishes and cover each of them with 2.5 g of flux mixture. Prepare a standard and a reagent blank pellet. Fuse and measure samples as described in Procedure 1. Calculate the apparent uranium content of each sample in $\mu g\ U\ mg^{-1}$ of sample, and plot the results against total sample weight on semilogarithmic paper. Extrapolate the straight line obtained to zero sample weight. The intercept on the logarithmic ordinate gives the true amount of uranium per mg of sample.

Some results obtained by using Procedures 1 and 2 are given in Table 3.

POTENTIAL AND LIMITS OF DIRECT FLUORIMETRY

The methods presented here for direct determination of uranium in minerals by fluorimetry represent a powerful tool for the rapid determination of about 20—5000 ppm of this element. Samples containing less than 20 ppm cannot be determined reliably by the direct method because of the considerable statistical fluctuation of the blank fluorescence. The method relies on complete decomposition and dissolution of the sample in the fluoride melt which can be safely assumed for most minerals; in a few cases this condition is not completely met and low values may be obtained. In such cases, however, other methods relying on sample decomposition (acid treatment, carbonate fusion etc.) are likely to involve similar problems.

A specific problem of direct fluorimetry is its sensitivity to excessive concentrations of quenching elements; while "normal" concentrations can be corrected for either by spiking or by the extrapolation method described in this paper, concentrations which give rise to Q values above 60% lead to systematically low results for uranium which cannot be corrected. To avoid this difficulty, sample weights should always be kept as small as possible considering the practical detection limit of the method and the minimum sample mass which can be weighed accurately.

When the spiking method is used, the nitric acid concentration of the uranium spike solution should not be excessive. To avoid adsorption losses at low acidity, concentrated standards should be stored in plastic bottles and diluted shortly before use.

TABLE 3

Results obtained by Procedure 1 or 2

Sample No.	Composition	Reference method[a]	U found (%)	
			Reference method	Proc. 1 or 2[b]
NBL 76	Monazite/Dunite	(Standard)	0.01	0.01 (2)
NBL 79	Monazite/Dunite	(Standard)	0.04	$0.041 \pm 0.001_8$ (4)
NBL 81	Monazite/Dunite	(Standard)	0.002	0.0018_2
NBL 82	Monazite/Dunite	(Standard)	0.0008	not detected
CUPAS 116	Unknown	(Standard)	0.0042	0.0045
S 2	Torbernite	Sp	0.26_5	0.26 ± 0.007 (4)
S 3	Carnotite	Sp	0.35_4	0.34_6
S 4	Uraninite	Sp	0.31_8	0.31_0
1382	Unknown	N.a.a.	0.054	0.050
1456	Unknown	N.a.a.	0.032	0.030 ± 0.001 (9) 0.032[c]
1458	Unknown	N.a.a.	0.03	0.028 ± 0.001 (2)
1462	Unknown	Fl.	0.070	0.071
1465	Unknown	N.a.a., Fl., γ-S	0.034 ± 0.005	0.031 ± 0.004 (3)
1687	Unknown	Fl.	0.0091	0.0085[c]
1711	Unknown	γ-S	0.0040	0.0040[c]

[a]The reference methods were : spectrophotometry (Sp), neutron activation analysis (N.a.a.), extractive fluorimetry including total sample decomposition and MIBK extraction of uranium (Fl.), and direct gamma spectrometry (γ-S). [b]The number of determinations is given in parentheses. [c]Determined by extrapolation of the quenching function; all others by procedure 1.

We thank the head of the low level radioactivity section of the IAEA Laboratory Seibersdorf, Dr. O. Suschny, for his interest in this work and for valuable comments.

REFERENCES

1 J. C. Veselsky and A. Wölfl, Anal. Chim. Acta, 85 (1976) 135.
2 G. R. Price, R. J. Ferretti and S. Schwartz, Anal. Chem., 25 (1953) 322.
3 F. S. Grimaldi, F. N. Ward and R. Kreher, AECD-2825 (1949).
4 I'. A. Vozella, A. S. Powell and J. E. Kelly, Anal. Chem., 32 (1960) 1430.
5 T. Schönfeld, M. El Garhy, C. Friedmann and J. C. Veselsky, Mikrochim. Acta, (1960) 883.
6 E. Singer and D. Cifkova, Fresenius Z. Anal. Chem., 202 (1964) 401.
7 G. R. Price, R. J. Ferretti and S. Schwartz, AECD-2282 (1945).

Analytica Chimica Acta, 104 (1979) 355—361

TRACE DETERMINATION OF GASEOUS CHLORINE: A COMPARISON BETWEEN AN ELECTROMETRIC METHOD AND THE METHYL ORANGE PHOTOMETRIC METHOD

M. D'AMBOISE* and F. MEYER-GRALL

Laboratoire GRAM, Département de Chimie, Université de Montréal, Montréal, Québec (Canada)

(Received 15th May 1978)

SUMMARY

Two methods for the determination of molecular chlorine in air are critically compared. An electrometric method based on measurement of the reduction current of chlorine to chloride is superior to the photometric determination based on bleaching of an acidic solution of methyl orange. The limit of detection for the electrometric method is 50 $\mu g\ m^{-3}$; the standard error of the mean is better than 2%, and the sensitivity is 5.9 $\mu g\ m^{-3}\ \mu A^{-1}$ at +50 mV applied potential versus SCE with a mercury cathode. The limit of detection for the photometric method is 300 $\mu g\ m^{-3}$; the precision is of the order of 5%, and the sensitivity is 80 $\mu g\ m^{-3}$ for an error of 1% in the absorption measurements. The accuracy of the electrometric method is good whereas the photometric method yields consistently low results. The electrometric method is less subject to interferences than the photometric method.

The methods currently used for the determination of molecular chlorine in air cannot distinguish between chlorine and other oxidizing agents such as chlorine dioxide. Furthermore, they generally offer poor sensitivity. In this paper, an evaluation of the amperometric method proposed by Kuempel and Shults [1] is presented. This method is highly sensitive, provides a good detection limit as well as precision and suffers little interference from chlorine dioxide. This method is compared to a photometric method [2] based on bleaching of methyl orange by chlorine, which has been proposed as a standard method for the determination of chlorine in air [3].

Principles

When a stream of chlorine-containing air is passed through an electrolytic cell having one polarizable platinum electrode, chlorine is reduced to chloride if the appropriate potential is applied to the electrode. The cathodic current produced by the reaction is proportional to the quantity of chlorine present in the gas stream. Generally, if another electroactive substance is present in the gas mixture, it will be reduced or oxidized at a different potential and should not interfere if the potentials are carefully chosen. A cell is constructed so as to admit a stream of gas simultaneously with a liquid flow of supporting electrolyte between three electrodes. The system

is calibrated by measuring the reduction currents corresponding to the addition of known amounts of chlorine generated electrolytically.

In the photometric method [3], a measured amount of chlorine-containing air is bubbled through a solution of methyl orange. Chlorine reacts with the dye to produce compounds that do not absorb at 505 nm, the absorption maximum for solutions of methyl orange buffered at pH around 3. The decrease in absorbance is thus directly proportional to the amount of chlorine admitted.

EXPERIMENTAL

Apparatus

The electrolytic cell, constructed from a rod of Dupont Teflon, contained three electrodes and was similar to the cell described by Kuempel and Shults [1]. A potentiostat (Tacussel model PRT 20—10) was used to maintain a constant potential between the indicating electrode and a saturated calomel reference electrode. A constant-potential source (Keithley model 260) was used as reference potential. The gas generating cell was fed with a constant-current source (Keithley model 225).

The flow rate of the supporting electrolyte was maintained at a constant value with an automatic buret (Radiometer type ABU 13). The total volume of the buret was 2.5 ml. The flow rate of the analyte gas was measured by two Gilmont size 2 flow-meters, one at the entrance of the system and the other at the outlet of the measuring cell. The flow-meters were calibrated by measuring the time required to displace the water contained in a 2-l flask. The pumping rate of a small suction pump connected at the outlet of the second flow-meter was adjusted to maintain a constant flow rate in the two meters.

The reduction currents were measured with a galvanometer (Verispot-Sefram type VS1B, no. 196) which had a constant internal resistance of 10 kΩ, thus insuring linear response over any of the scales used.

Absorbances were measured with a Unicam model SP-1700 recording spectrophotometer and 1-cm quartz cells.

Reagents and solutions

Chlorine-containing air mixtures were prepared by electrolysis of an acidic (pH 2.3) 2.3 M solution of sodium chloride. The chlorine thus generated was scrubbed from the solution into a stream of air from a cylinder; this air was found to be satisfactory for the purpose.

Chlorine dioxide was prepared by reacting chlorine with sodium chlorite: $NaClO_2 + \frac{1}{2} Cl_2 \rightarrow NaCl + ClO_2\uparrow$. Solid sodium chlorite (Mathieson Chemical, analytical reagent) was contained in a glass column, 12 cm long, 3.5 cm diameter. The ClO_2 was taken up by the air stream as in the case of chlorine.

Mercury was triply distilled. All other chemicals were of analytical-reagent grade.

The supporting electrolyte was a buffer solution of pH 7.2, containing

sodium sulfate (0.2 M), sodium hydrogenphosphate (0.05 M) and sodium dihydrogenphosphate (0.01 M).

The solutions required for the methyl orange method were prepared in the conventional manner in borosilicate volumetric flasks with doubly distilled water. A standard solution of chlorine (ca. 10 mg l^{-1}) was prepared by scrubbing the chlorine from a chlorine—air mixture (370 mg m^{-3}) prepared electrolytically as described above. The stream circulated for 2 h at a flow rate of 20 ml s^{-1}. The final volume was 1 l and 400 ml of this solution was standardized with 0.0100 N sodium thiosulfate just before use.

Working conditions

Electrometric method. The flow rate of the supporting electrolyte was chosen to give a linear relationship between the cathodic current and the concentration of oxidant in the air sample. The instrumentation allowed only a limited choice of fixed flow rates; a rate of 172 μl min^{-1} gave the best results over the concentration range studied. This agrees well with the value of 180 μl min^{-1} recommended earlier [1]. At small flow rates, a long time was needed to obtain a stable reading, whereas at high rates, a decrease in current was observed. The flow rate of the gas mixture was maintained at 20 ml s^{-1}. The cathodic current was linear with change in air flow around that value.

The time necessary to reach a steady-state signal after a concentration had been changed depended on whether the concentration of oxidant had been increased or decreased before the reading. In general, a 10—15-min period was necessary to reach a steady signal when changing from a low to a higher content, whereas only 5 min was required for the reverse order. The results reported here were obtained by first passing an air stream with a higher content of oxidant than the one to be determined, and then circulating the air mixture to be analysed for 1 min before taking the reading. Although complete equilibrium was not reached after this short time, the calibration curves were linear in the useful concentration range provided that the waiting period was maintained constant.

Photometric method. The sample solutions were prepared by scrubbing the chlorine from an air stream that contained varying amounts of chlorine, prepared electrolytically as before. The stream was circulated for 8 min at a flow rate of 20 ml s^{-1} in a total volume of 100 ml. The quantity of air thus sampled insured that the reproducibility was good and that the bleaching of methyl orange was due only to the presence of chlorine. The remainder of the procedure for the determination of chlorine with methyl orange was as described in the APHA method [3].

RESULTS AND DISCUSSION

Electrometric method

The current—potential curves for the reduction of chlorine and chlorine dioxide are shown in Fig. 1. At applied potentials more negative than —10 mV

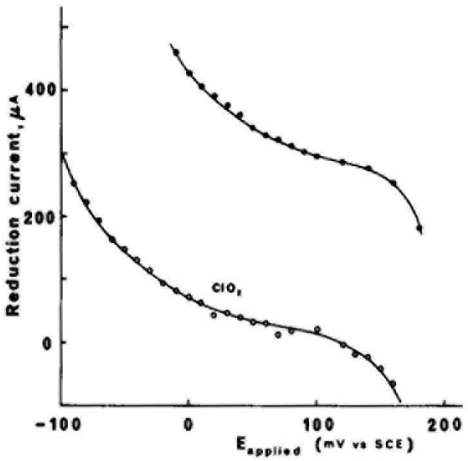

Fig. 1. Current—potential curves for chlorine (•) and chlorine dioxide (○); chlorine, 1.8 mg m^{-3}; chlorine dioxide, 3.5 mg m^{-3}.

vs. SCE, oxygen is reduced and interferes, whereas at potentials more positive than +140 mV, mercury is oxidized. Thus for chlorine, an applied potential of +50 mV was selected for all measurements. Chlorine dioxide was reduced at zero applied potential, which was the obvious choice after consideration of the calibration curves at different potentials (Fig. 2). It can be seen that at an applied potential of +50 mV the response is small, hence there is little interference with the determination of chlorine should the two gases be present in the air mixture.

Calibration curves. Current—concentration curves for chlorine were prepared over the concentration range of 0—20 mg m^{-3} of air. A linear response was obtained for chlorine contents above 70 μg m^{-3}; below that value, curvature was too pronounced for the method to be useful. Least-squares analysis of

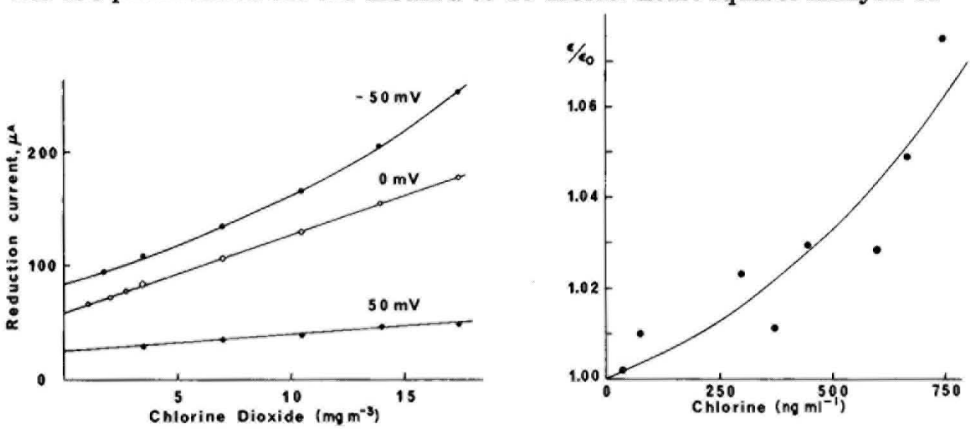

Fig. 2. Calibration curves for chlorine dioxide at different applied potentials.

Fig. 3. Variation of x (ϵ/ϵ_0) as a function of the chlorine added.

the linear part of the curve gave the equation $i(\mu A) = 170$ (mg Cl_2 m^{-3}) + 18.0. Least-squares analysis of the linear portions of the calibration curves for chlorine dioxide (Fig. 2) gave the equations $i(\mu A) = 6.84$ (mg ClO_2 m^{-3}) + 58.3 at 0 V vs. SCE, and $i(\mu A) = 1.40$ (mg ClO_2 m^{-3}) + 24.5 at +50 mV vs. SCE. These equations are valid over the concentration range 50 μg—20 mg ClO_2 m^{-3} in air. The strong curvature of the plot obtained at an applied potential of −50 mV is probably due to reduction of oxygen. The results at this potential were not reproducible.

Small discrepancies in the values of the intercepts obtained at the same applied potential are caused by day-to-day variations in the preparation of the supporting electrolyte.

Sensitivity, precision, accuracy and limit of detection. The sensitivities (dC/di) derived from the above equations are respectively, 5.9 μg m^{-3} μA^{-1} for Cl_2 at +50 mV, 720 μg m^{-3} μA^{-1} for ClO_2 at +50 mV, and 146 μg m^{-3} μA^{-1} for ClO_2 at 0 mV. Thus at +50 mV, the sensitivity is 120 times greater for chlorine than for chlorine dioxide. As a rule, in atmospheres contaminated with chlorine, the amounts of chlorine dioxide present are much smaller than those of chlorine; therefore, no significant interference from chlorine dioxide is likely when the electrometric method is used.

With the instrumentation used, currents could be measured with a precision better than 1 μA. This allowed changes in concentration smaller than 5.9 μg m^{-3} to be detected.

The precision and accuracy were evaluated for different chlorine levels; some results are shown in Table 1. The relative standard error of ca. 2% obtained for levels above ca. 3 mg Cl_2 m^{-3} can be reduced to less than 1% if calibration is done for each determination. The limit of detection ($s_{\bar{x}}/\bar{x}$ = 50%) is 50 μg m^{-3}.

Photometric methyl orange method

Calibration curve. Linear calibration plots were obtained for chlorine with measurement at 505 nm in 1-cm cells after reaction at pH 3 with 1.83

TABLE 1

Precision and accuracy of the electrometric determination of chlorine

Cl_2 (mg m^{-3})		Error[a] (%)	Degrees of freedom	Cl_2 (mg m^{-3})		Error[a] (%)	Degrees of freedom
Taken	Found			Taken	Found		
18.2	17.3	2.3	3	0.55	0.56	6.2	3
10.9	10.4	1.5	3	0.365	0.353	7.2	4
2.19	2.22	2.9	3	0.182	0.177	13	3
1.82	1.79	2.7	6	0.091	0.07	33	3
1.46	1.48	3.0	5	0.055	0.04	44	3
0.91	0.91	5.0	5				

[a]Relative standard error of the mean.

$\times 10^{-5}$ M methyl orange solution. Least-squares analysis gave the equation $A = -38550\,[Cl_2] + 0.735$. In this expression, the chlorine content refers to the amount of chlorine transferred to the solution rather than to the actual amount present in the solution; the standard solution of chlorine was used. If this equation is expressed in terms of the concentration of chlorine in the air that was added to the solution of methyl orange, it takes the form: $A = -0.0521$ (mg Cl_2 m^{-3}) + 0.735, which is valid over the range 0—10 mg Cl_2 m^{-3} of air sampled. No deviation from Beer's law was observed.

Sensitivity, precision, accuracy and limit of detection. The sensitivity (dC/dA) derived from this equation was 19.2 mg Cl_2 m^{-3} per absorbance unit. With the usual spectrophotometer, changes in absorption of 1% ($\Delta A = 0.0043$) correspond to a sensitivity of 80 μg m^{-3}. This value is to be compared with the value of 5.9 μg m^{-3} found for the electrometric method.

The precision and limit of detection were found to be of the same order of magnitude as those reported earlier [3]. The limit of detection is established practically by the presence of chlorine-consuming materials in the air sample and in the solution of methyl orange. It is of the order of 300 μg m^{-3}. The precision is of the order of 5%.

The reaction between chlorine and methyl orange (MO) may have a stoichiometry different from 1:1. If the reaction is $x[Cl_2] + [MO] \rightarrow [MO.x(Cl_2)]$, and if the only absorbing species is methyl orange, the absorbance (1-cm cells) of a methyl orange solution gradually bleached by chlorine is given by $A = -\epsilon_{MO}\,[Cl_2]/x + \epsilon_{MO}\,C^0_{MO}$, where ϵ_{MO} is the molar absorptivity of methyl orange, x represents the moles of Cl_2 that react with 1 mol of methyl orange, C^0_{MO} is the original concentration of indicator in the solution, and $[Cl_2]$ is the quantity of chlorine admitted to the solution, taken as a molar concentration. From the equation for the calibration graph, for $C^0_{MO} = 1.83 \times 10^{-5}$ M, the molar absorptivity for methyl orange is 4.02×10^4 l mol^{-1} cm^{-1} at 505 nm and pH 3.0 with $x = 1.04$.

Laitinen and Boyer [5] calculated an x value of 1.12 from their data and a value of 1.05 from the data of Sollo and Larson [4]. The value of x larger than 1 is accounted for by a second reaction requiring two moles of chlorine per mole of methyl orange, which becomes more important for local excesses of chlorine in the reaction vessel. The ratio x therefore depends on the manner of addition of chlorine to the reacting solution, smaller values being obtained when chlorine is added slowly to a large excess of methyl orange.

Similar quantities of chlorine were determined by the electrochemical and spectrophotometric methods. Representative results are shown in Table 2. The large discrepancies between the two sets of results seem to be due to occurrence of the above-mentioned 2:1 reaction ratio. This possibility was examined by measuring the absorbance of different methyl orange solutions containing increasing quantities of chlorine. The chlorine was scrubbed from an air—chlorine mixture in which chlorine was generated electrolytically during a fixed period of 8 min. A 1:1 stoichiometry was assumed and for each solution the unreacted methyl orange concentration was calculated.

TABLE 2

Comparison between the electrometric and photometric determinations of chlorine

Method	Concentration of Cl_2 (mg m^{-3})				
Electrochemical	9.12	7.29	5.47	3.65	1.82
Spectrophotometric	7.59	6.21	4.69	3.07	1.27
Difference (%)	17	15	14	16	30

From this value and from the absorbance reading, an apparent molar absorptivity (ϵ) was calculated. The ratio ϵ/ϵ_0 was then evaluated, ϵ_0 being the molar absorptivity of methyl orange in the solution without chlorine. This ratio ϵ/ϵ_0 is identical with the value x used previously. The results (Fig. 3) show clearly that x increases greatly as the content of chlorine is increased in the solution. This is considered to be due to the larger local excesses of chlorine which momentarily exist as larger quantities of chlorine are added, and which favor a 2:1 stoichiometry. As the reaction is irreversible, a larger quantity of chlorine will be necessary to bleach the solution, and results lower than expected will be obtained for the chlorine contents. Furthermore, the discrepancy between the value found and the actual value will be a function of the manner by which the reagents are added. This method cannot, therefore, produce accurate results in the determination of chlorine.

Conclusion

This comparison of the electrometric and photometric determinations of chlorine in air clearly shows the superiority of the electrometric method. Sensitivity, precision, accuracy and limits of detection are all better for the electrometric determination. The photometric method is subject to more interferences from various oxidizing agents than the electrometric method. In addition, a severe systematic error can be introduced in the photometric method, leading to low results; this error is a function of the manner of addition of the reagents and cannot be avoided easily. Finally, the electrometric method requires no pre-treatment of the sample and can be used for on-line determinations.

The electrometric method is therefore highly recommended for the determination of chlorine in air at the trace level.

This work was supported in part by the National Research Council of Canada, Grant number A-9807.

REFERENCES

1 J. R. Kuempel and W. D. Shults, Anal. Lett., 4 (1971) 107.
2 M. Taras, Anal. Chem., 19 (1947) 342.
3 Methods of Air Sampling and Analysis, method 204, Intersociety Committee, American Public Health Association (publisher), 1972.
4 F. W. Sollo and T. E. Larson, J. Am. Water Works Assoc., 57 (1965) 1575.
5 H. A. Laitinen and K. W. Boyer, Anal. Chem., 44 (1972) 920.

Analytica Chimica Acta, 104 (1979) 363—368

INDIRECT EXTRACTION—SPECTROPHOTOMETRIC METHOD FOR THE DETERMINATION OF TRACES OF TIN(II) BY MEANS OF 4,7-DIPHENYL-1,10-PHENANTHROLINE

ZBIGNIEW GREGOROWICZ and WOJCIECH BĄKOWSKI*

Department of Analytical and General Chemistry, Silesian Polytechnic University, 44—101 Gliwice (Poland)

(Received 14th April 1978)

SUMMARY

An indirect extraction—spectrophotometric determination of tin(II) is based on reduction of iron(III) and determination of the iron(II) formed with bathophenanthroline. Analysis is possible in strongly acidic samples even with large excesses of iron(III). The apparent molar absorptivity is 39,080 $dm^3\ mol^{-1}\ cm^{-1}$; the limit of determination is 32 ng cm^{-3} and the sensitivity is 64 ng cm^{-3}. Interferences are reported. The method is applicable to the determination of tin in samples soluble in non-oxidizing acids, and to the determination of tin in lead.

The preparation of high-purity compounds places great demands on analytical methods. For the determination of tin, instrumental methods such as spectrography, atomic absorption spectrometry and polarography often lack sufficient sensitivity, and spectrophotometric methods are still in use. The commonest spectrophotometric reagents for tin are substituted 2,6,7-trihydroxy-3-fluorones, pyrocatechol violet, hematoxylin, hematein, gallein, toluene-3,4-dithiol and quercetin [1]; most of these form sparingly soluble complexes with tin so that colloidal solutions are usually involved in the measurements. Precision, determination limits and interferences (through co-precipitation) thus tend to be unfavourable.

Accordingly, it seemed worthwhile to examine an alternative principle, to improve the sensitivity and selectivity of analysis. An indirect determination of tin based on the redox reaction of Sn^{2+} with Fe^{3+} ions and determination of the iron(II) formed in equivalent amounts was therefore studied.

EXPERIMENTAL

Apparatus and reagents

A Unicam SP1700 spectrophotometer was used with 1-cm glass cells.

All the reagents were of analytical grade. Iron(II) sulphate was purified by three recrystallizations from water and precipitation with ethanol.

Bathophenanthroline was used as a 0.015 M solution in absolute ethanol. Iron(II) sulphate stock solution (1 mg $Fe^{2+}\ cm^{-3}$) was prepared in 1 M HCl and standardized by titration with permanganate [2]. Working solutions were obtained by dilution with 1 M HCl.

Tin(II) stock solution. $SnCl_2$ (2 g) was dissolved, in a 50-cm^3 measuring flask, in hydrochloric acid of suitable concentration; 3, 2, 1.5, 1, 0.75, 0.5 and 0.25 M solutions were tested. Any opacity was removed by filtering. The solutions were standardized immediately before use by titration with bromate [2], and were stabilized by passing CO_2 for 5 min. The working solutions were obtained by dilution with the appropriate concentration of hydrochloric acid, previously deoxygenated with CO_2. Working solutions of tin(II) in 1 M hydrochloric acid, containing 1—5 μg Sn^{2+} cm^{-3}, were found to be stable for 45 min at the most (at about 20°C).

The acetate buffer solution was 1.3 M with pH about 5.6.

All the vessels used with working tin(II) solutions were flushed with CO_2.

Procedure

Place 0.5 cm^3 of 2.4×10^{-2} M $FeCl_3$ solution in 1 M HCl and the sample solution into a separatory funnel previously flushed with CO_2; if necessary, dilute the mixture to 4.5 cm^3 with 1 M hydrochloric acid (deoxygenated with CO_2). Set aside for about 20 min and then add 4.5 cm^3 of 1.3 M acetate buffer, 4 cm^3 of 0.125 M Na_2HPO_4 solution, 3 cm^3 of ethanol and 2 cm^3 of 0.015 M bathophenanthroline solution. Mix thoroughly and extract the iron(II)—bathophenanthroline complex with two 8-cm^3 portions of chloroform. Add 2.5 cm^3 of ethanol to the combined extracts and dilute with chloroform to 25 cm^3. Measure the absorbance at 533 nm against the pure solvent. Any opacity must be removed by filtration through dense filter paper before measurement.

RESULTS AND DISCUSSION

Determination of iron(II) with bathophenanthroline

The method requires an efficient procedure for determining iron(II) in the presence of more than 1000-fold amounts of iron(III) in strongly acidic medium. Several determinations [3—7] similar to the above have been described, but none was directly applicable. Detailed preliminary tests showed that: (a) the best solvent for extracting the $Fe(bath)_3^{2+}$ complex is chloroform; (b) the optimal pH range is 1.7—4, and the best solution for its adjustment is the acetate buffer described above; (c) of the eleven compounds investigated for masking iron(III), the most favourable is disodium hydrogenphosphate, the action of which is shown in Fig. 1; (d) the most reproducible results were obtained when the aqueous phase contained about 28% ethanol by volume, to prevent the precipitation of both iron(III) orthophosphate and the bathophenanthroline.

The criteria applied in these investigations were the value of the partition coefficient, the stability of colour, the precision, the molar absorptivity and the absorbance of the reagent blank. The optimal proportions of the reagents were as given in the Procedure. The ethanol added to the chloroform extracts not only prevented emulsion formation, but also had a favourable effect on the colour stability.

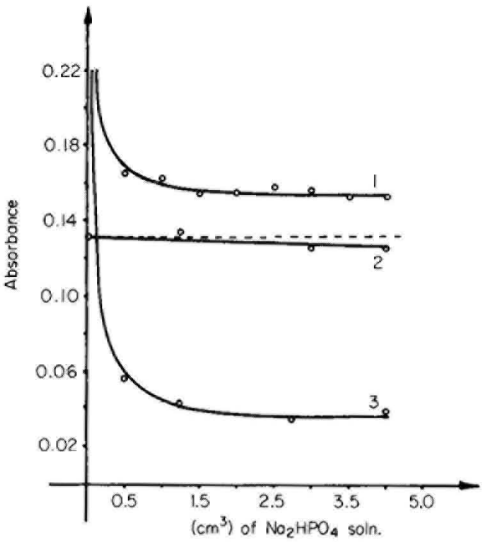

Fig. 1. Dependence of the absorbance of the chloroform extract on the volume of 0.125 M disodium hydrogenphosphate added. Curve 1, 10 μg Fe^{2+} and 600 μg Fe^{3+} in 7 cm^3 of solution. Curve 2, 10 μg Fe^{2+} without Fe^{3+}. Curve 3, 600 μg Fe^{3+} without Fe^{2+}.

Under the recommended conditions, iron(II) can be determined without difficulty even in the presence of a 5000-fold amount of tin(IV) (w/w) compared with iron(II), or even with Fe^{3+}/Fe^{2+} weight ratios up to 3000 if enough Na_2HPO_4 is added; samples containing up to 3 M HCl can be analyzed if enough buffer solution is used.

Reaction of tin(II) with iron(III)

The optimal conditions for the tin(II)—iron(III) reaction were then studied. The reaction rate of Sn^{2+} with Fe^{3+} was found to depend very greatly on the concentrations of hydrochloric acid and iron(III). The influence of HCl was tested in a medium containing 3.13×10^{-3} M iron(III) chloride. The greater the concentration of HCl, the greater the reaction rate: when the HCl concentration exceeded 3 M, the reaction time required to reach maximum absorbance of the chloroform extracts was shorter than 20 s, whèreas when the HCl concentration was less than 0.45 M, the time for complete reaction became almost infinite. With 1 M HCl the time required to achieve maximum absorbance of the final extract was 15.5 min. The effect of the iron(II) concentration on the time required for quantitative oxidation was studied for 1 M HCl. The time required decreased as the Fe^{3+} concentration increased, reaching its lowest value, (6 min) for $FeCl_3$ concentrations exceeding 1.6×10^{-2} M. When the $FeCl_3$ concentration was less than 1.6×10^{-3} M, the time increased asymptotically to infinity.

The time required for complete reaction was independent of the concentration of tin(II) within the range $1.22 \times 10^{-5} - 8.27 \times 10^{-5}$ M.

Other media were also examined for the reaction. The times required for complete oxidation were about 120 min in 0.5 M HCl—0.5 M H_2SO_4, 14 min in 0.5 M HCl—0.5 M NaCl, and 20 s in 0.5 M HCl—0.5 M NaBr, at about 20°C.

The kinetics and mechanism of the tin(II)—iron(III) reaction have often been studied with rather large concentrations of reagents [8—10]. The compatibility of the present results with earlier data suggests that the reaction mechanism proposed by Scott et al. [8] is valid even when the concentration of tin(II) is very low. According to this bridge mechanism, the reaction is controlled by the formation of an active $[FeSnL_n]^{5-n}$ complex, where L denotes a uninegative ligand group (usually chloride) capable of forming complexes with Fe^{3+} and/or Sn^{2+} ions and of conducting electrons comparatively well. Under such conditions, other reactions of iron(III) with metal cations frequently take the same course [9]. On the basis of this mechanism, it might be possible to enhance the selectivity of iron(III) as an oxidant by selecting a different ligand L which would form the active complex more quickly.

Effect of diverse ions

In the recommended procedure, the acidity and the $FeCl_3$ concentration are favourable for preventing at least some competitive reactions. Results obtained for the effects of diverse ions on the determination of tin(II) are presented in Fig. 2, but these effects may change even with small alterations of the reaction conditions.

Characterization of the method

Least-squares analysis of the data obtained in 38 measurements of various tin concentrations gave the equation $A = 0.01317c + 0.032$, where A is the absorbance and c is the tin concentration expressed in $\mu g/25\ cm^3$. The apparent molar absorptivity is 39080 $dm^3\ mol^{-1}\ cm^{-1}$ with a standard deviation of 180.

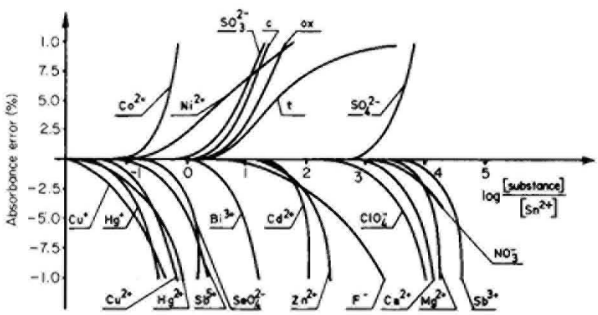

Fig. 2. The effects of diverse substances on the Sn^{2+}—Fe^{3+} reaction in 1 M HCl for 0.208 μ mol of tin; reaction volume, 7 cm^3. Pb^{2+} and Ag^+ do not interfere at any attainable concentration. The effect of antimony was checked in 3 M HCl for 0.0308 μ mol of tin. c = citrate, t = tartrate, ox = oxalate.

The standard deviation of the reagent blank absorbance is 0.0026. Application of the *F*-test showed that the absorbance—concentration relation is rectilinear up to 5 μg Sn/25 cm^3 (α = 0.001, n = 38). The limit of determination, established by standard methods based on the standard deviation of the absorbance [11], was 32 ng cm^{-3}. This result is somewhat arbitrary — as in all indirect extraction methods. It does not refer to the true minimal concentration of tin(II) in the solution tested (stable standard solutions at such low concentrations cannot be obtained from tin(II) chloride under the proposed conditions) but to a minimum concentration of the Fe (bath)$_3^{2+}$ complex in the chloroform extract. The sensitivity of the method [12] was calculated from the measurements used in establishing the analytical curve. If series of 5 measurements of each concentration are used, the suggested method makes it possible to discriminate (95% probability) between samples in which the difference in Sn^{2+} concentrations is 64 ng cm^{-3}.

Application to the analysis of lead

On the basis of literature data on the reactions of tin and lead metals [13] with mineral acids (tin dissolves as Sn^{2+} in hydrochloric acid), the proposed method was applied to determine tin in a sample of lead. The tin content was found to be 7.2×10^{-2}% (n = 8, $s = 2.4 \times 10^{-3}$). Comparative analysis by the toluene 3,4-dithiol method after separation of tin by distillation gave the result 6.9×10^{-2}% (n = 3, $s = 3.1 \times 10^{-3}$).

Conclusions

Utilization of the Fe^{3+}—Fe^{2+}—bathophenanthroline system provides a sensitive and selective method of determining trace amounts of tin. As was expected, the method can be applied in the presence of ions which interfere with most known colorimetric methods for tin(II) (e.g. Sb^{3+}, Pb^{2+} and Ag^{+}). Although the apparent molar absorptivity is not the highest available the sensitivity is excellent. The procedure is comparatively simple, and is suitable for the analysis of samples which dissolve in non-oxidizing acids with the production of tin(II). Analogous methods could be used for the determining of microgram amounts of other metal ions which reduce iron(III) such as Ti^{3+}, V^{4+} and Cu^{+}.

REFERENCES

1 W. B. Spivakovskij, Analiticheskaya Khimia Olova, Nauka (Publishers), Moskow, 1975.
2 J. Minczewski and Z. Marczenko, Chemia Analityczna, PWN, Warsaw, 1965.
3 G. F. Lee and W. Stumm, J. Am. Water Works Assoc., 52 (1961) 1567.
4 G. F. Ghosh, J. T. O'Connor and R. S. Engelbrecht, J. Am. Water Works Assoc., 59 (1967) 897.
5 L. J. Clark, Anal. Chem., 34 (1962) 348.
6 E. N. Pollock and A. N. Miguel, Anal. Chem., 39 (1967) 272.
7 T. Mizuno, Talanta, 19 (1972) 379.
8 P. D. Scott, D. Glasser and M. J. Nicol, J. Chem. Soc. Faraday Trans. 1, 71 (1975) 1413.

9 M. L. Tobe, Mekhanizmy Nieorganicheskikh Reakcji, Mir (Publishers) Moscow, 1975, pp. 1
10 F. R. Duke and R. C. Pinkerton, J. Am. Chem. Soc., 73 (1951) 3045.
11 B. Bułatow and I. Kalinkin, Prakticheskoye Rukovodstwo po Fotokolorimetricheskim i Spektrofotometricheskim Metodam Analiza, Chimia (Publishers) Leningrad, 1976, p. 28
12 J. Świętosławska, Spektrofotometria Absorpcyjna, PWN, Warsaw, 1962, p. 226.
13 J. W. Mellor, Comprehensive Treatise on Inorganic and Theoretical Chemistry, Vol. 7, Longman and Green, London, 1957.

Analytica Chimica Acta, 104 (1979) 369—377

EXTRACTION—SPECTROPHOTOMETRIC DETERMINATION OF TRACE AMOUNTS OF IRON IN WATERS WITH PYROGALLOL RED AND ZEPHIRAMINE

TAKASHI KORENAGA, SHOJI MOTOMIZU and KYOJI TÔEI*

Department of Chemistry, Faculty of Science, Okayama University, Tsushima-naka, Okayama-shi, 700 (Japan)

(Received 13th June 1978)

SUMMARY

The simple removal of excess of co-extracted reagent in the solvent extraction of metal complex anions with a quaternary ammonium salt greatly improves the determination of iron(II) with pyrogallol red and zephiramine. The method with pyrogallol red is suitable for the determination of trace amounts of iron in natural waters. The apparent molar absorptivities of the iron(II) complex in chloroform are 7.5×10^4 and 10.3×10^4 l mol^{-1} cm^{-1} at 560 and 298 nm, respectively. A large excess of reagent can be added, and the ternary complex can be completely extracted over the pH range 8.5—10. Masking agents allow most interferences to be suppressed. The method is suitable for the analysis of potable, river and sea waters.

Recent developments in the solvent extraction of metal complex anions with quaternary ammonium salts have provided highly sensitive and selective spectrophotometric methods for the determination of several metals. In many such extraction systems, chelating reagents with a sulfonic acid group have been used because of their powerful ability to form extractable ion pairs with quaternary ammonium salts; these ion pairs are extracted more readily than those formed from reagents possessing hydroxyl and carboxyl groups. In most of the extraction systems with quaternary ammonium ions, however, the excess of reagent is extracted into the organic phase along with the complex. The absorbance of the reagent itself is often large, and the reagent blank can be affected severely by co-existing monovalent anions [1]. This phenomenon is undesirable in the extraction—spectrophotometric methods for the determination of trace amounts of metals.

Motomizu and Tôei have reported a new method of removing excess of reagent from the organic phase in the solvent extraction of metal complex anions with quaternary ammonium salts [2]. The principle is as follows: the order of extractability of an anion with a quaternary ammonium ion is $R{-}SO_3^- > R{-}O^-$, where R is an organic radical; with a given chelating reagent ($HO{-}R{-}SO_3H$) which possesses both a hydroxyl group bonding with a metal ion (M^{n+}) and a sulfonic acid group, the order of extractability is expected to

be $HO—R—SO_3^-$, $[M(O—R—SO_3)_n]^{n-} > {}^-O—R—SO_3^-$. The ion pair formed between a quaternary ammonium ion and a monovalent anion (X^-) which does not absorb at the wavelength of measurement, e.g. chloride, bromide, nitrate and iodide, can also be extracted into organic solvents such as chloroform and 1,2-dichloroethane. Thus, at a defined concentration of the monovalent anion, the order of extractability is expected to be $[M(O—R—SO_3)_n]^{n-} > X^- > {}^-O—R—SO_3^-$. By adding a suitable anion to an extraction system, it is possible to transfer the excess of co-extracted reagent from the organic phase to the aqueous phase, and thus to improve considerably the sensitivity and selectivity of procedures.

Pyrogallol red reacts with many metal ions such as silver [3, 4], aluminum [5], copper [6] and germanium [7]. Some workers have also reported the extraction—spectrophotometric determination of molybdenum(VI) [8, 9] and tungsten(VI) [10] with pyrogallol red and quaternary ammonium salts (dodecanoltrimethylammonium bromide, dimethyldioctadecylammonium chloride and cetyltrimethylammonium chloride, respectively). In these methods, the absorption of the reagent blank is large, because the excess of reagent is also extracted along with the metal complex.

The present paper reports a procedure for extraction of the iron(II)—pyrogallol red complex anion with a quaternary ammonium salt (zephiramine) with subsequent removal of the excess of co-extracted reagent from the organic phase. The method can be applied to the determination of trace amounts of iron in natural waters.

EXPERIMENTAL

Reagents

All reagents used were of analytical-reagent grade.

Pyrogallol red solution (ca. 5×10^{-4} M). Dissolve 100 mg of pyrogallol red (Dojindo Co., Ltd.) in 450 ml of distilled water by heating to 60°C on a water bath. Transfer this solution into a 1-l separatory funnel; add 14.6 g of sodium chloride and 50 ml of 5×10^{-3} M zephiramine solution and 50 ml of chloroform. Shake for 30 min and discard the organic phase. Filter the aqueous phase through a wet filter paper and store this purified solution in an amber glass bottle. Standardize this stock solution by the mole ratio method by using thorium(IV) ion, which forms the 1:1 complex with pyrogallol red in aqueous solution without a quaternary ammonium salt [11]. This pyrogallol red solution containing 0.5 M sodium chloride is stable for at least 2 weeks.

Standard iron(II) solution. Prepare a stock solution from 702 mg of Mohr's salt ($FeSO_4(NH_4)_2SO_4 \cdot 6H_2O$) in 1 l of distilled water containing 10 g of hydroxylammonium sulfate and 1 ml of concentrated sulfuric acid. Standardize the solution by EDTA titration. Use this solution to prepare working iron(II) solution by accurate dilution.

Zephiramine solution (5×10^{-3} M). Dry the reagent (tetradecyldimethylbenzylammonium chloride; Dojindo Co., Ltd.) at reduced pressure (about 5

mm Hg) and 50—60°C to constant weight; dissolve the required amount in distilled water [12].

Masking agent. Dissolve 5.81 g of potassium fluoride, 4.41 g of sodium citrate dihydrate and 1.65 g of potassium pyrophosphate in 100 ml of distilled water.

Ammonia (1 + 4) and ammonia—ammonium sulfate buffer solutions were mainly used for pH adjustments.

Aqueous solutions of sodium chloride, bromide, nitrate and potassium iodide were used as the monovalent anion solutions.

Chloroform (extra pure-reagent grade) was used as the organic solvent.

Apparatus

All glassware was boiled in hydrochloric acid (1 + 1) before use.

A Hitachi-Perkin Elmer Model 139 spectrophotometer and a Hitachi Model EPS-3T recording spectrophotometer were used for measuring absorbances in quartz cells (1-cm path length). Other instruments were Hitachi-Horiba Model F-5ss pH meter equipped with a combined electrode (6026-05T), and an Iwaki Model V-S KM shaker. Stoppered test tubes (25 ml and 50 ml) were used for extractions.

General procedure

Transfer an aliquot of the iron(II) solution (1.83×10^{-5} M) to a stoppered 25-ml test tube. Add by pipet aliquots of the pyrogallol red (4.1×10^{-4} M), buffer, zephiramine (4.6×10^{-3} M) and monovalent anion solutions in that order. Dilute to 5 ml with distilled water and mix well. Add 5 ml of chloroform and shake for 30 min. After phase separation, measure the absorbance of organic phase in a 1-cm quartz cell against a reagent blank. Of the monovalent anions (Cl^-, Br^-, NO_3^- and I^-) examined for removing the excess of reagent from the organic phase, chloride gives the best results and is therefore recommended.

RESULTS AND DISCUSSION

Absorption spectra

The absorption spectra of the iron(II) complex with pyrogallol red and the reagent blank are shown in Fig. 1. When the excess of co-extracted reagent in the organic phase is removed, the absorption maxima are obtained at 298 and 560 nm with minimum reagent blanks. When the excess of reagent is not removed, although absorption maxima are obtained at similar wavelengths, the absorption of the reagent blanks are very high.

In this work, the absorbance at 560 nm was used to determine iron(II) because the reagent blank was lower than that obtained at 298 nm.

Effect of pH, chloride concentration and time

The effect of pH on the extraction of the iron(II) complex and the excess of pyrogallol red is shown in Fig. 2. The optimum pH range is 8.5—10; when

the pH is above 7, a little pyrogallol red decomposes. The iron(II) complex with pyrogallol red is, however, stable over the optimum pH range. The pK_a values of pyrogallol red (H_4L) have been reported as 2.56, 6.28, 9.75 and 11.94 in aqueous solution [13]. Figure 2 shows that the reagent present in the form H_3L^- is difficult to remove from the organic phase, whereas the reagent present as H_2L^{2-}, HL^{3-} and L^{4-} is very easily removed. Thus, the extraction was carried out at about pH 9.6.

The optimal concentration of chloride for removal of the excess of pyrogallol red from the organic phase is about 0.25 M (Fig. 3). At this concentration the

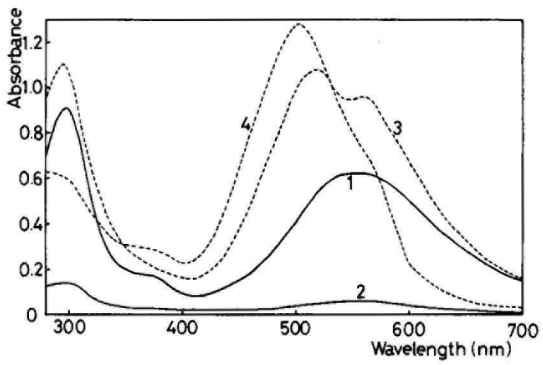

Fig. 1. Absorption spectra in chloroform. (1) Ternary complex with 7.3×10^{-6} M iron(II), 8.2×10^{-5} M pyrogallol red, 4.6×10^{-4} M zephiramine and 0.25 M sodium chloride at pH 9.6 measured against chloroform. (2) Reagent blank for the conditions used for spectrum (1). (3) Ternary complex with 7.3×10^{-6} M iron(II), 8.2×10^{-5} M pyrogallol red, 4.6×10^{-4} M zephiramine and no sodium chloride at pH 9.6 measured against chloroform. (4) Reagent blank for the conditions used for spectrum (3).

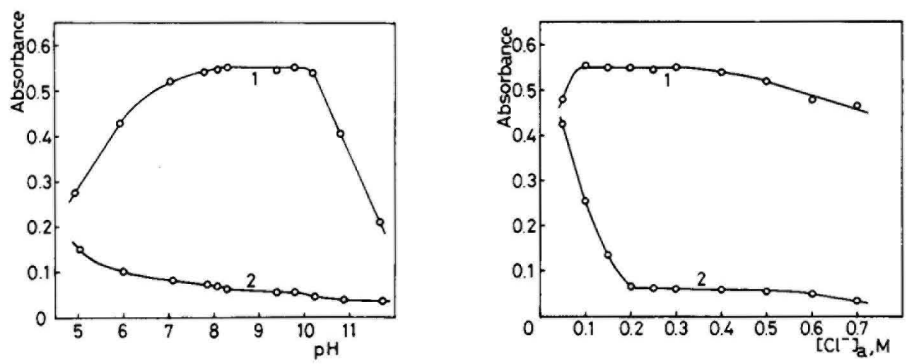

Fig. 2. Effect of pH. (1) Ternary complex; apart from pH and measurement against a reagent blank, conditions were those used for spectrum (1) of Fig. 1. (2) Reagent blank measured against chloroform.

Fig. 3. Effect of the concentration of chloride. (1) Ternary complex; apart from chloride concentration and measurement against a reagent blank, conditions were those used for spectrum (1) of Fig. 1. (2) Reagent blank measured against chloroform.

absorbances of the reagent blank and the complex are constant and the former is very small.

The time necessary for complete formation of the iron(II) complex with pyrogallol red was examined. Even when a 10-fold molar excess of pyrogallol red was added to an iron(II) solution at pH 9.6, about 10 min were required for complete reaction in aqueous solution; the time necessary for complete extraction of the complex into chloroform was 20 min. When the concentrations of iron(II), reagent and zephiramine were 7.3×10^{-6}, 8.2×10^{-5} and 4.6×10^{-4} M, respectively, the standing time for complete reaction, the shaking time for complete extraction and the standing time for complete separation of the two phases were found to be 10, 30 and 30 min, respectively.

Nature of the ternary complex and extraction mechanism

The ratio of iron(II) to pyrogallol red was found to be 1:2 by the mole ratio method (Fig. 4). The ratio of iron(II) to zephiramine was found to be 1:2 by the mole ratio method (Fig. 5). The experiments were carried out in the absence of sodium chloride and the absorbance in chloroform was measured at 620 nm at which wavelength the reagent blank was low. These results indicate that the species extracted into chloroform is the 1:2:2 iron(II)—pyrogallol red—zephiramine complex. Thus the ternary complex in chloroform appears to be the ion pair $Z_2[Fe(PR)_2]$. The same composition is probable when 0.25 M sodium chloride is present in the extraction system.

The extraction mechanism can be represented as follows.

$$Fe^{2+} + 2H_2L^{2-} \rightleftharpoons [Fe(H_2L)_2]^{2-}$$
$$[Fe(H_2L)_2]^{2-} + 2Z^+ \rightleftharpoons \{Z_2[Fe(H_2L)_2]\}_a \rightleftharpoons \{Z_2[Fe(H_2L)_2]\}_o$$
$$H_2L^{2-} + 2Z^+ \rightleftharpoons \{Z_2(H_2L)\}_a \rightleftharpoons \{Z_2(H_2L)\}_o$$
$$Cl^- + Z^+ \rightleftharpoons \{ZCl\}_a \rightleftharpoons \{ZCl\}_o$$

where L^{4-} is the tetravalent pyrogallol red anion and subscripts a and o refer to the aqueous and organic phase, respectively. When an excess of the reagent (assuming only H_2L^{2-}) is present in aqueous solution, the binary complex anion is easily produced; then when zephiramine solution is added, ion pairs of the iron(II) complex and the excess of reagent are produced. On shaking with chloroform, the ion pairs are distributed between the aqueous and organic phases. When a large excess of chloride ion is added in aqueous solution, the excess of zephiramine is also extracted as the chloride into chloroform, and the zephiramine associated with pyrogallol red is released. In this way, the excess of reagent in the organic phase can be transferred into the aqueous phase. However, the ternary 1:2:2 iron(II) complex in the organic phase is not transferred to the aqueous phase.

Calibration graph and reagent blank

When the excess of reagent was removed, the apparent molar absorptivities of the iron(II) complex at the wavelength of maximum absorption were measured at the optimum pH from the slopes of the calibration graphs. The

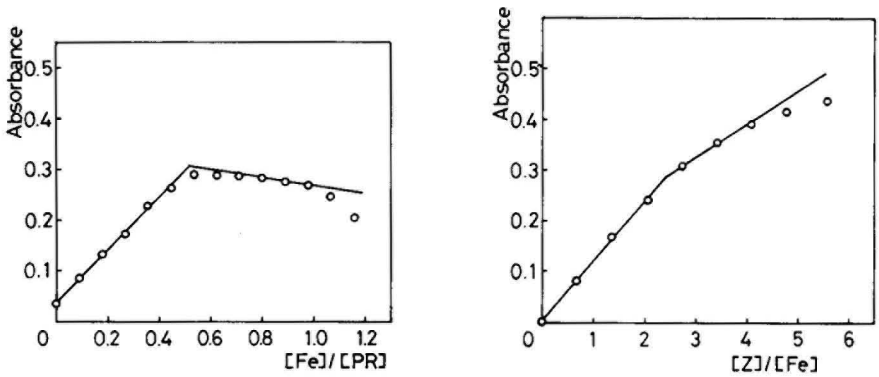

Fig. 4. Establishment of iron(II): pyrogallol red ratio by mole ratio method: 8.2×10^{-6} M pyrogallol red, 4.6×10^{-4} M zephiramine, no sodium chloride at pH 9.6, measured against chloroform at 620 nm.

Fig. 5. Establishment of iron(II): zephiramine ratio by mole ratio method: 7.3×10^{-6} M iron(II), 8.2×10^{-5} M pyrogallol red, no sodium chloride at pH 9.6 measured against chloroform at 620 nm.

concentrations of iron(II) and pyrogallol red were 0—1×10^{-5} M and 1×10^{-4} M, respectively. The absorbances were measured in a quartz cell of 1-cm path length at 298 and 560 nm in chloroform against the reagent blank. The calibration graphs obtained were straight lines that obeyed Beer's law. The apparent molar absorptivities calculated were 10.3×10^4 and 7.5×10^4 l mol^{-1} cm^{-1} at 298 and 560 nm, respectively. The reagent blanks at 298 and 560 nm were 0.126 and 0.060 ± 0.004, respectively. These values were reproducible, and the calibration graphs and reagent blanks were greatly superior to those obtained when the excess of co-extracted reagent was not removed.

Stability of the complex

The color of the iron(II) complex formed with pyrogallol red in chloroform was stable, and the absorbance of the complex at 560 nm was constant for at least 48 h.

The effect of EDTA was examined. When EDTA (10^{-4} M) was added before the addition of pyrogallol red (1×10^{-4} M), a negative error resulted. When the EDTA was added after the addition of pyrogallol red and buffer solutions, there was no error for 10^{-4} M EDTA but a negative error for 10^{-3} M EDTA. When the organic phase was shaken with EDTA solution (2×10^{-3} M) after extraction of the complex into chloroform at pH 9.6, correct results were obtained.

Reduction of iron(III) to iron(II)

As most of the iron in natural waters exists as iron(III), the efficiency of reduction of iron(III) with hydroxylammonium sulfate was examined. Concentrations of hydroxylammonium sulfate in the range 0.005—0.1 M were

effective; therefore 0.5 ml of 0.5 M hydroxylammonium sulfate solution was added to the aqueous solution.

Effect of diverse ions

Pyrogallol red is a ligand that possesses *o*-hydroxyl groups and reacts with many metal ions such as aluminum, manganese, iron, cobalt, nickel, copper, zinc, silver, cadmium, lead, bismuth, uranyl, etc. The tolerance limits for these metal ions and other ions often present in natural waters were examined (Table 1), masking agents being added when necessary. Aluminum was masked with fluoride ion. Copper(II) was reduced to copper(I) with hydroxylammonium sulfate and masked with pyrophosphate. Other interfering metal ions could be masked with citrate and pyrophosphate. Hence, 0.5 ml of 0.5 M hydroxylammonium sulfate and 1 ml of masking agent solution containing 1 M potassium fluoride, 0.15 M sodium citrate and 0.05 M potassium pyrophosphate were added to the aqueous solution.

Determination of iron in natural waters with pyrogallol red

Recommended procedure. Transfer the acidified (0.5 ml of concentrated sulfuric acid per liter) and filtered (0.45-μm pore size) sample solution (5—20 ml) to a stoppered 50-ml test tube; add 0.5 ml of 0.5 M hydroxylammonium sulfate solution and mix well. Add 1 ml of masking agent solution, 1 ml of 5×10^{-4} M pyrogallol red solution, 0.5 ml of 5×10^{-3} M zephiramine solution, 1 ml of ammonia—ammonium sulfate buffer solution (pH 9.6) and 1 ml of 5.75 M sodium chloride solution in this order. Dilute the resulting solution to the required volume (25 ml) and mix well. (In the case of sea-water samples, since the sample contains about 0.5 M chloride ion, the final concentration of

TABLE 1

Tolerance limits for diverse ions without and with masking agents

Ion	Tolerance limit (M)
Na^+, K^+, SO_4^{2-}	1[a]
F^-	0.2[a]
HPO_4^{2-}, citrate	0.05[a]
Mg^{2+}, Ca^{2+}, Sr^{2+}, Ba^{2+}, $P_2O_7^{4-}$	0.02[a]
Br^-, NO_3^-	2×10^{-3}
SCN^-, I^-	2×10^{-4}
Cu^+, Ag^+, Hg^{2+}, Cr^{3+}, ClO_4^-, dodecylbenzenesulfonate	1×10^{-5}
Cu^{2+}, Al^{3+}	2×10^{-4}[a, b]
Mn^{2+}, Ni^{2+}, Co^{2+}, Zn^{2+}	5×10^{-5}[b]
Cd^{2+}, Pb^{2+}, UO_2^{2+}	1×10^{-5}[b]

[a]Maximum tested.

[b]Add 0.5 ml of 0.5 M hydroxylammonium sulfate solution into the test solution and mix well, and then add 1 ml of masking agent solution.

chloride ion should be adjusted to be about 0.25 M by adding adequate amounts of sodium chloride.) Add 5 ml of chloroform and shake for 30 min. Add 0.5 ml of 0.02 M EDTA solution to the above solution after shaking, and again shake for 30 min to ensure masking of diverse metals. Stand for 30 min and measure the absorbance of the organic phase at 560 nm in a quartz (or glass) cell of 1-cm path length, against a reagent blank.

Results. The results obtained with city, river and sea waters are given in Table 2. To check the results obtained for iron in natural waters, the sample volumes taken were varied between 5 and 20 ml, and distilled water was added to each so as to give a constant volume of 20 ml. For all samples, linear graphs were obtained (Fig. 6) and the lines could be extrapolated to the same point which coincided with the point obtained for 20 ml of distilled water. Accordingly, the determination of iron in city, river and sea waters was quantitative and distilled water can be used for the reagent blank.

The recovery of iron was examined by adding variable amounts of iron(II) to the sample solutions (Fig. 7). The slopes obtained were all equal to that of the calibration graph obtained with distilled water. Iron in natural waters can thus be extracted quantitatively into chloroform as the ternary complex.

TABLE 2

Determination of iron in natural waters with pyrogallol red and zephiramine (All samples were taken during April 1977)

Sample[a]	Sampling date	Sample volume (ml)	Absorbance[b]	Iron content[b] ($\mu g\ l^{-1}$)
City water 1	10	20	0.570 ± 0.013	105 ± 2
	12	20	0.356 ± 0.010	66 ± 2
City water 2	13	20	0.241 ± 0.008	45 ± 1
City water 3	13	20	0.176 ± 0.004	32 ± 1
River water 4	13	10	0.089 ± 0.002	33 ± 0
		20	0.175 ± 0.005	32 ± 1
River water 5	23	20	0.224 ± 0.005	42 ± 1
River water 6	23	20	0.143 ± 0.007	26 ± 1
Sea water 7	13	10	0.131 ± 0.006	49 ± 2
Sea water 8	23	10	0.069 ± 0.004	25 ± 1

[a]Okayama city water: (1) at Tsushima; (2) at Saidaiji; (3) at Miyoshi. River water in Okayama prefecture: (4) Asahi river at Mino; (5) Yoshii river at Saidaiji; (6) Takahashi river at Sozya. Seto Inland Sea waters: (7) seashore at Sanban; (8) seashore at Ushimado.
[b]Average values of three determinations. The absorbance was measured (1-cm cells) against a reagent blank.

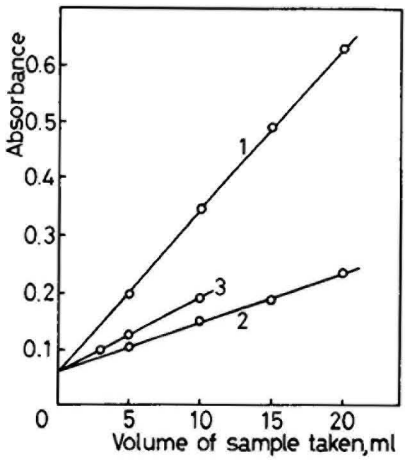

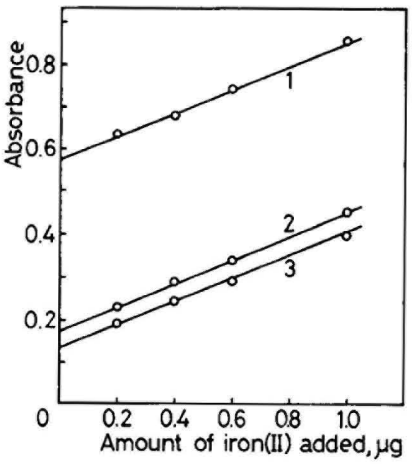

Fig. 6. Effect of volume of sample taken. (1) City water of Okayama city at Tsushima; sampled on April 10th, 1977. (2) Asahi river at Mino in Okayama prefecture; sampled on April 13th, 1977. (3) Sea water at Sanban; sampled on April 13th, 1977.

Fig. 7. Recovery of iron from sample solution. Samples as for Fig. 6; the amounts taken were 20, 20 and 10 ml, respectively.

REFERENCES

1 H. Kohara, N. Ishibashi and A. Yoshida, Jpn. Anal., 17 (1968) 616.
2 S. Motomizu and K. Tôei, Anal. Chim. Acta, 89 (1977) 167.
3 Z. Vodák and O. Leminger, Chem. Listy, 50 (1956) 2028.
4 R. M. Dagnall and T. S. West, Talanta, 8 (1961) 711.
5 T. Tanaka, Y. Nakagawa and S. Honda, Jpn. Anal., 10 (1961) 1148.
6 E. A. Bashirov, M. K. Akhmedli and T. E. Abdullaeva, Azerb. Khim. Zh., (1966) 122.
7 M. K. Akhmedli, D. G. Gasanov and R. A. Alieva, Uch. Zap. Azerb. Gos. Univ. Ser. Khim. Nauk, (1966) 3.
8 T. Takeuchi and Y. Shijo, Jpn. Anal., 15 (1966) 473.
9 E. A. Morgen, E. S. Rossinskaya and N. A. Vlasov, Zh. Anal. Khim., 30 (1975) 1384.
10 Y. Shijo and T. Takeuchi, Jpn. Anal., 22 (1973) 1341.
11 M. Kataoka, M. Tsukamoto and T. Kambara, J. Electrochem. Soc. Jpn., 45 (1977) 100
12 K. Tôei and K. Kawada, Jpn. Anal., 21 (1972) 1510.
13 V. Suk, Collect. Czech. Chem. Commun., 31 (1966) 3127.

Analytica Chimica Acta, 104 (1979) 379—384

Short Communication

TITRATION OF SULFITE IN WATER AND DIMETHYL SULFOXIDE WITH CERIUM(IV) SOLUTIONS

P. BRUNO*, M. CASELLI, A. DI FANO and A. TRAINI

Istituto di Chimica Analitica, Università degli Studi, Via Amendola 173, 70126 Bari (Italy)

(Received 23rd May 1978)

The titration of sulfite with oxidants has been very widely studied [1]. Bonner and Yost [2] considered many oxidizing titrations, and found that most of them were affected by errors caused by formation of some dithionate; an error of 3% was found with dichromate. Rao and Rao [3] pointed out that the reaction of sulfite with many oxidants proceeds quantitatively to sulfate in the presence of a catalyst. Good results were obtained with the following combinations of oxidant, catalyst, and acid concentration: (a) $KMnO_4$—$CuSO_4$—1 M acetic acid (or ICl in 0.5 M H_2SO_4); (b) $Ce(SO_4)_2$—ICl—3.75 M H_2SO_4; (c) $K_2Cr_2O_7$—$CuSC_4$—5 M HCl.

In the present communication, it is shown that accurate and reproducible results can be obtained in aqueous solutions by titrating sulfite with cerium(IV) solution in the absence of catalysts. The oxidation proceeds stoichiometrically according to the equation

$$7H_2SO_3 + 10Ce^{4+} + 3H_2O \rightleftharpoons 10Ce^{3+} + 3SO_4^{2-} + 2H_2S_2O_6 + 16H^+ \quad (1)$$

This stoichiometry is unchanged over the temperature range 20—70°C in 0.2—2 M sulfuric acid solutions.

Sulfur dioxide and sulfite can be determined in DMSO (dimethyl sulfoxide) by employing aqueous cerium(IV) solution as the titrant. In this case, all the sulfite is oxidized to dithionate. In both cases, the titration can be followed potentiometrically.

Experimental

Ammonium hexanitratocerate solutions were prepared as described by Smith and Fly [4] from analytical-grade reagent (C. Erba, RPE, ACS) and standardized against sodium oxalate [5]. Sodium sulfite (C. Erba, RPE, ACS) solutions were standardized by iodimetric titrations.

Titrations in the absence of oxygen were done in a cell fitted with inlet and outlet tubes for nitrogen. This cell, with suitable openings for the buret and electrodes (Pt and SCE), was used for potentiometric titrations. Potentials were measured by a Schulemberger 1240 voltmeter.

Results and discussion

The reproducibility of direct titrations of aqueous sulfite solutions with cerium(IV) is no better than 1% because sulfur dioxide is evolved by the acid present in the titrant. The reverse titration is far more reliable. Table 1 shows some results obtained with ferroin as indicator. The values of $N(SO_3^{2-})$ reported were calculated by dividing the amount (meq) of cerium(IV) taken by the volume (ml) of sulfite solution required for titration; the $M(SO_3^{2-})$ values were obtained by iodimetric titration. The mean value $f = 1.428$ is practically equal to 10/7. Equation (1) is therefore valid. This equation can be considered as the sum of the reactions:

$$2Ce^{4+} + H_2SO_3 + H_2O \rightleftharpoons 2Ce^{3+} + SO_4^{2-} + 4H^+ \quad (2)$$

$$2Ce^{4+} + 2H_2SO_3 \rightleftharpoons 2Ce^{3+} + H_2S_2O_6 + 2H^+ \quad (3)$$

in the ratio 3/2. The simultaneous progress of these reactions can be readily explained if a first step is postulated:

$$Ce^{4+} + SO_4^{2-} \rightleftharpoons Ce^{3+} + SO_3^{\cdot-} \quad (4)$$

The $SO_3^{\cdot-}$ radical can dimerize to form $S_2O_6^{2-}$ or undergo further oxidation. The ratio of the rates of the two reactions should determine the ratio between the amounts of sulfate and dithionate.

The system represented by eqns. (2) and (3) can be considered as an exampl of induced reaction [6, 7], where H_2SO_3 acts simultaneously as inductor and acceptor, and thus gives a constant value of the induction factor [8], defined as F_i = (equivalents of induced reaction)/(equivalents of primary reaction). The constant value of F_i suggests a coupled reaction, but a mechanism that takes account of the given stoichiometry has not been found. The hypothesis that the reaction of cerium(IV) with sulfite induces oxidation of sulfite by oxygen, as can happen with other oxidants [7], must be disregarded, because the $[SO_4^{2-}]/[S_2O_6^{2-}]$ ratio does not depend on the relative concentrations of cerium(IV) and oxygen or on the H_2SO_4 concentration.

Figure 1 shows a potentiometric titration curve for aqueous solutions; the value $E^0(Ce^{4+}/Ce^{3+}) = 1160 \pm 1.2$ mV (vs. SCE) was obtained from the points

TABLE 1

Titration of cerium(IV) with sodium sulfite solution

T (°C)	H_2SO_4 (M)	Ce(IV) taken (meq)	Ce(IV) taken (eq l^{-1})	Volume of SO_3^{2-} required (ml)	$N(SO_3^{2-})$ (eq l^{-1})	$M(SO_3^{2-})$ (mol l^{-1})	$f = N/M$[a]
20	0.50	0.4675[b]	9.6×10^{-2}	3.75	0.1247	0.0874	1.426
30	0.25	0.4810[c]	9.6×10^{-2}	4.50	0.1069	0.0748	1.429
40	1.00	0.4810[b]	9.6×10^{-3}	9.65	0.0498	0.0350	1.424
70	2.50	0.4810[c]	5.0×10^{-3}	13.55	0.0355	0.0248	1.431

[a] $\bar{f} = 1.428 \pm 0.003$. [b] Samples saturated with N_2. [c] Samples saturated with O_2.

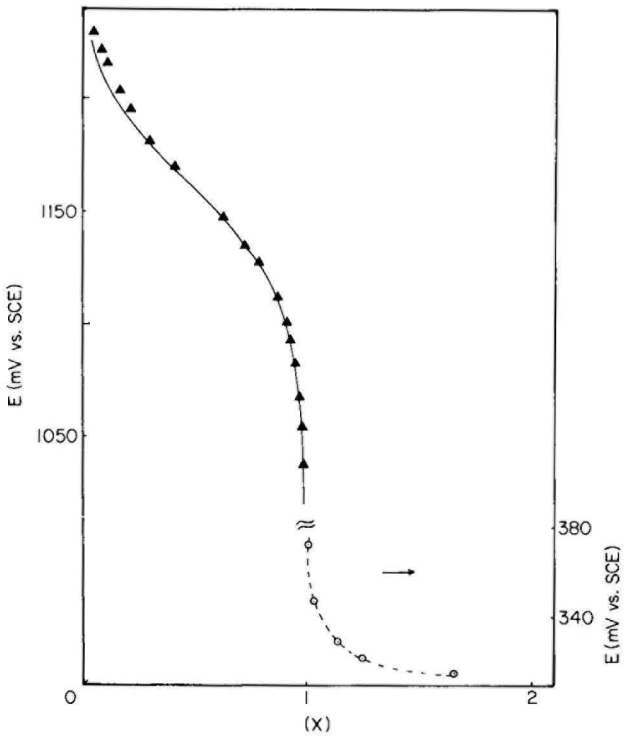

Fig. 1. Potentiometric titration for SO_3^{2-} with cerium(IV) in aqueous solution. The continuous curve was calculated by the Nernst equation for the couple Ce^{4+}/Ce^{3+}. The dotted curve was calculated for the SO_4^{2-}/SO_3^{2-} system. (▲) (○) Experimental points. V^0 = 58 ml; Ce^{4+} = 0.481 × 10^{-3} mol; 1 M H_2SO_4; $M(SO_3^{2-})$ = 0.0349; 25°C.

on the experimental curve in the range between $X = 0.1$ and $X = 1.0$ (where X is the fraction titrated). For the dotted portion of the curve, the SO_4^{2-}/SO_3^{2-} system was considered, and a value of $E'(SO_4^{2-}/SO_3^{2-}) = 237 \pm 2$ mV (vs. SCE) was obtained, but this potential is very far from the standard potential (170 mV vs. NHE) for the SO_4^{2-}/SO_3^{2-} couple [9]. This is understandable because the system is not reversible.

From the analytical point of view, the method is suitable for a titrimetric determination of sulfite. Better results can be obtained by addition of the sulfite solution to an excess of cerium(IV) solution in 1 M sulfuric acid followed by back-titration of the excess with standard oxalate solution. Typical results are reported in Table 2.

Titrations in dimethyl sulfoxide

Sulfite and sulfur dioxide in DMSO were titrated accurately and reproducibly with cerium(IV) solutions. This is of interest because most oxidants react with DMSO; for instance, permanganate [10] and dichromate [11] in dilute sulfuric acid solutions oxidize DMSO to sulphone. Although ammonium

TABLE 2

Results obtained by addition of sulfite to excess of cerium(IV) and back-titration

Na_2SO_3 taken (mg)	Ce(IV) taken (ml)	Ce(IV) (M)	Oxalate required[a] (ml)	Na_2SO_3 found (mg)	Error[b] (%)
94.6	27	0.0935	9.85	94.6	—
100.4	21	0.0935	6.95	99.9	−0.52
103.4	28	0.0935	10.10	104.0	+0.57
127.3	15	0.0962	3.57	128.0	+0.55
56.0	15	0.0962	5.60	56.0	—
98.2	15	0.0962	4.40	98.6	+0.41
53.3	15	0.0962	5.67	53.5	+0.37
140.9	15	0.0876	2.55	141.5	+0.42
66.0	5	0.0876	0.33	65.6	−0.60
132.5	15.5	0.0876	3.03	132.2	−0.23
57.7	5	0.0876	0.55	57.8	+0.17
220.7	25	0.0876	18.70	220.5	−0.09
226.8	25	0.0876	17.95	227.2	+0.17

[a]The $Na_2C_2O_4$ normality was 0.2010 in all cases except for the last two results when a 0.0502 N solution was used.
[b]The mean error is 0.32% (s.d. = 0.22).

cerium(IV) nitrate has been reported not to oxidize DMSO [12], it was found here that cerium(IV) in DMSO is gradually reduced to cerium(III). However, the kinetics of this reaction is slow (Fig. 2) and aqueous cerium(IV) solutions can be employed for titrations in DMSO. Table 3 shows some results for titrations of sulfite in DMSO at 50°C; end-points were detected visually by the appearance of the faint yellow colour of cerium(IV), persistent for a few minutes, or by potentiometry.

It is interesting to note that in DMSO only one electron is exchanged per

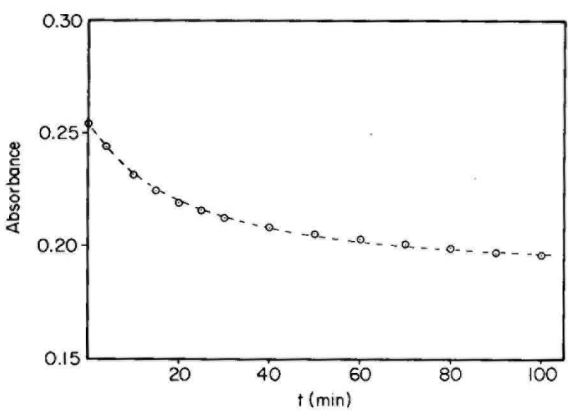

Fig. 2. Kinetics of 2×10^{-4} M cerium(IV) reduction in DMSO by spectrophotometric measurements at 305 nm.

TABLE 3

Titrations of sulfite in DMSO with aqueous 0.0962 M cerium(IV) solution

Na_2SO_3 taken (mg)	Ce(IV) required (ml)	Na_2SO_3 found (mg)	Error[a] (%)
108.4	4.45	107.9	−0.42
105.8	4.35	105.5	−0.27
128.5	5.30	128.6	−0.05
178.9	7.35	178.3	−0.34
218.6	9.00	218.3	−0.13
109.1	4.50	109.2	+0.07

[a]The mean error is 0.2% (s.d. = 0.15).

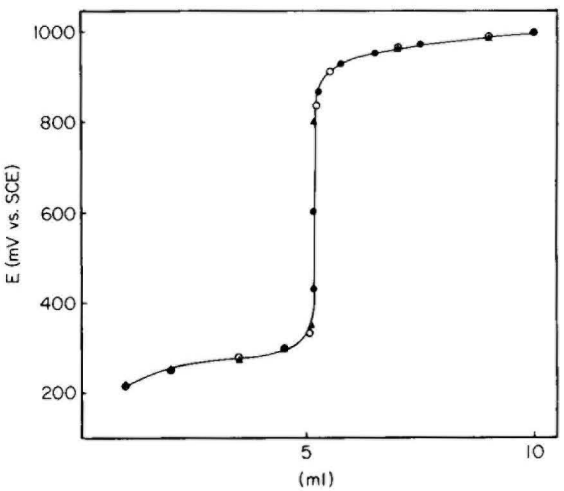

Fig. 3. Potentiometric titration of 0.49×10^{-3} mol of sulfite in DMSO with aqueous cerium(IV) solution (0.0962 M in 1 M H_2SO_4) at 50°C. V^0 = 55 ml.

molecule of sulfite (Fig. 3). If the reaction mechanism is the same as that in aqueous solution, dimerization of the $SO_3^{\cdot-}$ radical is very much faster than oxidation. Therefore eqn. (3) is the only reaction.

Titrations in mixed DMSO—water solvent

Sulfite—cerium(IV) titrations were also done in water—DMSO media. The number of electrons exchanged per molecule of sulfite remained one for solutions containing up to 15% (v/v) water. This number then increased almost linearly, becoming 10/7 in pure water.

REFERENCES

1 I. M. Kolthoff and R. Belcher, Volumetric Analysis, Vol. III, p. 195, Interscience, New York, 1957.
2 W. D. Bonner and D. M. Yost, Ind. Eng. Chem., 18 (1926) 55.
3 K. B. Rao and G. G. Rao, Anal. Chim. Acta, 13 (1955) 313.
4 G. F. Smith and W. H. Fly, Anal. Chem., 21 (1949) 1233.
5 H. H. Willard and P. Young, J. Am. Chem. Soc., 50 (1928) 1322; 55 (1933) 3260.
6 A. I. Medalia, Anal. Chem., 24 (1955) 1678.
7 H. Bassett and W. G. Parker, J. Chem. Soc., 352 (1951) 1540.
8 W. C. Bray and J. B. Ramsey, J. Am. Chem., Soc., 55 (1933) 2279.
9 W. M. Latimer, Oxidation Potentials, 2nd edn., Prentice-Hall, Englewood Cliffs, N.J., 195
10 T. B. Douglas, J. Am. Chem. Soc., 68 (1946) 1072.
11 K. Stelmach, Chem. Anal. (Warszawa), 11 (1966) 628.
12 L. H. Krull and M. Friedman, J. Chromatogr., 2 (1957) 336.

Analytica Chimica Acta, 104 (1979) 385—387

Short Communication

THE ATOMIC ABSORPTION SPECTROMETRIC DETERMINATION OF PALLADIUM WITH A CARBON-FILAMENT ELECTROTHERMAL ATOMIZER

E. A. BOUND***, J. D. NORRIS**, A. SANZ-MEDEL‡ and T. S. WEST*

Department of Chemistry, Imperial College of Science & Technology, London SW7 2AY (Gt. Britain)

(Received 21st June 1978)

Several methods have been described for the determination of palladium by atomic absorption spectrometry in flames. The best sensitivity, 0.01 ppm, appears to be that reported by Rubeska and Stupar [1]. A comprehensive study of the atomic absorption and atomic fluorescence of palladium has been described by Sychra et al. [2]. However, little work has been reported on the determination of palladium with electrothermal atomizers. This communication describes the atomic absorption determination of palladium with the carbon filament atom reservoir.

Experimental

The instrumentation employed was similar to that described by Oborne and West [3]. This included a 3.2-mm carbon filament, which allowed 5-μl aliquots of sample solutions to be used. The atomic line radiation source was a Techtron-ASL high-intensity hollow-cathode lamp. The operation of the carbon-filament atom reservoir was as described previously [3].

A 1000-ppm palladium stock solution was prepared by dissolving 0.2672 g of "Specpure" grade ammonium chloropalladite (Johnson Matthey and Co.) in a small volume of dilute hydrochloric acid and diluting to 100 cm^3 with deionized water. Working solutions were prepared by suitable dilution as required.

Results and discussion

The atomic absorption of palladium at seven wavelengths reported in flames [2] was investigated. With the carbon-filament atom reservoir, atomic absorption was found at 244.79 nm, 247.64 nm and 276.31 nm, but not at 324.27 nm, 340.46 nm, 360.96 nm and 363.47 nm. The latter four wavelengths correspond to transitions arising from energy levels above the ground

Present addresses:
*Macaulay Institute for Soil Research, Craigiebuckler, Aberdeen, Scotland.
**British Carbonization Research Association, Chesterfield, Derbyshire, S42 6JS.
***SGS (Kenya) Ltd., Mombasa, Kenya.
‡Chemistry Department, University of Madrid, Spain.

state. Therefore, although atomic absorption can be achieved at these wavelengths in a flame, because of thermal population of these levels by the flame, insufficient energy is available for this purpose with the resistively heated filament atomizer. This is a further example of the different atomizing characteristics of flames and other atom cells.

Optimal operating parameters for the atomic absorption determination of palladium at 244.79 nm were as follows: hollow-cathode lamp primary current, 16 mA; hollow-cathode lamp secondary current, 400 mA; slit-width (spectral band-pass), 0.2 nm; atomization voltage, 270 V; mean height of observation above filament, 0.9 mm; nitrogen flow rate, 3 l min^{-1}.

Sensitivities, detection limits, upper (linear) concentration limits, and relative standard deviations for the atomic absorption of palladium at 244.79 nm, 247.64 nm and 276.31 nm are given in Table 1. The best absolute sensitivity, 8×10^{-11} g, equivalent to 5 μl of a 0.16-ppm palladium solution, was obtained at 244.79 nm. For all three wavelengths, the detection limit was about one order of magnitude poorer than the absolute sensitivity. This is entirely attributable, in this instance, to the high noise from the hollow-cathode lamp employed, which was unfortunately nearing the end of its useful lifetime.

The effects of 1000-fold (weight) ratios of thirteen anions and cations on the atomic absorption of a 1-ppm solution of palladium at 244.79 nm were examined. In all cases a reduction in the atomic absorption signal was observed (Table 2).

Conclusion

The atomic absorption spectrometric determination of palladium with the carbon-filament atom reservoir is a feasible method. The sensitivity of 0.016 ppm obtained at 244.79 nm is similar to the best sensitivity previously reported with a flame [1]. However, the results obtained indicate that interference effects are likely to be significant, particularly at the 1000-fold level and above, although this is probably no more serious than for other elements with the carbon-filament atom reservoir.

TABLE 1

Analytical data for the atomic absorption of palladium with a carbon filament atomizer

Wavelength (nm)	Absolute sensitivity[a] (g)	Absolute detection limit[b] (g)	Upper concentration limit[c] (g)	% Relative standard deviation for 5×10^{-9} g[d]
244.79	8×10^{-11}	6×10^{-10}	6.5×10^{-9}	5.6
247.64	1×10^{-10}	1.5×10^{-9}	7.5×10^{-9}	5.5
276.31	3×10^{-10}	2.5×10^{-9}	7.5×10^{-9}	6.2

[a]Amount equivalent to an absorbance of 0.0044. [b]Amount that produces a signal twice the noise level. [c]Approximate upper end of linear range of calibration curve. [d]Calculated on 10 replicate analyses.

TABLE 2

Interference effects of 1000-fold ratios of various ions on the atomic absorption of 5×10^{-9} g of palladium at 244.79 nm

Ion	Compound used	% Depression of signal	Ion	Compound used	% Depression of signal
Cl^-	HCl	5.9	Fe^{3+}	$Fe_2(SO_4)_3$	25.7
SO_4^{2-}	H_2SO_4	14.7	Pb^{2+}	$Pb(NO_3)_2$	15.6
NO_3^-	HNO_3	16.8	Cu^{2+}	$CuSO_4$	6.8
PO_4^{3-}	H_3PO_4	32.2	Ag^+	$AgNO_3$	8.6
Ca^{2+}	$CaSO_4$	42.9	Ni^{2+}	$NiSO_4$	33.7
Mg^{2+}	$MgSO_4$	39.0	Co^{2+}	$CoCl_2$	10.6
Al^{3+}	$Al_2(SO_4)_3$	36.8			

J. D. N. thanks ICI Ltd. for the award of an ICI Research Fellowship and A. S. M. thanks the Spanish High Council for Scientific Research for the award of a Research Grant.

REFERENCES

1 I. Rubeska and J. Stupar, At. Absorpt. Newsl., 5 (1966) 69.
2 V. Sychra, P. J. Slevin, J. Matousek and F. Bek, Anal. Chim. Acta, 52 (1970) 259.
3 A. C. Oborne and T. S. West, Proc. Soc. Anal. Chem., 9 (1972) 198.

Analytica Chimica Acta, 104 (1979) 389—392

Short Communication

DETERMINATION OF COBALT IN BIOLOGICAL MATERIALS BY ATOMIC ABSORPTION SPECTROMETRY

MITSUYASU SUZUKI*, KENJIRO HAYASHI** and WARREN E. C. WACKER***

Department of Chemistry, Faculty of Liberal Arts, Yamaguchi University, Yamaguchi, 753 (Japan)

(Received 20th June 1978)

The formation of oxides and/or phosphates in the flame accounts for some of the difficulties in determining cobalt in biological materials by atomic absorption spectrometry. Moreover, the effects of cations and anions occurring in biological materials have not been adequately assessed in previous studies. The present method obviates these problems by the use of a 75% saturated oxine solution, a reagent which has been employed previously as a solvent in analyses for magnesium [1, 2] and manganese [3]. The optimization of several parameters which may affect the precision and accuracy for cobalt is reported below, as well as applications to vitamin B_{12} and some cobalt-containing proteins.

Experimental

Apparatus. A Westinghouse WL-22928 cobalt hollow-cathode lamp was used at a current of 13.5 mA, with a horizontal alumina (alundum) ceramic tube (length 25.5 cm; i.d. 1.6 cm) as the absorption cell, and a Beckman atomizer burner (no. 4020). The Zeiss M4Q III monochromator used had dispersions of 0.8 nm mm^{-1} at 200 nm and 3 nm mm^{-1} at 500 nm.

The lamp radiation was collimated by a quartz lens 11 cm from the window; after passage through the absorption cell the radiation was focused on the entrance slit (0.020 mm) of the monochromator. The optimal gas pressures were 11.5 psi air and 4.0 psi hydrogen. Samples were aspirated at 1.5 ml min^{-1}.

The strong cobalt resonance lines occur at 240.7 and 242.5 nm in atomic absorption spectrometry. The sensitivity of the Co 240.7-nm line is about 1.5 times greater than that of the Co 242.5-nm line, so that the former line was selected.

The electric circuits for the high-voltage power supply and amplifier were

**Present address: Department of Chemistry, Faculty of Science, Yamaguchi University, Yamaguchi, 753, Japan.

***Present address: Harvard University, University Health Services, 75 Mount Auburn St., Cambridge, Mass. 02138, U.S.A.

those used previously [3]. The output signal of the amplifier was displayed on a microammeter [3].

Reagents and solutions. Saturated oxine (8-hydroxyquinoline) solution was prepared by adding oxine slowly to 100 ml of metal-free 1 M hydrochloric acid until a saturated solution was obtained at room temperature; this was allowed to stand for 48 h before the supernatant solution was used. Cobalt standard solution (10 mg ml^{-1}) was prepared by dissolving the pure metal (Johnson Matthey) in metal-free 6 M hydrochloric acid and diluting with de-ionized distilled water. Working solutions containing 0.1—0.7 μg Co ml^{-1} were prepared by suitable dilution with water, after addition of the saturated oxine solution to give a 75% saturated solution. High-purity chromium, copper, iron, magnesium, manganese, nickel and zinc were dissolved in 6 M HCl (10 ml) and/or 7 M HNO_3 (5 ml) to give 1 M solutions of each metal; the solutions were evaporated almost to dryness and the resulting salts were dissolved in water. Calcium, potassium and sodium chlorides (Johnson Matthey) were dissolved in water. Hydrochloric acid, nitric acid, sulfuric acid and phosphoric acid were either Specpure or reagent-grade chemicals. De-ionized, distilled water was used throughout.

Results and discussion

It is well known that the absorption of the cobalt analytical lines is affected by the type and concentration of acids and co-existing elements in the sample solutions. In the present study the absorption of an aqueous cobalt solution (10^{-5} M) was found to decrease as the concentration of nitric acid, sulfuric acid or phosphoric acid increased (Fig. 1), possibly because of involatile salt formation in the flame or because of increased viscosity. However, even 10^{-1} M concentrations of these acids, or of Tris buffer, did not affect the absorption of a standard 10^{-5} M cobalt solution in 75% saturated oxine solution. The absorption of cobalt itself in the 75% saturated oxine solution was lowered slightly compared to pure cobalt solution (Fig. 1). The

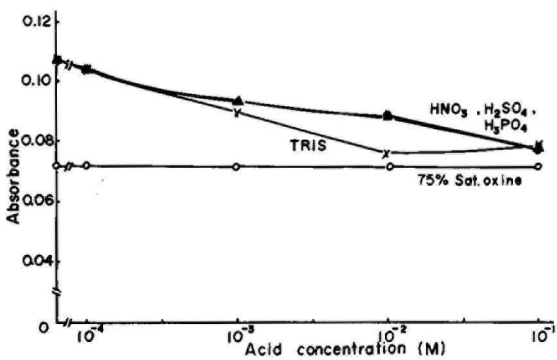

Fig. 1. Effect of various acids on the absorbance of cobalt.

absorption of 10^{-5} M solutions of cobalt in 75% saturated oxine was not affected by 10^{-3} M calcium, chromium, copper, iron, magnesium, manganese, nickel or zinc, or 10^{-2} M sodium or potassium.

The repeatability of the method was established for solutions containing four cobalt concentrations in the range 0.1—0.7 μg ml^{-1} in 75% saturated oxine solution; the relative standard deviation did not show a significant trend over the range, and the average was 2.5% (n = 6 at each level). The calibration graph was linear over the range 0—0.7 μg Co ml^{-1}. The sensitivity is 0.02 μg Co ml^{-1} for 1% absorption. The accuracy of the method was checked by analysis of the NBS standard sample No. 161 (nickel—chromium alloy). A sample of the standard (0.3 g) was dissolved in 5 ml of 6 M hydrochloric acid and 3 ml of 7 M nitric acid; the solution was evaporated almost to dryness and then diluted to 100 ml with water. An aliquot was diluted with the usual oxine solution for analysis. The average cobalt content found was 0.280 ± 0.0063% (n = 6); the certified value is 0.282%, so that the accuracy is 99.3%.

The proposed method was employed to determine cobalt in vitamin B_{12}. Samples of commercial crystalline vitamin B_{12} (0.05 or 0.10 g) were dissolved in water with gentle heating; after cooling to room temperature, the solutions were diluted, respectively, with 50 or 100 ml of water and then with 75% saturated oxine solution for the determination of cobalt. Vitamin B_{12} was also determined by direct spectrophotometry from the absorbance at 550 nm [4]. The results are shown in Table 1.

The proposed method was also used to determine cobalt in cobalt-containing alkaline phosphatase. In preliminary tests, alkaline phosphatase solutions containing known amounts of cobalt were diluted with 75% saturated oxine solution before aspiration; for final solutions which contained 4.3—8.7 × 10^{-5} M cobalt and about 4 × 10^{-5} M protein (determined from the absorbance at 278 nm), the recoveries of cobalt varied from 100.7 to 111%. Table 2 shows the results obtained for cobalt in treated alkaline phosphatase, thermolysin and carboxypeptidase by the proposed method.

It is well known that phosphate interference is usually severe in atomic absorption determinations of cobalt in biological materials. The use of oxine eliminates the interferences of phosphate and many other ions, and the pro-

TABLE 1

Analysis of vitamin B_{12} for cobalt

Sample taken (g)	Co found (μg ml^{-1})	Co found (M)	B_{12} content (M)[a]	Co: B_{12} (g-atom mol^{-1})
0.05025/50 ml	39.8 ± 0.8[b]	6.76 × 10^{-4}	6.64 × 10^{-4}	1.01
0.09860/100 ml	39.8 ± 0.8[b]	6.76 × 10^{-4}	6.35 × 10^{-4}	1.06

[a]By direct spectrophotometry at 550 nm.
[b]Mean and average deviation (n = 4).

TABLE 2

Results for cobalt in treated alkaline phosphatase, thermolysin and carboxypeptidase

Sample	Co found		Protein (M)	Co: Protein (g atom mol^{-1})
	($\mu g\ ml^{-1}$)	(M)		
Co—alkaline phosphatase[a]				
A	2.54	4.31×10^{-5}	2.30×10^{-5}	1.87
B	5.25	0.89×10^{-4}	2.47×10^{-5}	3.60
Co—thermolysin[b]				
A-1	3.89	6.60×10^{-5}	7.12×10^{-5}	0.93
A-2	8.13	1.38×10^{-4}	1.45×10^{-4}	0.95
Co—CPD[a]				
A-1	7.63	1.30×10^{-4}	1.27×10^{-4}	1.02
A-2	8.30	1.41×10^{-4}	1.43×10^{-4}	0.99

[a]Protein concentration determined by absorbance at 278 nm [5].
[b]Protein concentration determined by absorbance at 280 nm [6].

cedure is simple and practical. Systematic studies to clarify the complexing reaction between cobalt and oxine in the flame are in progress.

The authors express their appreciation to Dr. Bert L. Vallee for helpful comments.

REFERENCES

1 W. E. C. Wacker, C. Iida and K. Fuwa, Nature, 212 (1964) 659.
2 C. Iida, K. Fuwa and W. E. C. Wacker, Anal. Biochem., 18 (1967) 18.
3 M. Suzuki and W. E. C. Wacker, Anal. Biochem., 57 (1974) 605.
4 Handbook of Biochemistry, Selected data for Molecular Biology, 2nd. edn., 1970, K-37.
5 R. T. Simpson, J. F. Riordan and B. L. Vallee, Biochemistry, 2 (1963) 616.
6 Y. Ohta, Y. Ogura and A. Wada, J. Biol. Chem., 241 (1966) 5919.

Analytica Chimica Acta, 104 (1979) 393—395

Short Communication

DETERMINATION OF CADMIUM IN POLISHED RICE BY LOW-TEMPERATURE ASHING AND ATOMIC ABSORPTION SPECTROMETRY

HISATAKE NARASAKI

Department of Chemistry, Faculty of Science, Saitama University, Shimo-Okubo, Urawa (Japan)

(Received 11th July 1978)

In low-temperature ashing, the rates of reaction of oxygen plasma with specimens are constant regardless of the particle shapes [1]. In practice, however, the weight loss per unit time decreases as the reaction progresses, because the surface areas decrease. In the method proposed here for cadmium, samples were treated with the low-temperature asher until their weight was reduced by about half, and then decomposed by wet oxidation. Sulfuric acid and 60%(w/w) hydrogen peroxide were used for the wet oxidation. Cadmium was then extracted from the sample solution as its diethyldithiocarbamate (DDTC) into 4-methylpentan-2-one (MIBK), and determined by atomic absorption spectrometry [2].

Experimental

Instrumentation. An International Plasma Corporation 1001-B plasma machine was used for the treatment of samples. The Japan Jarrell-Ash AA-782 atomic absorption spectrometer used was fitted with a burner slit 10-cm long, and was attached to a Yanagimoto YR-110 recorder.

Cadmium solutions. A 1000 mg l^{-1} stock solution of cadmium was prepared by dissolving cadmium metal (minimum assay 99.999%) in 50 ml of 5 M hydrochloric acid and 5 ml of concentrated nitric acid and diluting to 1 l with water. Calibration solutions were prepared by suitable dilution with twice-distilled water.

Preparation of sample solutions. Treat 5 g of polished rice placed in a dish in a stream of oxygen (100 ml min^{-1}) for 10 h in the low-temperature asher. Transfer the treated sample to a 100-ml Kjeldahl flask. Add 3 ml of concentrated sulfuric acid and heat the flask until the organic material chars completely. Allow to cool first by standing and then by immersion of the flask in water. Then add about 1 ml of cold 60% (w/w) hydrogen peroxide. Warm gently until the decomposition of hydrogen peroxide ceases. Repeat the cooling and addition of 1-ml portions of hydrogen peroxide until a clear solution is obtained; this takes about 8 ml of the hydrogen peroxide.

Wash the original dish with a little 0.1 M hydrochloric acid, transferring the washings to the flask. Adjust the pH to 6—7 with 7 M ammonia solution, using bromothymol blue as indicator.

Extraction of cadmium. Transfer the cooled digest to a 300-ml separating funnel, add 5 ml of 25% (w/v) potassium sodium tartrate and dilute to 100 ml with water. Add 5 ml of 10% (w/v) sodium diethyldithiocarbamate and shake the funnel for 1 min. After 5 min, add 10.0 ml of 4-methylpentan-2-one and shake for 5 min. Leave for 1 h, remove the aqueous phase, and pass the ketone phase through a dry filter paper into a glass-stoppered tube.

For calibration, place 30—40-ml portions of water in the funnels and add up to 1.5 ml of cadmium standard (1 mg l^{-1}), 25 ml of 40% (w/v) ammonium sulfate and 5 ml of 25% (w/v) potassium sodium tartrate. Dilute to 100 ml and extract the DDTC complex as described above.

Measurement. Measure cadmium at 228.8 nm (lamp current, 5 mA; burner height, 3—4 mm) in fuel-lean air-acetylene flame (air flow, 13 l min^{-1}). Aspirate the ketone at a rate of 3 ml min^{-1} by opening the bypass air valve; then aspirate a reagent blank, the cadmium standards and the sample solutions, with ketone after each reading. Calculate the cadmium contents by reference to the calibration graph.

Results and discussion

Recoveries were checked by spiking the rice with 1 μg of cadmium and measuring as described above; the average recovery was 96.2% in duplicate runs. Table 1 shows typical results obtained for cadmium determinations in rice samples and in Orchard Leaves (NBS Standard Reference Material 1571).

The low-temperature ashing method is useful for treating large samples of organic materials, but a very long time is needed for complete ashing because the oxidation process is affected by the ash deposited on the surface of the sample. In the proposed method, the partial decomposition of the samples in the asher reduces the amount of oxidizing agent required for complete decomposition and so reduces the contamination from the usual wet oxidation technique. The use of hydrogen peroxide may be somewhat tedious because of the need for repetitive addition [3] but it is effective in preparing

TABLE 1

Determination of cadmium in rice samples and Orchard Leaves (SRM 1571) for 5-g samples

Sample	Cadmium range found (μg g^{-1})[a]
Polished rice 1	0.07—0.08 (0.08)
Polished rice 2	0.09—0.11 (0.10)
Polished rice 3	0.08—0.11 (0.10)
Orchard Leaves[b]	0.09—0.10 (0.10)

[a]Range for 4 determinations with the average result in parentheses.
[b]Certified value, 0.11 ± 0.01 μg g^{-1}.

clear solutions from charred digests [4]. Dithizone is a good chelating agent for cadmium [5], but is readily decomposed by residual hydrogen peroxide in the digest, so that diethyldithiocarbamate is more satisfactory for general purposes.

The author thanks Mr. K. Miyagi for technical assistance.

REFERENCES

1 R. H. Hansen, J. V. Pascale, T. De Benedictis and P. M. Rentzepis, J. Polym. Sci., Part A, 3 (1965) 2205.
2 S. Kanno, S. Fukui, S. Setsuda, S. Naito, M. Kaneko and J. Matsuzaki, Eisei Kagaku, 17 (1971) 24; Chem. Abstr., 75 (1971) 74243.
3 A. M. Ure and C. A. Shand, Anal. Chim. Acta, 72 (1974) 64.
4 H. Narasaki, J. L. Down and R. Ballah, Analyst, 102 (1977) 537.
5 J. C. Chambers and B. E. McClellan, Anal. Chem., 48 (1976) 2064.

Analytica Chimica Acta, 104 (1979) 397—402

Short Communication

PHOTOSENSITIZED GENERATION OF IODINE WITH ROSE BENGAL FOR PHOTOCHEMICAL TITRATIONS

C. SÁNCHEZ-PEDREÑO*, T. PÉREZ-RUIZ, C. MARTINEZ-LOZANO and M. HERNÁNDEZ-CÓRDOBA

Department of Analytical Chemistry, C.S.I.C. University of Murcia (Spain)

(Received 5th June 1978)

There are many examples known in which irradiation with visible light in the presence of a sensitizer causes a chemical change in a substrate which is transparent to the incident radiation. Experiments carried out by many different techniques have shown that in the absence of oxygen the photo-oxidation of certain compounds such as amino acids [1, 2], nucleic acids [3], amines [4—6], heterocyclic nitrogen compounds [7] and EDTA [8—12] takes place, the triplet-state dyestuff being the oxidant. In other instances [13], the presence of oxygen is necessary for photo-oxidation, the triplet-state dyestuff again being the active species.

The eosin-sensitized photochemical oxidation of iodide to iodine has been studied several times since Straub's first report [14]. Studies conducted with sinusoidally modulated radiation have shown that the main oxidant is the semi-oxidized dyestuff formed by the reduction of oxygen by triplet state eosin, so that the presence of oxygen is essential [15]. The formation of iodine by this photochemical reaction has been the basis for determinations of ascorbic acid, thiosulphate, arsenite, sulphite and sulphide [16, 17].

The present communication reports a study of the photo-generation of iodine from iodide in the presence of oxygen, sensitized by Rose Bengal dye, and its application to the determinations of arsenite, hydrazine, isonicotinic acid hydrazide (isoniazid) and uric acid, with amperometric end-point detection [18].

Experimental

Apparatus. A Radiometer PO4 polarograph was coupled to the illumination device (Arrosu Electromedidas, Murcia) described previously [12]. Biamperometric titrations were followed with two platinum electrodes of 1 cm^2 area.

Reagents. Reagent-grade chemicals were used without further purification. Double-distilled, deionized water was used throughout. An aqueous 0.001 M Rose Bengal solution (C.I. 45440) was prepared from the commercial product (K and K). Aqueous 0.01 N stock solutions of sodium arsenite, hydrazine sulphate, isonicotinic acid hydrazide and uric acid were standardized conventionally with iodine [18, 19]. Solutions of lower concentrations were prepared as required by suitable dilution. Buffer solutions were prepared by

mixing a solution 0.1 M in each of phosphoric, acetic and boric acids with an appropriate amount of 1 M sodium hydroxide solution. The pH values were always checked with a pH meter.

Procedure. The sample must always be prepared under diffuse light. To the reaction cell, add 10 ml of 5% sodium hydrogencarbonate solution, 2 ml of the 0.001 M Rose Bengal solution, various volumes of standard or analyte solution (arsenite, hydrazine sulphate, isoniazid or uric acid), and 2.5 g of potassium iodide. Dilute to exactly 50 ml with deionized water. Thermostat the cell to 25 ± 0.5°C. Apply an e.m.f. of 100 mV between the two platinum indicator electrodes. Switch on the halogen lamp of the illumination device and the polarograph recorder simultaneously, and record the current—time curve until the increase in the current is sufficient to obtain a straight line plot. The curves are equivalent to the biamperometric titration curves of the compounds with iodine and permit evaluation of the time required for total oxidation of the analyte (see Fig. 2). The time is related to concentration by calibration with standard solutions of the analyte.

Results and discussion

Photogeneration of iodine. When a solution containing iodide and Rose Bengal open to the atmosphere is subjected to the action of white light of sufficient intensity, iodine is very rapidly formed. This can be detected by the change in colour of the solution or, better, by recording the current flowing between two platinum electrodes at 100-mV applied voltage. The presence of oxygen is essential. In similar experiments in an inert atmosphere, no iodine was formed. These results show that the oxidation of iodide by triplet-state Rose Bengal, as with other sensitizers [15], is not significant even if energy considerations are favourable, perhaps because of fast quenching by the heavy atom. Oxygen introduces a new reaction path involving triplet-state Rose Bengal, which leads to the formation of a semi-oxidized form of the dye and to O_2^-, both of which oxidize iodide to iodine.

In order to establish the most appropriate conditions for the formation of iodine, the main variables affecting the photochemical process were studied. Figure 1 shows the effects of Rose Bengal and iodide concentrations on the iodine photogeneration process, measured as described above. With the source of excitation used, the presence of the dyestuff is essential for iodine generation. The rate of generation is almost constant when the concentrations of iodine and Rose Bengal are higher than 0.25 M and 4×10^{-5} M; respectively.

The rate of the photochemical reaction is strongly influenced by pH (Table 1). The small amount of iodine formed at pH 2 and 3 is probably because under these conditions most of the Rose Bengal is in its acid form, which is much less photosensitizing. The formation of iodine is also affected by temperature. The generation decreases substantially above 40°C (Table 2) because at the low concentration of dissolved oxygen under such conditions, the rate of the photochemical reaction depends mainly on the oxygen concentration, as has been observed with other photosensitizers [11, 15].

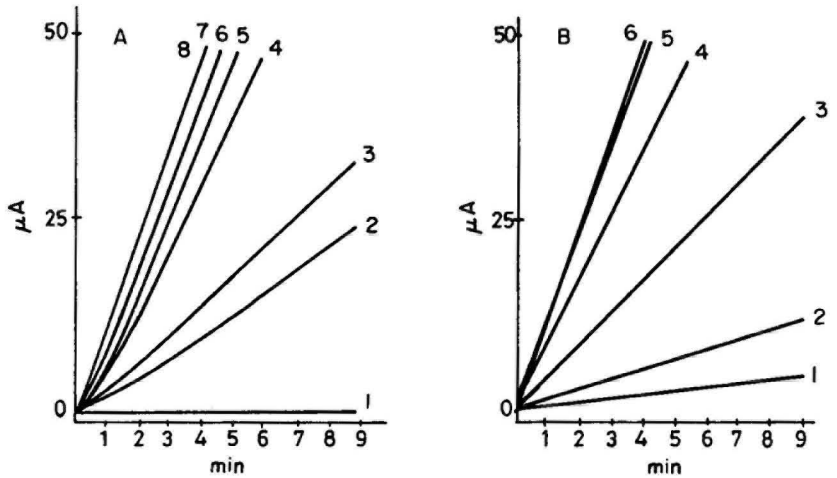

Fig. 1. Effect of reagent concentrations on photogeneration of iodine for 17,000 lux illumination (A) curves 1—8 correspond to Rose Bengal concentrations of 0.0, 1.0, 2.0, 5.0, 10.0, 20.0, 40.0 and 100.0 X 10^{-6} M, respectively, with 0.3 M iodide present. (B) Curves 1—6 correspond to iodide concentrations of 0.01, 0.02, 0.05, 0.10, 0.25, and 0.50 M, respectively, with 4 x 10^{-5} M Rose Bengal present.

TABLE 1

Influence of pH on photogeneration of iodine
(For 2 ml of 10^{-3} M Rose Bengal, 10 ml of buffer and 2.5 g KI diluted exactly to 50 ml; 25 ± 0.5°C; 13,000 lux for 10 min.)

pH	2.0	3.0	4.0	6.2	7.7	9.1
Iodine formed (μeq)	0.20	0.30	1.18	2.46	2.24	0.65

TABLE 2

Effect of temperature on photogeneration of iodine
(Conditions as Table 1, with 5% sodium hydrogencarbonate buffer instead of BR buffer.)

Temp. (°C)	18	25	30	35	40	50
Iodine formed (μeq)	1.95	2.20	2.22	2.16	2.10	1.46

The effects of various salts on the rate of iodine formation are shown in Table 3; 0.1 M salt solutions had no significant influence on the photochemical process. Sulphate and phosphate above 0.5 M had an inhibiting effect.

At the concentrations of Rose Bengal and iodide used, the rate of photogeneration is proportional to the light intensity. The light is adjusted to the value desired by using suitable filters, but always keeping the solid angle subtended by the reaction vessels constant, so that the incident intensity is the same for all samples.

TABLE 3

Influence of salts on photo-generation of iodine
(Conditions as in Table 2.)

Salt		NaCl		KBr		$NaNO_3$		Na_2SO_4		Na_2HPO_4	
Conc. (M)	0.0	0.1	0.5	0.1	0.5	0.1	0.5	0.1	0.5	0.1	0.5
Iodine formed (μeq)	4.10	4.10	4.00	4.20	3.94	4.20	3.82	3.82	3.08	3.90	3.10

For reproducible results, all these parameters must be kept constant throughout a series of measurements on standards and unknowns. For ten determinations of the amount of iodine formed, under the conditions given in Table 2 at 25°C, the relative standard deviation was 2.5%.

Photochemical determinations. The photo-generation of iodine with Rose Bengal sensitizer under the established optimal conditions was applied to the determinations of arsenite, hydrazine sulphate, isoniazid and uric acid, in a hydrogencarbonate medium [18—20]. The determinations of reducing substances with iodine photogenerated with Rose Bengal as photosensitizer can be thought to proceed by direct reaction with the iodine produced. However, the possibility of the triplet-state dye oxidizing the reductant directly cannot be excluded, especially with amines of nitrogen heterocycles; the presence of oxygen is essential for such reactions to take place. The time of photolysis necessary to arrive at the end-point of the determination will be affected by the contribution of the latter reaction to the overall oxidation. In the present investigations, it was established that arsenite is not oxidized by the excited form of the dye, but that for hydrazine sulphate, isoniazid and uric acid, the contribution of the triplet-state oxidation is significant.

Figure 2 shows the biamperometric determination of various amounts of hydrazine sulphate with photogenerated iodine. The end-point (complete oxidation) can be determined with great accuracy. The ascending portion

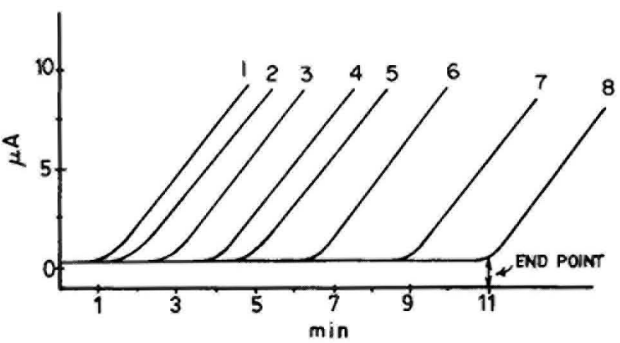

Fig. 2. Determination of the end-point for the determination of hydrazine sulphate. Curves 1—8 correspond to 0.2, 0.4, 0.8, 1.2, 1.6, 2.4, 3.2 and 4 μeq of hydrazine.

of the curve measures the increase of current beyond the equivalence point, when the iodine-iodide ratio increases.

Calibration diagrams (Fig. 3) were constructed representing the time required for complete oxidation of the analyte as a function of its concentration. The slope of the straight line for each reductant decreases as the relative contribution of triplet-state dye oxidation increases. Photolysis times are 30—900 s, if appropriate filters are used to adjust the light intensity. Table 4 summarizes the results obtained for the determination of the compounds mentioned.

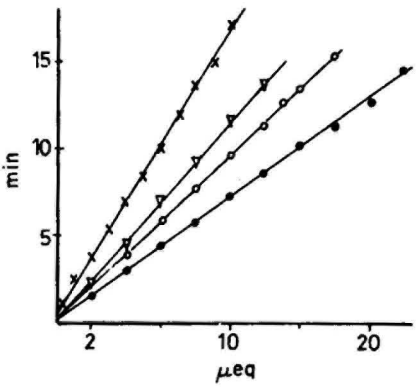

Fig. 3. Calibration curves for titrations with photogenerated iodine. (•) Hydrazine sulphate; (×) arsenite; (▽) isoniazid; (○) uric acid. Least-squares fit of data points shown as solid lines.

TABLE 4

Titrations of reductants with photogenerated iodine

Reductant	Range (μeq)	R.s.d. (%)
Arsenite	0.5—10	1.3[a]
Hydrazine sulphate	2—20	1.1[a]
Hydrazine sulphate[b]	0.2—4	2.1[b]
Isoniazid	0.5—8	1.2[a]
Uric acid	0.5—10	0.9[a]

[a]3 Determinations of 6 μeq. [b]3 Determinations of 0.6 μeq; light intensity was 30% of that used in the other determinations

REFERENCES

1 T. Gomyo, Y. Yang and M. Fujimaki, Agric. Biol. Chem., 32 (1968) 1061.
2 L. Well, Arch. Biochem. Biophys., 110 (1965) 57.
3 F. W. Morthland, P. P. H. De Bruyn and N. H. Smith, Exp. Cell Res., 7 (1954) 201.
4 R. F. Bartholomew and R. S. Davidson, J. Chem. Soc. C, (1971) 2347.

5 L. Well, Science, 107 (1948) 426.
6 H. Obata and M. Koizumi, Bull. Chem. Soc. Jpn., 30 (1957) 136 and 30 (1957) 142.
7 M. I. Simons and H. Van Vonakis, Arch. Biochem. Biophys., 111 (1965) 308.
8 J. R. Merkel and W. J. Nickerson, Biochim. Biophys. Acta, 14 (1954) 303.
9 G. Oster and N. Wotherspoon, J. Am. Chem. Soc., 79 (1957) 4836.
10 J. Faure and J. Joussot-Dubbien, J. Chem. Phys., 63 (1966) 621.
11 M. Koizumi, Mol. Photochem., 4 (1972) 57.
12 F. Sierra, C. Sánchez-Pedreño, T. Pérez Ruiz, C. Martinez and M. Hernández, Anal. Chim. Acta, 78 (1975) 277.
13 C. S. Foote and R. W. Denny, J. Am. Chem. Soc., 93 (1971) 5168.
14 J. Straub, Arch. Exp. Pathol. Pharmakol., 51 (1904) 383.
15 A. G. Kepka and L. I. Grossweiner, Photochem. Photobiol., 14 (1971) 621.
16 E. I. Dodin, I. P. Kharlamov and A. M. Pavlova, Zh. Anal. Khim., 31 (1976) 935; 31 (1976) 1181.
17 E. I. Dodin, A. M. Pavlova, N. P. Zakharova and I. P. Kharlamov, Zh. Anal. Khim., 31 (1976) 1570.
18 See e.g. J. T. Stock, Amperometric Titrations, Wiley-Interscience, New York, 1965.
19 I. M. Kolthoff and R. Belcher, Volumetric Analysis, Vol. 3, Interscience-Wiley, New York, 1957.
20 A. Berka and J. Vulterin, Chem. Anal., 52 (1963) 56.

Analytica Chimica Acta, 104 (1979) 403—406

Book Reviews

R. W. May, E. F. Pearson and D. Scothern, *Pyrolysis Gas Chromatography*, The Chemical Society, London, 1977, vii + 109 pp., price £7.20.

This Chemical Society publication is a valuable laboratory guide to the technique of pyrolysis gas chromatography, containing a well balanced account of the theory, practice and results obtainable. The material is organised into chapters on gas chromatography, pyrolysis apparatus, applications, peak identification, and standardization of methods and techniques. Finally, there is a library of pyrograms, produced under carefully described standard conditions, which more than anything else in the book display the power of, and information provided by, the technique.

The major uses of this book will be as an introduction to the power and scope of the method, showing how it may help in particular problems, and as a laboratory handbook, where the authors' careful attention to details of practice will enable many workers to improve their own procedures. This having been said, however, it must be noted that the expectation of the reader's commonsense is sometimes rather low, as in the comment that differing chart speeds can lead to problems in comparing pyrograms.

Many workers in the field will wish to purchase this excellent book, and all polymer libraries ought to possess a copy.

I. W. Parsons

T. R. Roberts, *Radiochromatography*, Elsevier, Amsterdam, 1978, x + 174 pp., price Dfl. 90.00, U.S. $ 39.95.

This book, Part 14 in the Journal of Chromatography Library, gives a concise and up-to-date account of the chromatography and electrophoresis of radio-labelled compounds. Following a very brief introductory chapter, the second chapter reviews the various types of radio-activity detectors used in conjunction with chromatography. Subsequent chapters each deal with a separate chromatographic technique e.g. radio-paper chromatography, radio-thin layer chromatography, radio-column chromatography and radio-gas liquid chromatography; there are also short chapters on radio-electrophoresis and miscellaneous applications related to radiochromatography. There is a detailed Table of Contents; a subject index, but no author index; and an Appendix that lists the names of the manufacturers of instruments used frequently in radio-chromatography, and offers brief comments on the capability of their instruments.

The production reaches the high standard set by previous volumes in this Library: there are very few misprints. The book is well illustrated with figures

and block schematic diagrams. There are also numerous reproductions of photographs, depicting the external appearance of commercial pieces of apparatus; these contribute little, other than to extend the length of the book by several pages, and may well lead to giving the book a prematurely "dated" appearance within a few years. Regular users of radio techniques in conjunction with chromatography and electrophoresis will probably gain little from this book, but it offers a good general introduction to a somewhat specialised field for students and those inexperienced in the specialised techniques involved.

J. Turkova, *Affinity Chromatography*, Elsevier , Amsterdam, 1978, ix + 405 pp price Dfl. 167.00, U.S. $ 69.75.

This, Volume 12 of the Journal of Chromatography Library, is a splendid book that gives an authoritative, up-to-date and comprehensive account of affinity chromatography in its broadest sense - indeed the final chapter, devoted to immobilized enzymes, is particularly valuable. Although this book, according to its cover, is intended mainly for those working in biochemistry, biology, and clinical laboratories concerned with human and veterinary medicin there is also a great deal in it for those specialising in the chemistry of natural products.

The literature coverage is comprehensive (ca. 1400 references), and considering that a translation into English was necessary, surprisingly up-to-date: there are many references to material published in 1976. Incidentally, the translator, Dr. Z. Prochazka, deserves considerable commendation in achieving a lucid and readable text in which only very occasional mis-spellings or quaint turns of phrase attract attention. Those responsible for preparing and proof-reading the index fared rather less well: there are quite a few slips e.g. concavalin (concanavalin); Arrenius (Arrhenius); heterogenous (heterogeneous); specifity (specificity); dephenylmethane (diphenyl); lecitin (lectin); Poissin (Poisson); guadines (guanidines); enthropy (entropy); hydrophylic (hydrophilic) sulpher (sulphur) etc., but these do not detract from the importance of this work. Chapter 11 "Examples of the Use of Affinity Chromatography" is particularly valuable; it incorporates a Table (74 pages in length) listing the uses of affinity chromatography for the isolation of biologically active products.

As is usual for books produced in The Netherlands, the price is high by British standards, although it will probably be considered a good buy on the American market. This is an outstandingly successful book, however, and, regardless of cost, it must go on the acquisition list of all libraries catering for scientists concerned with proteins, glycoproteins, polysaccharides, nucleic acids, nucleotides, lectins, lipids, hormones, enzymes, cells, viruses etc.

Roger Epton (Ed.), *Chromatography of Synthetic and Biological Polymers, Volume 1, Column Packings, Gel Permeation Chromatography, Gel Filtration,*

and Gradient Elution, Ellis Horwood, Chichester, 1978, ix + 368 pp., price £18.00.

This is the first of two volumes, published by Ellis Horwood Ltd. for the Macromolecular Group of the Chemical Society, which present the texts of the papers read at an International Symposium held at Birmingham University on July 7—9, 1976. Of the 28 contributions, 14 are from laboratories in Britain, 10 from elsewhere in Europe, and 4 from U.S.A., of which 3 were from one particular Corporation. The Editor has performed efficiently, and has given an excellent, concise introduction to the topics involved. As usual with Conference Proceedings, one wonders why the production of the book took around 20 months, especially as it is based on the reproduction of typed copy. This format is not in itself objectionable, as the edited manuscripts have all been re-typed, cleanly and free from trivial errors, on one machine: when this is done professionally, a very satisfactory appearance can be achieved. In terms of the general production of the book, the binding and presentation of the various Figures & Tables are excellent, but the reviewer's copy is marred by the occurrence of several pages in which the print is smudgy, and some other pages carry a pale brown stain—possibly a slight flaw in the otherwise good quality paper, and possibly only in reviewer's copies, if slightly substandard copies are distributed for their use! Incidentally, the National Institute for Research in Dairying is in Shinfield, not Sheffield (p. vi).

The Contents are arranged in three sections. Part 1 (11 papers) — General Developments; Part 2 (3 papers) — Preparative and Industrial Scale Chromatography; Part 3 (14 papers) — Specialised Applications, Theory and Techniques. There is a good subject Index, but no Author Index. The quality of the papers varies a great deal, as is to be expected in Conference Proceedings: the book is worth reading, if only for the first paper, by Jerker Porath, in which he reviews Polysaccharide Supports — their Synthesis, Derivatization and Application. But although the price is reasonable by present standards, this book cannot be placed high on the personal purchase priorities list. Take your turn in the queue for a library copy.

D. M. W. Anderson

G. Mamantov (Ed.), *Characterization of Solutes in Non-aqueous Solvents*, Plenum Press, New York, 1978, viii + 325 pp. $____.

The book is a collection of contributions by participants in the Symposium "Spectroscopic and Electrochemical Characterization of Solute Species in Non-Aqueous Solvents" which took place at the meeting of the Division of Analytical Chemistry of the American Chemical Society at San Francisco, California in the Fall of 1976.

The editor claims that the contributions represent reviews of research topics. This applies to contributions by J. F. Coetzee and collaborators (an evaluation

of solvent effects on ligand substitution of nickel(II) complexes), M. Szwarc (on the use of e.s.r. and absorption spectra as well as of potentiometric and polarographic measurements in studies of reactions of radical anions and dianio G. Mamantov and R. Osteryoung (on acid—base reactions accompanying oxidation—reduction processes in molten chloroaluminates) and D. L. Manning and G. Mamantov (on recent electrochemical studies in molten fluorides). In all other cases the contribution corresponds to a description of recent results of contributors dealing in most cases with specialized, rather narrow subjects and usually described in more detail in journal publications.

The appeal of this volume to the general analytical audience is limited, but electroanalytical chemists working with non-aqueous systems — both solutions and melts — can find it a useful, up-to-date source of information, if they are interested in the nature of reacting species rather than in practical application.

P. Zuman

ANALYTICA CHIMICA ACTA, Vol. 104 (1979)

AUTHOR INDEX

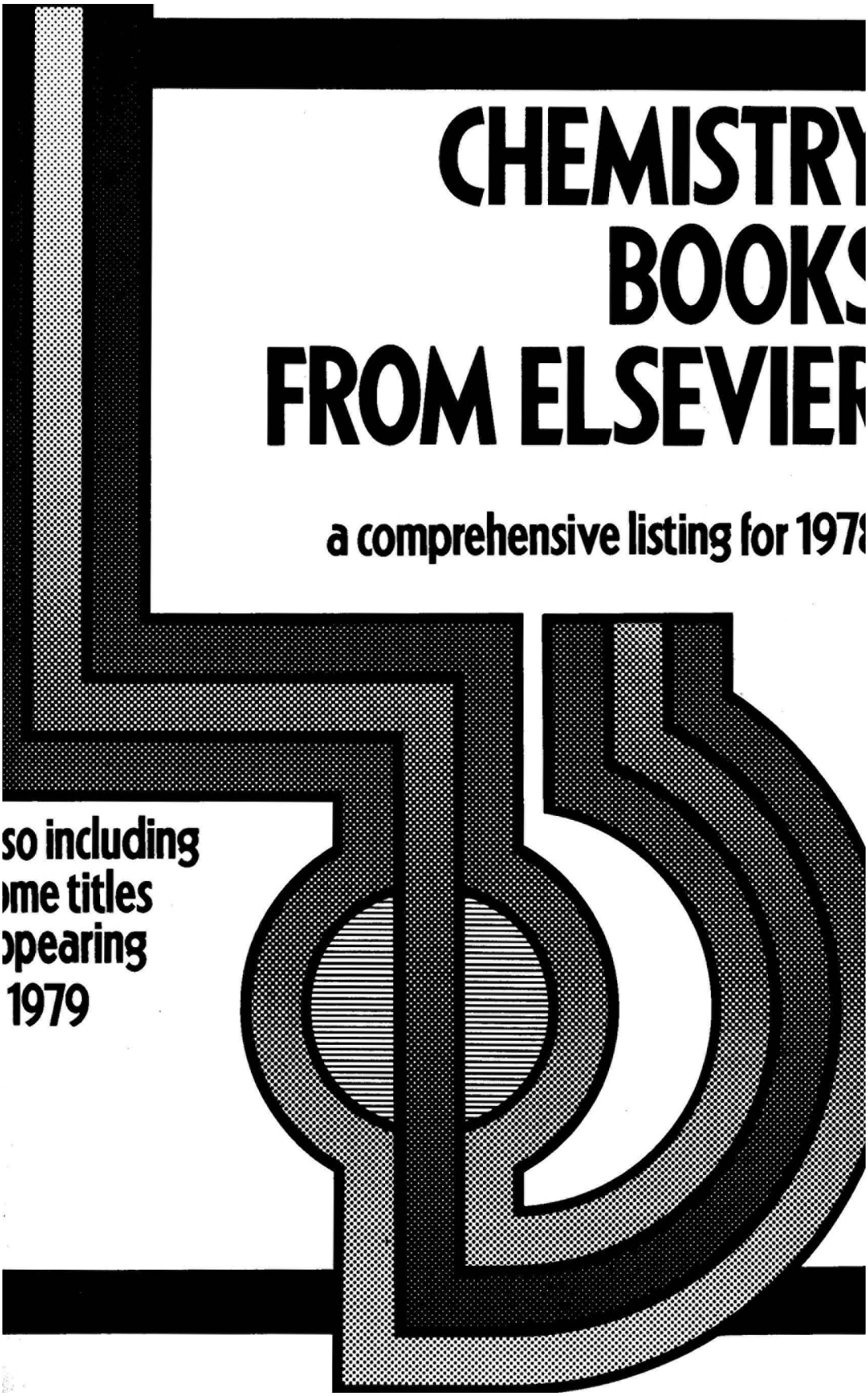
CHEMISTRY
BOOKS
FROM ELSEVIER
a comprehensive listing for 1978
so including
ome titles
ppearing
1979

ANALYTICAL CHEMISTRY

INTRODUCTION TO RADIOANALYTICAL PHYSICS

G. DECONNINCK, *Facultés Universitaires de Namur and Université de Louvain-la-Neuve, Belgium.*

Nuclear Methods Monograph 1

Covering the physical principles of radioanalytical methods (excluding neutron activation), this work discusses nuclear reaction mechanisms, the interaction of charged particle beams with matter, and practical formulae for elemental analysis. Suitable as a basic text for scientists of diverse backgrounds.

Aug. 1978 242 pp. US $49.75 / Dfl. 114.00
0-444-99796-2

QUANTITATIVE MASS SPECTROMETRY IN LIFE SCIENCES II

Proceedings of the Second International Symposium held at the State University of Ghent, June 13-16, 1978

A.P. DE LEENHEER, R.R. RONCUCCI *and* **C. VAN PETEGHEM** (Editors).

This volume reports the 5 plenary lectures presented at the symposium by recognized leaders in the field, as well as the 42 communications. Topics include: drug metabolism, clinical chemistry, biochemistry, toxicology and environmental hygiene.

Dec. 1978 514 pp. US $49.50 / Dfl. 109.00
0-444-41760-5

ANALYSIS OF STEROID HORMONE DRUGS

S. GÖRÖG, *Chemical Works, G. Richter Ltd., and* **GY. SZÁSZ,** *Semmelweis University Medical School, Budapest.*

This is the first monograph devoted to the analysis of steroid hormones from the point of view of the pharmaceutical industry and pharmaceutical analysis. Includes various physico-chemical methods for their analysis, with special emphasis on chromatographic methods.

Jan. 1978 426 pp. US $59.00 / Dfl. 138.00
0-444-99805-5

AFLATOXINS: CHEMICAL AND BIOLOGICAL ASPECTS

J. G. HEATHCOTE, *The University of Salford, U.K., and* **J. R. HIBBERT,** *Manchester Polytechnic, U.K.*

Developments in Food Science, 1

The book will encourage a wider recognition of the hazards of the aflatoxins among researchers in the fields of agriculture, food harvesting and storage, pathology, toxicology and preventive medicine. It will also serve as a valuable reference guide to the aflatoxins for both the inexperienced and experienced worker.

Oct. 1978 222 pp. US $53.50 / Dfl. 120.00
0-444-41686-2

INSTRUMENTATION FOR HIGH-PERFORMANCE LIQUID CHROMATOGRAPHY

J. F. K. HUBER (Editor), *Institute of Analytical Chemistry, University of Vienna.*

Journal of Chromatography Library - Vol. 13

Providing an up-to-date review of the large selection of instrumentation currently available, this book describes the general design features as well as the specific technical solutions in the instrumentation for high-performance liquid chromatography.

Aug. 1978 216 pp. US $34.75 / Dfl. 80.00
0-444-41648-X

EVALUATION AND OPTIMIZATION OF LABORATORY METHODS AND ANALYTICAL PROCEDURES

A Survey of Statistical and Mathematical Techniques

D. L. MASSART, A. DIJKSTRA and **L. KAUFMAN;** *with contributions by S. Wold, B. Vandeginste, and Y. Michotte.*

Techniques and Methods in Analytical Chemistry - Vol. 1

Formal methods for optimization in analytical chemistry are discussed in detail. This work will be useful to those involved with optimization in analytical chemistry as well as in other fields such as clinical chemistry and chromatography. Also suitable as an introduction to Chemometrics.

Oct. 1978 612 pp. US $57.75 / Dfl. 130.00
0-444-41743-5

ION-SELECTIVE ELECTRODES

E. PUNGOR, *Hungarian Academy of Sciences,* and **I. BUZÁS (Editors)**

This volume, containing 55 papers by participants from 18 countries, covers current trends of research as well as applications of ion-selective electrodes. Of interest to: researchers, analytical chemists, and those dealing with technical aspects of instrument development.

May 1978 624 pp. US $78.25 / Dfl. 180.00
0-444-99799-7

RADIOCHROMATOGRAPHY

The Chromatography and Electrophoresis of Radiolabelled Compounds

T. R. ROBERTS, Shell Biosciences Laboratory, *Sittingbourne Research Centre, U.K.*

Journal of Chromatography Library - Vol. 14

This book describes and discusses all of the various radiochromatography and radioelectrophoresis methods in a single volume. It will be of great value in enabling the inexperienced worker to select the optimum method for his particular situation.

May 1978 194 pp. US $39.95 / Dfl. 90.00
0-444-41656-0

(continued from outside of cover)

Printed in The Netherlands

CONTENTS

(continued on inside page of the cover)